Profiling and structural investigation of dihydrotriazine-based DHFR inhibitors and hydantoin-derived DprE1 inhibitors in search of novel antimycobacterials

Profilering en structureel onderzoek van op dihydrotriazine gebaseerde DHFR-remmers en van hydantoïne afgeleide DprE1-remmers op zoek naar nieuwe antimycobacteriële middelen

Proefschrift voorgelegd tot het behalen van de graad
van doctor in de Farmaceutische Wetenshappen
aan de Universiteit Antwerpen, te verdedigen door

Olga Balabon

Promotoren:
Prof. dr.Koen Augustyns
Prof. dr. Pieter Van der Veken
Dr. Robert Bates   Antwerpen, 2021

To my family

Table of Contents

List of Abbreviations

[Pd(allyl)Cl]$_2$	allylpalladium(II) chloride dimer
°C	degrees Celsius
µM	micromolar
1D	one-dimentional
2D	two-dimentional
2-MeTHF	2-methyltetrahydrofuran
ACN	acetonitrile
ADME	absorption, disctibution, metabolism, excretion
AIDS	acquired immune deficiency syndrome
Am	amikacin
APT	attached proton test
ART	antiretroviral therapy
ATP	adenosine triphosphate
BBB	blood-brain barrier
BCG	Bacillus Calmette–Guérin
Bdq	bedaquiline
br	broad signal (spectral)
calcd	calculated
CFU	colony forming unit
Cfz	clofazimine
c-Hex	cyclohexane
chrom	chromatographic
ChromlogD	chromatographic logarithmic value of distribution coefficient
Cl$_{int}$	hepatic intrinsic clearance
CLND	chemiluminescent nitrogen detection
CLND	kinetic aqueous solubility
Cs	cycloserine
δ	chemical shift (spectral)
DCM	dichloromethane
dd	doublet of doublets
DDIs	drug-drug interactions
DHFR	dihydrofolate reductase
DHFS	dihydrofolate synthase
DHPS	dihydropteroate synthase
Dlm	delamanid
DMF	dimethylformamide
DMSO	dimethyl sulfoxide
DMSO-d$_6$	deuterated dimethyl sulfoxide
DNA	deoxyribonucleic acid
DOT	directly observed therapy
DPA	decaprenyl-phosphoryl D-arabinose
DPR	decaprenylphosphoryl-D-ribose
DprE1	decaprenylphospho-beta-D-ribofuranose 2-oxidase
DPX	decaprenylphosphoryl-2-ketoribose

_____

DR-TB	drug-resistant tuberculosis
DS-TB	drug-susceptible tuberculosis
dt	doublet of triplets (spectral)
E	ethambutol
EMB, E	ethambutol
eq.	equivalent
ESI	electrospray ionization
Et	ethyl
Eto	ethionamide
EtOAc	ethyl acetate
EtOH	ethanol
EU	European Union
FBDD	fragment-based drug discovery
FDA	Food and Drug Administration
FQs	Fluoroquinolones
g	gram
GSK	GlaxoSmithKline
H2L	hit to lead
HCl	hydrogen chloride
HepG2	human hepatocellular carcinoma
hERG	human ether-a-go-go-related gene
HIV	human immunodeficiency virus
HMBC	heteronuclear multiple bond correlation
HMQC	heteronuclear multiple quantum coherence
HPLC	high performance liquid chromatography
HRMS	High Resolution Mass Spectrometry
hrs	hours
HSQC	heteronuclear single quantum coherence
HTS	high-throughput screening
Hz	Hertz
IC_{50}	half maximal inhibitory concentration
INH, H	isoniazid
Ipm-Cln	imipenem-cilastatin
IRIS	immune reconstitution inflammatory syndrome
J	coupling constant (spectral)
K_2CO_3	potassium carbonate
L	liter
LCMS	liquid chromatography–mass spectrometry
Lfx	levofloxacin
LTBI	Latent tuberculosis infection
Lzd	linezolid
M	molar (moles per liter)
m	multiplate (spectra), meter, meta-(subsitution)
M.tuberculosis	*Mycobacterium tuberculosis*
m/z	mass-to-charge ratio
M^+	parent molecular ion
max	maximum

_____

mbr	millibar
MDR-TB	multidrug-resistant tuberculosis
Me	methyl
MeCN	acetonitrile
MeOH	methanol
Mfx	moxifloxacin
MHz	megahertz
MIC	minimum inhibitory concentration
min	minute, minimum
mL	milliliter
mM	millimolar (millimoles per liter)
mol	mole (unit in chemistry)
Mpm	meropenem
Mtb	*Mycobacterium tuberculosis*
MW	microwave, molecular weight
N.D.	not determined
Na_2SO_4	sodium sulfate
NADH	nicotinamide adenine dinucleotide
nm	nanometers
NMR	nuclear magnetic resonance
NNRTIs	nonnucleoside reverse-transcriptase inhibitors
NOE	nuclear Overhauser effect
NOESY	2D nuclear Overhauser effect method
n-PrOH	1-propanol
o-	ortho-
p-	para-
PAS	para-aminosalicylic acid
Ph	phenyl
POA	pyrazinoic acid
ppm	parts per million (spectral)
Pr	propyl
Pto	prothionamide
PZA, Z	pyrazinamide
q	quartet (spectral)
quin	quintet (spectral)
R&D	Research&Development
RIF, RMP, R	rifampicin
RNA	ribonucleic acid
RR-TB	rifampicin-resistant tuberculosis
R_t	Retention time
S	streptomycin
s	singlet (spectral), second
SAR	structure-activity relationship
sept	septet (spectral)
t	triplet (spectral)
TB	tuberculosis
t-BuXPhos	2-di-tert-butylphosphino-2',4',6'-triisopropylbiphenyl
td	triplet of doublets (spectral)

_____

TDR-TB	term totally drug-resistant tuberculosis
TFA	trifluoroacetic acid
THF	tetrahydrofuran
THP-1	human acute monocytic leukemia cell line
TLC	thin-layer chromatography
TMS	tetramethylsilane
Trd	terizidone
TS	thymidylate synthase
UPLC-MS	ultra-performance liquid chromatography-mass spectrometry
USA	United States of America
UV	ultraviolet
VCD	vibrational circular dichroism
WHO	World Health Organization
XDR-TB	extensively drug-resistant tuberculosis
Z	pyrazinamide

1. Introduction[1]

1.1 Background. General info on TB

Tuberculosis (TB) is a widely known bacterial infectious disease, which has been plaguing humanity for millennia. Although reports date the oldest signs of infection to 9000 years old human remains,[1] and hospitals dedicated to this disease are believed to have existed in ancient Egypt as early as 1500 BC,[2] it was not until late 19th century that the etiological agent – *Mycobacterium tuberculosis* (Figure 1.1) was discovered. Often referred to as consumption or white plague TB managed to become a significant burden to the society over the centuries, accounting for as high as a quarter of all deaths in 1800s in some European countries.[3,4] The 19th century brought significant breakthroughs in understanding of the pathogenesis of the diseases. With the works of René Laennec, the inventor of the stethoscope, through demonstration of transmissibility by Jean Antoine Villemin and finally, in 1882, the identification of the tubercle bacillus by Robert Koch, the disease could be properly described under the name tuberculosis.[5]
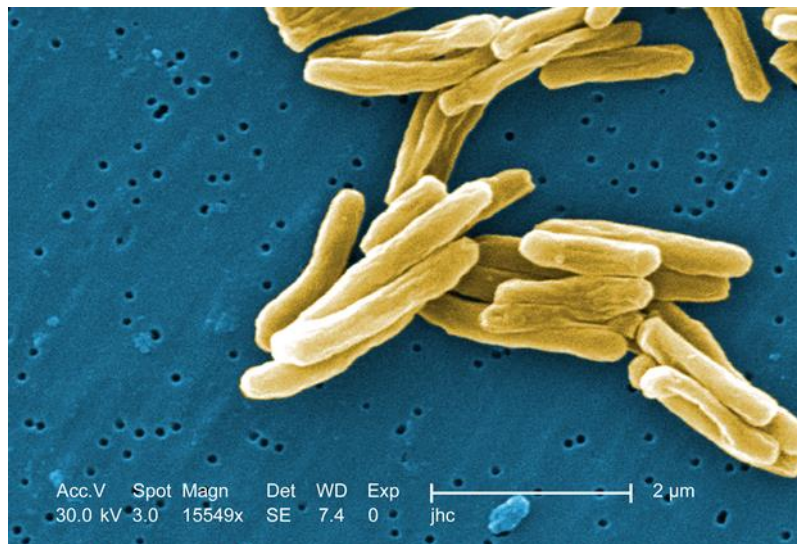
Figure 1.1. Mycobacterium tuberculosis under scanning electron microscopy (Center for Disease Control and Prevention's Public Health Image Library (PHIL), with identification number #9997).

Increased understanding of the microbiological nature allowed to implement guidelines and measures based on increased hygiene to reduce the transmission and mortality from the disease. Followed by the invention of diagnostic skin tests by Charles Mantoux and the Albert Calmette and Camille Guérin's vaccine in early 20th century, the overall infection burden started to decrease.[6] With the development of the first antibiotics – 4-aminosalicylic acid and streptomycin in the 1940s and isoniazid and cycloserine in the 1950s – the disease was thought to soon be eradicated (see Section 1.7.1 for more details). However the rise of the drug-resistant strains of the bacterium, together with the infection rates continuously increasing in the poorest regions of Africa and Asia, led the World Health Organization (WHO) to declare tuberculosis a global health emergency in 1993.[7] Although significant

_____

[1] Olga Balabon and Maciej K Rogacki contributed equally to the preparation Chapter 1.

_____

focus has been put on development of new drugs and vaccines, as well as improving the living conditions in the most affected regions, the disease remains a huge burden and a major threat to human health worldwide (see Section 1.7.6 for a detailed description of the current challenges).

1.2 Epidemiology

Tuberculosis today is the leading cause of death worldwide from infectious disease.[8] The World Health Organization estimates that 2018 alone brought approximately 10 million new infections and 1.5 million TB-associated deaths. While it is suggested that one third of the world's population is currently infected with the bacterium, prevalence of the disease is not homogenous. In fact, only 30 countries account for as much as 87% of cases (Figure 1.2).[9] The list is made up of mainly countries from the south-east Asia, sub-Saharan Africa and Western Pacific. The regions most affected are predominantly associated with poorer economy, lower quality of life and often insufficient access to medical assistance, which significantly hampers the efforts to control the disease. Simultaneously, the TB burden in the poorest regions – especially in Africa – to a large extent overlaps with prevalence of infections with Human Immunodeficiency Virus (HIV). HIV-TB coinfection has been shown to be a major risk factor leading to progression of the disease (Section 1.7.6.2). HIV positive patients account for 8.6% of all TB cases as well as an estimated 251 thousand TB-associated deaths in 2018 alone.[8]
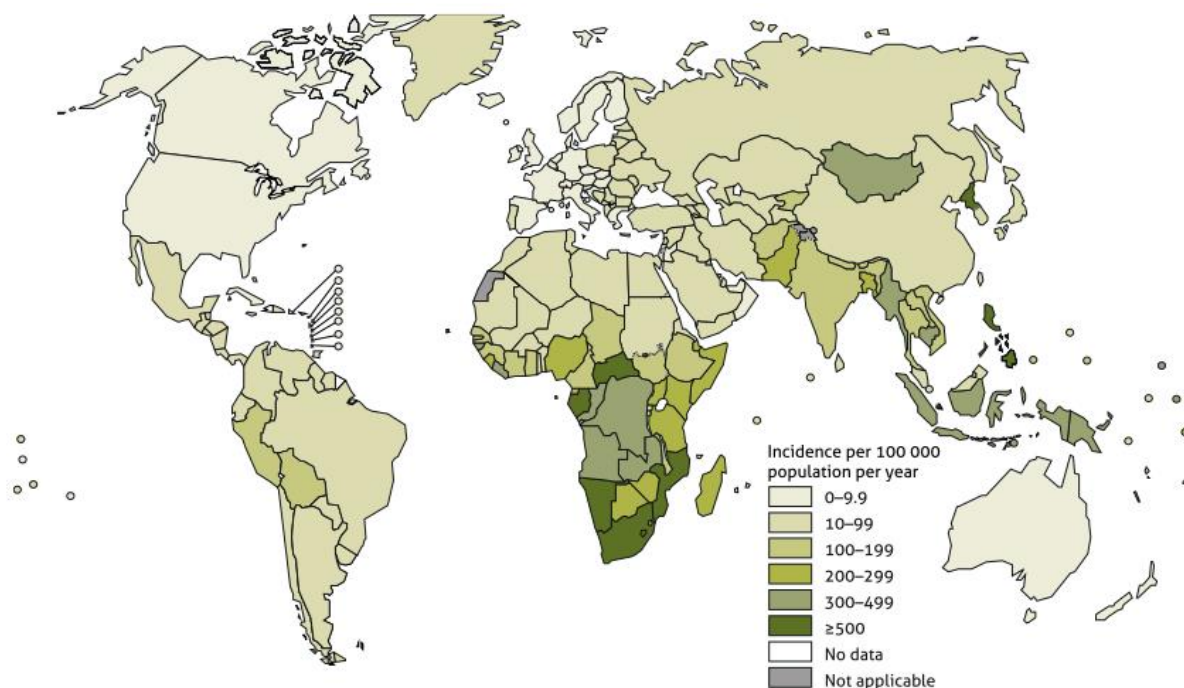
Figure 1.2. Estimated global tuberculosis incidence rates in 2018.[8]

Public health measures combined with the use of several chemotherapeutics led to a significant drop in the disease incidence and mortality rates in the western world over the last century and are showing similar results in the countries with heavier TB burden.

In 2018, over 52 thousand cases of tuberculosis TB were reported in 30 European Union and European Economic Area (EU/EEA), 4.2% of which were coinfected with HIV.[10] This corresponds to a notification rate of 10.2 per 100,000 inhabitants. The overall notification rate and the rates in most countries have been decreasing over the last five years. 35% of all TB cases reported in the EU/EEA were of foreign

origin. The rate of notified MDR TB cases remained at 0.3 per 100 000 population from 2014 to 2016 and then decreased to 0.2 in 2017 and 2018.

Belgium is a low-incidence country for tuberculosis, with 8.6 new tuberculosis cases per 100,000 inhabitants in 2018 with 52.1% of the those reported among people who did not have a Belgian nationality (88.9% of those come from countries with high prevalence of the disease).[11] Expectedly, more cases were registered in big cities, where there is a higher concentration of risk groups.

Unfortunately, the efforts to completely eradicate the disease have been largely set back by rapid development of drug resistant strains of *Mycobacterium*. The first cases of drug resistance date back to the very first trials of streptomycin and have led to development of combination therapies required for effective treatment[12] (for further information see in Sections 1.7.3, 1.7.4). Nevertheless, decades of poorly controlled, lengthy antibiotic administration led to emergence of bacteria resistant not only to one, but multiple chemotherapeutics (Section 1.7.6.1, Figure 1.3). With the onset of multidrug-resistant (MDR-TB), extremely drug-resistant (XDR-TB) and more recently identified strains grouped under a suggested term totally drug-resistant tuberculosis (TDR-TB)[13,14] the need for increased drug-discovery efforts as well as global initiatives to control and stop the spread of the disease was critical. Therefore, in 2014 World Health Assembly passed a resolution to implement a global program named 'End TB Strategy'.[15] The program's ultimate goal is to bring the global infection rates down by 90% and cut mortality rates 95% by 2035. The strategy requires increased financing and commitment from governments to engage in facilitating access to health services and improving quality of life especially in the highly disease-struck areas of low economic status. At the same time the program assumes increased funding in order to fill the antitubercular pipeline with novel vaccines and chemotherapeutics. Although the ongoing efforts are already showing positive results, the latest reports suggest that the planned 2030 milestones might not be met and additional actions and financing is required.[8]
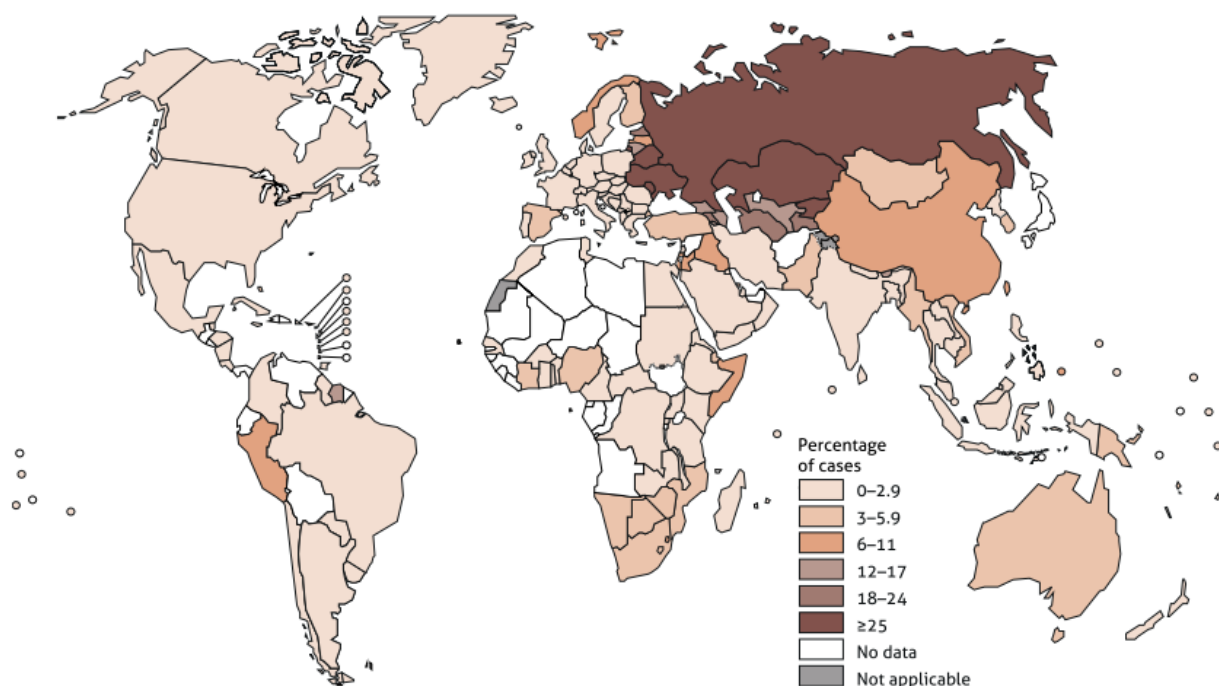
Figure 1.3. Percentage of new TB cases with MDR/Rifampicin-resistant tuberculosis. Percentage shown for the most recent data point.[8]

1.3   Mechanism: transmission, pathogenesis

Tuberculosis is caused by members of Mycobacterium tuberculosis complex – a subgroup of the *Mycobacterium* genus formed by a range of acid-fast, non-motile, aerobic bacteria.[16] Although the disease is predominantly associated with *Mycobacterium tuberculosis*, a minority of cases are found to be also caused by related species e.g. *Mycobacterium africanum* or their zoonotic relatives such as *Mycobacterium bovis*, *Mycobacterium caprae* or *Mycobacterium canetti* (Section 1.4).[17] The bacteria are usually spread in aerosol released through cough. The pathogen-containing droplets are inhaled and enter the lower respiratory tract, where they are recognized and phagocytosed mainly by alveoli macrophages (Figure 1.4).[18] After internalization, the phagosomes are normally fused with lysosomes in order to degrade the contents – including the pathogen. However, some mycobacteria are able to evade the process. Amongst the main mechanisms identified so far are the recruitment of host's protein TACO/coronin1 and secretion of the PknG serine/threonine kinase and the SapM phosphatase.[19] The latter was found to be responsible for proteolysis of the phosphatidylinositol 3-kinase (PI3 kinase), believed to be involved in docking of a number of enzymes responsible for the phagosome maturation.[20] Subsequently bacteria can gain access to the lung interstitium, either through migration of the macrophage or direct infection of lung epithelial cells. At the same time, infected dendritic cells and monocytes migrate to lymph nodes were T cell priming can occur. As a result, T cells and B cells can be recruited to the infection site eventually forming a multicellular structure called a granuloma. Formation of granulomas is an important step in control and progression of the disease. On one hand, the host's immune system can contain the infection within the structure, sealing it from the surrounding tissues with layers of immune cells expressing anti-inflammatory signals.[21] On the other hand, the expanding granuloma provides a growing number of immune cells available for the bacteria to infect and multiply. In most cases granulomas are able to contain the pathogens stopping further spread of the disease. This is what is called the 'Latent Tuberculosis Infection' (LTBI).
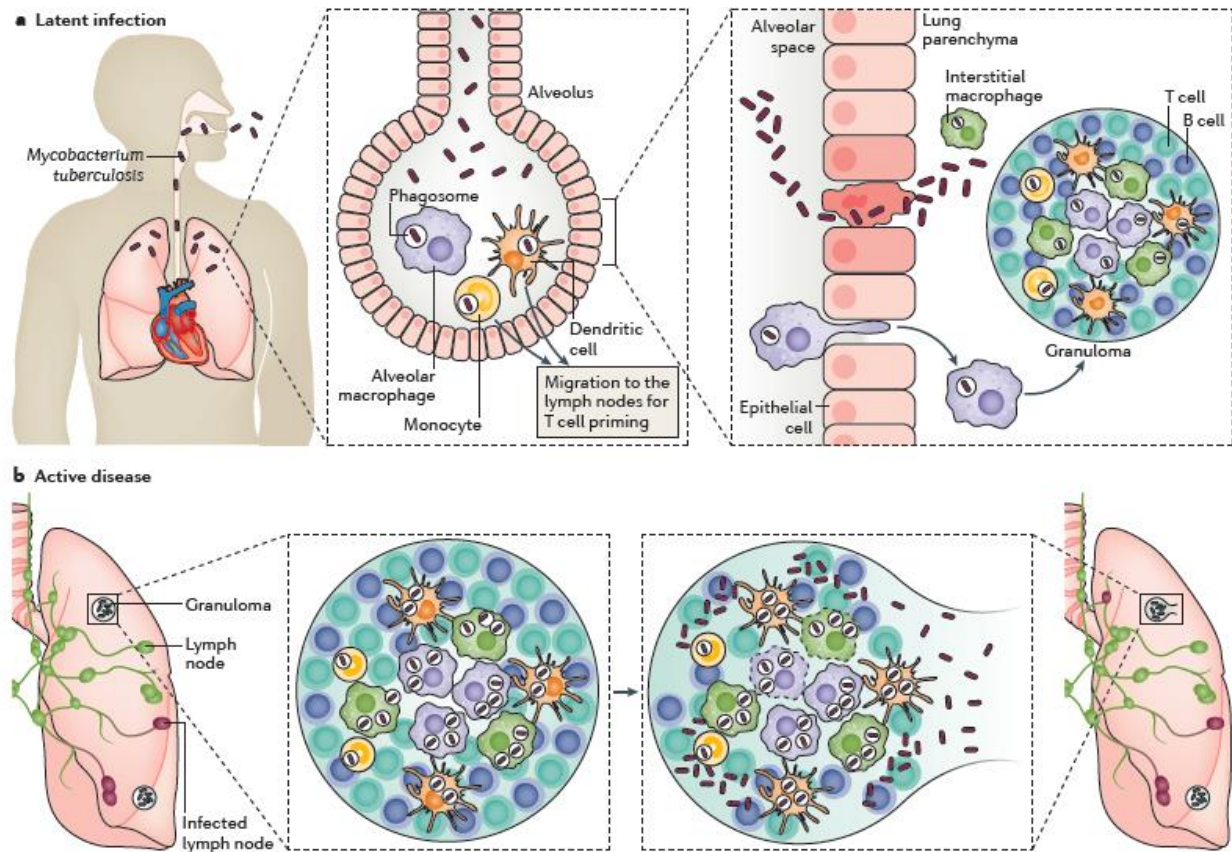
Figure 1.4. Progressive stages of infection with Mycobacterium tuberculosis; a. latent disease; b. active disease.[18]

Although in most individuals the disease remains in this asymptomatic form, the granulomas may sometimes be unable to control multiplication of bacteria. The mechanisms of progression are not fully understood, however, impaired function of the host's immune system, such as in case of co-infection with HIV has been identified as a major risk factor. Insufficient supply of nutrients and oxygen to the center of a granuloma leads to necrosis and formation of the so-called caseum.[22] At a certain point, the granuloma may break, releasing the content and enabling progression of the disease into the clinical stage. Release of the infected necrotic tissue to the lung alveoli is manifested by a persistent cough – the classic symptom of pulmonary tuberculosis. At this stage, the infected individual is highly infectious and the bacteria spread via aerosol, may infect another host. At the same time, the released bacteria may also enter the blood stream and disseminate into other organs where the infection can progress into the extrapulmonary form of the disease.[23]

1.4   Non-tuberculous Mycobacteria

Overall, the genus *Mycobacteria* (the only genus of the *Mycobacteriaceae* family) consists of nearly 200 species[24] commonly classified by varying rate of growth in the laboratory setting or the ability to produce pigmentation. However, for diagnostic purposes the group is generally divided based on their pathogenic potential into two main subgroups: tuberculous Mycobacteria (forming the *M. tuberculosis* complex), and non-tuberculous Mycobacteria. In addition, the Mycobacteria genus also contains *Mycobacterium leprae*, a known human pathogen and the etiological agent of leprosy. However, due to distinct phenotypic and genetic features, *M. leprae* is commonly classified outside of the two main groups.

Non-tuberculous Mycobacteria (NTM) are generally saprophytic organisms that are ubiquitous in the environment. The majority are commonly found in soil, rivers, lakes, as well as drinking water[25] and new species continue to be isolated every year.[24] Although members of the *M. tuberculosis* are of primary clinical importance within Mycobacteriaceae, NTMs are considered to be opportunistic human pathogens of rising significance. The ability of *Mycobacteria* to survive and persist in man-made environments, and in particular the piping systems providing homes with water, allows for high exposure to these organisms.[25] Household water and plumbing are conducive to NTM survival and growth due to several characteristics: pipe surfaces give opportunities for biofilm formation, low organic matter content permits growth of the oligotrophic NTM, while residual disinfectant favors the growth of disinfectant-resistant NTM.[26]

Although NTMs lack the pathogenic capabilities of the tuberculous bacteria, under some conditions, they can lead to development of a disease in humans. The main risk factors involve immunosuppression and lung diseases.

Historically, it was often difficult to determine the actual cause of infection. However, over the course of time, owing to improved techniques, it has become easier to precisely identify new pathogenic NTM species and get a better image of the prevalence of the NTM-mediated infections. Although NTM-caused disease are typically not mandatorily reported,[27] multiple studies report rising incidence rates of infections with non-tuberculous bacteria across different countries. In Germany annual incidence of NTM pulmonary disease (NTMPD) rose from 2.2 to 3.3 cases per 100 thousand population over a 5 year period,[28] while in Japan the disease was found in 14.7 patients per 100 thousand population, increasing 2.6 times over 7 years.[29] Similar trends were observed in reports from studies done in USA and other regions of the world, showing that in fact in the industrialized countries, incidence rates of NTM infections are often surpassing the numbers of new cases of tuberculosis.[29,30]

The most important non-tuberculous mycobacteria known to be responsible for human infections are the members of the *Mycobacterium avium* complex (*M. avium*, *M. intracellulare*, *M. chimaera*) and *Mycobacterium abcessus* complex (*M. abscessus*, *M. bolletii*, *M. massiliense*) as well as several other species such as *M. kansasii* or *M. xenopi*. Clinical symptoms of NTM infections are diverse, and are species-dependent. Although the pulmonary form of the disease is the most prevalent in immunocompetent patients, most other organs can also be affected especially in immunocompromised individuals.[31] Although the routes of transmission are not well described, it is suspected that bacteria often enter hosts lungs via aerosol inhalation.[32] The overall infection process often mimics mechanisms known from tuberculosis. The bacteria trigger a response of the innate immune system, leading to recruitment of macrophages and neutrophils, which attempt to phagocytose the microorganism. However, as in the case of *M. tuberculosis*, the bacteria may evade the phagosomal machinery and survive, leading to further recruitment of immune cells and creation of granulomas.[24]

Due to similarity to *M. tuberculosis*, infections with NTM were usually treated with standard of care antitubercular therapy. However, it has become increasingly evident that a lot of non-tubercular mycobacteria can be less susceptible to the set of primarily administered antibiotics. It has been found that NTMs are often resistant, not only to the wide-spectrum antibiotics such as beta-lactams but also to drugs typically administered for TB, such as rifampicin or ethambutol in case of *M. abcessus*.[33] (See sections 1.6.3, 1.6.4 for a review of antibiotics used for treatment of tuberculosis). Additionally, it has been observed that potent antitubercular bactericidal drugs such as bedaquiline may exert only

_____

bacteriostatic effects on NTMs as witnessed for *Mycobacterium avium*.[33] Since the biology of non-tuberculous mycobacteria is not yet well-understood and their clinical importance has classically been assessed as low in comparison to Mtb, it is unsurprising that the drug discovery pipeline is not well developed and consists mostly of repurposed drugs. Taking into account the heterogeneity of pathogenic mycobacteria, the rising incidence of infections, insufficient drug discovery efforts, non-tuberculous mycobacteria are becoming an increasing threat to healthcare, especially in the developed countries.

1.5   TB vaccines

After identification of *M. tuberculosis* and distinguishing it from *M. bovis,* it was hypothesized that administration of bovine bacilli, could provide protection against tuberculosis in humans. Initial trials performed at the end of 19th century, however, clearly showed that *M. bovis* is also highly virulent in humans and infection may lead to development of the disease.[34] In 1908, nonetheless, Albert Calmette and Camille Guérin first identified a less virulent strain of the bovine pathogen. Further subculturing work, continued over the course of 13 years, finally led to identification of an avirulent strain which was unable to cause development of the disease in animal studies.[35] In 1921, Bacillus Calmette-Guérin (BCG) was administered to human patients and until this day, almost one hundred years later, it remains the only available clinically approved vaccine against tuberculosis.

However, despite a century of global use and numerous studies performed, the protective efficacy against the disease is still largely unpredictable. In multiple trials, BCG was shown to provide immune protection ranging from as low as 0% to as high as 80%.[36] What is more, the length of immune memory persisting after vaccination was also found to be inconsistent. Although the general analysis shows the duration of protection to last until 10-15 years after vaccination,[37] antigen reactivity has been observed to be waning already within the first years in some cases, while persisting for more than 40 years in other individuals.[38] The protective efficacy was also suggested to correlate with geographical latitude,[39] with higher response observed in northern regions such as UK and poor results obtained closer to the equator, such as in sub-Saharan Africa. However other factors were also suggested to be of importance, such as the disease spread in the population, pre-exposure to environmental non-tuberculous Mycobacteria,[40] as well as even the BCG vaccine strain used.[41]

Although BCG's efficacy in adults seems to be largely unpredictable, it was shown to give high protective immunity against the infection in infants, especially against disseminated, so-called 'miliary' TB and tuberculosis meningitis.[42] The results could be consistent with findings that the higher efficacy is obtained especially in TB-naive individuals and prior contact with mycobacteria was suggested to lead to priming of the immune system causing a quick response against bovine bacilli administration and silencing of the expected stimulatory effect.[40] These findings support the continuous neonatal administration, especially in countries with an increased disease prevalence (Figure 1.5). On the other hand, administration of live bacilli in BCG may lead to an infection especially in immunocompromised patients. Therefore, the vaccine is not recommended anymore for infants infected with HIV.[43]
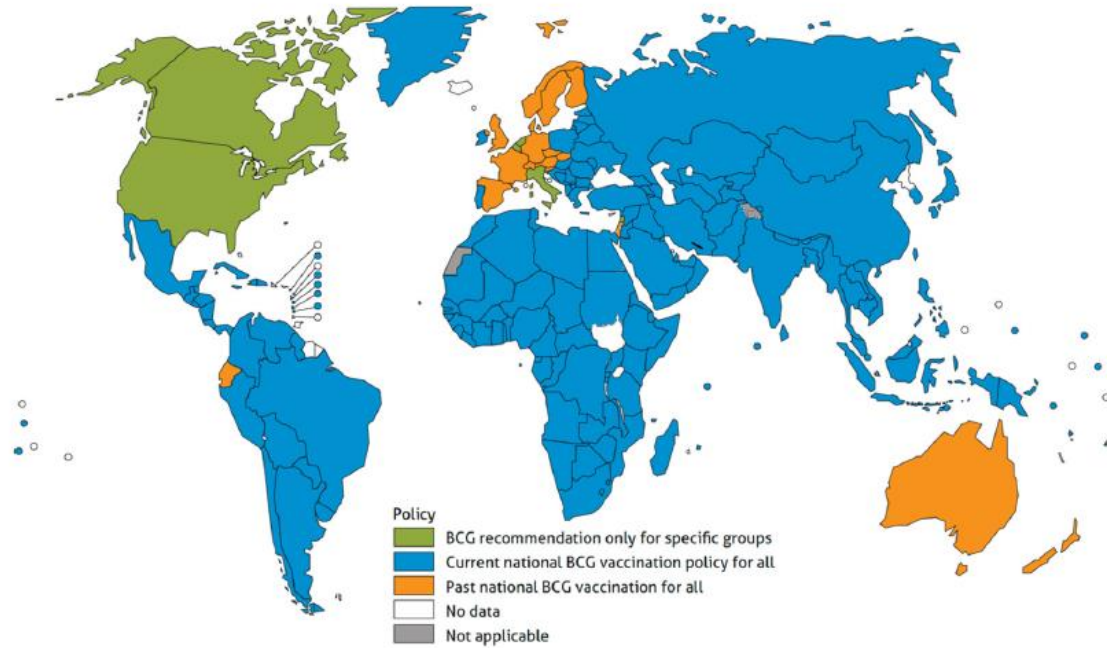
Figure 1.5. Current global BCG vaccination policy (reproduced from Martin et al.[44])

Given the lack of predictable efficacy, low expected benefit in adults, especially pre-exposed to mycobacteria and higher risk of adverse effects in HIV-positive patients, the need for new vaccines is evident. However, development of an antitubercular vaccine is not straightforward as proven by the lack of any new products entering the market over the past century. The new vaccine should be safe in adults as well as in children and immunocompromised individuals. At the same time, it should preferably be efficacious not only in naïve individuals but also in those pre-exposed to mycobacteria, in order to effectively control the disease in high-burden regions. Proper design and selection of a mechanism of action is not trivial, especially for an intracellular pathogen such *M. tuberculosis* which cannot be easily targeted by a set of antibodies. Additionally, lack of predictive biomarkers[45] and suboptimal animal infection models[46] lead to lengthy clinical trials requiring thousands of volunteers in order to properly evaluate the efficacy of a new vaccine in a human organism.

Given these obstacles, the 20th century brought little success in developing BCG's successor. The first new agent to reach human efficacy trial since 1921 was MVA85A, based on a virus engineered to produce a mycobacterial antigen Ag85A.[47] The vaccine was meant to boost the efficacy of BCG and was given several months after the original immunization. Although successful in animal models, MVA85A failed to show clinical efficacy.[48] Following development of MVA85A, new candidates based on different vaccine technologies and formulation strategies, started filling the antitubercular vaccine pipeline. As of 2020, there are 14 vaccine candidates ongoing clinical trials at various stages of progression.[44] The most successful so far is M72/AS01E developed by GlaxoSmithKline, combining the M72 subunit fusion protein of Mtb antigens (32A and 39A) and the company's proprietary adjuvant protein AS01E.[8] M72/AS01E is the first vaccine that was able to provide efficacy against clinical disease, showing 54% protection against progression to pulmonary tuberculosis in *M. tuberculosis* infected patients in Kenya.[49] The vaccine has successfully completed Phase IIb clinical trials and has been licensed to the Bill & Melinda Gates Medical Research Institute for further stages of development.[50]

_____

1.6   TB diagnosis

The effective management of tuberculosis relies on the rapid diagnosis of TB, rapid detection of drug resistance (drug-susceptibility testing DST), and prompt initiation of an effective treatment regimen.

To detect M. tuberculosis bacteria in the body, one of two kinds of tests are used: the TB skin test (Mantoux tuberculin skin test TST) or TB blood tests. Their positive outcome only shows that a person has been infected with the bacteria, but provides no information on whether the person has latent TB infection (LTBI) or has progressed to TB disease. Therefore, other tests (e.g. a chest x-ray and a sample of sputum), are needed for the diagnosis of TB disease.

Sputum-smear microscopy remains the primary diagnostic technique for evaluating persons with symptoms and signs of tuberculosis in many high TB burden settings. Nevertheless, it has several disadvantages such as relatively low sensitivity and no distinction between drug-susceptible and drug-resistant TB strains. Culture using commercially available liquid media remains the current gold standard method for the bacteriological confirmation of TB. However, it is not used as a primary diagnostic test in many high TB burden settings due to its costs, biosafety requirements, and long time for result generation. Nevertheless, conventional microscopy and culture are necessary to monitor a patient's response to treatment.

The initial tests for the diagnosis of TB are broadly grouped as WHO-approved rapid diagnostic tests (WRDs) and employ molecular or biomarker-based techniques, described in detail WHO operational handbook on tuberculosis. Module 3: Diagnosis - Rapid diagnostics for tuberculosis detection 2021 update.[51]

1.7   TB chemotherapy treatment

1.7.1   History of TB treatment

Although Robert Koch presented his research on the causative agent of tuberculosis already in 1882, the advent of effective antitubercular chemotherapy fell behind for another 60 years. Streptomycin, an antibiotic isolated from *Streptomyces griseus* in 1943, became the first antibiotic with proven activity against *Mycobacterium tuberculosis*, giving hope for tuberculosis-specific drug-based therapy. A year later, a patient with tuberculosis treated by it was declared cured, followed with more successful treatment cases.[52]

During the next decade, two other anti-TB agents, *para*-aminosalicylic acid (PAS, P), and thiacetazone, were marketed. Their administration, in combination with streptomycin, led to cure rate growth and reduction of antibiotic resistance.[53] The development of other anti-tuberculosis drugs with different mechanisms of action, including isoniazid (INH, H), pyrazinamide (PZA, Z), cycloserine, ethionamide, rifampicin (RIF, RMP, R), and ethambutol (EMB, E), soon followed (Figure 1.6). Highly efficient and easy to administer, rifampin revolutionized tuberculosis chemotherapy treatment.[54,55] Figure 1.7 shows the main milestones of the discovery of anti-TB drugs and regimens.[56–58]
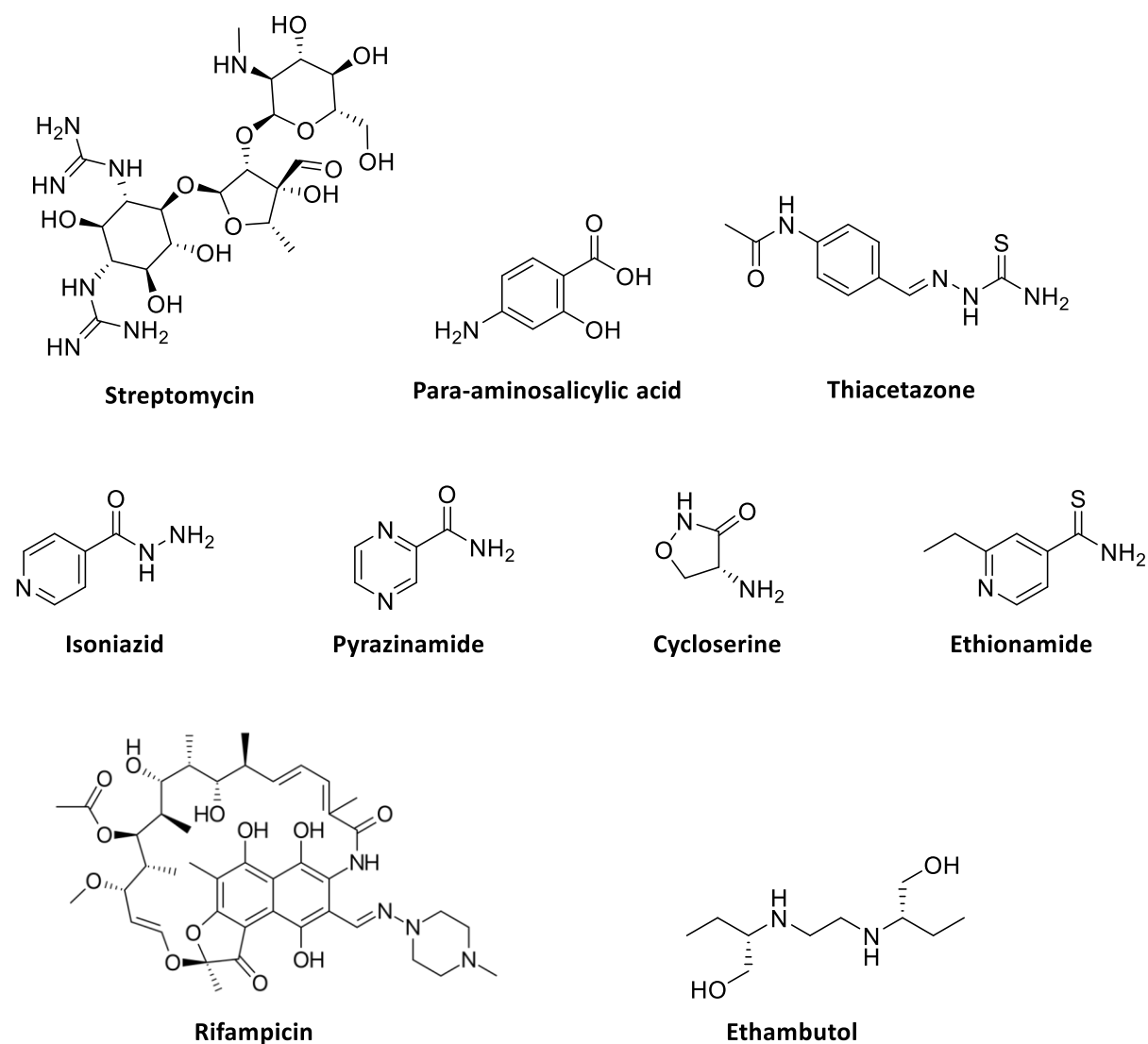
Figure 1.6. Chemical structures of anti-TB drugs

It was observed starting from the earliest studies that the introduction of any single antibiotic led to a rapid onset of resistance to it. Laboratory data from trials showed that receiving isoniazid as monotherapy caused resistance development, while it was suppressed when isoniazid was administered in combination with streptomycin or *para*-aminosalicylic acid.[59] Those findings led to the implementation of multi-drug therapy of a combination of antibiotics – nowadays, a widely-accepted strategy for the treatment of a range of infectious diseases and cancers.

Until the early 1970s, anti-tuberculosis treatment duration was typically 18 months or longer. Several multi-country clinical trials were led by the British Medical Research Council to provide more efficient anti-TB regimens. Addition of rifampicin into clinical use allowed to shorten the therapy duration to 9 months. Finally, the replacement of streptomycin with pyrazinamide in the 1980s led to the modern short-course oral treatment regimen of 6 month.[59]
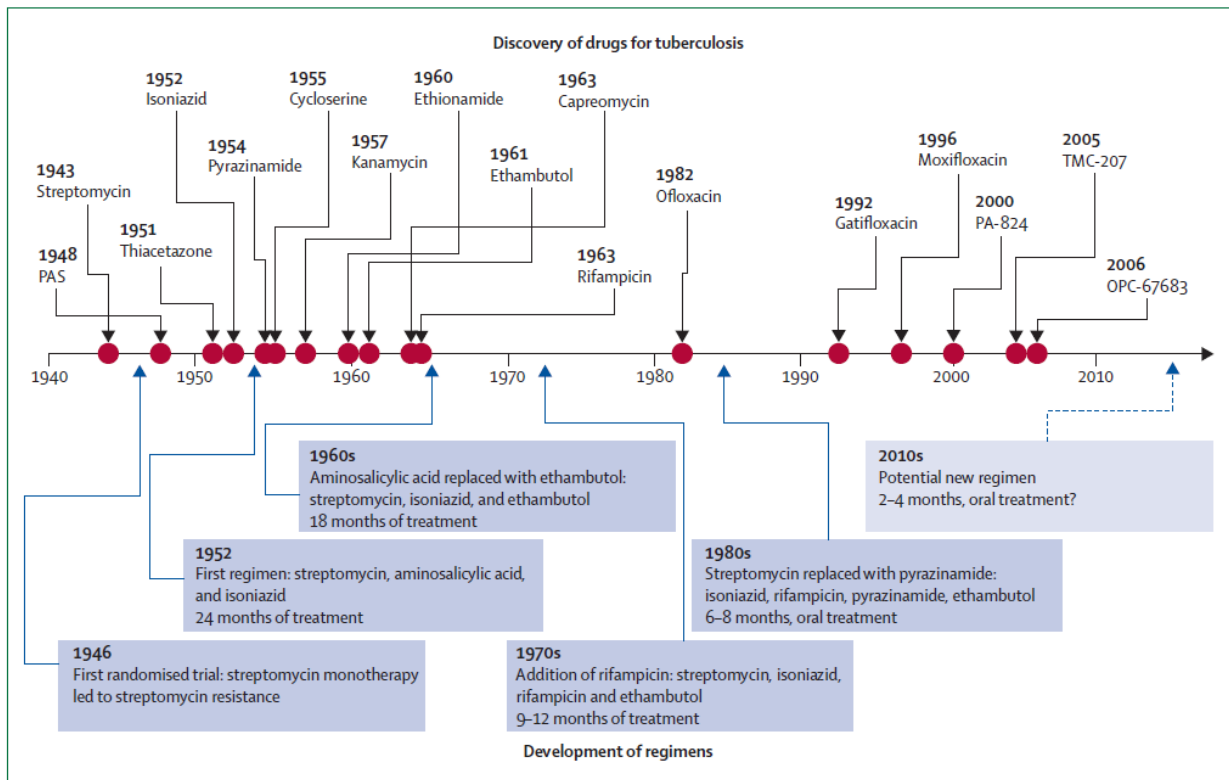
Figure 1.7. Timeline of the discovery of anti-tuberculosis drugs and the development of treatment regimens. Adopted from Ma, Z. *et al.*[60]

1.7.2 Mode of action of the approved anti-TB drugs

Most of the approved anti-TB drugs or drug classes possesses an established specific target, generally in cell wall biosynthesis, DNA/RNA synthesis, protein synthesis, or metabolism. Figure 1.8 provides a diagram representation of anti-tuberculosis drugs and their respective drug targets.

All anti-TB drugs can be broadly categorized into two big groups:

1) standard first-line treatment for drug-susceptible (DS)-TB,

2) second-line medicines for drug-resistant TB treatment. They are described in detail in Sections 1.7.3.2 and 1.7.4.3.

Figure 1.8. Approved anti-tuberculosis drugs and their corresponding drug targets.
Picture adopted from Bahuguna, A. *et al.*, 2020[61]

1.7.3 First-line treatment for drug-susceptible tuberculosis

No significant changes in drug-susceptible tuberculosis treatment were made since the 1970s up to date.[62,63] Typically, drug susceptibility is unknown for new TB cases at the time of therapy start. Unless there is an identified risk of drug-resistance disease (for example, if the patient has been in contact with individuals with proven drug-resistant TB), a drug-susceptible anti-tuberculosis regimen is started.
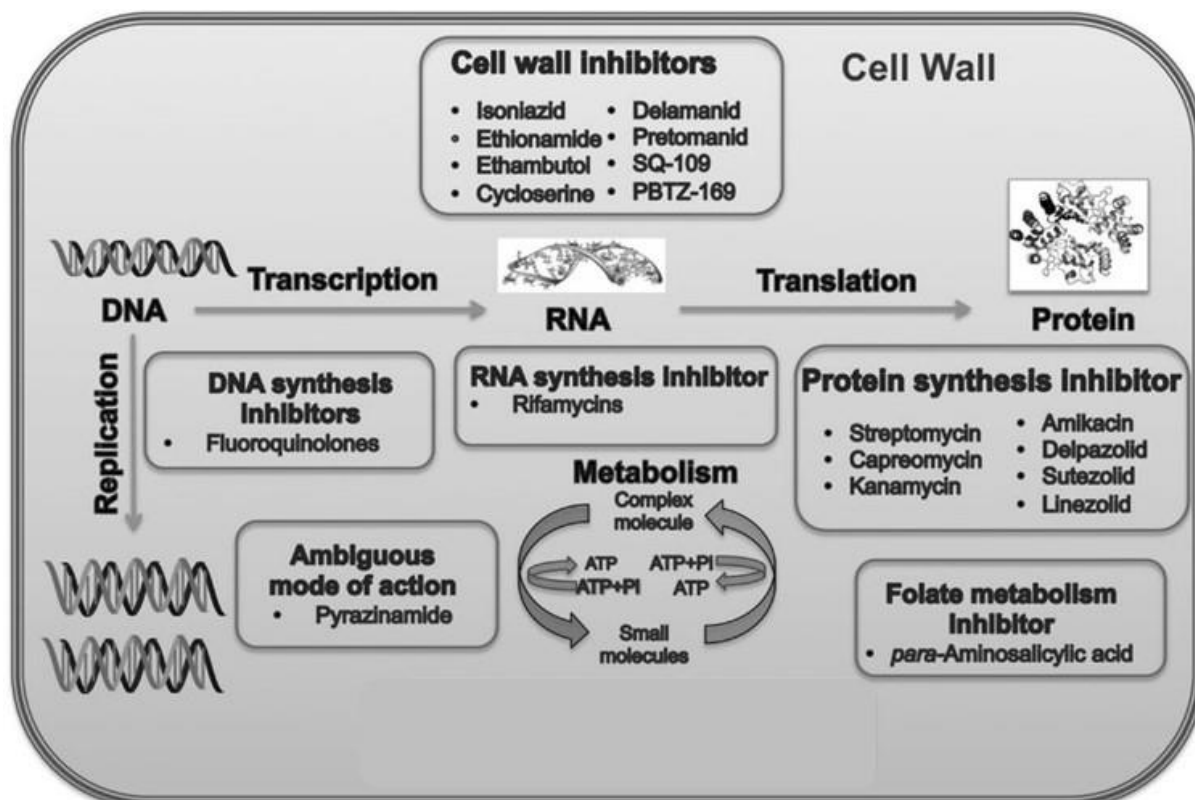
1.7.3.1   Drug-susceptible anti-tuberculosis regimen

The drug-susceptible anti-tuberculosis regimen consists of 4 first-line drugs: isoniazid (INH, H), rifampicin (RMP, R), pyrazinamide (PZA, Z), and ethambutol (EMB, E) (Figure 1.9).[62,64]

The 6-month 2HRZE/ 4RH treatment regimen of pan-susceptible tuberculosis consists of 2 consecutive phases: the intensive phase and the continuation phase. The first intensive phase consists of a once-daily 4-drug therapy for two months. It allows rapid bacillary burden reduction as the antibiotics kill rapidly growing bacteria, and a marked decrease in the intensity of clinical symptoms is observed.[65] The continuation phase consists of 2-drug therapy for four additional months. It is required to kill slow-growing persistent strains of *M.tuberculosis* for complete sterilization and cure.[66,67]

This four-drug regimen achieves up to 95% cure rates for DS-TB in 6 months when administered under directly observed therapy (DOT).[58,68,69] It is currently implemented for pulmonary and most forms of extrapulmonary tuberculosis, regardless of HIV co-infection presence[58,62,64,70] Complications associated with co-administration of antitubercular and antiretroviral agents are discussed in Section 1.7.6.2.

The sterilizing activity of a drug is defined as its ability to kill either dormant or non-replicating bacteria under hypoxic conditions, as well as the ability to shorten antituberculosis therapy duration and reduce

relapse (after the completion of treatment) in a long-term, while early bactericidal activity refers to the initial rapid kill of actively replicating mycobacteria.
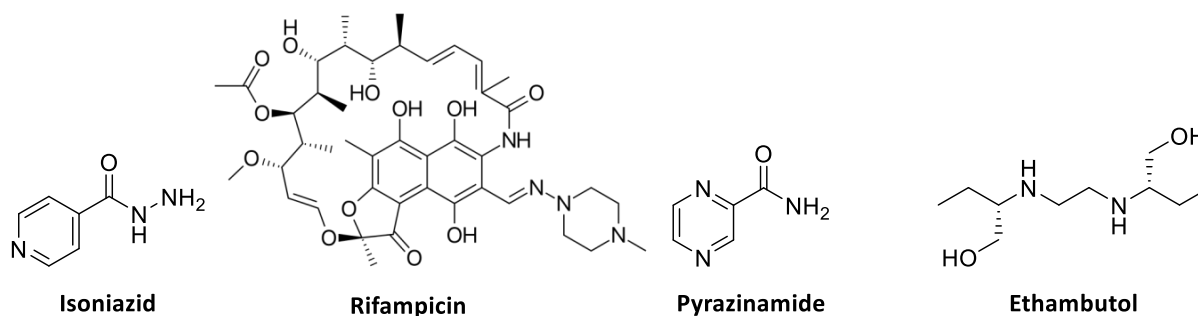

Figure 1.9. Chemical structures of the first-line anti-TB drugs.

1.7.3.2 First-line anti-TB drugs

Each first-line drug has a unique contribution to the overall efficacy of this short-course treatment regimen.

Isoniazid (INH, H)

Isoniazid, isonicotinic acid hydrazide, is considered one of the most specific and effective anti-tuberculosis drugs for DS-TB since its introduction in 1952.[71] It inhibits cell wall production and shows a high early bactericidal effect on actively growing *M. Tuberculosis*, causing rapid decrease in sputum bacilli within the first two weeks of treatment.[72] It is not active against the non-replicating bacterial subpopulation or under anaerobic conditions.[67]

The isoniazid mechanism of action is very complex, affecting many pathways related to macromolecular synthesis, in particular mycolic acid synthesis. INH is a pro-drug activated by catalase-peroxidase hemoprotein (KatG). Its active products inhibit InhA, an NADH-specific enoyl-acyl carrier protein (ACP) reductase, and beta-ketoacyl ACP synthase (KasA), both involved in fatty acid synthesis.[73–75]

Isoniazid can be used as a monotherapy for latent tuberculosis infection to prevent the reactivation of disease (Section 1.7.6.4).[72,75] Hepatotoxicity (including hepatitis development) and neurotoxicity (in particular peripheral neuropathy) are the most significant adverse reactions associated with isoniazid administration.[67,72]

Rifampicin (RIF, RMP, R)

Rifampicin, also known as rifampin or rifaldazine, is a semisynthetic derivative of the natural rifamycins, a family of structurally-related compounds. Its parent compound, rifamycin, was initially identified as a natural product isolated from *Amycolatopsis ryfamycinica* in 1957.[76] Rifampin was first synthesized in 1959 and was introduced into clinical practice in 1972 as an anti-tuberculosis drug with excellent sterilizing activity.

Rifampicin specifically inhibits the essential rpoB gene product, β-subunit of bacterial DNA-dependent RNA polymerase, the enzyme responsible for mycobacterial DNA transcription and expression, by forming a stable drug-enzyme complex. It results in bacterial transcription activity inhibition, killing the organism.[77–80] RIF exhibits exposure-dependent killing of actively growing and non-growing (slowly

metabolizing) bacilli, achieving elimination of all mycobacteria, including persistors.[81] RIF does not inhibit the mammalian enzyme.[80]

Analogues of rifampicin are also used in clinics. For instance, it was reported that treatment regiments containing rifapentine (brand name Priftin) may permit further shortening of the tuberculosis treatment regimen.[82]

The administration of rifampin leads to relatively few adverse reactions. It may provoke gastrointestinal upset, whereas hepatotoxicity is generally rare with RIF alone and occurs less frequently than with isoniazid administration.[67,80] Rifampicin induction of the cytochrome P450 enzymes leads to drug-drug interactions (DDIs) with many antiretroviral agents (Section 1.7.6.2).[70,83]

Pyrazinamide (PZA, Z)

Pyrazinamide, a nicotinamide analogue, played a crucial role in shortening TB treatment, and the creation of the modern 6-month first-like treatment regimen for DS-TS.[59] PZA is able to kill a population of semi-dormant, non-replicating *M. tuberculosis* persisters, residing in acidic environments present during inflammation, that other TB drugs fail to kill.[84] That makes pyrazinamide one of the keystone drugs of combined chemotherapies against drug-resistant TB such as MDR-TB.[85]

This sterilizing activity is unique among TB drugs, including new drug candidates in clinical trials. For example, recent preclinical efforts to identify optimal drug combinations with new drug candidates for shortening TB therapy suggested that PZA is the only drug that cannot be replaced without compromising treatment efficacy.[82,86,87]

Pyrazinamide is a pro-drug, converted into its active form, pyrazinoic acid (POA), by the cytoplasmic enzyme pyrazinamidase/nicotinamidase (PZase).[88] It is commonly accepted that POA may not have a specific target but rather gives rise to cytoplasmic acidification. This leads to disruption of major cellular processes: inhibition of vital enzymes, inhibition of membrane transport, protein and RNA synthesis.[89–91] At the same time, it showed little to no activity against growing tubercle bacilli.[84,92]

Side effects of pyrazinamide administration include hypersensitivity reactions (such as urticaria, pruritis, and skin rashes), liver injury, as well as gastrointestinal upset.

Ethambutol (EMB, ETH, E)

Ethambutol, discovered in 1961, is an essential antimycobacterial drug for chemotherapy treatment of both drug-susceptible and drug-resistant TB.[67] It enhances the effect of other medicines, including rifamycins, aminoglycosides, and quinolones.

Ethambutol is a bacteriostatic drug active against actively growing microorganisms of the genus *Mycobacterium*, including *M. tuberculosis,* but shows no effect on non-replicating tubercle bacilli.[93] Its target is arabinosyl transferase, an enzyme involved in cell-wall arabinogalactan biosynthesis.[94–96]

Ethambutol demonstrates significant dose-dependent risk of optic neuropathy, including color blindness, visual changes, and decreased visual acuity.[93] Those effects are reversible in most cases when its administration is discontinued promptly. It is a current practice in the USA to immediately suspend EMB administration when susceptibility to INH, RIF, and PZA is confirmed.[62]

1.7.4 Second-line treatment for drug-resistant tuberculosis

Second-line anti-tuberculosis drugs are employed when resistance to first-line therapy was manifested. Patients with RR-TB and MDR-TB (definitions are given in Section 1.7.6.1) are treated with different combinations of second-line drugs, usually for extended periods (18 months or more) (see Section 1.7.4.2 "Longer MDR-TB regimens").[85,97]

The WHO regularly issues new recommendations on the usage and combinations of new and repurposed antibiotics for the treatment of MDR-TB based on available evidence.[97] They are focused on optimizing all aspects of MDR-TB treatment: developing new combination regimens, shortening treatment duration, optimizing dosages.

Repurposed drugs, initially developed to treat other infections but shown to exhibit anti-TB activity, are frequently employed in MDR-TB and XDR-TB treatment regimens as they are already proven to be safe and more readily accessible. These include later generation fluoroquinolones, linezolid, aminoglycosides, and carbapenems. In fact, the majority of the second-line medicines, recommended by the WHO guidelines for MDR-TB treatment, were not developed for this purpose.

Bedaquiline and delamanid are the two exceptions that received a conditional license for MDR-TB treatment from the European Medicines Agency in 2014. The US Food and Drug Administration (FDA) granted accelerated approval to bedaquiline to treat resistant tuberculosis, making it the first FDA-approved tuberculosis drug in 40 years.

1.7.4.1 Shorter MDR-TB regimens for eligible MDR/RR-TB patients

Recently, numerous attempts to reduce the length of conventional MDR-TB regimens and to use better-tolerated drug combinations have been ongoing through various studies. In 2016 WHO updated its treatment guidelines for DR-TB and included a recommendation on the use of the shorter MDR-TB regimen under specific conditions.

The WHO evidence-based guidelines for the treatment of drug-resistant TB (released in December 2018 and incorporated into Consolidated Guidelines published in March 2019), recommend the usage of the shorter standardized MDR-TB regimen (known as the 'Bangladesh regimen'), under specific conditions.[69,85,97,98] The Bangladesh regimen consisted of seven drugs and is schematically referred to as '4-6 Km-Mfx-Pto-Cfz-Z-Hh-E / 5 Mfx-Cfz-Z-E' (see Section 1.7.4.3 for details on second-line drugs that are involved). More specifically, an initial phase of 4-6 months consists of treatment with kanamycin, moxifloxacin, prothionamide, clofazimine, pyrazinamide, high-dose isoniazid, and ethambutol, followed by 5 months of moxifloxacin, clofazimine, pyrazinamide, and ethambutol.[85,99] It is characterized by lowered costs and expected improvement in patients' compliance due to the shorter duration, while its programmatic use is feasible in most settings worldwide.

This regimen is indicated conditionally for patients who have not been previously treated for more than one month with second-line drugs used in this regimen and in whom resistance to fluoroquinolones has been excluded, regardless of patient age or HIV status.[97,100] Extrapulmonary disease, pregnancy, intolerance, or toxicity risk (for example, due to drug-drug interactions) for one or more medicine in the shorter MDR-TB regimen makes individuals not eligible for this regimen. In case of the emergence of any exclusion criterion or in case of return after treatment interruption for more than two months, the shorter MDR-TB regimen cannot be employed any longer, and the patient should be transferred to a longer individualized MDR-TB treatment regimen.

More recently, a shorter all-oral, bedaquiline-containing BPaL (bedaquiline, pretomanid and linezolid) regimen was studied clinically in the Phase 3 Nix-TB trial (in South Africa) to see if it improves patient outcomes when compared to a standardized shorter regimen with injectables recommended in previous WHO guidelines.[101] The trial enrolled 109 people with XDR-TB as well as treatment-intolerant or non-responsive MDR-TB. Nix-TB data demonstrated a favorable outcome in a high percentage of patients at 6 months after the end of therapy. Limitations in study design, the small number of participants and observed adverse events (including blood disorders, hepatotoxicity, peripheral and optic neuropathy) preclude programmatic implementation of the regimen worldwide until additional evidence has been generated. However, the BPaL regimen may be used under operational research conditions conforming to WHO standards for eligible MDR/RR-TB patients.[100,102]

Based on these findings, one recommendation on shorter regimens to treat MDR/RR-TB has been updated in the 2020 edition of the WHO consolidated guidelines on tuberculosis. A shorter all-oral regimen of 9-12 months was conditionally recommended in this update for eligible patients with confirmed MDR/RR-TB who have not been exposed to treatment with second- line TB medicines used in this regimen for more than 1 month, and in whom resistance to fluoroquinolones has been excluded. This regiment consists of two phases: '6 Bdq with 4–6 Lfx[Mfx]-Cfz-Z-E-Hh-Eto/ 5 Lfx[Mfx]-Cfz-Z-E' (orally-administered bedaquiline replace injectable amikacin from the previous guidances).[100,102]The initial, intensive phase of 4-6 months combines 4 second-line drugs (bedaquiline for 6 months, levofloxacin or moxifloxacin, ethionamide and clofazimine). It is followed by the 5-month continuation phase of 2 second-line drugs (levofloxacin or moxifloxacin and clofazimine). Both phases are supported by the selected first-line TB Drugs (ethambutol and pyrazinamide for both phases, while high-dose isoniazid only for the first phase). See Section 1.7.4.3 for the details on the second-line drugs.

1.7.4.2 *Longer MDR-TB regimens*
The individualized longer MDR-TB regimens are typically designed to include a minimum number of second-line TB drugs, which are considered effective based on drug-resistance patterns and patient history, using the WHO priority grouping of medicines and last 18 months or more.[97,100,102] Previously, the term "conventional" was used to refer to such regimens, but its usage was discontinued in 2016.

Table 1.1 summarizes the second-line drugs currently recommended to be included in the longer MDR-TB regimens and their division in three groups A-C (see Section 1.7.4.3 for the details on each medicine).[97,102] It is intended to guide the design of individualized treatments. Group A fluoroquinolones (levofloxacin or moxifloxacin), bedaquiline, and linezolid are considered highly effective. Therefore, it is strongly recommended to include them in all regimens unless contraindicated. Group B medicines are conditionally recommended as agents of the second choice. All other drugs that can be added to complete the regimen, when it cannot be composed with Group A and B agents alone, are included into Group C, ranking by the predicted relative balance of benefit *vs.* harm.[102]

The general guidelines suggest that the regimens should be composed of all three Group A medicines plus at least one Group B agent so that treatment starts with at least four drugs likely to be effective. At least three medicines are continued for the remaining duration of treatment after bedaquiline is stopped after six months.

There are other known anti-TB drugs that are no longer included in Groups A-C for various reasons. Capreomycin and kanamycin were associated with poorer outcomes and, therefore, are no longer

_____

recommended for use in MDR-TB regimens. Thioacetazone is not suggested for contemporary longer regimens, while gatifloxacin is withdrawn from the market due to concerns about dysglycaemia.[103]

Table 1.1. Grouping of second-line drugs recommended by WHO for use in longer MDR-TB regimens[97]

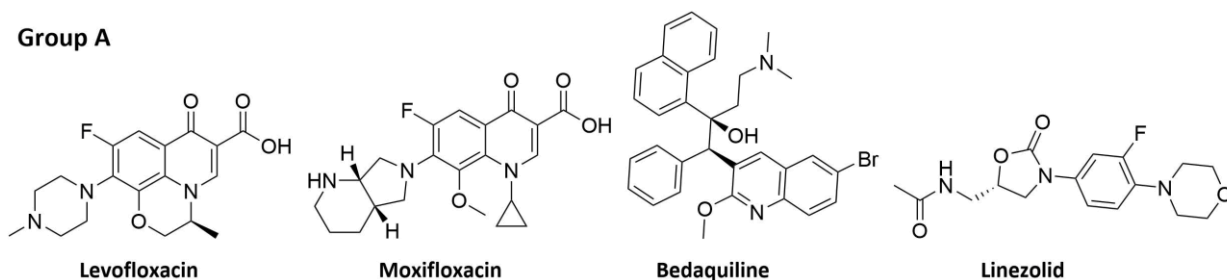| Group	Consideration	Medicines	Abbreviation
Group A	Include all 3 medicines	levofloxacin *OR* moxifloxacin	Lfx Mfx
		Bedaquiline	Bdq
		Linezolid	Lzd
Group B	Add 1 or both medicines	Clofazimine	Cfz
		cycloserine *OR* terizidone	Cs Trd
Group C	Add to complete the regimen and when medicines from Groups A and B cannot be used	Ethambutol	E
		Delamanid	Dlm
		Pyrazinamide	Z
		imipenem-cilastatin *OR* meropenem[a]	Ipm-Cln Mpm
		amikacin (*OR* streptomycin)	Am (S)
		ethionamide *OR* prothionamide[b]	Eto Pto
		p-aminosalicylic acid[b]	PAS

[a]Imipenem-cilastatin and meropenem are administered with clavulanic acid, which is available only in formulations combined with amoxicillin. Amoxicillin-clavulanic acid is not counted as an additional effective TB agent and should not be used without imipenem-cilastatin or meropenem.
[b]These agents showed effectiveness only in regimens without bedaquiline, linezolid, clofazimine, or delamanid, and are thus proposed only when other options to compose a regimen are not possible.
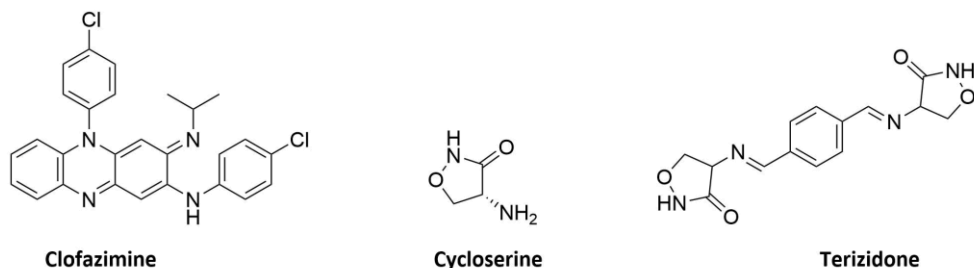
1.7.4.3   *Second-line drugs recommended for drug-resistant tuberculosis treatment.*

The chemical structures of the second-line drugs recommended by the current WHO guidelines for MDR-TB and XDR-TB treatment are shown in Figure 1.1010.

Group A

Levofloxacin Moxifloxacin Bedaquiline Linezolid

Group B

Clofazimine Cycloserine Terizidone

Group C

Delamanid Imipenem Meropenem

Amikacin Streptomycin

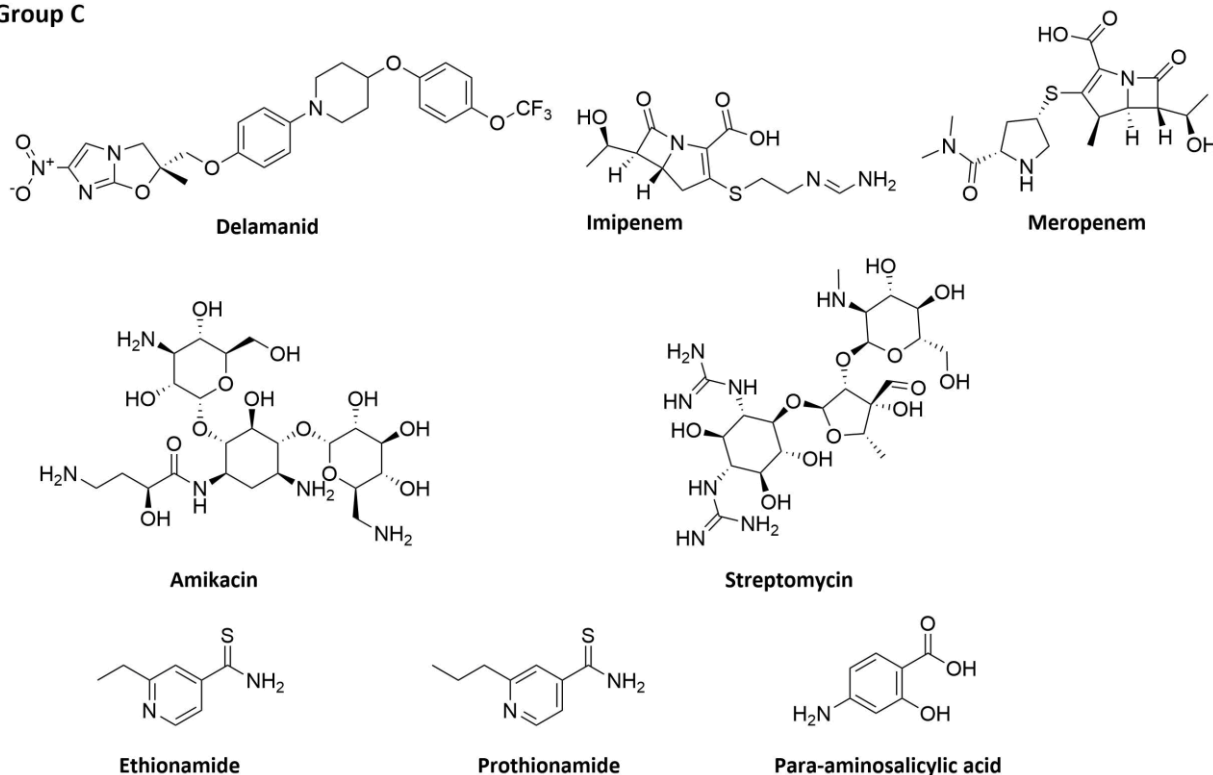Ethionamide Prothionamide Para-aminosalicylic acid

Figure 1.10. Chemical structures of the approved second-line anti-TB drugs.

Fluoroquinolones: levofloxacin (Lfx), moxifloxacin (Mfx)

Fluoroquinolones (FQs) are broad-spectrum antimicrobial agents. They are widely used for the treatment of bacterial infections of the respiratory, urinary and gastrointestinal tract and in sexually transmitted diseases.[104]

Levofloxacin and moxifloxacin, second-generation fluoroquinolones, are core drugs for the treatment of MDR-TB.[97] They demonstrate bactericidal and sterilizing activity.[105] Their cellular target in *M.*

tuberculosis is ATP-dependent topoisomerase II (DNA gyrase), an essential enzyme involved in the bacterial DNA replication, transcription and repair.[106,107]

Overall, these FQs demonstrate a good safety profile, their adverse effects (rashes dizziness, headache, gastrointestinal intolerance) are relatively infrequent, and the benefits of their administration outweigh potential risks.[107,108] Prolongation of the QT interval is a general feature of the fluoroquinolones; therefore, precaution should be taken, and patients should be monitored when they simultaneously receive other drugs with a QT prolongation risk (such as bedaquiline or clofazimine). Levofloxacin is less prone to QT prolongation. It is, therefore, the fluoroquinolone of choice in bedaquiline-containing regimens.[18]

Bedaquiline (Bdq)

Bedaquiline (commercial name Sirturo, previously TMC207) is a diarylquinoline that became the first drug in a novel class approved for TB treatment since rifampin's approval in 1971.[109] In December 2012 FDA granted it accelerated approval.[110] Currently, it is recommended by WHO as a core drug to be included in all longer MDR-TB regimens for patients aged 18 years for the first 6 months. Its longer administration should follow best practices in "off-label" use.[97] It is also a part of the novel all-oral shorter MDR-TB regimen.[100]

Bdq inhibits mycobacterial adenosine triphosphate (ATP) synthase, an essential membrane-bound enzyme, disrupting intracellular metabolism and interfering with energy production.[111–113] It kills both dormant and actively replicating mycobacteria. Bedaquiline selectively inhibits the ATP synthase in mycobacteria and does not interfere with mammalian ATP synthase activity.[109,114]

Among the most-pronounced side effects is moderate QTc prolongation, and additional care should be taken when administered with other drugs that possess similar effects (fluoroquinolones, clofazimine).[115]

Oxazolidinones: linezolid (Lzd)

Oxazolidinones represent a new class of synthetic antibacterial agents, active against a broad range of Gram-positive organisms and certain Gram-negative bacteria. They have shown highly promising antimycobacterial activities.

Oxazolidinones possess a novel mechanism of action and showed no cross-resistance with other antibiotics. They bind to 23S rRNA, targeting early-step translation by preventing the proper binding of formyl-methionine tRNA to the ribosome.[116] As protein synthesis inhibitors, they stop bacterial growth by disrupting protein production. Oxazolidinones were shown to be bacteriostatic agents, not bactericidal *in vitro*.

Linezolid (commercial name Zyvox) was the first-in-class oxazolidinone antibiotic to reach the market in 2000.[117] It was recently re-classified as a Group A drug by WHO for MDR-TB and XDR-TB.[97] Its administration for at least six months was shown to increase effectiveness, although toxicity may limit use.

Linezolid is often poorly tolerated because of the side effects of anemia/thrombocytopenia and peripheral neuropathy.[118,119] Several novel oxazolidinones are currently in different phases of preclinical and clinical development in the TB drug pipeline (Section 1.7.5).[120]

Clofazimine (Cfz)

Clofazimine, a riminophenazine, developed initially as an anti-TB drug but overlooked for decades, is the standard component of the WHO-recommended triple-drug regimen for the treatment of multibacillary leprosy.[121] Recently, it was repurposed for the treatment of MDR-TB, as it has shown sterilizing and treatment-shortening potential for MDR-TB treatment.[122,123] Currently it is included by WHO as a second-line agent of Group B.[97]

It was recently demonstrated that clofazimine has a unique mode of action among all antibiotics, including antimycobacterial agents. It inhibits mycobacterial integration host factor (mIHF), an essential nucleoid-associated protein in *M.tuberculosis,* and interferes with mycobacterial gene expression.[124] Another study showed that clofazimine inhibits human Kv 1.3 potassium channel by interfering with calcium signaling in T lymphocytes.[125]

Cfz side effect includes QTc prolongation together with skin and conjunctival pigmentation.[126]

Cycloserine (Cs), terizidone (Trd)

Cycloserine is an analogue of the amino acid d-alanine. It is a broad-spectrum bacteriostatic antibiotic that inhibits the growth of both Gram-positive and Gram-negative bacteria. It is an important second-line drug for MDR-TB treatment and currently classified as a Group B agent by WHO. [97]

Cycloserine inhibits alanine racemase (Alr) and d-alanine:d-alanine ligase (Ddl), which synthesizes the pentapeptide core using d-alanine. Both enzymes are crucial in the peptidoglycan synthesis, cell-wall biosynthesis and maintenance.[127] Cycloserine displays no cross-resistance with any other known antitubercular drugs.[128]

Severe toxicity has limited cycloserine use as it can elicit adverse psychiatric and nervous system reactions.[127,129] Terizidone, a structural analogue of cycloserine, can substitute the latter in the anti-TB therapy. It may be better tolerated, although also associated with neurologic and psychiatric disturbances, such as severe depression, anxiety, panic attacks, and psychosis.[129] Therefore, greater attention to MDR-TB patients' mental health should be devoted, and they should be informed on possible adverse drug reactions.

Delamanid (Dlm)

Delamanid (previously OPC-67683) is a novel drug of the dihydro-nitroimidazole class with potent anti-TB activity. It is an oral agent with bactericidal properties, currently classified in the Group C for MDR-TB treatment by WHO.[97]

Delamanid is a pro-drug that requires metabolic activation, mediated via the mycobacterial F420 coenzyme system.[130] It is thought to primarily inhibit the synthesis of primary components of the mycobacterial cell wall: methoxy-mycolic and keto-mycolic acids.[131] In contrast to isoniazid, delamanid does not inhibit alpha-mycolic acid. It also showed no action against gram-negative or gram-positive bacteria, which may be clinically advantageous as its use restriction to mycobacterial infection might help prevent the resistance generation.[132]

In general, delamanid is well tolerated, although showed mild QTc prolongation.[115,133]
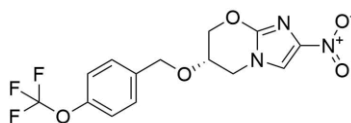
Pretomanid

Pretomanid (previously known as PA-824) is an oral nitroimidazooxazine antimycobacterial agent that possesses significant anti-TB activity and a unique mechanism of action (Figure 1.11). It is a potent

inhibitor of actively replicating and hypoxic, non-replicating, *M. tuberculosis*. The latter is particularly important for the development of new TB drugs.

Pretomanid is a pro-drug that possesses a very complex mechanism of action. Its activation within the target bacteria results in nitric oxide production, causing nonspecific damage of intracellular macromolecules, such as proteins and cell wall lipids.[134,135]

Pretomanid was administered as part of the BPaL (bedaquiline, pretomanid, and linezolid) and BPaMZ (bedaquiline, pretomanid, moxifloxacin, and pyrazinamide) regimens.[100] The Global Alliance for TB Drug Development (TB Alliance) developed PA-824 as an oral tablet formulation for the treatment of tuberculosis in combination with other anti-tuberculosis agents. It was approved for medical use in the USA in August 2019 and in the European Union in July 2020. The FAD approved it in the Nix-TB (BPaL) regimen for treatment of XDR-TB and or treatment-intolerant/non-responsive MDR-TB.

Figure 1.11. Chemical structure of Pretomanid.

Carbapenems: imipenem-cilastatin (Ipm-Cln), meropenem (Mpm)

Carbapenems imipenem and meropenem belong to the β-lactam antibiotics and possess a broad-spectrum activity against several clinically relevant, both aerobic and anaerobic, Gram-positive and Gram-negative bacteria.[136,137] They are used for MDR-TB and XDR-TB, despite the limited published evidence of their efficacy, safety, and tolerability.[138] They are classified as Group C drugs in the WHO's latest guidelines and included into the treatment regimen especially when the number of other recommended active drugs necessary to design an effective regimen is lacking.[97]

β-lactam antibiotics were previously considered ineffective against *M. tuberculosis* as they are rapidly hydrolyzed by the endogenous mycobacterial BlaC enzyme. However, it was shown that clavulanic acid is the only FDA-approved β-lactamase inhibitor that irreversibly inhibits BlaC, rendering *M. tuberculosis* susceptible to β-lactam antibiotics[139,140]

Carbapenems target L, D-transpeptidases, inhibiting peptidoglycan cross-linking in *M.tuberculosis*.[141] Both drugs are administered together with clavulanic acid, which is available only in formulations combined with amoxicillin. Amoxicillin–clavulanic acid is not counted as an additional effective TB agent and should not be used without imipenem-cilastatin or meropenem.[97] This drug combination is effective also against XDR-TB and kills both exponentially growing and dormant forms of the tubercle bacilli.[141]

The carbapenems are generally well-tolerated. Seizures are the most severe adverse effect, especially in the case of imipenem.[142]

Aminoglycosides (streptomycin, amikacin)

Streptomycin (S) and amikacin (Am) are both injectable aminoglycosides. They inhibit protein synthesis in *M. tuberculosis* by binding tightly to the conserved A site of 16S rRNA in the 30S ribosomal subunit.[143,144]

Streptomycin is the first-in-class aminoglycoside antibiotic identified (Section 1.7.1). Although it is no longer used routinely due to its high resistance probability, it can still be used to substitute amikacin when the latter is not available, or there is a confirmed resistance to it.[85] The latest WHO guidelines do not recommend unnecessary exposure of patients with DS-TB because of its significant toxicity.[64] The related drugs kanamycin and capreomycin and are no longer recommended for MDR-TB regimens.[97]

All aminoglycosides may affect the eighth cranial nerve resulting in hearing loss, loss of balance, or both.[145] Moreover, neurotoxicity (muscle paralysis and apnea) and nephrotoxicity have been observed together with milder side effects such as rashes, headache, nausea.[143,144]

Thioamides: ethionamide (Eto), prothionamide (Pto)

Thioamide drugs ethionamide and prothionamide are clinically effective in the treatment of mycobacterial infections, caused by *M. tuberculosis*, *M. avium,* and *M. leprae*. Both drugs are bactericidal, currently included in Group C of the longer MDR-TB treatment recommended by WHO and used interchangeably.[97]

Both thioamides are structurally similar to isoniazid and inhibit cell-wall mycolic acid biosynthesis. They were shown to form covalent adducts with nicotinamide adenine dinucleotide (NAD) which are tight-binding inhibitors of the inhA gene product enoyl-ACP reductase.[146]

Prothionamide and ethionamide may be included in the treatment of MDR-TB patients on longer regimens given that bedaquiline, linezolid, clofazimine, or delamanid are not used or if better options to compose a regimen are not possible.[97] They are usually contraindicated during pregnancy.

The most common adverse reactions are dose-related gastrointestinal disturbances, such as nausea and vomiting. Hypothyroidism, drug-induced hepatitis, or pancreatitis are among other side effects.[147,148]

P-aminosalicylic acid (PAS)

Para-aminosalicylic acid was one of the first agents found in the 1940s to be effective against tuberculosis but was later on replaced by more efficient ethambutol for the first-line TB treatment in early 1960.[149,150] PAS is a bacteriostatic agent, currently included into Group C for the MDR-TB treatment regiments recommended by WHO.[97]

Its exact mode of action remained elusive and largely speculative for a long time. In 2013 it was shown by Zheng et al. that *para*-aminosalicylic acid is a pro-drug, ultimately targeting dihydrofolate reductase (DHFR) through an unusual and novel mechanism of action by incorporation into the folate pathway by dihydropteroate synthase (DHPS) and dihydrofolate synthase (DHFS) to generate a hydroxyl dihydrofolate antimetabolite, which in turn inhibits DHFR enzymatic activity.[151]

Para-aminosalicylic acid may be included in the treatment of MDR/RR-TB patients on longer regimens only if bedaquiline, linezolid, clofazimine, or delamanid are not used or if better options to compose a regimen are not possible.[97]

PAS is quite poorly tolerated due to its gastrointestinal toxicity, leading to reduced compliance.

_____

1.7.5 Perspective: drugs in clinical development

The last few years have been transformative for the TB-treatment as several compounds from new classes (i.e., that have new targets and/or novel mechanisms of action) or with advantageous properties are advancing through the drug development pipeline (Figure 1.122, Table 1.2).[152]

Those new TB drugs work by inhibiting four processes: energy production, cell wall synthesis, protein synthesis, and DNA synthesis (Table 1.2). The interruption of these processes affects the TB bacteria's ability to survive and/or replicate, making them the key targets for anti-tuberculosis drug development.

Table 1.2. Anti-TB drugs in the pipeline (clinical phases I-IV).[152]

Drug	Class	Mechanism of action	Phase
Energy Production			
bedaquiline[a]	diarylquinoline	Inhibits ATP synthase and bacterial respiration	III
pyrifazimine (TBI-166)	riminophenazine	Inhibits ion transport and bacterial respiration	I
telacebec (Q203)	imidazopyridine	Inhibits ATP synthesis (QcrB) and bacterial respiration	IIa
Cell Wall Synthesis			
delamanid[b]	nitroimidazole	Inhibits cell wall synthesis and bacterial respiration	IV
pretomanid[c]	nitroimidazole	Inhibits cell wall synthesis and bacterial respiration	III
BTZ-043	benzothiazinone	Inhibits cell wall synthesis (DprE1)	Ib/IIa
macozinone (PBTZ169)	benzothiazinone	Inhibits cell wall synthesis (DprE1)	Ib
OPC-167832	carbostyril	Inhibits cell wall synthesis (DprE1)	Ib/IIa
TBA-7371	azaindole	Inhibits cell wall synthesis (DprE1)	Ia/Ib
SQ109	1,2-ethylene diamine	Inhibits cell wall synthesis (MmpL3)	IIb
Protein Synthesis			
contezolid acefosamil (MRX-4)	oxazolidinone	Inhibits protein synthesis (23S ribosome)	II
delpazolid (LCB01-0371)	oxazolidinone	Inhibits protein synthesis (23S ribosome)	IIa
sutezolid (PNU-100480)	oxazolidinone	Inhibits protein synthesis (23S ribosome)	IIb
TBI-223	oxazolidinone	Inhibits protein synthesis (23S ribosome)	Ia
GSK3036656 (GSK-656)	oxaborole	Inhibits protein synthesis (LeuRS)	IIa
DNA Synthesis			
SPR720	benzimidazole	Inhibits bacterial DNA synthesis (GyrB)	Ia/Ib

[a]Bedaquiline is recommended by the latest WHO guidelines as a core drug to be included in all longer MDR-TB regimens (Group A).[97] [b]Delamanid is currently classified in the Group C for MDR-TB treatment by the latest WHO guidelines.[97] [c]Pretomanid was approved by the FDA in the Nix-TB regimen for treatment of XDR-TB and or treatment-intolerant/non-responsive MDR-TB.
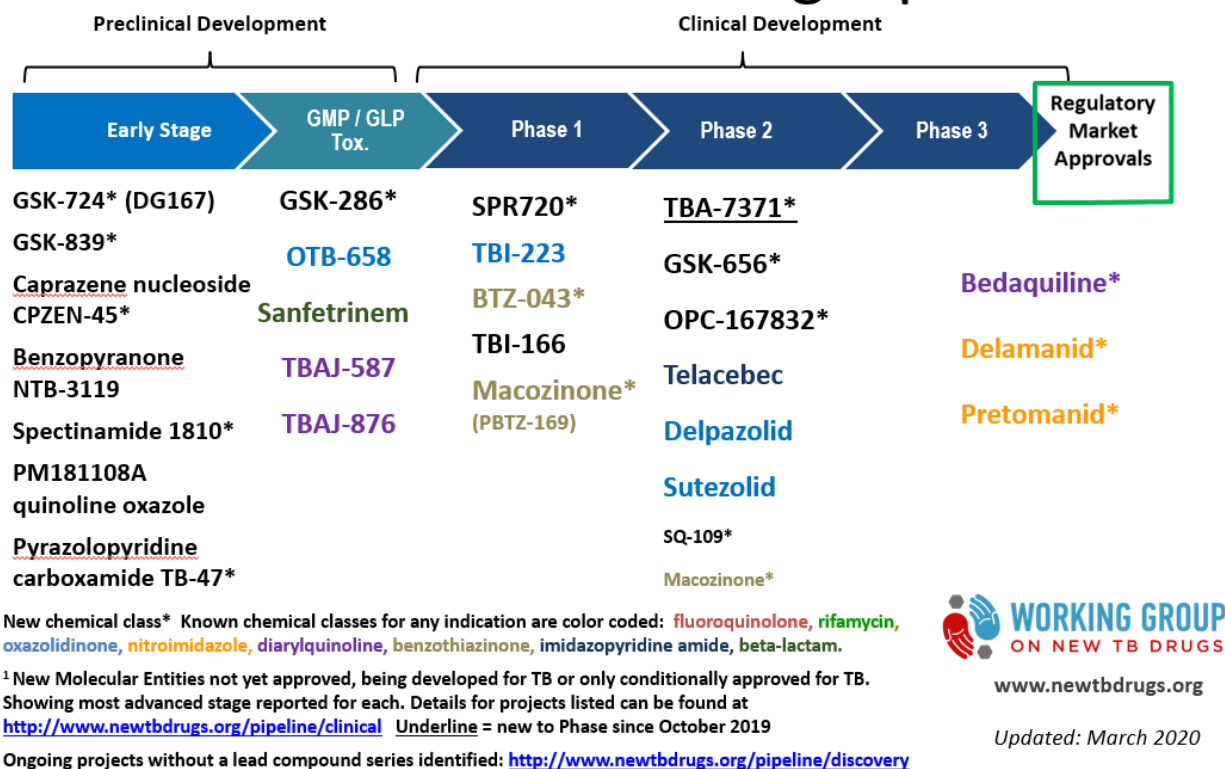
_____

2020 Global New TB Drug Pipeline [1]

Preclinical Development   **Clinical Development**

Early Stage	GMP / GLP Tox.	Phase 1	Phase 2	Phase 3	Regulatory Market Approvals

GSK-724* (DG167)

GSK-839*

Caprazene nucleoside **CPZEN-45***

Benzopyranone NTB-3119

Spectinamide 1810*

PM181108A quinoline oxazole

Pyrazolopyridine carboxamide TB-47*

GSK-286*

OTB-658

Sanfetrinem

TBAJ-587

TBAJ-876

SPR720*

TBI-223

BTZ-043*

TBI-166

Macozinone* (PBTZ-169)

TBA-7371*

GSK-656*

OPC-167832*

Telacebec

Delpazolid

Sutezolid

SQ-109*

Macozinone*

Bedaquiline*

Delamanid*

Pretomanid*

WORKING GROUP ON NEW TB DRUGS

www.newtbdrugs.org

Updated: March 2020

New chemical class* Known chemical classes for any indication are color coded: fluoroquinolone, rifamycin, oxazolidinone, nitroimidazole, diarylquinoline, benzothiazinone, imidazopyridine amide, beta-lactam.

[1] New Molecular Entities not yet approved, being developed for TB or only conditionally approved for TB. Showing most advanced stage reported for each. Details for projects listed can be found at http://www.newtbdrugs.org/pipeline/clinical Underline = new to Phase since October 2019

Ongoing projects without a lead compound series identified: http://www.newtbdrugs.org/pipeline/discovery

Figure 1.12. New anti-TB drugs in the pipeline: https://www.newtbdrugs.org/pipeline/clinical (accessed May 21, 2020).[153]

Results from a landmark study on the treatment of drug-susceptible TB were presented at the 51st virtual Union World Conference on Lung Health in October 2020. One of the key findings from the study was that the four-month regimen which included a combination of high-dose rifapentine, isoniazid, pyrazinamide and moxifloxacin, was shown to be non-inferior in terms of efficacy to the currently recommended six-month regimen, plus safe and well-tolerated by patients.[154]

1.7.6 Challenges and unmet treatment needs

Effective chemotherapy options together with declining incidence rates influenced the general perception of tuberculosis as a treatable disease of low significance.[155] Nonetheless, according to the World Health Organization (WHO), tuberculosis remains among the top 10 causes of death worldwide, and it still is the leading cause of death from a single infectious agent.[6]

For decades, the drug development process for novel anti-TB medicines remained stagnant. Sudden progress was achieved during the last 10 years, resulting in highly promising drugs, including bedaquiline, delamanid, and pretomanid (Sections 1.7.4.3, 1.7.5).

Many issues contribute to TB persistence, among which absence of shorter treatments, drug costs, and side effects, the rapid emergence of drug resistance (Section 1.7.6.1), HIV co-infection (Section 1.7.6.2), treatment of latent infection (Section 1.7.6.4), global mobility together with poor infection control.

Therefore, the development of new antimycobacterial drugs remains a pressing need. New antimycobacterials should preferably have novel modes of action, good safety profile, show no cross-

resistance with current therapies, be effective in the management of MDR and XDR TB. The new treatment regimens should be shorter, safer, and cheaper.

1.7.6.1 Development of drug-resistant TB

Tuberculosis drug resistance has remained a major concern. Lengthy regimens, coupled with pronounced side effects, are the primary causes of poor patient compliance. Failure to complete the prescribed adequate chemotherapy course, in many cases, leads to disease relapse. This requires re-treatment of patients, accelerating the emergence of drug-resistant strains of mycobacteria.

Solely in 2018, about half a million people developed tuberculosis resistant to rifampicin (RR-TB), the most effective first-line anti-TB drug.[6] Multidrug-resistant TB (MDR-TB), defined as *M. Tuberculosis* with demonstrated resistance to at least rifampicin and isoniazid, represented 78% of these cases.

Extensively drug-resistant tuberculosis (XDR-TB) is a sub-type of MDR-TB that is resistant to at least four of the core anti-TB drugs: first-line isoniazid and rifampicin, any of the fluoroquinolones (levofloxacin or moxifloxacin) alongside at least one of the three injectable second-line drugs (amikacin, capreomycin or kanamycin). Its remaining treatment options are relatively limited, less effective, cause more pronounced side effects and higher costs.

The WHO has issued guidelines on drug-resistant tuberculosis treatment since 1997 with the latest consolidated guidelines published in 2019.[97]

1.7.6.2 Treatment of tuberculosis and HIV co-infection

Tuberculosis is the most common opportunistic disease in patients infected with the human immunodeficiency virus (HIV). Treatment of drug-susceptible tuberculosis (DS-TB) for such patients is complicated due to high pill burden, drug-drug interactions (DDIs), programmatic challenges, and elevated cost.

Fortunately, the cure rate for HIV-positive patients on antiretroviral therapy (ART) is similar to that of non-HIV-infected ones.[62,156] For HIV-seropositive individuals not receiving ART at the time of the tuberculosis diagnosis, it is recommended to start ART early.

Co-administration of antitubercular and antiretroviral agents is associated with three major complications.[70,83] First, their overlapping toxicities occur frequently, which increases the risk of nonadherence and may require discontinuation of therapy.

Second, rifampicin has DDIs with many ART drugs owing to its induction of the cytochrome P450 family of enzymes and P-glycoprotein. It results in reduced concentrations of nonnucleoside reverse-transcriptase inhibitors (NNRTIs) and, particularly, protease inhibitors that may potentially lead to the loss of antiviral efficacy and the development of viral resistance. Rifabutin should be considered as its substitute as it is a less potent inducer of cytochrome P450 enzymes and does not significantly affect the concentrations of antiretroviral agents.[62] Moreover, an extended 7-month continuation phase should be prescribed for individuals not on ART due to recurrence and reinfection risks.[157,158]

Third, immunopathological reactions, termed "*Immune Reconstitution Inflammatory Syndrome*" (IRIS), occur frequently when antiretroviral therapy is initiated in patients co-infected with tuberculosis. Nonetheless, several randomized clinical trials demonstrated that in case ART therapy initiation is postponed, a higher mortality rate in many cases due IRIS.[159–161]

1.7.6.3 Extrapulmonary tuberculosis

The chemotherapy treatment regimens for extrapulmonary tuberculosis do not differ significantly from standard pulmonary treatment.[62] There is no difference in the intensive phase for DS-TB. The continuation phase is extended to 6-9 months if considered necessary.

Meningitis is an exception as the therapy should be extended to at least 7 months due to the suboptimal blood-brain barrier (BBB) penetration and drug accumulation coupled with a high risk of relapse. In addition, corticosteroids should be administered upfront for 6 to 8 weeks.[162]

Response to treatment should be followed on radiologic and clinical findings rather than repeat specimen sampling unless there is a concurrent pulmonary disease.[62]

1.7.6.4 Latent tuberculosis infection (LTBI)

Latent tuberculosis infection is defined by the presence of detectable immune responses to *M. tuberculosis* antigens in the absence of clinical evidence of active TB disease.[163] Approximately 1.7 billion individuals globally were estimated to have LTBI in 2014, almost one-quarter of the world population.[164] Therefore, LTBI screening and treatment are essential components of overall tuberculosis control and elimination efforts.[163,165]

Currently, there are four main antimicrobial regimens available for LTBI treatment: isoniazid monotherapy, rifampin monotherapy, combinations of isoniazid plus rifampin or rifapentine.[165] Isoniazid monotherapy is efficacious in preventing progression to TB disease in approx. 90% of cases, but its prolonged duration and hepatotoxicity cause low adherence and completion rates.[166,167] Rifampin and rifapentine-containing regimens are shorter, possess similar efficacy, and are increasingly used. They are associated with higher completion rates and reduced risk of hepatotoxicity compared with isoniazid monotherapy.[165,168] Notably, no increased risk of isoniazid-resistant or rifamycin-resistant TB disease development after receiving preventive LTBI treatments containing these drugs has been demonstrated.[169,170]

1.8 Aims of the presented research

Recent advances in the TB-drug pipeline give hope for the development of more advanced treatment regiments (Section 1.7.5). Nonetheless, there is a continuing need to discover new anti-TB agents with novel mechanism of actions to overcome emerging resistance and improve treatment outcomes, especially in case of HIV-coinfection and latent infection (Section 1.7.6).

The presented research was performed as part of the OpenMedChem project, funded by Marie Curie Initial Training Networks. The OpenMedChem project comprises collaboration between a major industrial Research&Development (R&D) unit of GlaxoSmithKline (GSK I+D, Madrid, Spain) and academia (University of Antwerp, Belgium).

The performed investigation was focused on two projects:

1. Investigation of a library of *Mtb* DHFR inhibitors, identified in a phenotypic HTS campaign (described in detail in Chapters 2-3)
2. SAR exploration of a novel hydantoin family of DprE1 inhibitors (described in detail in Chapters 4-7).

_____

Based on the analysis of the GSK HTS campaign results (Sections 2.1-2.2), several representatives based on dihydro-2,4-diamino-1,3,5-triazine scaffold were identified as potential *Mtb* DHFR inhibitors. The main objectives of this project were:

1. Determination if the identified hits were inhibitors of *Mtb* DHFR
2. SAR exploration around the initial hits, including scaffold-hopping on the dihydrotriazine core
3. Evaluation of cytotoxicity and physicochemical parameters of synthesized compounds
4. Identification of more potent inhibitors with optimized cytotoxicity and physicochemical profile

A literature overview of the DHFR enzyme in *M. tuberculosis* and its known inhibitors is presented in Section 2.3. Chapter 3 describes the design and synthesis of analogues of the initial hits, including the scaffold hopping approach, together with the biological evaluation of all synthesized compounds.

A novel hydantoin-based family of antimycobacterials was discovered as a promising hit series in the target-based HTS for DprE1 inhibitors performed by GSK (Chapter 4). The main objectives of this project are described in detail in the Section 4.4 and included:

1. SAR exploration around the initial hits to obtain higher potency and enzyme affinity
2. Removal of potential liabilities and safety evaluation of the series
3. *In vivo* proof of concept

The two rounds of Hit-to-Lead optimization are reported in Chapters 5 and 6 and the further biological evaluation is described in Chapter 7.

2. Mtb DHFR inhibitors: scaffold selection and project objectives

2.1 Whole-cell HTS performed by GSK

GlaxoSmithKline (GSK) performed an antimycobacterial whole-cell phenotypic high throughput screening (HTS) campaign against *Mycobacterium bovis* BCG with hit confirmation in the *M. tuberculosis* H37Rv strain. The results were made publicly accessible by GSK in 2013 and provided many potential new starting points for synthetic lead-generation activities.[171]

Mycobacterium bovis and *Mycobacterium tuberculosis* are closely related pathogens, responsible for bovine and human tuberculosis, respectively. The *M. bovis* BCG genome vis > 99% identical to that of the *M. tuberculosis* H37Rv strain.[172] However, distinct phenotypes, virulence and host tropism differentiate both pathogens.[17] The high genome sequence homology and the lack of species-specific genes for *M. bovis,* suggest that distinctive mechanisms of gene expression might be involved in determining the differences among these bacilli.

M. bovis BCG was employed as a surrogate for *M. tuberculosis* for first-line screening purposes, being much safer to manipulate (possible within a biosafety level (BSL) 2 environment) than the virulent *Mtb* strains (infectious, BSL 3). Nevertheless, conducting primary screens using model mycobacterial species could limit the potential for identifying new inhibitors with efficacy against *M. tuberculosis*.[173]

For that reason, a subset of ~$2\cdot10^4$ compounds from the GSK compound collection was selected in order to assess the predictive value of BCG as an *M. tuberculosis* surrogate.[171] The included compounds possessed good cell membrane permeability as well as other properties that fall clearly into the predefined drug-like parameters.[174] Based on the obtained results, the BCG surrogate was considered as a feasible compromise for detecting H37Rv inhibitors.[171] Nevertheless, the outcome also suggested that any BCG-based screening campaign is bound to generate a significant number of BCG-specific compounds that, although interesting for the basic understanding of mycobacterial biology, would not prove useful for anti-tuberculosis drug discovery.

More than 2 million entities from the GSK corporate compound collection were evaluated in the initial HTS BCG screening. The primary hit list was subsequently narrowed down by the application of several similarity and physicochemical property filters. As a general observation, most TB drugs and antibacterials do not follow Lipinski's "rule of 5", which is typically used to define optimal drug-like features.[68] The screening hits and certain drugs often possess higher lipophilicity, which favors better permeability through the highly lipophilic mycobacterial cell wall. This factor accounted for using the relatively large cut-off values for the trimming of the initial hit list. An overall workflow, depicted in Figure 2.1, was established by GSK and included the following considerations and parameters:

- Calculated logP < 6 and MW < 600 Da
- > 90% Inhibition of BCG at 10 μM
- Known antibacterials discarded (in search of new chemical diversity)
- Structures containing reactive functional groups eliminated
- Therapeutic index T.I.= (IC$_{50}$ HepG2)/(IC$_{50}$ BCG) > 50

The obtained subset of 960 compounds was progressed to subsequent MIC determination against *Mtb* H37Rv under standard 7H9 medium growth conditions. A threshold application of H37Rv MIC < 10 μM

and a therapeutic index (T.I., calculated as (IC_{50}(HepG2)/MIC) > 50 resulted in 177 positives, among which GSK initially marked out 7 active chemical families (Figure 2.1).[171]
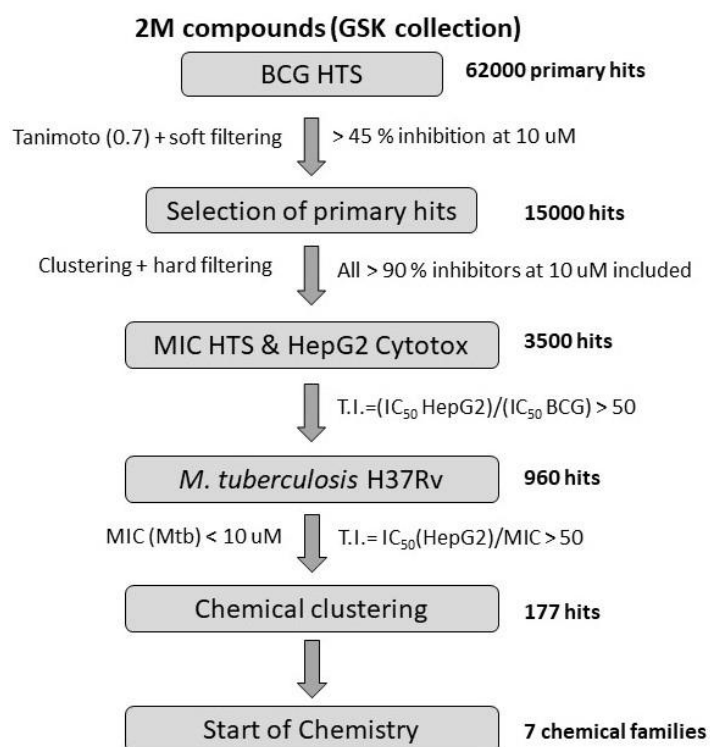
Figure 2.1 The whole-cell phenotypic HTS progression cascade: filter workflow details. Adapted from Ballell *et al.*[171]

2.2 OpenMedChem project: cluster selection
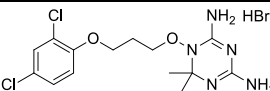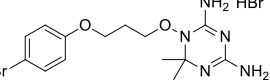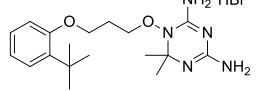
Access to these screening results was provided (in advance of their subsequent publication) within the framework of the FP7 ITN project OpenMedChem. All compound design and synthesis were performed within the OpenMedChem project, while the biological evaluation was performed by GSK representatives. The thesis covers part of these endeavors.

At the OpenMedChem project onset, a further examination of the 960 compound subset was performed. Compound clustering was carried out using visual comparison and the molecular modeling and bioinformatics package MOE[175], delivering several highly potent structural families and some representatives deprioritized in the initial screen.[171] In addition, an extensive literature overview was performed to collect data on prior reports of the selected clusters, their related structures, and potential targets (if determined).

Dihydro-2,4-diamino-1,3,5-triazine derivatives were found to be one of the promising chemical families and were therefore selected for further investigation. An analogue search revealed a total of 8 analogues in the narrowed-down library. The three most active compounds (Table 2.1) showed very promising whole-cell inhibition in the H37Rv strain. The number of representatives in the cluster was not sufficient to make reliable SAR conclusions concerning the *Mtb* inhibition efficiency.

GSK had previously performed in antifolate drug discovery focused on antimalarials, developing a large antifolate chemical space, to which those analogues probably belong.[176] Later on, a separate research on a dedicated GSK Antifolate Library preparation and screening was published by Kumar *et. al* in 2016 (see Section 2.4 for more details).[177] The reference compounds presented herein (Table 2.1) were discussed as well.

Table 2.1 Dihydro-2,4-diamino-1,3,5-triazine initial hits and their biological activity

Structure		MIC (μM)[a]
2.1		1.3
2.2		16
2.3		0.6
[a] MIC [μM] against Mycobacterium tuberculosis (H37Rv). Reference: Isoniazid, MIC = 1.8 μM		

For organizational purposes, the initial hit structure was formally divided into three main parts: the "core," "linker," and "aryl" regions (Figure 2.2). All representatives had two methyl substituents in the core and identical linker lengths. Their structures differed solely by the aryl substitution pattern. The limited structural diversity of the identified hits may be rooted in (1) the initial absence of structurally related compounds inside the tested GSK library or, alternatively, (2) the inactivity in the performed assays of other structural congeners present among the screened molecules.
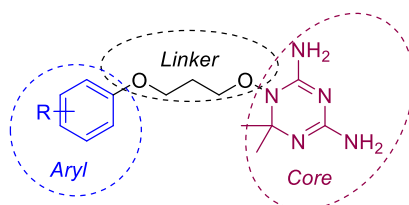
In magenta: heterocyclic core, in blue: aryl substituent, in black: linker

Figure 2.2. General cluster structure

All the initial hits possessed in their structure the 1,6-dihydro-1,3,5-triazine-2,4-diamine core. This structural fragment was previously demonstrated to be capable of dihydrofolate reductase (DHFR) inhibition in different organisms.[178–184] This finding led to the hypothesis that the series' mode of action in mycobacteria could involve inhibition of *Mtb* DHFR.

2.3   DHFR as a drug target in *M. tuberculosis*

Dihydrofolate reductase (DHFR) is a well-validated and clinically important drug target for over 50 years. It is an essential enzyme involved in the metabolism of folic acid, ubiquitously expressed in all living organisms. It catalyzes the NADPH-dependent reduction of dihydrofolate (DHF) to tetrahydrofolate (THF) as shown in Figure 2.3. The latter is the primary carrier of one-carbon units necessary for the biosynthesis of thymidine monophosphate (dTMP), nucleotides (purine and pyrimidine), and amino acids (methionine, serine, and glycine) that are required for RNA, DNA, and

protein synthesis.[185–187] Inhibition of DHFR activity leads to the arrest of DNA synthesis and, eventually, cell death.

Inhibition of human DHFR is essential to the action of antifolate medications used to treat cancer and some inflammatory diseases.[188–191] Methotrexate (MTX) is used in combinational therapy for cancer treatment as an anti-inflammatory and immunosuppressive agent (Figure 2.4).[192,193] Selective DHFR inhibitors are the basis of some antibacterial and antiparasitic (such as toxoplasmosis and malaria) therapies.[191,194–197] Pyrimethamine (PYR) and trimethoprim (TMP) are potent inhibitors of protozoal and bacterial DHFRs, respectively, being weak inhibitors of mammalian DHFRs (Figure 2.4).
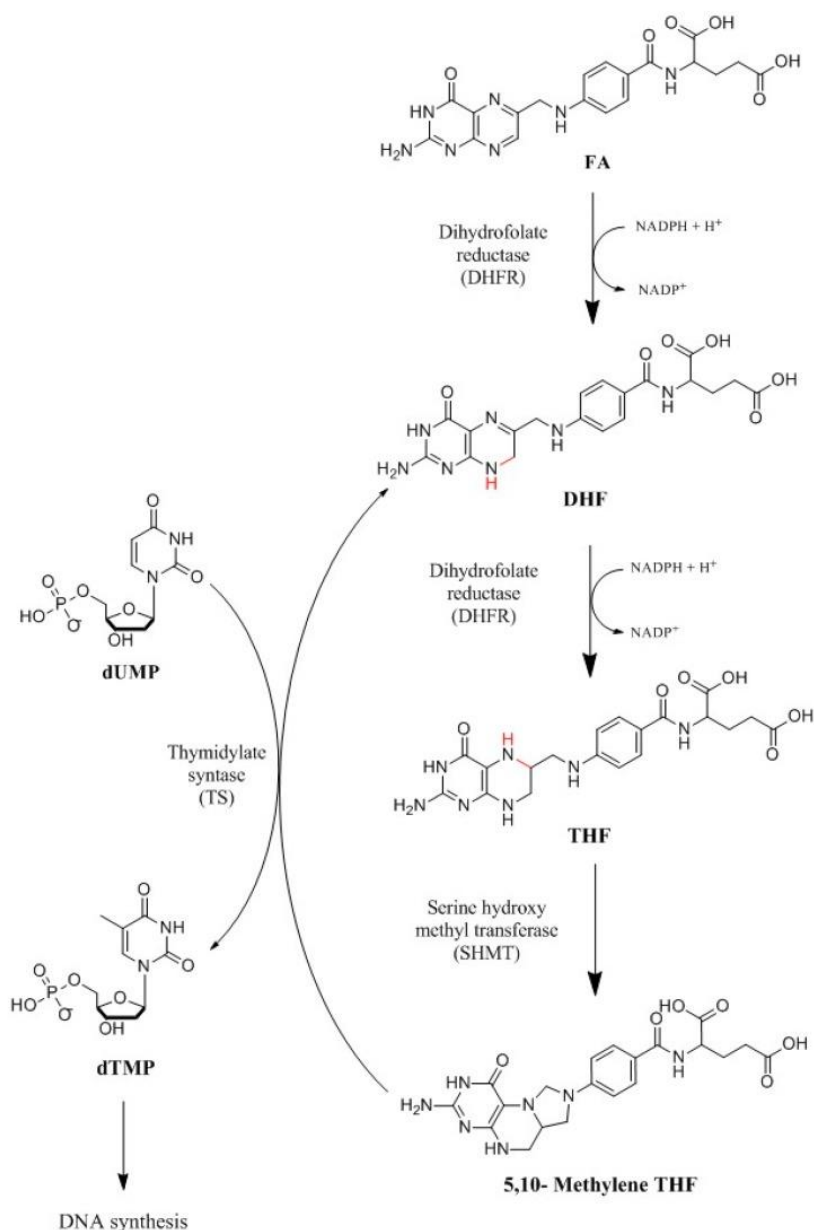
Figure 2.3. Synthetic pathway of folate metabolism. DHFR catalyses the passage of a hydride from the cofactor NADPH, used as an electron donor, to dihydrofolate (DHF), through a protonation to produce tetrahydrofolate (THF). DHFR couples with thymidylate synthase (TS), which catalyses the reductive methylation of deoxyuridine monophosphate (dUMP) in deoxythymidine monophosphate (dTMP) 5,10-Methylene THF as a cofactor. Adopted from the publication by Raimondi MV, et al., 2019[198]
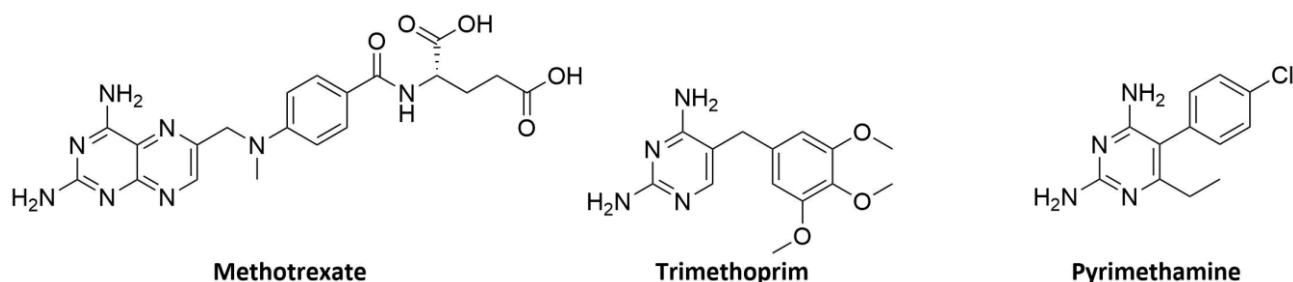
Figure 2.4. Clinically approved antifolates

One approach to identifying new lead compounds is to exploit recognized drug targets that are not currently used in existing treatment regimens. Meanwhile, dihydrofolate reductase has several potential advantages as a drug target for *M.tuberculosis*:

- the biochemistry of the folate pathway and the DHFR enzyme, in particular, are well characterized
- due to a long history of different DHFR inhibitors usage, their safety and selectivity inhibitors have been intensively studied
- compounds selective against microbial DHFR over the human one have been identified already[191,199]

High species selectivity, essential to avoid undesired side effects and toxicity, especially those associated with the typical long duration of anti-TB therapies, is among the challenges connected to the development of novel DHFR inhibitors. Mycobacterial cell wall permeability is another pitfall that should not be underestimated as it may prevent compounds, otherwise active and selective against *Mtb* DHFR enzyme from killing tubercle bacilli.

Although the folate pathway has effectively been exploited to treat various diseases, antifolates are not currently used in tuberculosis's recommended treatment regimens. Some clinically approved antifolates such as pyrimethamine, trimethoprim, and methotrexate inhibit *Mtb* DHFR enzyme *in vitro* but do not affect the growth of live M.tuberculosis bacilli efficiently.[200,201] Methotrexate binds to both human DHFR and *Mtb* DHFR without pronounced selectivity. It was recently shown that *para*-aminosalicylic acid, a second-line anti-TB agent, is a prodrug activated by the folate pathway and possibly inhibiting DHRF (see Section 1.6.4.3 for more details).[151]

Several DHFR inhibitors showed reasonable efficacy against other mycobacteria. In particular, the experimental antimalarial compound WR99210 with reported DHFR activity was shown to inhibit *Mycobacterium avium* growth both *in vitro* and in animal models.[183,184,202,203] PS-15, the biguanide precursor of WR99210, was demonstrated to convert *in vivo* into the active triazine form.[202] It substantially improved the bioavailability, problematic in the case of WR99210, and gave another chance to this compound series.

A number of published studies focused on the preparation of analogues of known DHFR inhibitors by exploiting differences in human and *M.tuberculosis* enzyme structures to gain selectivity and activity against TB.[204–208] Analysis of the crystal structures of MTX binding human and *M. tuberculosis* DHFR indicated that a glycerol molecule binds in a pocket of the *Mtb* DHFR:MTX complex, while in the human enzyme this pocket is filled with hydrophobic side-chains. This glycerol binding site is a relatively small pocket, located very close to the dihydrofolate binding site so that it might be treated as its extension.

It was assumed that the glycerol binding site, why not essential for *Mtb* DHFR enzyme activity, could be critical for developing new inhibitors that specifically bind to *M. tuberculosis* DHFR.

Bromo-WR99210 was shown to bind to the active site of *Mtb* DHFR (Figure 2.6).[205] WR99210 and several of its analogues showed the reasonable *in vitro* activity against *M. tuberculosis* using a genetically modified *Saccharomyces cerevisiae* strain.[206] El-Hamamsy, M. *et al.* reported the design and synthesis of a compound family with glycerol-like side chains, including El-7a, that showed notable selectivity for inhibition of *Mtb* DHFR against human one in the assay based on TB5 *Saccharomyces cerevisiae* carrying the DHFR genes from *M. tuberculosis* and human (Figure 2.6).[207] It is worth noting that no direct evidence that WR99210 or El-7a can inhibit *M. tuberculosis* bacilli's growth was provided in those studies as no experimentation was done on the living cells.

In 2016, Kumar A. et al. reported the preparation of the GSK Antifolate Library of 2508 compounds with its subsequent screening against the *M. tuberculosis* H37Rv strain (Figure 2.5).[209] The 17 hit compounds that could be divided into five subgroups based on their chemotype were identified. It was concluded that due to their poor selectivity, toxicity, or DMPK profiles, none of the hit was suitable for further progression, but they could become a valuable starting points for subsequent chemical modifications and optimization. The described study was published subsequently to the research reported in this thesis.
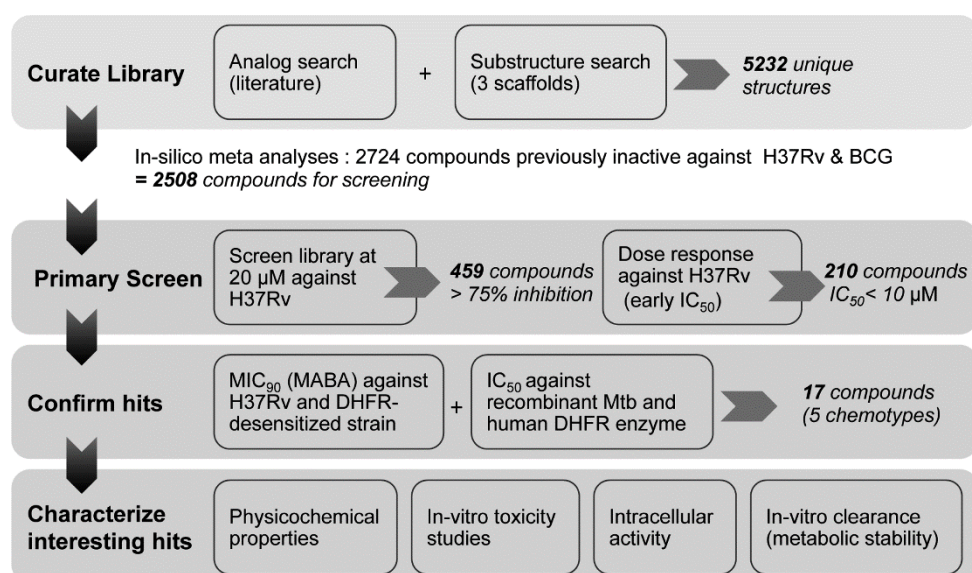
Figure 2.5. Flowchart of the GSK Antifolate Library screening. Adopted from the publication by Kumar et al., 2016[209]

Several molecular modeling and virtual screening studies of potential *Mtb* DHFR inhibitors were published.[208,210–213] A modeling study by Hong, W. *et al.* suggested that hydrophilic side groups could, in fact, occupy the crucial glycerol site in *Mtb* DHFR.[208] It should be stressed that novel compounds with hydrophilic side groups capable of specific inhibition of *Mtb* DHFR might not be able to cross the mycobacterial cell wall efficiently to act on *M.tuberculosis* whole cells.

Wang N. *et al.* performed a virtual screening followed by the *in vitro* evaluation, where compound G3 showed activity against *M.tuberculosis* H37Rv strain (Figure 2.6).[210] In 2019, Sharma K. *et al.* reported synthesis and optimization of new chemical series with compound KC-11 to be the most potent analogue with in vitro activity against *M.tuberculosis* H37Rv strain and >18-fold selectivity towards *Mtb* DHFR over the human enzyme (Figure 2.6).[214] Ribeiro, J. *et al.* has recently reported the application of

fragment-based drug discovery (FBDD) approach to the Mtb DHFR and a series of compounds with completely novel scaffolds that bind in non-explored regions of the enzyme active site.[215,216]
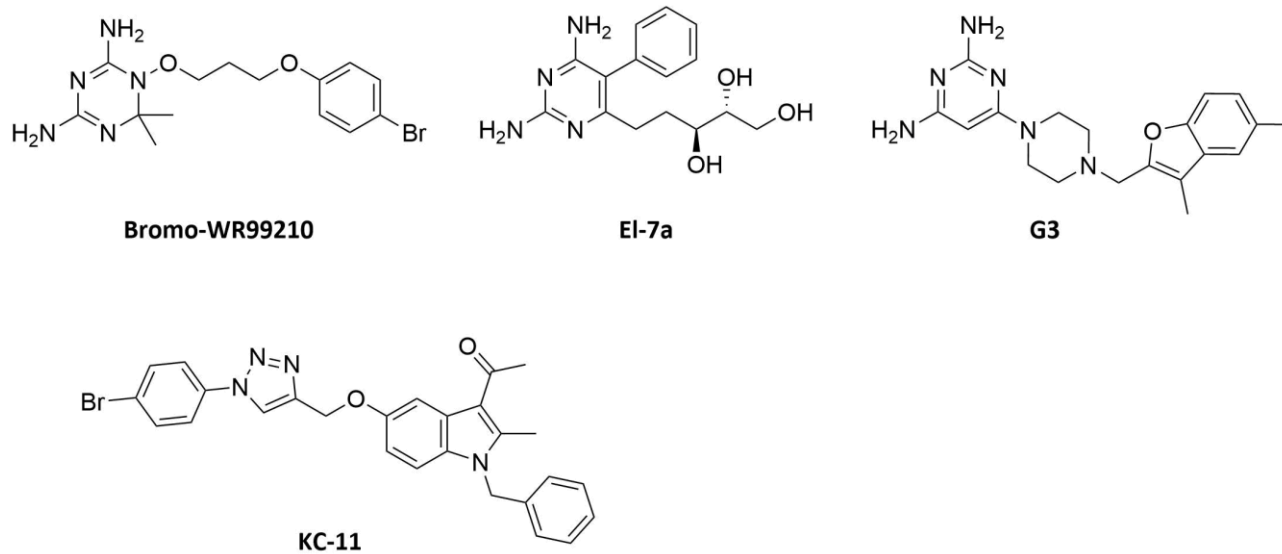
Figure 2.6 Representative compounds with reported Mtb DHFR activity.

35

_____

3. Mtb DHFR inhibitor analogues: synthesis and evaluation

3.1 Compound design and synthesis

This chapter is dedicated to the synthesis and biological evaluation of dihydrotriazines and related compounds in search of novel *Mtb* DHFR inhibitors. The compound design was based on the initial hits **2.1**-**2.3**, identified by analysis of the phenotypic HTS performed by GSK.[171] The performed modifications, described herein, include:

- Preparation of direct analogues of the initial hits **2.1-2.3**
- Scaffold hopping approach
  - Introduction of different heterocyclic scaffolds
  - Aryl substitution variation
  - Alternations in the inker length and nature

In total, 24 analogues were synthesized and evaluated within this DHFR inhibitor research project.

3.1.1 Dihydrotriazines: synthesis of direct analogues

In the beginning, our attention was concentrated on the direct analogue synthesis of the initial hits **2.1-2.3**, preserving the partially saturated dihydrotriazine core. The published data concerning the dihydrotriazine core synthesis were found to be scarce and not reproducible.[203,217–219]

Final products **2.1a** and **2.2a** are hydrochloride analogues of the original hits **2.1** and **2.2** respectively. They were resynthesized using procedures reported in the literature (Figure 3.1).[219,220]
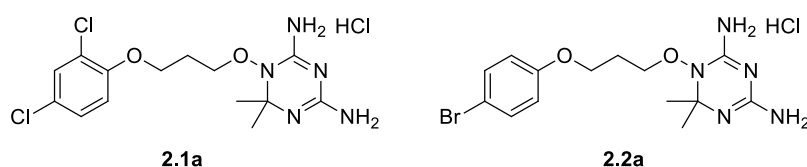
Figure 3.1. Structures of compounds 2.1a and 2.2a, prepared within the OpenMedChem project

Additionally, the direct analogue **3.5** was synthesized as an attempt to introduce and evaluate the influence of an alkyl substitution pattern variation in the *6*-position of dihydrotriazine core on compound activity and selectivity. Initially, the key precursor **3.3** was synthesized according to the previously established workflow, followed by the late-stage dihydrotriazine core formation (Scheme 3.1).[221,222]

Scheme 3.1. Synthesis of 3.5 with an alkyl substitution pattern variation

3.1 X = Br
3.2 X = ONH-Boc
3.3 X = ONH₂ HCl
3.4
3.5
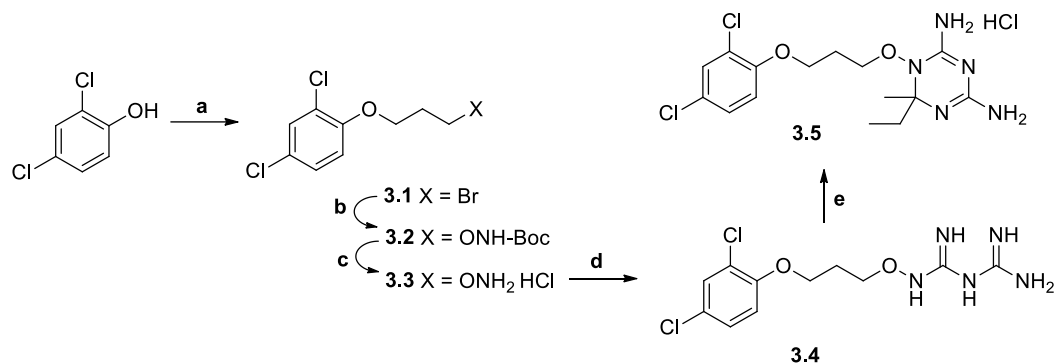
Reagents and conditions: (a) 1,3-dibromopropane, K₂CO₃, DMF, r.t., 48 hrs; (b) N-Boc-hydroxylamine, DBU, DCM, 0 °C, 17 hrs; (c) TFA, DCM, HCl, r.t., 15 min; (d) cyanoguanidine, EtOH, reflux, 3 hrs; (e) 2-butanone, HCl, MeOH, r.t., 100 hrs.

In the dihydrotriazine-containing compound preparation, we faced numerous structure elucidation and synthetic issues, such as limited reaction reproducibility and very low yields. For instance, the first step reported in the literature included phenol alkylation by 1,3-dibromopropane, which resulted in the formation of double-alkylation and elimination side products, rendering purification complicated and lowering the yields.[223,224] In order to overcome this hurdle, we developed an alternative approach to the *O*-substituted hydroxylamine preparation through the direct transformation of alcohols as shown in Scheme 3.2.[220]

Scheme 3.2 Alternative approach for the preparation of *O*-substituted hydroxylamines
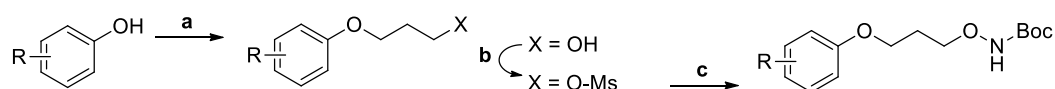
R = varied (4-Br, 2,4-diF)

Reagents and conditions: (a) 3-bromo-1-propanol, K₂CO₃, DMF/ACN, r.t., 24-72 hrs; (b) methanesulfonylchloride, Et₃N, DCM, 0 °C, 1 hr; (c) N-Boc-hydroxylamine, DBU, DCM, 0 °C, 24-100 hrs.

Dihydrotriazine core formation was the major obstacle for the current synthetic pathway. Typically the reaction progress (Scheme 3.1, step "**e**") was followed up by real-time UPLC analysis of the reaction mixture. Several diverse carbonyl-containing reagents were tested in order to introduce substituent variation in the dihydrotriazine core. It is worth noting that under different reaction conditions, usually only one new peak was detected by real-time UPLC analysis, predominantly possessing the *m/z* corresponding to the desired product. Nevertheless, the follow-up product purification and isolation were not straightforward or reproducible and, in most cases, failed to deliver the pure final product. The isolated residue often possessed unknown and unquantifiable impurities. The structural determination and/or impurity identification employing NMR analysis were complicated further by extreme peak broadening, described in detail in Section 3.1.2.

3.1.2 Structure elucidation by NMR

A characteristic feature of this compound series is significant peak broadening in ¹H and ¹³C NMR spectra. This phenomenon may be related to the coexistence of numerous tautomeric structures for this particular heterocyclic core (Figure 3.2). In each tautomer, exchangeable amine protons and R₁, R₂

substituents would possess slightly different chemical shifts, contributing to the averaged spectrum appearance. On the other hand, no clear explanation for peak broadening in ^{13}C NMR was found.
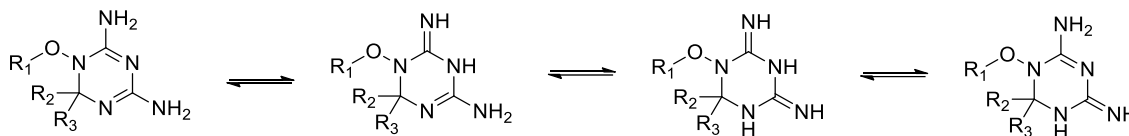
Figure 3.2. Some tautomeric structures, feasible for substituted 1,6-dihydro-1,3,5-triazine-2,4-diamine core

The broadening obstructs the precise peak integration in ^{1}H NMR. Moreover, in the measured ^{13}C or APT NMR spectra, the broadened peaks were at times not distinguishable from the noise. Some of these missing peaks could be tentatively assigned by 2D NMR cross-peak analysis. Nevertheless, some correlations, expected to be observed in HMBC spectra, resulted in a very weak signal, lost in the noise.

A characteristic example of ^{1}H and ^{13}C NMR spectra (zoomed areas) of **3.5** is presented in Figure 3.3 (A and B, respectively). The broadened peaks in the region 0-2.3 ppm in ^{1}H NMR (Figure 3.3A) correspond to the methyl (1.38 ppm) and ethyl (0.84, 2.13 ppm) substituents in the *6-position* of the dihydrotriazine ring, which can be expected to be influenced the most by the presence of different tautomeric forms. The signal at 2.18 ppm belongs to the middle CH$_2$ in the linker. The ^{13}C NMR signals of the 6-ethyl substituent of the dihydrotriazine core (7.7, 29.3 ppm) were noticeably broadened, while the 6-methyl peak at 22.9 ppm was not visually detectable (in the area inside the circle, Figure 3.3B), its position was determined by careful examination of HMQC spectrum of **3.5**.
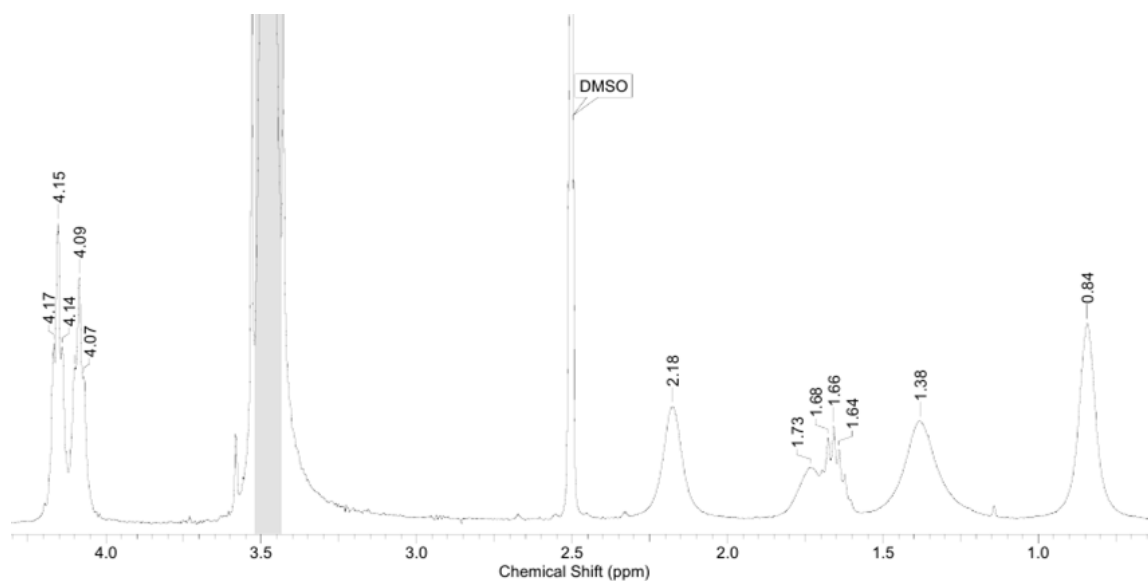
(A) ^{1}H *NMR of* **3.5***, zoomed area (0-4.5 ppm)*
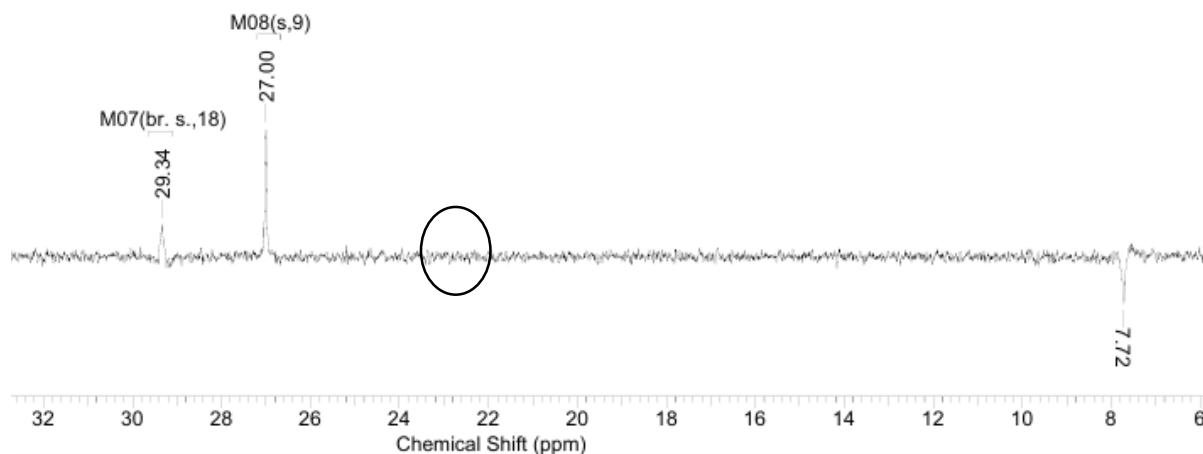
(B) ^{13}C (APT) NMR of 3.5, zoomed area (6-32 ppm). Red circle: non detected peak, identified by 2D NMRs.

Figure 3.3. ^{1}H and ^{13}C (APT) NMRs (zoomed areas) of 3.5.

3.1.3 Scaffold hopping: compound design

Based on the described synthetic challenges and the biological evaluation results of compounds **2.1a**, **2.2a,** and **3.5** (*vide infra*, Section 3.2), the next stage of our research was concentrated on a scaffold hopping approach to replace the dihydrotriazinone core. Critical considerations for the compound design were the following:

- The 2,4-diamino-1,3-diaza pharmacophore reported being essential for DHFR inhibition, should be preserved in all new analogues
- Aromatic diazines and triazines were deemed to be preferable as they could have improved permeability compared to non-aromatic dihydrotriazines
- Special attention is to be given to the toxicity evaluation of all new compounds

The general structure of designed compounds is displayed in Figure 3.4B with the crucial pharmacophore highlighted in magenta.
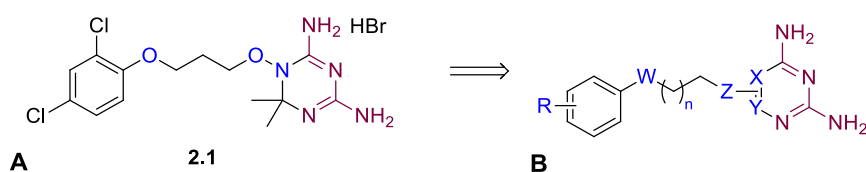
(A) The initial hit 2.1 structure, (B) Scaffold hopping: general compound structure, indicating the crucial 2,4-diamino-1,3-diaza pharmacophore (magenta) and the structural features to be varied during this project (blue).

Figure 3.4. The identified hit 2.1 and the general structure of the designed series

Based on the abovementioned general structure, a few substituted heterocyclic scaffolds were proposed as new cores for further investigation and synthetic approach development (Figure 3.5 A-D). The synthesis of compounds comprising those heterocyclic cores is described below.
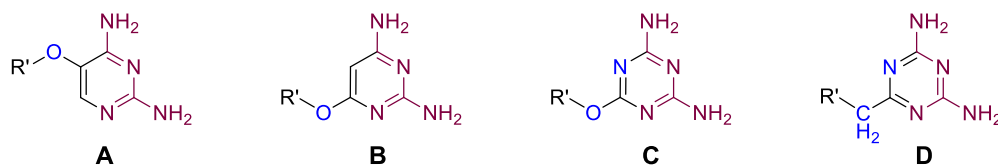
Figure 3.5. Proposed heterocyclic scaffolds A-D, indicating the crucial 2,4-diamino-1,3-diaza pharmacophore (magenta) and the key structural features to be modified (blue).

3.1.3.1 5-O-substituted pyrimidine-2,4-diamine derivatives

5-*O*-substituted pyrimidine-2,4-diamine derivatives were considered the closest analogues of the initial hits (Figure 3.5 A). In those compounds, the relative position of the linker to the core was preserved to the greatest extent possible while providing the aromatic heterocyclic pharmacophore.

The synthesis of target compounds was based on the alkylation of 2,4-diaminopyrimidin-5-ol **3.6** with the halo-alkyl counterpart (Scheme 3.3). The key intermediate **3.6** was obtained by oxidation of pyrimidine-2,4-diamine with ammonium persulfate.[225] The reaction turned out to lack reproducibility. The structural confirmation of **3.6** posed an additional challenge, as its structure consists mainly of exchangeable OH and NH protons and only one well-defined CH signal (singlet). As the molecular ion detected by UPLC corresponded to the desired product **3.6**, the obtained compound was used directly for further alkylation with **3.7**-**3.8** analogously to a described procedure[226].

Scheme 3.3. Synthesis of 5-O-substituted pyrimidine-2,4-diamine derivatives
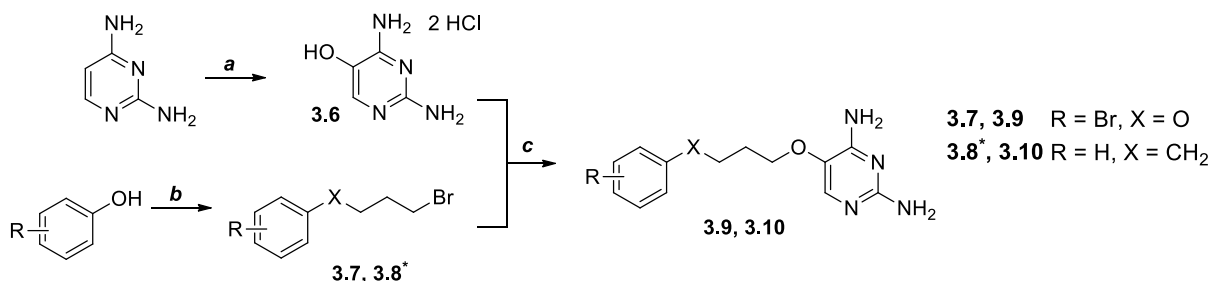
Reagents and conditions: (a) ammonium persulfate, NaOH, water, 0 °C, 2 hrs, followed by HCl/water; (b) 1,3-dibromopropane, K$_2$CO$_3$, ACN, r.t., 24 hrs; (c) NaOEt, EtOH, reflux, 48 hrs. *commercially available*

As mentioned before, phenol alkylation with 1,3-dibromopropane was found to be challenging, leading to limited accessibility of such analogues as intermediate **3.7**. Compound **3.8** was instead commercially available and used to probe the substitution of the oxygen in the linker by X = CH$_2$. In both cases, final products **3.9-3.10** were isolated in low yields (9% and 27% correspondingly).

3.1.3.2 6-O-substituted pyrimidine-2,4-diamine derivatives

In this compound sub-series, a different substitution pattern of the pyrimidine core was offered (Figure 3.5 B). The linker flexibility was hypothesized to at least partially compensate for the substituent shift from the *5*-position to the *6*-position of the heterocycle.

The synthesis of 6-*O*-substituted pyrimidine-2,4-diamine derivatives was based on the described reaction of the commercially available 6-chloropyrimidine-2,4-diamine with the appropriate sodium alkoxide (Scheme 3.4)[227].

Scheme 3.4. Synthesis of 6-*O*-substituted pyrimidine-2,4-diamine derivatives
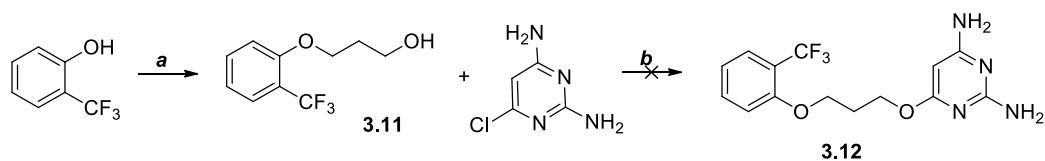
Reagents and conditions: (a) 3-Bromo-1-propanol, K$_2$CO$_3$, DMF/ACN, r.t., 3-7 days; (b) NaH, DMF, 100 °C, 24 hrs.

The synthetic approach was tested on the precursor **3.11** (R = 2-CF$_3$). Although the formation of the desired product was observed by UPLC, the purification failed to deliver any pure final product **3.12**. As this reaction also failed under similar conditions with other precursors, we shifted our attention to the preparation of closely related 6-*O*-substituted 1,3,5-triazine-2,4-diamine derivatives (Section 3.1.4.3).

3.1.3.3   6-O-substituted 1,3,5-triazine-2,4-diamine derivatives

A similar approach to the pyrimidine-2,4-diamines synthesis was used for the preparation of analogous 6-O-substituted 1,3,5-triazine-2,4-diamine derivatives (Figure 3.5 C, Scheme 3.5). In this case, the alkylation of the 2-chloro-4,6-diamino-1,3,5-triazine using sodium hydride as a base was proven to be more successful, as two desired products **3.16** and **3.17** were isolated in the pure state, although in very low yields (4% and < 1% correspondingly). On the other hand, isolation of **3.18** was unsuccessful, even though its formation was observed by UPLC.

Taking into account the very low yields in the case of **3.16-3.17**, we decided to test different reaction conditions for the alkylation step. Basic (KO^{t}Bu) and acidic (HCl solution) catalysis were evaluated for preparation of **3.19** from **3.15**; nevertheless, no desired product formation was detected in the reaction mixture by UPLC in both cases.

Scheme 3.5. Synthesis of 6-*O*-substituted 1,3,5-triazine-2,4-diamine derivatives
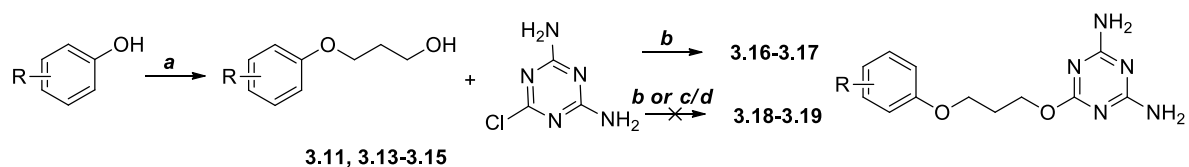
R =

4-Br	2-iPr	2-CF$_3$	2-^{t}Bu
3.13	**3.14**	**3.11**	**3.15**
3.16	**3.17**	**3.18**	**3.19**

Reagents and conditions: (a) 3-Bromo-1-propanol, K$_2$CO$_3$, DMF/ACN, r.t., 3-7 days; (b) NaH, DMSO or THF, 100 °C, 5 hrs; (c) KO^{t}Bu, THF, reflux, 6 hrs; (d) HCl, dioxane, reflux, 6 hrs;

Boc-protection of amino-groups in 2-chloro-4,6-diamino-1,3,5-triazine was tested in order to reduce the probability of amine group alkylation during the last step and to improve reaction yield and reproducibility. To our disappointment, no desired product **6.20** formation was detected under the standard reaction conditions (Scheme 3.6).

Scheme 3.6. 1,3,5-triazine-2,4-diamine Boc protection attempt
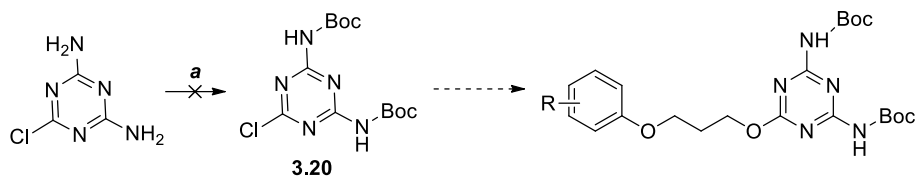
Reagents and conditions: (a) Di-t-butyldicarbonate, THF, r.t. 17 hrs or reflux 2 hrs.

As a result, it was decided to put this scaffold's synthesis on hold until more indications were obtained on its utility in DHFR inhibitors. Preliminary biological evaluation results of the available analogues were expected to be indicative of this.

3.1.3.4 6-CH₂-substituted 1,3,5-triazine-2,4-diamine derivatives

Compounds described in this section (Figure 3.5 D) are close analogues of **3.16-3.17** but differ from the latter by the 6-CH_2-substitution on the triazine ring (highlighted in magenta, Figure 3.6). A different synthetic approach, based on last-stage triazine ring synthesis from the corresponding nitrile-substituted precursors, was developed.
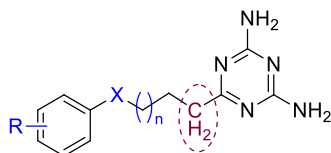
Key difference: 6-CH₂ substitution (in magenta); variable moieties: in blue
Figure 3.6. General structure of 6-CH₂-substituted 1,3,5-triazine-2,4-diamine derivatives

Compounds were proven to be easily accessible in a two-step synthesis (Scheme 3.7-3.9), providing the final products in good yields. First, the appropriate phenols or anilines were alkylated with bromoalkylnitriles. The formed precursors were then cyclized with dicyandiamide to form the triazine core with the 6-CH_2-substitution pattern.[227] Various modifications were further exploited for this compound cluster in order to provide comprehensive SAR data, including the introduction of:

- several aryl substituents (R)
- different linker length (n = 1-3)
- diverse connector group X at the aryl (O, NH or NMe)

Based on the original hits **2.1-2.3**, the three aryl substitution patterns (R = 2,4-diCl, 4-Br, 2-^{t}Bu) were chosen for further investigation in the current sub-series. An array of compounds with varying linker lengths were prepared to test the influence on compound binding and activity. The nature of the linker was addressed via the introduction of diverse connector group X, bound to the aryl.

Scheme 3.7 describes the synthesis of final compounds **3.30-3.38**, all containing X = O (ethers).

Scheme 3.7. Synthesis of 6-CH₂-substituted 1,3,5-triazine-2,4-diamine derivatives with linker length variation
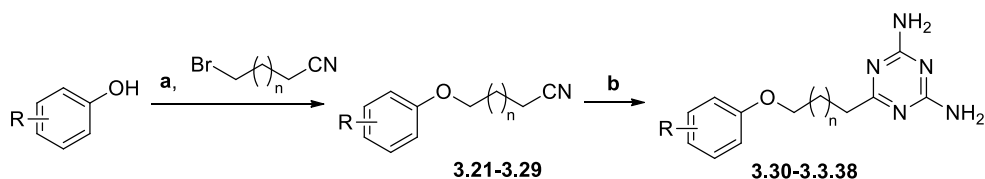
	R =		
	2,4-diCl	**4-Br**	**2-^{t}Bu**
n = 1	**3.21**	**3.24**	**3.27**
	3.30	**3.33**	**3.36**
n = 2	**3.22**	**3.25**	**3.28**
	3.31	**3.34**	**3.37**
n = 3	**3.23**	**3.26**	**3.29**
	3.32	**3.35**	**3.38**

Reagents and conditions: (a) K$_2$CO$_3$, DMF/ACN, r.t., 3-7 days; (b) cyanoguanidine, KOH or KO^{t}Bu, 2-methoxyethanol, 100 °C, 3-7 hrs.

In order to provide precursors **3.39-3.44** (X = NR'), two different amine alkylation approaches were explored (Scheme 3.8): (a) a two-component (aniline with bromoalkylnitrile) reaction with no solvent or catalyst; and (b) an alkylation in solution, using NaH as a base. The necessary intermediates were delivered without major difficulties in most of the cases and smoothly transformed into the desired compounds.

Scheme 3.8. Synthesis of 6-CH$_2$-substituted 1,3,5-triazine-2,4-diamine derivatives with additional linker modifications
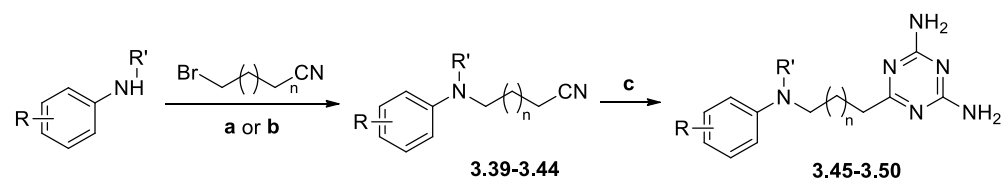
	R = 2,4-diCl, R' = H	R = 2-^{t}Bu, R' = H	R = 2,4-diCl, R' = Me
n = 1	-	**3.41**	-
		3.47	
n = 2	**3.39**	**3.42**	**3.44**
	3.45	**3.48**	**3.50**
n = 3	**3.40**	**3.43**	-
	3.46	**3.49**	

Reagents and conditions: (a) solvent-free, 100 °C, 4-7 hrs; (b) NaH, THF, r.t., 24-48 hrs; (c) cyanoguanidine, KOH or KO^{t}Bu, 2-methoxyethanol, 100 °C, 3-7 hrs.

Compounds **3.53-3.54**, bearing a phenothiazine moiety in place of the aromatic ring, were prepared to assess the effect of a bulky and lipophilic tricyclic moiety on the proposed pharmacophore. The products were prepared analogously to the amine-bearing compounds **3.45-3.50** (Scheme 3.9).

Scheme 3.9. Synthesis of 6-CH₂-substituted 1,3,5-triazine-2,4-diamine derivatives with phenothiazine moiety
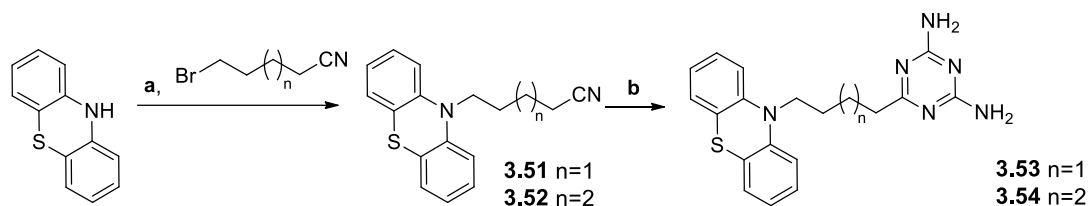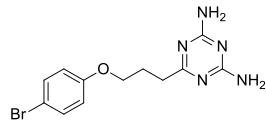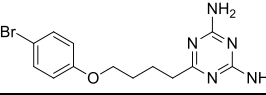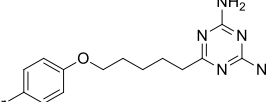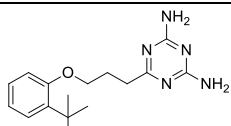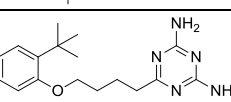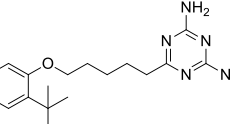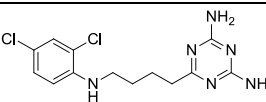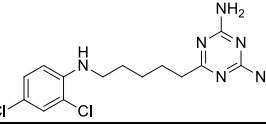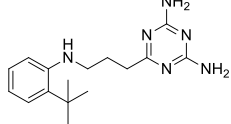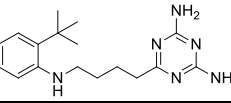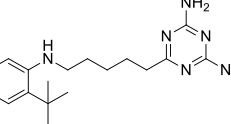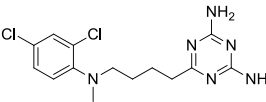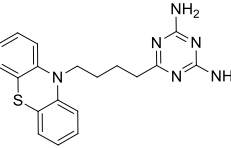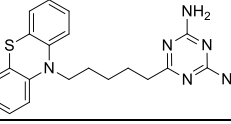
Reagents and conditions: (a) NaH, THF, r.t., 24-48 hrs; (b) cyanoguanidine, KOH or KO^{t}Bu, 2-methoxyethanol, 100 °C, 3-7 hrs.

3.2 Results and discussion

All final compounds were evaluated for their ability to inhibit the *Mtb* DHFR enzyme (pIC$_{50}$ values) as well as for their ability to inhibit the growth of the H$_{37}$Rv strain (whole-cell MIC values). In addition, the cytotoxicity in HepG$_2$ cells was evaluated together with two physicochemical parameters: kinetic aqueous solubility (using chemiluminescent nitrogen detection, CLND) and ChromLogD. The biological and physicochemical evaluation results of all prepared analogues in this series are summarized in Table 3.1.

Table 3.1. Biological and physicochemical profile of synthesized analogues of DHFR inhibitors

Structure		DHFR pIC$_{50}$[a]	MIC (µM)[b]	Cytotoxicity HepG$_2$ (µM)[c]	Solubility (µM)[d]	Chrom logD[e]
2.1a		8.2	2.0	0.005	405	3.66
2.2a		7.4	15.6	0.008	361	3.32
3.5		7.8	1.4	0.003	230	3.69
3.9		4.3	> 80	11.7	≥ 306	3.90
3.10		4.3	> 80	5.3	≥ 404	3.68
3.16		< 4	> 80	> 100	139	3.80
3.17		< 4	> 80	> 100	≥ 383	4.62
3.30		< 4	> 80	> 100	116	3.89
3.31		< 4	> 80	> 100	103	4.32
3.32		< 4	> 80	> 100	97	4.79

	Structure	DHFR pIC$_{50}$[a]	MIC (µM)[b]	Cytotoxicity HepG$_2$ (µM)[c]	Solubility (µM)[d]	Chrom logD[e]
3.33		< 4	> 80	> 100	171	3.28
3.34		< 4	> 80	> 100	237	3.72
3.35		< 4	> 80	25.0	60	4.17
3.36		< 4	> 80	> 100	332	4.68
3.37		< 4	> 80	> 100	252	5.23
3.38		< 4	> 80	57.3	101	5.75
3.45		< 4	> 80	> 100	339	4.18
3.46		< 4	> 80	100	187	4.67
3.47		< 4	> 80	> 100	≥ 410	4.11
3.48		< 4	> 80	> 100	≥ 384	4.49
3.49		< 4	> 80	> 100	≥ 381	4.95
3.50		< 4	> 80	> 100	360	4.38
3.51		4.6	> 80	> 100	74	4.89
3.52		< 4	> 80	100	24	5.11

_____

Structure	DHFR pIC$_{50}$[a]	MIC (µM)[b]	Cytotoxicity HepG$_2$ (µM)[c]	Solubility (µM)[d]	Chrom logD[e]
[a] *Mtb* DHFR enzyme inhibition pIC$_{50}$; [b] MIC [µM] against *Mycobacterium tuberculosis* (H37Rv). Reference: Isoniazid, MIC = 1.8 µM; [c] Cytotoxicity HepG$_2$ IC$_{50}$ [µM]; [d] kinetic aqueous solubility (CLND) [µM]; [e] ChromlogD (pH 7.4); [f] N.D. – not determined.					

During the biological evaluation, all the dihydrotriazine-bearing compounds displayed micromolar anti-mycobacterial potencies along with exceptionally potent human cytotoxicity in the HepG2 assay (IC$_{50}$ < 0.01 µM) (see Table 3.1). This behavior is likely related to a lack of compound selectivity between *M. tuberculosis* and human DHFR enzymes so that compounds which showed high affinity against *Mtb* DHFR were able to inhibit efficiently human DHFR leading to the intrinsic series toxicity. Nevertheless, the performed evaluation did not allow us to exclude with all the certainty the off-target toxicity of this compound series.

The possibility of toxicity problems with dihydrotriazine-based molecules has been discussed in other literature reports as well.[178] Furthermore, the limited solubility and membrane permeability of those compounds indicate a higher risk of poor bioavailability. Taken together, the dihydrotriazine-based compounds discovered during HTS do not seem to be a promising starting point for TB drug development, a factor that might be intrinsically related to the biopharmaceutical properties of the dihydrotriazine ring itself. These data also justify the scaffold hopping approach that was explored.

All new compounds obtained in the framework of this approach, however, were found to be inactive in the enzymatic and whole-cell assays (pIC$_{50}$ < 4.5, MIC ≥ 80 µM). None of the alternative ring systems, therefore, seems competitive with the 1,6-dihydro-1,3,5-triazine-2,4-diamine for achieving *Mtb* DHFR activity.

The 5-*O*-substituted pyrimidine-2,4-diamines **3.9** and **3.10** are the closest analogues of the original dihydrotriazine references. These molecules have limited, tens of micromolar *Mtb* DHFR affinity, and also seem to have suboptimal (*Mtb* DHFR/*Hs* DHFR) selectivity as suggested by the significant cytotoxicities in the HepG2 assay (IC$_{50}$ = 5-10 µM).

3.3   Conclusions

As both *M. tuberculosis* and human cells possess orthologous forms of DHFR with similar general structure and functionality, high species selectivity is of extreme importance for DHFR inhibitors against tuberculosis (see Section 2.3). All dihydrotriazine derivatives reported herein caused severe human cytotoxicity in the HepG$_2$ assay. This series furthermore showed numerous synthetic issues, rendering an extensive SAR investigation not feasible in the course of this research. Scaffold hopping was applied in an attempt to overcome toxicity and low bioavailability issues of the hit molecules. Unfortunately, the prepared analogues did not demonstrate inhibitory potency on DHFR and did not demonstrate whole-cell activity on *M. tuberculosis*. Based on this consideration, the project was discontinued.

_____

3.4 Experimental section

3.4.1 General information: reagents and analytical methods

Laboratory reagent grade solvents were used unless stated otherwise. All reagents were purchased from Sigma-Aldrich, AcrosOrganics, Apollo scientific, Fluorochem, Enamine Ltd. or TCI and were used without further purification, unless otherwise mentioned.

Characterization of intermediates and final compounds was done using ^{1}H, ^{13}C, or APT NMR spectroscopy and mass spectrometry. In selected cased HSQC, HMQC, HMBC, NOE, NOESY spectra were used for structure determination. ^{1}H NMR (400 MHz) and ^{13}C NMR (100 MHz) spectra were recorded on a Bruker Avance III Nanobay Ultrashield 400 spectrometer or a Bruker DPX 400 spectrometer. The chemical shifts (δ) are expressed in parts per million (ppm), and coupling constants are in Hertz (Hz). DMSO-d_6, Acetone-d_6, CDCl$_3$, or Methanol-d_4 were used as standard NMR solvents. The chemical shifts δ were given relative to tetramethylsilane (TMS) (where available) or, in most of the cases, to the residual ^{1}H and ^{13}C signals of the solvent peak as an internal standard: in ^{1}H NMR (400 MHz) δ 2.50 ppm (quin, C$_2$D$_5$HOS) for DMSO-d_6, δ 2.05 ppm (quin, C$_3$D$_5$HO) for Acetone-d_6, δ 7.27 ppm (s, CHCl$_3$) for CDCl$_3$, δ 3.31 ppm (pent, CD$_2$HOD) for Methanol-d_4; in ^{13}C NMR (101 MHz) δ 39.51 ppm (sept) for DMSO-d_6, δ 29.84 ppm (sept), δ 206.26 ppm (s) for Acetone-d_6, δ 77.1 ppm (t) for CDCl$_3$, δ 49.00 ppm (sept) for Methanol-d_4. Legend: s = singlet, d = doublet, t = triplet, q = quartet, quin = quintet, sept = septet, m = multiplet (denotes complex pattern), br = broad signal, dd = doublet of doublets, dt = doublet of triplets, td = triplet of doublets, etc.

The reaction progress was monitored by UPLC/LCMS or TLC. TLC was performed on Polygram® pre-coated silica gel TLC sheets SIL G/UV$_{254}$ with detection by UV light (254 nm) using ethyl acetate/cyclohexane or ethyl acetate/*n*-heptane as solvent systems.

UPLC (Ultra Performance Liquid Chromatography) was performed according to methods A, B, or C. In all cases, ESI (electrospray ionization) was used. The quasi-molecular ions [M+H]$^+$ or [M-H]$^-$ were typically detected, unless stated otherwise. Retention time R$_t$ is indicated for the described method. In method A, a Waters Acquity UPLC system coupled to a Waters SQ detector and an Acquity UPLC BEH C18 1.7 µm, 3x50 mm column was used; the concentration of the measured samples was 0.1 mg/mL and flow 0.8 mL/min. The method A involved the following: Acetate NH$_4$ 25mM + 10% ACN at pH 6.6 /ACN, 0.0-0.2 min 99.9: 0.1, 0.2-1.0 min 10:90, 1.0-1.8 min 10:90, 1.9-2.0 min 99.9:0.1 at temperature 40 °C; the UV detection was an averaged signal from wavelength of 210 nm to 400 nm.

A Waters Acquity H-class UPLC system coupled to a waters TQD ESI mass spectrometer and a Waters TUV detector was used with a Waters Acquity UPLC BEH C18 1.7 µm 2.1 × 50 mm column. In methods B and C, the wavelength for UV detection was 254 nm unless stated otherwise. Solvent A consisted of water with 0.1% formic acid. Solvent B consisted of acetonitrile with 0.1% formic acid. Method B involved the following: flow 0.7 mL/min, 0.15 min isocratic elution (A:B = 95:5), followed by gradient elution during 1.85 min (A:B = from 95:5 to 0:100), then 0.25min of isocratic elution (A:B = 0:100), 0.75 min of isocratic elution (A:B = 95:5). Method C involved the following: flow 0.4 mL/min, 0.15 min isocratic elution (A:B = 95:5), followed by gradient elution during 4.85 min (A:B = from 95:5 to 0:100), then 0.25min of isocratic elution (A:B = 0:100), 0.75 min of isocratic elution (A:B = 95:5).

For the High-Resolution Mass Spectrometry (HRMS) measurements, positive ion mass spectra were acquired using a QSTAR Elite System (AB Sciex Instruments) mass spectrometer, equipped with a

turbospray source, over a mass range of 250–700. HRMS spectra were measured for selected compounds.

Where necessary, flash purification was performed on a Biotage® ISOLERA One and Four flash systems equipped with an internal variable dual-wavelength diode array detector (200-400 nm). Typically, the UV detection was performed at 254 nm. For normal phase purifications, SNAP cartridges (10-340 g; flow rate 10-100 mL/min) were used. Reversed-phase purifications were usually performed on Grace™Reveleris™ C18 Flash cartridges (12 g; flow rate 20-25 mL/min). Liquid sample loading was performed with small amounts of the appropriate solvents; dry sample loading was done by Self-Packing Samplet® cartridges using silica or Celite 545 for normal and reversed-phase purifications respectively. Common eluents used: *n*-heptane (Hep), cyclohexane (*c*-Hex), and ethyl acetate (EtOAc) for the normal phase purifications; water and acetonitrile (ACN) for the reversed-phase purifications. Used gradients varied by purification.

The preparative HPLC purification was conducted on the Agilent 1200 or Agilent 1100 instrument, employing either X-Bridge C_{18} columns (19 mm x 150 mm or 30 mm x 150 mm, 5 µm packing diameter) or SunFire C18 column (4.6 mm X 50 mm, 100Å, 3.5 µm). The solvents employed were: A = 0.1 M ammonium bicarbonate in water; B = acetonitrile ("basic" method) or A = 0.1 M formic acid in water; B = 0.1 M formic acid in acetonitrile ("acidic" method) respectively. The purification was run as a gradient (A:B) typically from 40 to 100% over either 20 min or 25 min, with a flow rate of 17 mL/min (19 mm column) or 35 mL/min (30 mm column). The UV detection wavelengths were 210 nm and 254 nm.

The isolated yields are reported. The purity of all final compounds, tested on *in vitro* and *in vivo* assays, was 95% or higher (unless stated otherwise), verified by interpretation of ESI-MS (LCMS/UPLC) and ^{1}H NMR data. All products were obtained as amorphous solids; melting points were not measured. All the biological and physicochemical evaluation of the final compounds was performed in GSK; the assay description can be found in Chapter 7.2.

3.4.2 General methods

General method A: phenol alkylation. To a stirred solution of the appropriate phenol (1.2-2.0 eq.), potassium carbonate K_2CO_3 (2.0-3.0 eq.) and DMF (1 mL) in acetonitrile, the corresponding alkyl halide was added (4.0-40.0 mmol, 1.0 eq.) at 0 °C (reaction molarity ≈ 0.30-0.70 mol/L). The reaction mixture was warmed to room temperature and stirred for 3-7 days. After the solid residue was separated by filtration, the solvent was removed under reduced pressure. The residue was directly purified by normal phase column chromatography (gradient *n*-Hep:EtOAc = 100:0 to 70:30, solid loading). The fractions containing the desired product were collected and evaporated under reduced pressure.

General method B: 6-CH₂-substituted 1,3,5-triazine-2,4-diamine core synthesis. The heterocyclic core formation was performed according to a described procedure[227] with some modifications. A stirred solution of the appropriate alkyl nitrile (1.9-7.1 mmol, 1.0 eq.) in 2-methoxyethanol was treated with cyanoguanidine (1.2-1.3 eq.), followed by potassium *tert*-butoxide (2.0 eq.) or potassium hydroxide (1.2-5.0 eq.) as a base (reaction molarity ≈ 0.30-0.90 mol/L). The reaction mixture was stirred at 100 °C for 3-7 hrs. Next, the reaction mixture was cooled down to room temperature, diluted with water, and extracted with ethyl acetate. The combined organic phases were washed with brine, dried over Na_2SO_4, filtered, and evaporated to dryness. The residue was purified by recrystallization from

_____

isopropanol or by normal phase column chromatography (solvent A: EtOAc or DCM, gradient A:MeOH = 100:0 to 80:20, solid loading). In the latter case, the fractions containing the desired product were collected and evaporated under reduced pressure. The final product was additionally dried in the oven (100 °C) to remove any solvent impurity.

General method C: aniline alkylation. A mixture of the appropriate alkyl halide (1.2-2.0 eq.) with the corresponding aniline (12.0-17.0 mmol, 1.0 eq.) was heated at 100 °C for 4-7 hrs. Next, the reaction mixture was cooled down to room temperature, and the residue was directly purified by flash column chromatography (gradient Hep:EtOAc = 100:0 to 60:40). The fractions containing the desired product were collected and evaporated under reducd pressure. The obtained product sometimes contained the impurity of the starting alkyl halide (proven by NMR), it was used for the next reaction step without any further purification.

General method D: amine alkylation with sodium hydride. To a stirred solution of the appropriate amine (1.2 eq.) in THF (15 mL) sodium hydride (60% Wt. in the mineral oil, 1.3 eq.) was added at room temperature. After 30 min, the corresponding alkyl halide (7.5-9.5 mmol, 1.0 eq.) was added (reaction molarity $\approx$ 0.50-0.65 mol/L). The reaction mixture was stirred at room temperature for 1-2 days. After the solid residue was separated by filtration, the solvent was removed under reduced pressure. The residue was directly purified by normal phase column chromatography (gradient *n*-Hep:EtOAc = 100:0 to 70:30, solid loading). The fractions containing the desired product were collected and evaporated under reduced pressure.

3.4.3 Chemistry

Compound **3.8** was commercially available.

1-(3-(2,4-Dichlorophenoxy)propoxy)-6,6-dimethyl-1,6-dihydro-1,3,5-triazine-2,4-diamine hydrochloride (2.1a)
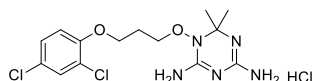
The title compound was prepared according to an optimized literature procedure.[218] Off-white amorphous solid, purity ≥ 95%.

¹H NMR (400 MHz, DMSO-d_6) δ 9.05 (br. s., 1H), 8.61 (br. s., 1H), 8.08 (s, 1H), 7.76 (br. s, 1H), 7.58 (d, *J*=2.53 Hz, 1H), 7.39 (dd, *J*=2.53, 8.84 Hz, 1H), 7.21 (d, *J*=8.84 Hz, 1H), 7.07 (br. s., 1H), 4.18 (t, *J*=6.06 Hz, 2H), 4.10 (t, *J*=6.06 Hz, 2H), 2.19 (br. s., 2H), 1.39 (br. s., 6H). **¹³C NMR** (101 MHz, DMSO-d_6) δ 161.7, 156.6, 153.2, 129.8, 128.6, 125.0, 122.8, 115.5, 74.4, 72.7, 65.8, 27.4, 11.0* (br. s). **ESI-MS (A):** *m/z* 360 [M+H]⁺ (R$_t$ = 1.06 min). **HRMS** (ESI) *m/z* calcd for $C_{14}H_{19}Cl_2N_5O_2$ [M+H]⁺: 360.0989; found: 360.0988. *Methyl signals were broadened in ¹³C NMR; its chemical shift was determined by 2D NMRs.

1-(3-(4-Bromophenoxy)propoxy)-6,6-dimethyl-1,6-dihydro-1,3,5-triazine-2,4-diaminehydrochloride (2.2a)
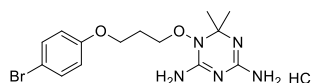
The title compound was prepared according to a modified literature procedure.[218] Off-white amorphous solid, purity ≥ 95%.

¹H NMR (400 MHz, DMSO-d_6) δ 9.20 (s, 1H), 8.63 (s, 1H), 8.08 (s, 1H), 7.76 (br. s., 1H), 7.38-7.53 (m, 2H), 7.14 (br. s., 1H), 6.84-7.00 (m, 2H), 4.06 (t, J=6.06 Hz, 4H), 2.15 (br. s., 2H), 1.39 (br. s., 6H). **ESI-MS (A):** *m/z* 370, 372 [M+H]⁺ (R_t = 1.04 min). **HRMS** (ESI) *m/z* calcd for $C_{14}H_{20}BrN_5O_2$ [M+H]⁺: 370.0873; found: 370.0887.

1-(3-Bromopropoxy)-2,4-dichlorobenzene (3.1)
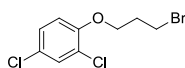
A solution of 2,4-dichlorophenol (23.52 g, 144 mmol) in DMF (100 mL) was added dropwise to a stirred solution of 1,3-dibromopropane (29.3 mL, 289 mmol) and potassium carbonate K_2CO_3 (39.9 g, 289 mmol) in DMF (200 mL) at 0 °C. The reaction mixture was warmed to room temperature and stirred for 48 hrs. The solution was diluted with water and extracted with diethyl ether. The combined organic phases were washed with water and brine, dried over $MgSO_4$, filtered, and evaporated to dryness. In order to remove the 1,3-dibromopropane impurity in the residue, co-evaporation with toluene was performed, resulting in the crude mixture (24.2 g, the title compound content > 80%), which was used directly for the next reaction step without any further purification. The title compound was not isolated in the pure form.

¹H NMR (400 MHz, CDCl₃) δ 7.35 - 7.39 (m, 1H), 7.15 - 7.22 (m, 1H), 6.86 - 6.92 (m, 1H), 4.16 (t, J = 5.65 Hz, 2H), 3.66 (t, J = 6.27 Hz, 2H), 2.30 - 2.43 (m, 2H).

tert-Butyl 3-(2,4-dichlorophenoxy)propoxycarbamate (3.2)
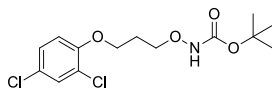
The crude mixture (22.4 g) containing 1-(3-bromopropoxy)-2,4-dichlorobenzene **3.1** was dissolved in DCM (15 mL), *N*-Boc-hydroxylamine (9.85 g, 74 mmol) was added. The resulting solution was cooled down to 0 °C, and 1,8-diazabicyclo[5.4.0]undec-7-ene (DBU) (11.15 mL, 74 mmol) was slowly added. The reaction mixture was warmed to room temperature and stirred overnight. The solution was diluted with ethyl acetate and washed with water and brine, dried over $MgSO_4$, filtered and evaporated to dryness. The residue was purified by normal phase column chromatography (gradient *n*-Hep:EtOAc = 100:0 to 40:60, solid loading). The fractions containing the desired product were collected and evaporated under reduced pressure, resulting in the title compound. Yield* 21.018 g, 62.5 mmol, purity ≥ 90%. **No % was measured as the precise amount of the starting 3.1 in the crude mixture was unknown.*

¹H NMR (400 MHz, CDCl₃) δ 7.37 – 7.32 (m, 1H), 7.21 (br s, 1H, ex), 7.18 – 7.14 (m, 1H), 6.89 – 6.84 (m, 1H), 4.15 (t, J = 6.1 Hz, 2H), 4.07 (t, J = 6.0 Hz, 2H), 2.21 – 2.10 (m, 2H), 1.47 (s, 9H). **ESI-MS (B):** *m/z* not detectable (R_t = 2.24 min).

O-(3-(2,4-Dichlorophenoxy)propyl)hydroxylamine hydrochloride (3.3)
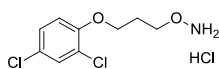
Trifluoroacetic acid (30 mL) was slowly added to a solution of *tert*-butyl 3-(2,4-dichlorophenoxy) propoxycarbamate **3.2** (9.039 g, 26.9 mmol) in DCM (30 mL). The reaction mixture was stirred at room temperature for 15 min, then evaporated under reduced pressure. The residue was dissolved in DCM (10 mL) and added to a 2M hydrogen chloride solution in anhydrous diethyl ether (54 mL). The formed precipitate was collected by filtration and washed with DCM, resulting in the title compound. Yield 32% (2.376 g, 8.72 mmol).

¹H NMR (400 MHz, DMSO-*d₆*) δ 11.07 (br. s., 3H, ex), 7.61 (d, *J* = 2.6 Hz, 1H), 7.41 (dd, *J* = 8.9, 2.6 Hz, 1H), 7.22 (d, *J* = 8.9 Hz, 1H), 4.23 (t, *J* = 6.4 Hz, 2H), 4.16 (t, *J* = 6.2 Hz, 2H), 2.13 (p, *J* = 6.3 Hz, 2H). **ESI-MS (B):** *m/z* 236.4 [M+H]⁺ (Rₜ = 1.50 min).

N-(3-(2,4-Dichlorophenoxy)propoxy)imidodicarbonimidic diamide hydrochloride (3.4)
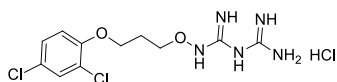
The title compound was prepared *in situ* and not isolated. O-(3-(2,4-dichlorophenoxy)propyl)hydroxylamine hydrochloride **3.3** (0.654 g, 2.4 mmol) and cyanoguanidine (0.242 g, 2.88 mmol) were dissolved in ethanol (9 mL), the resulting mixture was refluxed for 3 hrs. The product formation was followed by UPLC. The reaction mixture was evaporated under reduced pressure; the solid residue was directly used for the next reaction step without isolation of the title compound.

ESI-MS (B): *m/z* 320.4 [M+H]⁺ (Rₜ = 1.65 min).

1-(3-(2,4-Dichlorophenoxy)propoxy)-6-ethyl-6-methyl-1,6-dihydro-1,3,5-triazine-2,4-diamine hydrochloride (3.5)
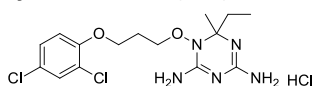
To a solution of *N*-(3-(2,4-dichlorophenoxy)propoxy)imidodicarbonimidic diamide hydrochloride **3.4** (0.285 g of the residue obtained) in methanol (1 mL) 4M hydrogen chloride solution (0.80 mL, 3.20 mmol) was added, followed by 2-butanone (0.122 g, 1.692 mmol). The solution was stirred at room temperature and the reaction progress was monitored by UPLC. The reaction was completed in 4 days, the reaction mixture was evaporated, the residue was re-crystallized from methanol to produce the title compound. Yield 24% (80.0 mg, 0.195 mmol), white amorphous solid, purity ≥ 95%.

¹H NMR (400 MHz, DMSO-*d₆*) δ 8.96 (br. s., 1H), 8.55 (br. s., 1H), 8.04 (br. s., 1H), 7.52-7.87 (m, 2H), 7.38 (dd, *J*=2.53, 8.84 Hz, 1H), 7.01-7.29 (m, 2H), 4.15 (t, *J*=5.05 Hz, 2H), 4.09 (t, *J*=5.81 Hz, 2H), 2.18 (br. s., 2H), 1.56-1.88 (m, 2H), 1.38 (br. s., 3H), 0.84 (br. s., 3H). **¹³C NMR** (101 MHz, DMSO-*d₆*) δ 156.3, 152.8, 129.4, 128.3, 124.6, 122.4, 115.1, 75.1 (br. s.), 73.8*(br. s.), 65.4, 29.3 (br. s.), 27.0, 22.9* (br. s.), 7.7 (br. s.). **ESI-MS (A):** *m/z* 374 [M+H]⁺ (Rₜ = 1.08 min). **HRMS** (ESI) *m/z* calcd for $C_{15}H_{21}Cl_2N_5O_2$ [M+H]⁺: 374.1151; found: 374.1141. *Those signals were not detected in ¹³C NMR, their chemical shift was determined by 2D NMRs.*

2,4-Diaminopyrimidin-5-ol dihydrochloride (3.6)
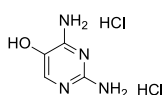
The title compound was prepared according to a described procedure.[228] A solution of ammonium persulfate (6.22 g, 27.2 mmol) in water (10 mL) was added dropwise in course of 2 hours to a stirred suspension of pyrimidine-2,4-diamine (2 g, 18.16 mmol) in 4N sodium hydroxide solution (30 mL) at 0 °C. The solution was warmed up to room temperature and stirred overnight, then it was cooled to 0 °C and acidified with concentrated hydrochloric acid. The precipitate was collected by filtration and washed with ice-cold water. The residue was dissolved in concentrated hydrochloric acid (5 mL) and water (5 mL) and the resulting solution was refluxed for 30 min. The solution was then cooled down to room temperature. The formed precipitated was collected by filtration resulting in the title compound. The compound identity was predominantly judged by the UPLC result due to the presence of mostly exchangeable protons in the structure. Yield 24% (872 mg, 4.38 mmol).

¹H NMR (400 MHz, DMSO-d_6) δ 11.60 (br. s., 1H), 10.27 (br. s., 1H), 8.27 (br. s., 1H), 8.09 (br. s., 1H), 7.80 (br. s., 1H), 7.22 - 7.31 (m, 3H). **ESI-MS (B)***: *m/z* 127 [M+H]⁺ (R_t = 0.23 min). *The product was detected as a base.*

1-Bromo-4-(3-bromopropoxy)benzene (3.7)
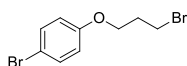
To a stirred solution of 1,3-dibromopropane (26 mL, 256 mmol) and potassium carbonate K_2CO_3 (35.4 g, 256 mmol) in acetonitrile (280 mL) a solution of 4-bromophenol (23.7 g, 137 mmol) in acetonitrile (100 mL) was added dropwise at 0 °C. The reaction mixture was stirred at room temperature for 24 hrs. After the solvent was removed under reduced pressure, diluted with water and extracted with diethyl ether. The combined organic phases were washed with brine, dried over $MgSO_4$, filtered and evaporated to dryness. The purification by normal phase column chromatography (gradient *n*-Hep:EtOAc = 100:0 to 70:30, solid loading) failed due to co-elution with unreacted started materials and side products. The pure product crystallized from the crude mixture in toluene on evaporation, it was collected and washed with toluene. Yield 29% (11.726 g, 39.9 mmol).

¹H NMR (400 MHz, CDCl₃) δ 7.35 - 7.43 (m, 2H), 6.80 (d, *J* = 9.04 Hz, 2H), 4.08 (t, *J* = 5.77 Hz, 2H), 3.60 (t, *J* = 6.40 Hz, 2H), 2.32 (quin, *J* = 6.09 Hz, 2H). **ESI-MS (B):** *m/z* 309, 311, 313 [M-H+H₂O]⁻ (R_t = 2.25 min).

5-(3-(4-Bromophenoxy)propoxy)pyrimidine-2,4-diamine (3.9)
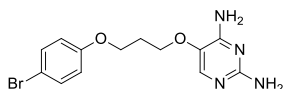
The title compound was prepared analogously to a described procedure.[226] 2,4-diaminopyrimidin-5-ol dihydrochloride **3.6** (0.200 g, 1.005 mmol) was added to a solution of freshly prepared sodium ethoxide (0.069 g, 3.01 mmol of Sodium in 20 mL of absolute ethanol) and the solution was refluxed for 30 min. 1-Bromo-4-(3-bromopropoxy)benzene **3.7** (0.481 g, 1.636 mmol) was then added and the mixture was refluxed under stirring during 48 hrs. After the reaction mixture was cooled down to room temperature and the solvent was removed under reduced pressure. The solid residue was washed with hot DCM, the non-soluble residue was filtrated and discarded, while DCM was removed under reduced pressure. The residue was purified by normal phase column chromatography (gradient EtOAc:MeOH = 100:0 to 80:20, solid loading). The fractions, containing the desired product, were collected and evaporated under reduced pressure. The final product was additionally dried in the oven (100 °C) to remove any solvent impurity. Yield 9% (31.4 mg, 0.093 mmol), off-white amorphous solid, purity ≥ 95%.

_____

¹H NMR (400 MHz, DMSO-*d₆*) δ 7.41-7.47 (m, 3H), 6.90-6.96 (m, 2H), 6.84 (br. s., 2H), 6.05 (br. s., 2H), 4.16 (t, *J*=6.44 Hz, 2H), 3.98 (t, *J*=6.06 Hz, 2H), 2.12 (quin, *J*=6.19 Hz, 2H). **¹³C NMR*** (101 MHz, DMSO-*d₆*) δ 157.8, 157.2, 156.4, 132.1, 132.1, 116.8, 111.8, 66.2, 64.6, 28.5.**ESI-MS (A):** *m/z* 339, 341 [M+H]⁺ (R$_t$ = 1.08 min). **HRMS** (ESI) *m/z* calcd for C$_{13}$H$_{15}$BrN$_4$O$_2$ [M+H]⁺: 339.0451; found: 339.0459. **One aromatic CH signal was not detected, probably overlapping with another one with the same chemical shift. 2D NMR (HSQC and HMBC) did not provide the unambiguous assignment to the signals*

5-(4-Phenylbutoxy)pyrimidine-2,4-diamine (3.10)
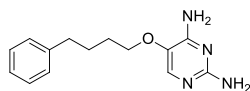
The title compound was prepared analogously to **3.9** from 2,4-diaminopyrimidin-5-ol dihydrochloride **3.6** (0.200 g, 1.005 mmol) and 4-phenyl-1-butylbromide **3.8** (0.407 g, 1.910 mmol). Yield 27% (70.6 mg, 0.273 mmol), off-white amorphous solid, purity ≥ 95%.

¹H NMR (400 MHz, DMSO-*d₆*) δ 7.40 (s, 1H), 7.24-7.31 (m, 2H), 7.12-7.24 (m, 3H), 6.20 (br. s., 2H), 5.51 (s, 2H), 3.82 (t, *J*=5.94 Hz, 2H), 2.62 (t, *J*=6.95 Hz, 2H), 1.62-1.76 (m, 4H). **¹³C NMR** (101 MHz, DMSO-*d₆*) δ 158.0, 156.5, 142.0, 138.2, 132.3, 128.3, 128.2, 125.6, 69.5, 34.8, 28.5, 27.2. **ESI-MS (A):** *m/z* 259 [M+H]⁺ (R$_t$ = 1.05 min).

3-(2-(Trifluoromethyl)phenoxy)propan-1-ol (3.11)
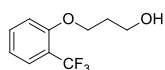
The title compound was prepared according to general method A from 2-(trifluoromethyl)phenol (4.034 g, 24.88 mmol) and 3-bromo-1-propanol (2 mL, 22.12 mmol). Yield 83% (4.292 g, 18.320 mmol).

¹H NMR (400 MHz, CDCl₃) δ 7.55 - 7.61 (m, 1H), 7.46 - 7.53 (m, 1H), 6.98 - 7.05 (m, 2H), 4.22 (t, *J* = 5.90 Hz, 2H), 3.90 (q, *J* = 5.69 Hz, 2H), 2.09 (quin, *J* = 5.83 Hz, 2H), 1.82 (t, *J* = 5.40 Hz, 1H). **ESI-MS (B):** *m/z* 262 [M+CH₃CN+H]⁺, 265 [M+HCOO]⁻ (R$_t$ = 1.71 min).

3-(4-Bromophenoxy)propan-1-ol (3.13)
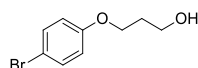
The title compound was prepared according to general method A from 4-bromophenol (7.46 g, 43.1 mmol) and 3-bromo-1-propanol (3 mL, 33.2 mmol). Yield 58% (4.450 g, 19.260 mmol).

¹H NMR (400 MHz, CDCl₃) δ 7.35 - 7.41 (m, 2H), 6.76 - 6.83 (m, 2H), 4.10 (t, *J* = 5.90 Hz, 2H), 3.86 (q, *J* = 5.52 Hz, 2H), 2.05 (quin, *J* = 5.96 Hz, 2H), 1.70 (t, *J* = 4.64 Hz, 1H). **¹³C NMR** (101 MHz, CDCl₃) δ 157.9, 132.3, 116.3, 113.0, 65.8, 60.2, 31.9. **ESI-MS (B):** *m/z* 275, 277 [M+HCOO]⁻ (R$_t$ = 1.70 min).

3-(2-Isopropylphenoxy)propan-1-ol (3.14)
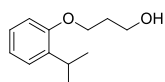
The title compound was prepared according to general method A from 2-isopropylphenol (9.47 g, 69.5 mmol) and 3-bromo-1-propanol (3.62 mL, 40 mmol). Yield 77% (5.972 g, 30.70 mmol).

_____

¹H NMR (400 MHz, CDCl₃) δ 7.24 (dd, *J* = 1.51, 7.53 Hz, 1H), 7.17 (dt, *J* = 1.76, 7.78 Hz, 1H), 6.92 - 6.98 (m, 1H), 6.88 (d, *J* = 8.03 Hz, 1H), 4.14 (t, *J* = 5.77 Hz, 2H), 3.91 (q, *J* = 5.52 Hz, 2H), 3.31 (spt, *J* = 6.90 Hz, 1H), 2.10 (quin, *J* = 5.90 Hz, 2H), 1.82 (t, *J* = 4.52 Hz, 1H), 1.24 (d, *J* = 6.78 Hz, 6H). **ESI-MS (B):** *m/z* 195 [M+H]⁺, 236 [M+CH₃CN+H]⁺ (Rₜ = 1.81 min).

3-(2-(tert-Butyl)phenoxy)propan-1-ol (3.15)
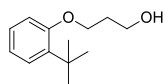
The title compound was prepared according to general method A from 2-*tert*-butylphenol (4.08 mL, 26.5 mmol) and 3-bromo-1-propanol (2 mL, 22.12 mmol). Yield 66% (3.033 g, 14.56 mmol).

¹H NMR (400 MHz, CDCl₃) δ 7.30 (dd, *J* = 1.76, 8.03 Hz, 1H), 7.15 - 7.22 (m, 1H), 6.87 - 6.94 (m, 2H), 4.15 (t, *J* = 6.02 Hz, 2H), 3.94 (t, *J* = 6.15 Hz, 2H), 2.13 (quin, *J* = 6.15 Hz, 2H), 1.56 (s, 1H), 1.40 (s, 9H). **ESI-MS (B):** *m/z* 209 [M+H]⁺(Rₜ = 2.00 min).

6-(3-(4-Bromophenoxy)propoxy)-1,3,5-triazine-2,4-diamine (3.16)
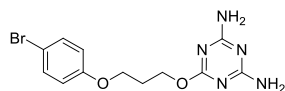
Sodium hydride (60% Wt. in the mineral oil) (0.260 g, 6.49 mmol) was added to a solution of 2-chloro-4,6-diamino-1,3,5-triazine (0.630 g, 4.33 mmol) and 3-(4-bromophenoxy)propan-1-ol **3.13** (1 g, 4.33 mmol) in dry DMSO (3 mL). The solution was stirred for 5 hrs at 100 °C. After the reaction mixture was cooled down to room temperature and the solid residue was filtrated away and washed with MeOH. The organic phases were combined and the solvent was removed under reduced pressure. The residue was diluted with ethyl acetate and the organic phase was washed with brine, dried over Na₂SO₄, filtered and evaporated to dryness. The residue was purified by normal phase column chromatography (gradient DCM:MeOH = 100:0 to 85:15, solid loading). The fractions, containing the desired product, were collected and evaporated under reduced pressure. The final product was additionally dried in the oven (100 °C) to remove any solvent impurity. Yield 0.6% (10.0 mg, 0.028 mmol), off-white amorphous solid, purity ≥ 94%.

¹H NMR (400 MHz, DMSO-*d₆*) δ 7.40-7.48 (m, 2H), 6.88-6.97 (m, 2H), 6.59 (s, 4H), 4.28 (t, *J*=6.44 Hz, 2H), 4.06 (t, *J*=6.19 Hz, 2H), 2.08 (quin, *J*=6.32 Hz, 2H). **¹³C NMR** (101 MHz, DMSO-*d₆*) δ 170.6, 168.3, 157.7, 132.1, 116.7, 111.9, 64.6, 62.2, 28.3. **ESI-MS (A):** *m/z* 340, 342 [M+H]⁺ (Rₜ = 1.08 min). **HRMS** (ESI) *m/z* calcd for C₁₂H₁₄BrN₅O₂ [M+H]⁺: 340.0404; found: 340.0401.

6-(3-(2-Isopropylphenoxy)propoxy)-1,3,5-triazine-2,4-diamine (3.17)
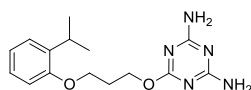
The title compound was prepared analogously to **3.17** from 2-chloro-4,6-diamino-1,3,5-triazine (294 mg, 2.023 mmol), 3-(2-isopropylphenoxy)propan-1-ol **3.14** (393 mg, 2.023 mmol) and sodium hydride (60% Wt. in the mineral oil) (97 mg, 2.428 mmol) refluxing in THF (3 mL) for 5 hrs. The work up was the same as in case of **3.17**. Yield 4.2% (26.1 mg, 0.086 mmol), off-white amorphous solid, purity ≥ 95%.

¹H NMR (400 MHz, DMSO-*d₆*) δ 7.10-7.21 (m, 2H), 6.86-6.96 (m, 2H), 6.57 (s, 4H), 4.33 (t, *J*=6.19 Hz, 2H), 4.06 (t, *J*=6.06 Hz, 2H), 3.17-3.30 (m, 1H), 2.11 (quin, *J*=6.19 Hz, 2H), 1.15 (d, *J*=7.07 Hz, 6H). **¹³C**

NMR (101 MHz, DMSO-*d₆*) δ 170.6, 168.3, 155.5, 136.1, 126.7, 125.7, 120.5, 111.5, 64.2, 62.2, 28.6, 26.3, 22.5. **ESI-MS (A):** *m/z* 304 [M+H]⁺ (Rₜ = 1.13 min).
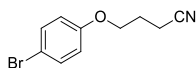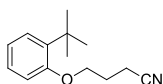
4-(2,4-Dichlorophenoxy)butanenitrile (3.21)
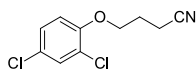
The title compound was prepared according to general method A from 2,4-dichlorophenol (4.26 g, 26.2 mmol) and 4-bromobutyronitrile (2 mL, 20.12 mmol). Yield 91% (4.210 g, 18.30 mmol).

¹H NMR (400 MHz, CDCl₃) δ 7.38 (d, *J* = 2.51 Hz, 1H), 7.20 (dd, *J* = 2.64, 8.66 Hz, 1H), 6.86 (d, *J* = 8.78 Hz, 1H), 4.13 (t, *J* = 5.65 Hz, 2H), 2.67 (t, *J* = 7.03 Hz, 2H), 2.15 - 2.24 (m, 2H). **¹³C NMR** (101 MHz, CDCl₃) δ 152.7, 130.1, 127.7, 126.5, 123.9, 119.0, 114.3, 66.7, 25.4, 14.1. **ESI-MS (B):** *m/z* 274 [M+HCOO]⁻ (Rₜ = 2.00 min).

5-(2,4-Dichlorophenoxy)pentanenitrile (3.22)
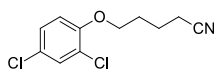
The title compound was prepared according to general method A from 2,4-dichlorophenol (1.815 g, 11.14 mmol) and 5-bromopentanenitrile (1.0 mL, 8.57 mmol). Yield 91% (1.900 g, 7.78 mmol).

¹H NMR (400 MHz, CDCl₃) δ 7.37 (d, *J* = 2.51 Hz, 1H), 7.19 (dd, *J* = 2.51, 8.78 Hz, 1H), 6.83 (d, *J* = 9.04 Hz, 1H), 4.06 (t, *J* = 5.65 Hz, 2H), 2.51 (t, *J* = 6.90 Hz, 2H), 1.89 - 2.07 (m, 4H). **ESI-MS (B):** *m/z* 288 [M+HCOO]⁻ (Rₜ = 2.09 min).

6-(2,4-Dichlorophenoxy)hexanenitrile (3.23)
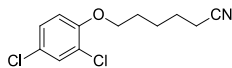
The title compound was prepared according to general method A from 2,4-dichlorophenol (1.475 g, 9.05 mmol) and 6-bromocapronitrile (1 mL, 7.54 mmol). Yield 94% (1.830 g, 7.09 mmol), purity ≥ 90%. 2,4-Dichlorophenol impurity (0.13 eq. by NMR, ~8% Wt.) was detected; the collected product was used for the next reaction step without any further purification.

¹H NMR (400 MHz, CDCl₃) δ 7.37 (d, *J* = 2.51 Hz, 1H), 7.18 (dd, *J* = 2.51, 8.78 Hz, 1H), 6.83 (d, *J* = 8.78 Hz, 1H), 4.02 (t, *J* = 6.02 Hz, 2H), 2.41 (t, *J* = 7.03 Hz, 2H), 1.85 - 1.93 (m, 2H), 1.65 - 1.83 (m, 4H). **ESI-MS (B):** *m/z* 302 [M+HCOO]⁻ (Rₜ = 2.18 min).

4-(4-Bromophenoxy)butanenitrile (3.24)

The title compound was prepared according to general method A from 4-bromophenol (1.671 g, 9.66 mmol) and 4-bromobutyronitrile (0.8 mL, 8.05 mmol). Yield 86% (1.668 g, 6.95 mmol).

¹H NMR (400 MHz, CDCl₃) δ 7.36 - 7.43 (m, 2H), 6.75 - 6.82 (m, 2H), 4.06 (t, *J* = 5.77 Hz, 2H), 2.59 (t, *J* = 7.15 Hz, 2H), 2.09 - 2.21 (m, 2H). **¹³C NMR** (101 MHz, CDCl₃) δ 157.5, 132.4, 119.0, 116.3, 113.5, 65.5, 25.4, 14.2. **ESI-MS (B):** *m/z* not detectable (Rₜ = 1.92 min).

5-(4-Bromophenoxy)pentanenitrile (3.25)
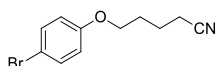
The title compound was prepared according to general method A from 4-bromophenol (1.601 g, 9.25 mmol) and 5-bromovaleronitrile (0.9 mL, 7.71 mmol). Yield 83% (1.617 g, 6.36 mmol).

¹H NMR (400 MHz, CDCl₃) δ 7.34 - 7.42 (m, 2H), 6.73 - 6.81 (m, 2H), 3.98 (t, *J* = 5.65 Hz, 2H), 2.45 (t, *J* = 6.90 Hz, 2H), 1.83 - 2.01 (m, 4H). **ESI-MS (B):** *m/z* 298, 300 [M+HCOO]⁻ (R$_t$ = 2.00 min).

6-(4-Bromophenoxy)hexanenitrile (3.26)
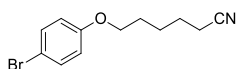
The title compound was prepared according to general method A from 4-bromophenol (1.56 g, 9.02 mmol) and 6-bromocapronitrile (0.6 mL, 4.53 mmol). Yield 71% (0.954 g, 3.20 mmol), purity ≥ 90%. 4-Bromophenol impurity (0.15 eq. by NMR, ~9% Wt.) was detected; the collected product was used for the next reaction step without any further purification.

¹H NMR (400 MHz, CDCl₃) δ 7.35 - 7.41 (m, 2H), 6.75 - 6.80 (m, 2H), 3.95 (t, *J* = 6.15 Hz, 2H), 2.39 (t, *J* = 6.90 Hz, 2H), 1.71 - 1.87 (m, 4H), 1.61 - 1.70 (m, 2H). **ESI-MS (B):** *m/z* not detectable (R$_t$ = 2.10 min)

4-(2-(tert-Butyl)phenoxy)butanenitrile (3.27)

The title compound was prepared according to general method A from 2-*tert*-butylphenol (1.854 mL, 12.07 mmol) and 4-bromobutyronitrile (1 mL, 10.06 mmol). The title compound co-eluted with the starting 2-*tert*-butylphenol (~1:1 mixture by NMR) resulting in the crude mixture (0.520 g), which was used directly for the next reaction step without any further purification.

5-(2-(tert-Butyl)phenoxy)pentanenitrile (3.28)
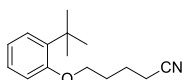
The title compound was prepared according to general method A from 2-*tert*-butylphenol (1.579 mL, 10.28 mmol) and 5-bromopentanenitrile (1.0 mL, 8.57 mmol). The title compound co-eluted with the starting 2-*tert*-butylphenol (~0.19 eq. of impurity by NMR) resulting in the crude mixture (1.900 g), which was used for the next reaction step without any further purification.

¹H NMR (400 MHz, CDCl₃) δ 7.29 - 7.34 (m, 1H), 7.15 - 7.23 (m, 1H), 6.82 - 6.97 (m, 2H), 4.06 (t, *J* = 5.77 Hz, 2H), 2.48 (t, *J* = 6.90 Hz, 2H), 1.92 - 2.10 (m, 4H), 1.40 (s, 9H). **ESI-MS (B):** *m/z* not detectable (R$_t$ = 2.22 min).

6-(2-(tert-Butyl)phenoxy)hexanenitrile (3.29)
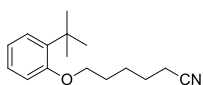
The title compound was prepared according to general method A from 2-*tert*-butylphenol (1.390 mL, 9.05 mmol) and 6-bromocapronitrile (1 mL, 7.54 mmol). Yield 65% (1.200 g, 4.89 mmol).

¹H NMR (400 MHz, CDCl₃) δ 7.30 (dd, *J* = 1.51, 7.78 Hz, 1H), 7.18 (dt, *J* = 1.63, 7.72 Hz, 1H), 6.83 - 6.94 (m, 2H), 4.02 (t, *J* = 6.27 Hz, 2H), 2.37 - 2.44 (m, 2H), 1.87 - 1.95 (m, 2H), 1.66 - 1.84 (m, 4H), 1.40 (s, 9H). **ESI-MS (B):** *m/z* 246 [M+H]⁺ (R_t = 2.38 min).
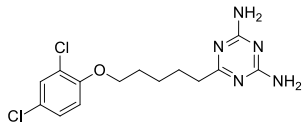
6-(3-(2,4-Dichlorophenoxy)propyl)-1,3,5-triazine-2,4-diamine (3.30)
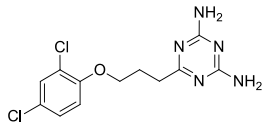
The title compound was prepared according to general method B from 4-(2,4-dichlorophenoxy)butanenitrile **3.21** (552 mg, 2.40 mmol) and cyanoguanidine (242 mg, 2.88 mmol), using potassium hydroxide (673 mg, 12.00 mmol) as a base and water (0.8 mL) as co-solvent. Yield 16% (118.5 mg, 0.377 mmol), white amorphous solid, purity ≥ 95%.

¹H NMR (400 MHz, DMSO-*d₆*) δ 7.55 (d, *J*=2.78 Hz, 1H), 7.36 (dd, *J*=2.78, 8.84 Hz, 1H), 7.17 (d, *J*=9.09 Hz, 1H), 6.58 (br. s., 4H), 4.11 (t, *J*=6.44 Hz, 2H), 2.47-2.54 (m, 2H), 2.03-2.14 (m, 2H). **¹³C NMR** (101 MHz, DMSO-*d₆*) δ 176.9, 167.0, 153.0, 129.2, 128.1, 124.2, 122.3, 115.0, 68.5, 34.1, 26.1. **ESI-MS (A):** *m/z* 314 [M+H]⁺ (R_t = 1.07 min).

6-(4-(2,4-Dichlorophenoxy)butyl)-1,3,5-triazine-2,4-diamine (3.31)
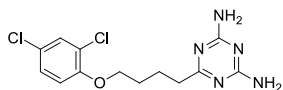
The title compound was prepared according to general method B from 5-(2,4-dichlorophenoxy)pentanenitrile **3.22** (0.700 g, 2.87 mmol) and cyanoguanidine (0.289 g, 3.44 mmol), using potassium hydroxide (0.193 g, 3.44 mmol) as a base and water (0.8 mL) as co-solvent. Yield 27% (250 mg, 0.762 mmol), white amorphous solid, purity ≥ 95%.

¹H NMR (400 MHz, DMSO-*d₆*) δ 7.55 (d, *J*=2.53 Hz, 1H), 7.35 (dd, *J*=2.53, 8.84 Hz, 1H), 7.16 (d, *J*=8.84 Hz, 1H), 6.56 (br. s., 4H), 4.01-4.11 (m, 2H), 2.39 (t, *J*=7.07 Hz, 2H), 1.70-1.83 (m, 4H). **¹³C NMR** (101 MHz, DMSO-*d₆*) δ 177.4, 167.0, 153.0, 129.2, 128.1, 124.2, 122.3, 114.9, 68.7, 37.5, 28.2, 23.4. **ESI-MS (A):** *m/z* 328 [M+H]⁺ (R_t = 1.12 min). **HRMS** (ESI) *m/z* calcd for C₁₃H₁₅Cl₂N₅O [M+H]⁺: 328.0726; found: 328.0724.

6-(5-(2,4-Dichlorophenoxy)pentyl)-1,3,5-triazine-2,4-diamine (3.32)

The title compound was prepared according to general method B from 6-(2,4-dichlorophenoxy)hexanenitrile **3.23** (1.831 g, 7.09 mmol) and cyanoguanidine (0.716 g, 8.51 mmol), using potassium hydroxide (0.478 g, 8.51 mmol) and DMF (1 mL) as co-solvent. Yield 8% (204 mg, 0.595 mmol), white amorphous solid, purity ≥ 95%.

¹H NMR (400 MHz, DMSO-*d₆*) δ 7.55 (d, *J*=2.53 Hz, 1H), 7.35 (dd, *J*=2.53, 8.84 Hz, 1H), 7.15 (d, *J*=8.84 Hz, 1H), 6.53 (br. s., 4H), 4.04 (t, *J*=6.44 Hz, 2H), 2.33 (t, *J*=7.45 Hz, 2H), 1.61-1.81 (m, 4H), 1.44 (m, 2H). **¹³C NMR** (101 MHz, DMSO-*d₆*) δ 177.6, 167.0, 153.1, 129.2, 128.1, 124.2, 122.3, 115.0, 68.8, 37.9, 28.3, 26.7, 25.2. **ESI-MS (A):** *m/z* 342 [M+H]⁺ (R_t = 1.15 min).

_____

### *6-(3-(4-Bromophenoxy)propyl)-1,3,5-triazine-2,4-diamine (3.33)*
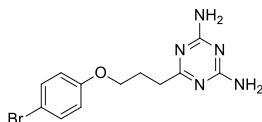
The title compound was prepared according to general method B from 4-(4-bromophenoxy)butanenitrile **3.24** (0.809 g, 3.37 mmol) and cyanoguanidine (0.368 g, 4.38 mmol), using potassium *tert*-butoxide (0.756 g, 6.74 mmol) as a base. Yield 70% (769 mg, 2.372 mmol), white amorphous solid, purity ≥ 95%.

¹H NMR (400 MHz, DMSO-d_6) δ 7.39-7.47 (m, 2H), 6.86-6.93 (m, 2H), 6.57 (br. s., 4H), 3.99 (t, *J*=6.44 Hz, 2H), 2.47 (t, *J*=7.80 Hz, 2H), 2.00-2.09 (m, 2H). **¹³C NMR** (101 MHz, DMSO-d_6) δ 177.0, 167.0, 157.8, 132.1, 116.7, 111.7, 67.3, 34.1, 26.2. **ESI-MS (A):** *m/z* 324, 326 [M+H]⁺ (R$_t$ = 1.03 min).

6-(4-(4-Bromophenoxy)butyl)-1,3,5-triazine-2,4-diamine (3.34)
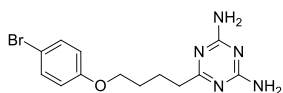
The title compound was prepared according to general method B from 5-(4-bromophenoxy)pentanenitrile **3.25** (0.851 g, 3.35 mmol), cyanoguanidine (0.366 g, 4.35 mmol), using potassium *tert*-butoxide (0.752 g, 6.70 mmol) as a base. Yield 59% (662 mg, 1.957 mmol), white amorphous solid, purity ≥ 95%.

¹H NMR (400 MHz, DMSO-d_6) δ 7.31-7.50 (m, 2H), 6.82-6.96 (m, 2H), 6.55 (br. s., 4H), 3.96 (t, *J*=6.06 Hz, 2H), 2.37 (t, *J*=7.20 Hz, 2H), 1.65-1.81 (m, 4H). **¹³C NMR** (101 MHz, DMSO-d_6) δ 177.4, 167.0, 157.9, 132.1, 116.7, 111.7, 67.5, 37.5, 28.2, 23.5. **ESI-MS (A):** *m/z* 338, 340 [M+H]⁺ (R$_t$ = 1.07 min).

6-(5-(4-Bromophenoxy)pentyl)-1,3,5-triazine-2,4-diamine (3.35)
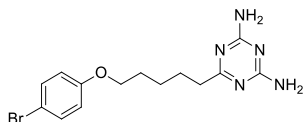
The title compound was prepared according to general method B from 6-(4-bromophenoxy)hexanenitrile **3.26** (0.524 g, 1.954 mmol) and cyanoguanidine (0.214 g, 2.54 mmol), using potassium *tert*-butoxide (0.439 g, 3.91 mmol) as a base. Yield 48% (332 mg, 0.943 mmol), white amorphous solid, purity ≥ 95%.

¹H NMR (400 MHz, DMSO-d_6) δ 7.38-7.46 (m, 2H), 6.85-6.93 (m, 2H), 6.54 (br. s., 4H), 3.93 (t, *J*=6.57 Hz, 2H), 2.33 (t, *J*=7.58 Hz, 2H), 1.61-1.76 (m, 4H), 1.35-1.47 (m, 2H). **¹³C NMR** (101 MHz, DMSO-d_6) δ 177.6, 167.0, 157.9, 132.0, 116.7, 111.7, 67.7, 37.9, 28.4, 26.8, 25.3. **ESI-MS (A):** *m/z* 352, 354 [M+H]⁺ (R$_t$ = 1.11 min).

6-(3-(2-(tert-Butyl)phenoxy)propyl)-1,3,5-triazine-2,4-diamine (3.36)
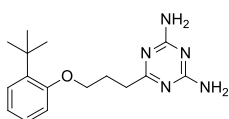
The title compound was prepared according to general method B from the crude mixture containing 4-(2-(*tert*-butyl)phenoxy)butanenitrile **3.27** (0.520 g)and cyanoguanidine (0.241 g, 2.87 mmol), using

_____

potassium hydroxide (0.161 g, 2.87 mmol) as a base and DMF (1 mL) as co-solvent. Yield 35% (250 mg, 0.829 mmol), white amorphous solid, purity ≥ 95%.

^{1}H NMR (400 MHz, DMSO-d_6) δ 7.21 (dd, J=1.64, 7.71 Hz, 1H), 7.11-7.18 (m, 1H), 6.93 (d, J=8.08 Hz, 1H), 6.85 (dt, J=1.01, 7.45 Hz, 1H), 6.58 (br. s., 4H), 4.03 (t, J=6.32 Hz, 2H), 2.53-2.59 (m, 2H), 2.04-2.24 (m, 2H), 1.35 (s, 9H). **^{13}C NMR** (101 MHz, DMSO-d_6) δ 177.0, 167.0, 157.3, 136.9, 127.1, 126.1, 120.0, 112.1, 67.2, 34.9, 34.4, 29.7, 26.7. **ESI-MS (A):** m/z 302 [M+H]$^+$ (R_t = 1.16 min).

6-(4-(2-(tert-Butyl)phenoxy)butyl)-1,3,5-triazine-2,4-diamine (3.37)
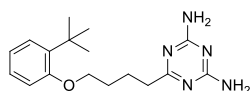
The title compound was prepared according to general method B from the crude mixture containing 5-(2-(*tert*-butyl)phenoxy)pentanenitrile **3.28** (1.350 g) and cyanoguanidine (0.589 g, 7.00 mmol), using potassium hydroxide (0.393 g, 7.00 mmol) as a base and DMF (1 mL as co-solvent). Yield 29% (540 mg, 1.711 mmol), white amorphous solid, purity ≥ 95%.

^{1}H NMR (400 MHz, DMSO-d_6) δ 7.20 (dd, J=1.64, 7.71 Hz, 1H), 7.11-7.17 (m, 1H), 6.94 (dd, J=0.88, 8.21 Hz, 1H), 6.84 (dt, J=1.14, 7.52 Hz, 1H), 6.56 (br. s., 4H), 3.98 (t, J=5.68 Hz, 2H), 2.40 (t, J=6.95 Hz, 2H), 1.74-1.87 (m, 4H), 1.33 (s, 9H). **^{13}C NMR** (101 MHz, DMSO-d_6) δ 177.4, 167.0, 157.4, 137.0, 127.1, 126.1, 119.9, 112.2, 67.2, 37.5, 34.4, 29.7, 28.7, 23.9. **ESI-MS (A):** m/z 316 [M+H]$^+$ (R_t = 1.19 min).

6-(5-(2-(tert-Butyl)phenoxy)pentyl)-1,3,5-triazine-2,4-diamine (3.38)
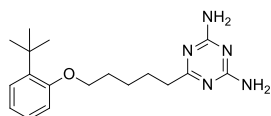
The title compound was prepared according to general method B from 6-(2-(*tert*-butyl)phenoxy)hexanenitrile **3.29** (1.20 g, 4.89 mmol) and cyanoguanidine (0.493 g, 5.87 mmol), using potassium hydroxide (0.329 g, 5.87 mmol) as a base and DMF (1 mL) as co-solvent. Yield 5% (84 mg, 0.253 mmol), white amorphous solid, purity ≥ 95%.

^{1}H NMR (400 MHz, DMSO-d_6) δ 7.20 (dd, J=1.64, 7.71 Hz, 1H), 7.10-7.17 (m, 1H), 6.93 (dd, J=0.88, 8.21 Hz, 1H), 6.84 (dt, J=1.14, 7.52 Hz, 1H), 6.53 (br. s., 4H), 3.96 (t, J=6.32 Hz, 2H), 2.34 (t, J=7.45 Hz, 2H), 1.75-1.84 (m, 2H), 1.70 (quin, J=7.58 Hz, 2H), 1.45-1.55 (m, 2H), 1.32 (s, 9H). **^{13}C NMR** (101 MHz, DMSO-d_6) δ 177.5, 167.0, 157.3, 136.9, 127.1, 126.1, 119.9, 112.0, 67.0, 37.9, 34.4, 29.6, 28.8, 26.7, 25.6. **ESI-MS (A):** m/z 330 [M+H]$^+$ (R_t = 1.23 min).

5-((2,4-Dichlorophenyl)amino)pentanenitrile (3.39)
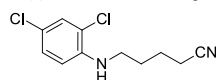
The title compound was prepared according to general method C from 2,4-dichloroaniline (3.89 g, 23.99 mmol) and 5-bromovaleronitrile (1.4 mL, 11.99 mmol). Yield 20% (570 mg, 2.344 mmol).

^{1}H NMR (400 MHz, DMSO-d_6) δ 7.33 (d, J = 2.51 Hz, 1H), 7.16 (dd, J = 2.26, 8.78 Hz, 1H), 6.72 (d, J = 8.78 Hz, 1H), 5.52 (t, J = 5.65 Hz, 1H), 3.11 - 3.20 (m, 2H), 2.51 - 2.56 (m, 2H), 1.58 - 1.67 (m, 4H). **ESI-MS (B):** m/z 243 [M+H]$^+$ (R_t = 2.08 min).

6-((2,4-Dichlorophenyl)amino)hexanenitrile (3.40)
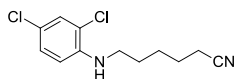
The title compound was prepared according to general method D from 2,4-dichloroaniline (1.613 g, 9.96 mmol) and 6-bromocapronitrile (1.1 mL, 8.30 mmol). Yield 41% (883 mg, 3.43 mmol).

^{1}H NMR (400 MHz, CDCl$_3$) δ 7.24 - 7.29 (m, 1H), 7.12 (dd, *J* = 2.51, 8.78 Hz, 1H), 6.58 (d, *J* = 8.53 Hz, 1H), 3.19 (t, *J* = 7.03 Hz, 2H), 2.39 (t, *J* = 7.03 Hz, 2H), 1.73 (m, 4H), 1.53 - 1.66 (m, 2H). **ESI-MS (B):** *m/z* 257 [M+H]$^+$ (R$_t$ = 2.18 min).

4-((2-(tert-Butyl)phenyl)amino)butanenitrile (3.41)
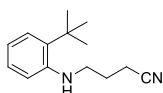
The title compound was prepared according to general method C from 2-*tert*-butylaniline (2.5 mL, 16.03 mmol) and 4-bromobutyronitrile (1.2 mL, 12.07 mmol). The title compound co-eluted with the starting 4-bromobutyronitrile (~0.25 eq. by NMR, 15% Wt.) resulting in the crude mixture (0.426 g), which was used directly for the next reaction step without any further purification.

ESI-MS (B): *m/z* 217 [M+H]$^+$ (R$_t$ = 2.08 min).

5-((2-(tert-Butyl)phenyl)amino)pentanenitrile (3.42)
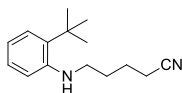
The title compound was prepared according to general method C from 2-*tert*-butylaniline (3.21 mL, 20.56 mmol) and 5-bromovaleronitrile (2 mL, 17.13 mmol). The title compound co-eluted with the starting 4-bromobutyronitrile (~1:1 by NMR), resulting in the crude mixture (2.050 g), which was used directly for the next reaction step without any further purification.

ESI-MS (B): *m/z* 231 [M+H]$^+$, *m/z* 275 [M+HCOO]$^-$ (R$_t$ = 2.17 min).

6-((2-(tert-Butyl)phenyl)amino)hexanenitrile (3.43)
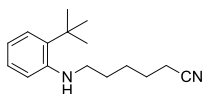
The title compound was prepared according to general method C from 2-*tert*-butylaniline (2.82 mL, 18.10 mmol) and 6-bromocapronitrile (2 mL, 15.09 mmol). The title compound co-eluted with the starting 4-bromobutyronitrile (~1:1 by NMR) resulting in the crude mixture (1.924 g), which was used directly for the next reaction step without any further purification.

ESI-MS (B): *m/z* 245 [M+H]$^+$ (R$_t$ = 2.24 min).

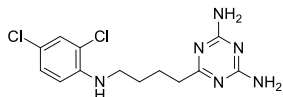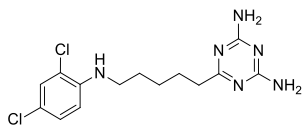### 5-((2,4-Dichlorophenyl)(methyl)amino)pentanenitrile (3.44)
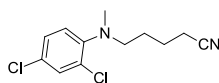
The title compound was prepared according to general method D from *N*-methyl-2,4-dichloroaniline (1.991 g, 11.31 mmol) and 5-bromovaleronitrile (1.1 mL, 9.42 mmol). As no conversion was observed

at room temperature, the reaction was promoted by heating for 6 hrs at 70 °C. The title compound co-eluted with the starting and 5-bromovaleronitrile (~1:1 mixture by NMR), resulting in the crude mixture (0.368 g), which was used directly for the next reaction step without any further purification.

ESI-MS (B): *m/z* 257 [M+H]$^+$ (R$_t$ = 2.14 min).

6-(4-((2,4-Dichlorophenyl)amino)butyl)-1,3,5-triazine-2,4-diamine (3.45)

The title compound was prepared according to general method B from 5-((2,4-dichlorophenyl)amino)pentanenitrile **3.39** (0.352 g, 1.448 mmol) and cyanoguanidine (0.158 g, 1.882 mmol) using potassium *tert*-butoxide (0.325 g, 2.90 mmol) as a base. Yield 62% (294 mg, 0.898 mmol), white amorphous solid, purity ≥ 95%.

^{1}H NMR (400 MHz, DMSO-*d$_6$*) δ 7.32 (d, *J*=2.27 Hz, 1H), 7.16 (dd, *J*=2.53, 8.84 Hz, 1H), 6.69 (d, *J*=8.84 Hz, 1H), 6.55 (br. s., 4H), 5.44 (t, *J*=5.68 Hz, 1H), 3.12 (q, *J*=6.74 Hz, 2H), 2.35 (t, *J*=7.45 Hz, 2H), 1.68 (quin, *J*=7.39 Hz, 2H), 1.49-1.61 (m, 2H). **^{13}C NMR** (101 MHz, DMSO-*d$_6$*) δ 177.5, 167.0, 143.2, 128.1, 127.8, 118.4, 118.0, 111.9, 42.4, 37.6, 27.8, 24.4. **ESI-MS (A):** *m/z* 327 [M+H]$^+$ (R$_t$ = 1.12 min). **HRMS** (ESI) *m/z* calcd for C$_{13}$H$_{16}$Cl$_2$N$_6$ [M+H]$^+$: 327.0886; found: 327.0885.

6-(5-((2,4-Dichlorophenyl)amino)pentyl)-1,3,5-triazine-2,4-diamine (3.46)

The title compound was prepared according to general method B from 6-((2,4-dichlorophenyl)amino)hexanenitrile **3.40** (0.646 g, 2.51 mmol) and cyanoguanidine (0.275 g, 3.27 mmol) using potassium *tert*-butoxide (0.564 g, 5.02 mmol) as a base. Yield 16% (137 mg, 0.401 mmol), white amorphous solid, purity ≥ 95%.

^{1}H NMR (400 MHz, DMSO-*d$_6$*) δ 7.33 (d, *J*=2.53 Hz, 1H), 7.16 (dd, *J*=2.40, 8.72 Hz, 1H), 6.68 (d, *J*=8.84 Hz, 1H), 6.53 (br. s., 4H), 5.39 (t, *J*=5.68 Hz, 1H), 3.10 (q, *J*=6.74 Hz, 2H), 2.32 (t, *J*=7.58 Hz, 2H), 1.50-1.69 (m, 4H), 1.33 (quin, *J*=7.58 Hz, 2H). **^{13}C NMR** (101 MHz, DMSO-*d$_6$*) δ 178.1, 167.5, 143.7, 128.6, 128.3, 118.9, 118.5, 112.4, 43.1, 38.4, 28.6, 27.3, 26.8. **ESI-MS (A):** *m/z* 341 [M+H]$^+$ (R$_t$ = 1.17 min).

6-(3-((2-(tert-Butyl)phenyl)amino)propyl)-1,3,5-triazine-2,4-diamine (3.47)
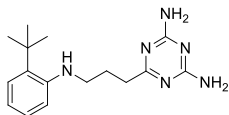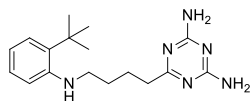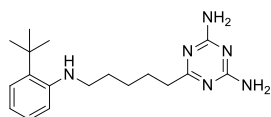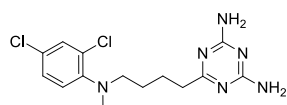

The title compound was prepared according to general method B from the crude mixture (0.426 g) containing 4-((2-(*tert*-butyl)phenyl)amino)butanenitrile **3.41** and cyanoguanidine (0.215 g, 2.56 mmol) using potassium *tert*-butoxide (0.442 g, 3.94 mmol) as a base. Yield 14% (83.2 mg, 0.277 mmol), white amorphous solid, purity ≥ 95%.

^{1}H NMR (400 MHz, DMSO-*d$_6$*) δ 7.10 (dd, *J*=1.52, 7.83 Hz, 1H), 6.97-7.04 (m, 1H), 6.43-6.66 (m, 6H), 4.41 (t, *J*=5.68 Hz, 1H), 3.20 (q, *J*=6.57 Hz, 2H), 2.42 (t, *J*=7.71 Hz, 2H), 1.88-2.01 (m, 2H), 1.34 (s, 9H).

_____

13C NMR (101 MHz, DMSO-d_6) δ 177.4, 167.0, 145.8, 132.5, 126.8, 125.7, 115.7, 111.1, 43.1, 35.9, 33.8, 29.5, 26.2. **ESI-MS (A):** *m/z* 301 [M+H]+ (R$_t$ = 1.10 min).

6-(4-((2-(tert-Butyl)phenyl)amino)butyl)-1,3,5-triazine-2,4-diamine (3.48)

The title compound was prepared according to general method B from the crude mixture containing 5-((2-(*tert*-butyl)phenyl)amino)pentanenitrile **3.42** (0.901 g) and cyanoguanidine (0.428 g, 5.08 mmol) using potassium *tert*-butoxide (0.878 g, 7.82 mmol) as a base. Yield 8% (101 mg, 0.322 mmol), white amorphous solid, purity ≥ 95%.

1H NMR (400 MHz, DMSO-d_6) δ 7.10 (dd, *J*=1.52, 7.83 Hz, 1H), 6.98-7.04 (m, 1H), 6.42-6.64 (m, 6H), 4.29 (t, *J*=5.56 Hz, 1H), 3.15 (q, *J*=6.65 Hz, 2H), 2.37 (t, *J*=7.45 Hz, 2H), 1.67-1.77 (m, 2H), 1.55-1.66 (m, 2H), 1.34 (s, 9H). **13C NMR** (101 MHz, DMSO-d_6) δ 177.6, 167.0, 146.0, 132.4, 126.8, 125.7, 115.7, 111.1, 43.1, 37.7, 33.8, 29.6, 28.4, 24.8. **ESI-MS (A):** *m/z* 315 [M+H]+ (R$_t$ = 1.13 min).

6-(5-((2-(tert-Butyl)phenyl)amino)pentyl)-1,3,5-triazine-2,4-diamine (3.49)

The title compound was prepared according to general method B from the crude mixture containing 6-((2-(*tert*-butyl)phenyl)amino)hexanenitrile **3.43** (0.877 g) and cyanoguanidine (0.392 g, 4.67 mmol) using potassium *tert*-butoxide (0.805 g, 7.18 mmol) as a base. Yield 26% (304 mg, 0.926 mmol), off-white amorphous solid, purity ≥ 95%.

1H NMR (400 MHz, DMSO-d_6) δ 7.10 (dd, *J*=1.52, 7.83 Hz, 1H), 6.97-7.05 (m, 1H), 6.43-6.64 (m, 6H), 4.25 (t, *J*=5.43 Hz, 1H), 3.13 (q, *J*=6.20 Hz, 2H), 2.32 (t, *J*=7.58 Hz, 2H), 1.57-1.72 (m, 4H), 1.29-1.43 (m, 2H), 1.33 (s, 9H). **13C NMR** (101 MHz, DMSO-d_6) δ 177.6, 167.0, 146.0, 132.4, 126.8, 125.7, 115.8, 111.0, 43.1, 37.9, 33.8, 29.6, 28.4, 26.8, 26.5. **ESI-MS (A):** *m/z* 329 [M+H]+ (R$_t$ = 1.18 min).

6-(4-((2,4-Dichlorophenyl)(methyl)amino)butyl)-1,3,5-triazine-2,4-diamine (3.50)

The title compound was prepared according to general method B from the crude mixture containing 5-((2,4-dichlorophenyl)(methyl)amino)pentanenitrile **3.44** (0.368 g, 1.431 mmol) and Cyanoguanidine (0.156 g, 1.860 mmol) using potassium *tert*-butoxide (0.321 g, 2.86 mmol) as a base. Yield 2.4% (12 mg, 0.034 mmol), off-white amorphous solid, purity ≥ 95%.

1H NMR (400 MHz, DMSO-d_6) δ 7.49 (d, *J*=2.27 Hz, 1H), 7.32 (dd, *J*=2.53, 8.59 Hz, 1H), 7.16 (d, *J*=8.59 Hz, 1H), 6.53 (br. s., 4H), 2.97 (t, *J*=7.30 Hz, 2H), 2.67 (s, 3H), 2.31 (t, *J*=7.45 Hz, 2H), 1.61 (quin, *J*=7.45 Hz, 2H), 1.45-1.55 (m, 2H). **13C NMR** (101 MHz, DMSO-d_6) δ 177.5, 167.0, 148.7, 129.6, 128.3, 127.6, 126.1, 122.8, 54.6, 40.4, 37.7, 26.4, 24.4. **ESI-MS (A):** *m/z* 341 [M+H]+ (R$_t$ = 1.14 min). **HRMS** (ESI) *m/z* calcd for $C_{14}H_{18}Cl_2N_6$ [M+H]+: 341.1043; found: 341.1042.
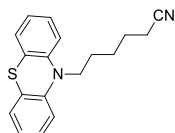
5-(10H-phenothiazin-10-yl)pentanenitrile (3.51)
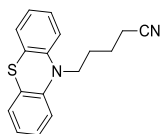
The title compound was prepared according to general method D from phenothiazine (2.048 g, 10.28 mmol) and 5-bromovaleronitrile (1 mL, 8.57 mmol). Yield 84% (2.025 g, 7.220 mmol).

¹H NMR (400 MHz, CDCl₃) δ 7.15 - 7.22 (m, 4H), 6.92 - 7.00 (m, 2H), 6.89 (d, *J* = 8.28 Hz, 2H), 3.96 (t, *J* = 6.27 Hz, 2H), 2.35 (t, *J* = 7.03 Hz, 2H), 1.92 - 2.04 (m, 2H), 1.74 - 1.87 (m, 2H).
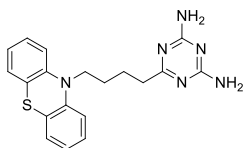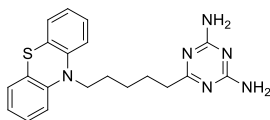
6-(10H-phenothiazin-10-yl)hexanenitrile (3.52)

The title compound was prepared according to general method D from phenothiazine (1.804 g, 9.05 mmol) and 6-bromocapronitrile (1.0 mL, 7.54 mmol). Yield 35% (781 mg, 2.650 mmol).

¹H NMR (400 MHz, DMSO-*d₆*) δ 7.17 - 7.23 (m, 2H), 7.15 (dd, *J* = 1.38, 7.66 Hz, 2H), 7.02 (d, *J* = 8.03 Hz, 2H), 6.94 (dt, *J* = 0.88, 7.47 Hz, 2H), 3.87 (t, *J* = 6.90 Hz, 2H), 2.45 (t, *J* = 6.90 Hz, 2H), 1.71 (quin, *J* = 7.15 Hz, 2H), 1.44 - 1.61 (m, 4H).

6-(4-(10H-phenothiazin-10-yl)butyl)-1,3,5-triazine-2,4-diamine (3.53)

The title compound was prepared according to general method B from 5-(10*H*-phenothiazin-10-yl)pentanenitrile **3.51** (0.452 g, 1.612 mmol) and cyanoguanidine (0.176 g, 2.096 mmol) using potassium *tert*-butoxide (0.362 g, 3.22 mmol) as a base. Yield 44% (258 mg, 0.709 mmol), white amorphous solid, purity ≥ 95%.

¹H NMR (400 MHz, DMSO-*d₆*) δ 7.16-7.23 (m, 2H), 7.13 (dd, *J*=1.52, 7.58 Hz, 2H), 7.00 (d, *J*=7.83 Hz, 2H), 6.88-6.97 (m, 2H), 6.55 (br. s., 4H), 3.87 (t, *J*=6.44 Hz, 2H), 2.34 (t, *J*=7.07 Hz, 2H), 1.62-1.83 (m, 4H). **¹³C NMR** (101 MHz, DMSO-*d₆*) δ 177.4, 167.0, 144.7, 127.6, 127.1, 123.4, 122.4, 115.7, 46.3, 37.3, 25.8, 24.2. **ESI-MS (A):** *m/z* 365 [M+H]⁺ (R$_t$ = 1.15 min).

6-(5-(10H-phenothiazin-10-yl)pentyl)-1,3,5-triazine-2,4-diamine (3.54)

The title compound was prepared according to general method B from 6-(10*H*-phenothiazin-10-yl)hexanenitrile **3.52** (0.401 g, 1.362 mmol) and cyanoguanidine (0.149 g, 1.771 mmol) using potassium *tert*-butoxide (0.306 g, 2.72 mmol) as a base. Yield 57% (293 mg, 0.774 mmol), white amorphous solid, purity ≥ 95%.

_____

¹H NMR (400 MHz, DMSO-d_6) δ 7.17-7.23 (m, 2H), 7.14 (dd, *J*=1.39, 7.71 Hz, 2H), 7.00 (d, *J*=7.58 Hz, 2H), 6.93 (dt, *J*=0.88, 7.52 Hz, 2H), 6.53 (br. s., 4H), 3.84 (t, *J*=7.07 Hz, 2H), 2.28 (t, *J*=7.58 Hz, 2H), 1.55-1.76 (m, 4H), 1.34-1.47 (m, 2H). **¹³C NMR** (101 MHz, DMSO-d_6) δ 177.5, 167.0, 144.7, 127.6, 127.1, 123.6, 122.4, 115.8, 46.4, 37.9, 26.7, 26.2, 26.1. **ESI-MS (A):** *m/z* 379 [M+H]⁺ (R$_t$ = 1.19 min).

_____

_____

4. DprE1 inhibitors: scaffold selection and project objectives

4.1 DprE1 as a drug target in *M. tuberculosis*

In 2009 a new antimycobacterial family of 1,3-benzothiazin-4-ones (BTZs) was described by Makarov V. *et al.*[229] Using genetic and biochemistry approaches, they identified DprE1, the flavoprotein subunit of decaprenylphosphoryl-β-D-ribose-2'-epimerase, as the main BTZ target. BTZ and several analogues were then demonstrated to be covalent suicide inhibitors of DprE1.[230–234]

Since then, DprE1 has been established as a highly-promising druggable target for antimycobacterial research. Numerous compound series based on structurally different chemical scaffolds have been reported to inhibit DprE1 either in an irreversible covalent or reversible non-covalent mode.[235–243] A comprehensive review of various DprE1-inhibitors as anti-TB agents and their binding modes was recently published by Chikhale, R. *et al.*[244]

Benzothiazinones BTZ043 and macozinone (MCZ, PBTZ-169), carbostyril OPC-167832, and azaindole TBA-7371 have entered the early clinical development phase (Figure 4.1).[152,245] All antituberculosis drugs currently in the clinical trials pipeline are listed in Section 1.5.6.

BTZ043   **macozinone**   **OPC-167832**   **TBA-7371**
                (MCZ, PBTZ-169)
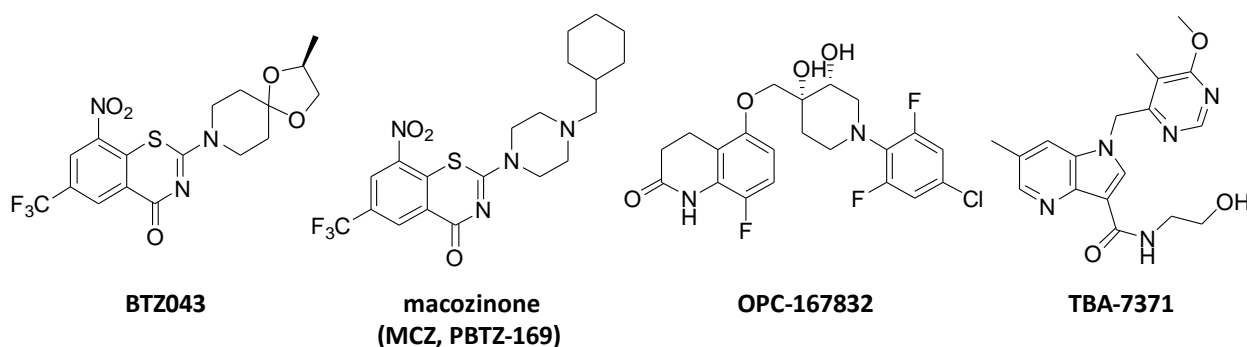
Figure 4.1. Chemical structures of the DprE1 inhibitors in clinical trials.[152]

DprE1 is a flavoprotein enzyme that catalyzes a key epimerization step in the decaprenyl-phosphoryl D-arabinose (DPA) pathway. DPA is the only known donor of arabinose residues in bacteria for the synthesis of arabinogalactan and lipoarabinomannan, two essential components of the mycobacterial cell wall.[246] More specifically, DprE1 causes the FAD-dependent oxidation of decaprenylphosphoryl-D-ribose (DPR) to the corresponding keto-intermediate, decaprenylphosphoryl-2-ketoribose (DPX). The latter is subsequently reduced by the enzyme DprE2 to DPA, relying on NADH as a cofactor (Figure 4.2).[247–249]

Inhibition of DprE1 interrupts the cell wall biosynthesis, leading to mycobacteria death. The periplasmic localization of DprE1 makes the enzyme more accessible to drugs and might be a crucial factor that explains the remarkable vulnerability of the target for mycobacteria.[247] Drugs targeting DprE1 do not have to enter the cytoplasm to exert their effects on the enzyme, therefore escaping the action of the efflux pumps and potential cytoplasmic inactivation mechanisms that might confer intrinsic resistance.
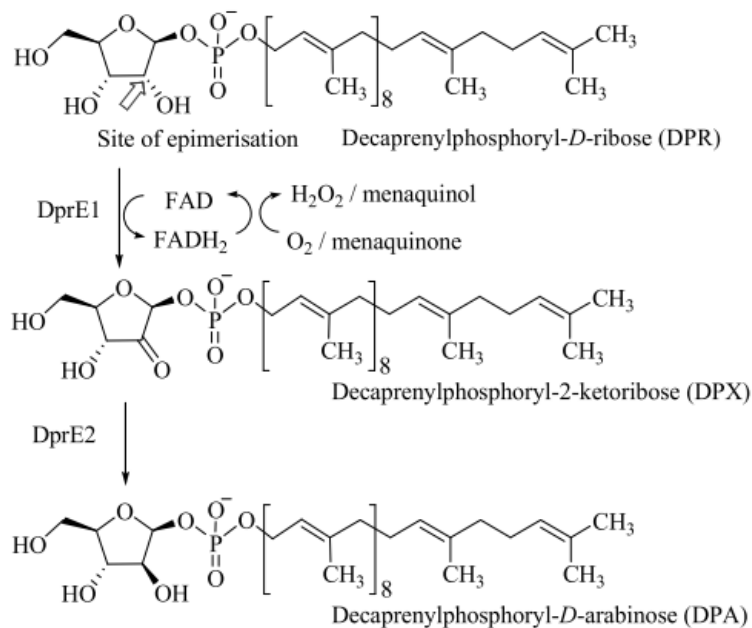
Figure 4.2. Epimerization of 2'-OH group of ribose by DprE1 and DprE2 into arabinose in the presence of cofactor FAD. The arrow indicates the site of epimerization. Adapted from the publication by Chikhale, R. *et al.*, 2018.[244]

4.2 Target-based HTS for DprE1 inhibitors performed by GSK

Recently GlaxoSmithKline (GSK) performed a target-based high-throughput screening (HTS) campaign in search of novel DprE$_1$ inhibitors. More than 1.8 million compounds were evaluated in a fluorescence-based biochemical assay. Based on the primary results obtained, ~4000 compounds were progressed to dose-response studies which allowed preliminary pIC$_{50}$ estimation and hit ranking based on potency and ligand efficiency. In order to reconfirm (or dismiss) the primary hits, the RapidFire™ assay was performed subsequently. It is an orthogonal mass spectrometry assay, which allows monitoring based directly on an intrinsic compound property (m/z) without the risk of fluorescence interference, providing therefore an attractive screening alternative to fluorescent assays.[250,251]

The confirmed hits, which showed DprE$_1$ inhibitory activity in both assays, were then profiled further with several physicochemical and *in vitro* properties evaluated. The selected compounds were clustered into chemical families based on their structural similarity. At that point, an analogue search was performed within the GSK compound library. Identified structurally related analogues were evaluated for their DprE$_1$ inhibitory activity to allow preliminary SAR indications. For each chemical family, the potential risk evaluation (PAINS, reactive moieties, etc.) was performed, and the synthetic accessibility was addressed.

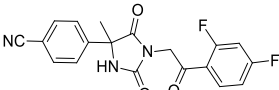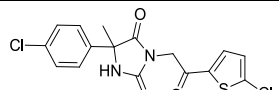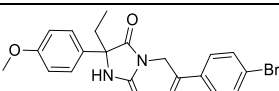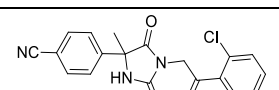The clusters were prioritized based on all the set of parameters:
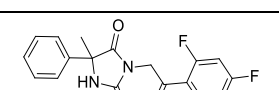
- DprE$_1$ inhibitory activity pIC$_{50}$ ≥ 5 (preferably ≥ 6);
- Whole-cell potency MIC ≤ 50 µM;
- Cytotoxicity HepG$_2$ IC$_{50}$ > 100 µM or ratio HepG$_2$ IC$_{50}$/MIC > 10;
- Chrom logD ≤ 5.

_____

4.3 Hydantoins as DprE1 inhibitors: project background

A novel hydantoin-based family of antimycobacterials was discovered as a promising hit series in the above-mentioned target-based HTS. The hydantoin derivative **4.1** possessed strong DprE$_1$ enzymatic inhibition activity (pIC$_{50}$ = 6.8) as well as very promising whole-cell potency (MIC = 8.3 µM) (Table 4.1). Overall, compound **4.1** demonstrated an encouraging hit profile with no detectable cytotoxicity in HepG$_2$ assay coupled with satisfactory solubility and lipophilicity.

An analogue search revealed 11 congeners with DprE$_1$ pIC$_{50}$ > 4 inside the cluster. Due to the small number of closely related structures tested, only a limited structure-activity relationship (SAR) was obtained. All the initial cluster representatives (Table 4.1) possessed an identical linker, providing no information about modifications allowed in this position. This might indicate the particular importance of the acetophenone linker for activity within the series, although the further investigation was indispensable in order to make any firm conclusions. Several representatives with modifications around aromatic rings preserved significant inhibitory activity (pIC$_{50}$ > 6, Table 4.1), indicating opportunities for further improvement via substituent variation.

Table 4.1. Biological and physicochemical profile of the hydantoin-based compounds from the HTS

	Structure	DprE1 pIC$_{50}$[a]	MIC (µM)[b]	Cytotoxicity HepG$_2$ (µM)[c]	Solubility (µM)[d]	Chrom logD[e]
4.1		6.8	8.3	> 100	202	4.54
4.2		6.4	40	88.1	N.D.	N.D.
4.3		6.8	> 80	49.0	N.D.	N.D.
4.4		6.2	40	> 100	N.D.	N.D.
4.5		4.4	> 80	N.D.	N.D.	N.D.

[a] MtbDprE1 enzyme inhibition pIC$_{50}$; [b] MIC [µM] against Mycobacterium tuberculosis (H37Rv). Reference: Isoniazid, MIC = 1.8 µM; [c] Cytotoxicity HepG$_2$ IC$_{50}$ (µM); [d] kinetic aqueous solubility (CLND) [µM]; [e] ChromlogD (pH 7.4); [f] N.D. – not determined.

The current research forms a part of a collaborative effort on the hit-to-lead investigation of the presented chemical family by GSK with the University of Antwerp in the framework of the FP7 ITN project OpenMedChem. All the compound design and synthesis were performed in a team of three medicinal chemistry Ph.D. students (Olga Balabon, Maciek Rogacki and Eleni Pitta), while all the biochemical and biological evaluations were performed within GSK.[252,253]

4.4 Hydantoins: project objectives

Additional optimization of several different parameters, removal of any potential liabilities, and an extensive SAR investigation was required in order to produce a high-quality lead compound. Therefore,

this series was progressed for the analogues library design and synthesis along with more extensive biological profiling.

4.4.1 Enhanced potency and enzyme affinity and balanced physicochemical profile

In order to be able to progress this compound series into a lead optimization program, it was necessary to obtain very potent DprE1 enzyme inhibitors ($pIC_{50} > 7$) with sub-micromolar whole-cell activity (MIC < 1 µM). Additionally, a more diverse understanding of the SAR was essential to demonstrate the true potential of the series.

The reference compound **4.1** had most of its physicochemical parameters within the acceptable ranges for the initial hit. Nevertheless, some further improvements were desirable to produce a high-quality lead. For instance, compound solubility and a balance between hydrophilicity and lipophilicity were to be monitored in the course of the H2L program. Drug candidates with chromlogD ≤ 4 are typically observed to have reduced possibility of non-specific compound binding, better solubility, and slower intrinsic clearance when compared to more lipophilic analogues. In contrast, very low values of chromlogD in highly hydrophilic compounds can potentially result in permeability and bioavailability issues.[254]

4.4.2 Removal of potential liabilities

The initial hit **4.1** possesses in its structure two moieties with potential safety and metabolic stability liabilities (Figure 4.3): (1) the acetophenone fragment (in blue) and (2) the carbonitrile group (in magenta).
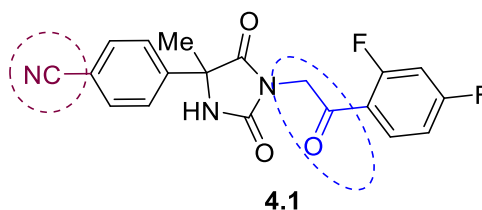

Figure 4.3. Potential liabilities present in the reference hit 4.1

Notably, the aromatic ketone in the linker could contribute to increased metabolic instability of the compounds and potential non-specific covalent binding due to its intrinsic chemical reactivity. Moreover, the activated methylene group adjacent to the keto-function was considered potentially susceptible to oxidative metabolism. Therefore, in order to assess this possible series liability, a number of compounds with different linker modifications were synthesized and evaluated within the OpenMedChem project. Additionally, several analogues were tested for *in vitro* metabolic stability in human and murine microsomes (results are described in Section 7.1.4).

Aliphatic and aromatic carbonitrile moieties were reported to be able to react covalently with cysteine residues in proteins, resulting in thiazoline derivative formation.[255] This potential reactivity may lead to undesirable off-target covalent binding, toxicity, and idiosyncratic reactions.[256] Comparison of the hit **4.1** with its closely related analogue **4.5** indicated the importance of the carbonitrile substituent as the unsubstituted anologue **4.5** proved to be completely inactive. Although there exist several clinically approved carbonitrile-containing drugs, its replacement in the series would lower the potential risks of nonspecific covalent binding. This would provide a decreased risk of undesirable side effects, especially pressing for the lengthy anti-tuberculosis treatments that imply the possibility of

accumulated chronic toxicity. To tackle this point, several compounds with cyano-group replacements in ring A were synthesized, and their biological evaluation results are described in Section 5.2.2.

4.4.3 In vivo proof of concept

The final goal of this hit-to-lead optimization project was to obtain an *in vivo* proof of concept, namely the statistically significant reduction of tuberculosis burden in an *in vivo* murine model of *M. tuberculosis* infection, available at GSK. A few compound representatives with the best overall profile were to be selected for their *in vivo* efficacy evaluation.

4.5 Hydantoins: library design

In order to reach the established project objectives, the hit-to-lead (H2L) optimization process was divided into two rounds. The compound library preparation was based on iterative cycles of structure design, followed by compound synthesis and evaluation. The initial hit **4.1** or the most closely-related analogue were used as a reference for a direct comparison of the corresponding biological results. The design of new compounds typically included modifications to one or two parts of the reference molecule per time. For organizational purposes, the structure of **4.1** was divided into five main moieties, as shown in Figure 4.4:

1. Ring A
2. Hydantoin core
3. Core substituent (methyl)
4. Linker
5. Ring B
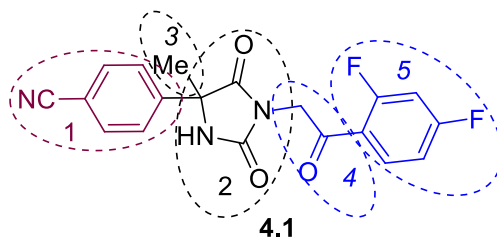
Figure 4.4. The formal structure division of the compound 4.1 into 5 parts

During the initial assessment of the compound series, our attention was focused on the evaluation of the potential liabilities, present in the initial hit **4.1** (Section 4.4.22), and their removal together with collecting primary SAR information. The results of the first round of the Hit-to-Lead (H2L) investigation are described in Chapter 5.

The most promising compounds, prepared within the first round, were selected for further investigation in course of the second round of the H2L program (described in Chapter 6). In particular, an extensive SAR exploration was performed on ring B along with introduction of some additional ring A and linker modifications.

Investigation of compound mode of action, selectivity and metabolic stability is described in detail in Chapter 7.1. The hit compound **4.1** and all other analogues were evaluated as racemates. An enantiomeric separation was performed for some analogues in order to investigate the contribution of each enantiomer to the overall activity (see section 7.1.3).

5. Hydantoins as DprE1 inhibitors: first round of Hit-to-Lead optimization

5.1 Compound design and synthesis

This chapter describes the results of the first round of Hit-to-Lead optimization of hydantoin-based DprE1 inhibitors. The introduced modifications mostly addressed the potential liabilities of the initial hit **4.1** together with exploration of wider chemical space around it, in particular including (Figure 5.1):

- *Modifications of the linker*:
  - elongation or shortening of the linker
  - removal or replacement of the keto-group
- *Side chain modifications*:
  - introduction of iso-propyl or proton substituents instead of methyl side-chain
- *Ring A modifications*:
  - replacement of cyano-group in *4*-position.
  - substitution pattern variation
  - introduction of heterocycles
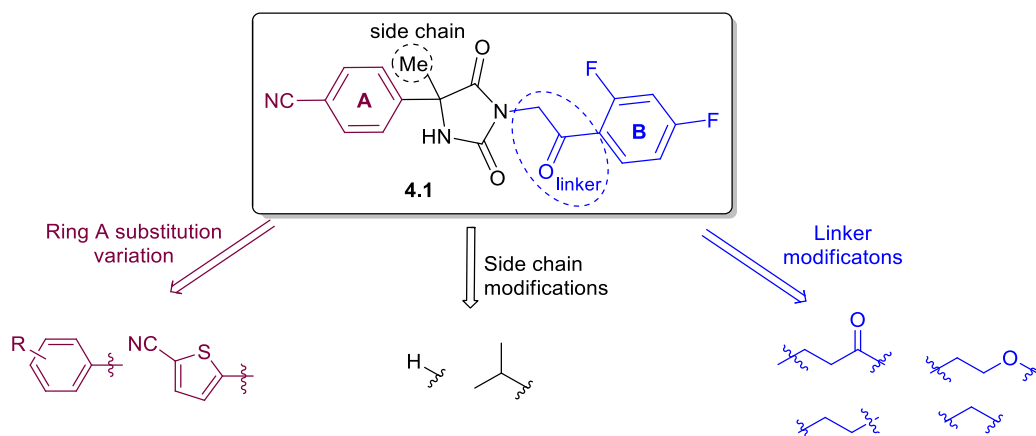
Figure 5.1. Compound design for the first round Hit-to-Lead optimization

In the course of this first round of hit-to-lead (H2L) optimization, a total of around 100 compounds with these modification types were synthesized and evaluated under the OpenMedChem project. Around 30 of these analogues (designed and synthesized by Olga Balabon) are described in this thesis in detail. The biological results for some relevant analogues, evaluated within the OpenMedChem project, will be discussed as well.

5.1.1 Linker modifications

Our initial structural analysis of hit **4.1** pointed to the acetophenone linker moiety as a potential liability of the series due to its potential for poor metabolic stability. As a result, in the beginning we focused effort on assessing the importance of this part of the molecule for the series activity.

In order to explore a broader part of chemical space, we decided to perform the linker modifications on the precursors with several different substituents in ring A. More specifically, R_1 = 4-CN substitution was kept as a direct analogue of the initial hit **4.1**. Together with 4-Cl, it probes the importance of the electron withdrawing groups (EWG) in this part of the molecule. In contrast, the 4-OMe and 4-Me substitutions were exploited as examples of electron donating groups (EDG).

This chapter mainly covers compounds with R_1 = 4-Me substitution in the ring A and additional modifications on the hydantoin ring's side chain (R_2 = Me to *i*-Pr, H), summarized in Figure 5.2. Analogues with elongated linker and carbonyl group removal were prepared. The hydantoin acylation was explored as well. In majority of the cases, the 4-fluoro substituted ring B (R_3 = H) was introduced as a surrogate for the corresponding 2,4-difluoro substitution present in reference **4.1**. Commercial availability of the of the 4-fluorinated chemical building blocks required for synthesis (*vide infra*) was a decisive factor to choose this surrogate.
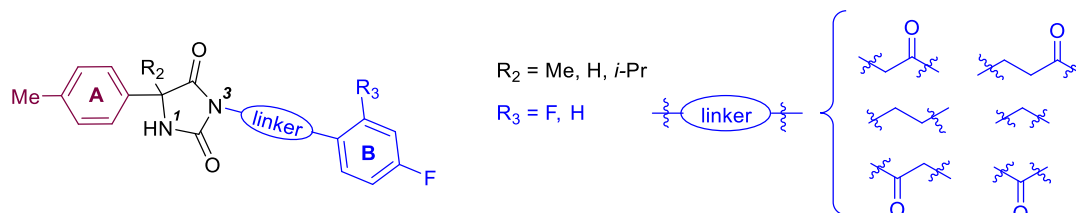
Figure 5.2. Overview of linker modifications for compounds with R_1 = 4-Me substitution in the ring A

Additionally, I prepared two examples with R_1 = CN (compounds **5.30**-**5.31**) which are described herein.

A two-step synthesis was used in order to introduce different linker modifications. First, the hydantoin core was synthesized, followed by its alkylation with different alkyl halides (Scheme 5.1). This synthetic approach allowed late-stage introduction of different linkers using common precursor. The initial hydantoin **5.1** was synthesized according to a modified Bucherer–Bergs synthesis (*vide infra*, Section 5.1.2), while the precursors **5.2**-**5.3** were available in house and were used directly. The final compounds **5.9**-**5.19** with modified linkers were prepared by alkylation of **5.1**-**5.3** with alkyl halides **5.4**-**5.8** in the presence of potassium carbonate as a base according to a literature procedure (Scheme 5.1)[257].

Scheme 5.1. Synthesis of compounds 5.9-5.19 with linker modifications
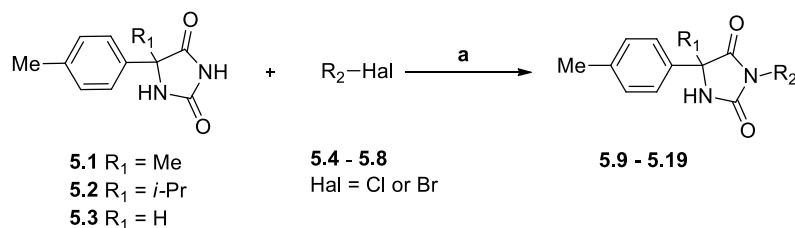
	$R_1 =$		
	Me	*i*-Pr	H
$R_2 =$			
	5.9	**5.14**	**5.19**
	5.10	**5.15**	-
	5.11	**5.16**	-

_____

|			
	5.12	**5.17**	-
	5.13	**5.18**	-
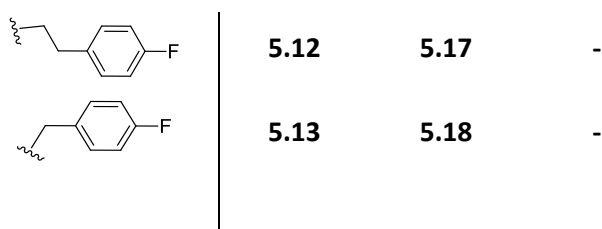
Reagents and conditions: (a) K_2CO_3, DMF or acetone, r.t., 20-72 hrs

First, compounds **5.9, 5.14, 5.19** as well as **5.10, 5.15** were synthesized for direct comparison purposes, preserving the same linker as in the initial hit **4.1**. Introduction of linker elongation led to products **5.11** and **5.16**, while in compounds **5.12-5.13**, **5.17-5.18** the linker carbonyl group was removed. In case of compounds **5.9-5.19** the alkylation occurred selectively at the N-3 position under the reported conditions. The unambiguous structural assignment was carried out by means of 2D NMR spectroscopy (as described in Section 5.2).

While alkylation of precursors **5.1**-**5.2** with different alkyl halides did not present any major synthetic issues, **5.3** (R_1 = H) alkylation with **5.7** and **5.8** resulted in complex mixture formation, and the desired products were never obtained. Surprisingly, the only product isolated in the reaction of **5.3** with **5.6** demonstrated the substitution of C-5 on the hydantoin ring (compound **5.21**), while no expected *N-3* alkylated product **5.20** was obtained (Scheme 5.2). The mechanism of the transformation was not explored but it was hypothesized that the R_1 = H permits the enol formation at C-5 from the carbonyl CO-4, leading to alkylation at the C-5 position.

Scheme 5.2. Formation of unexpected C-5 substituted product on alkylation of the hydantoin 5.3
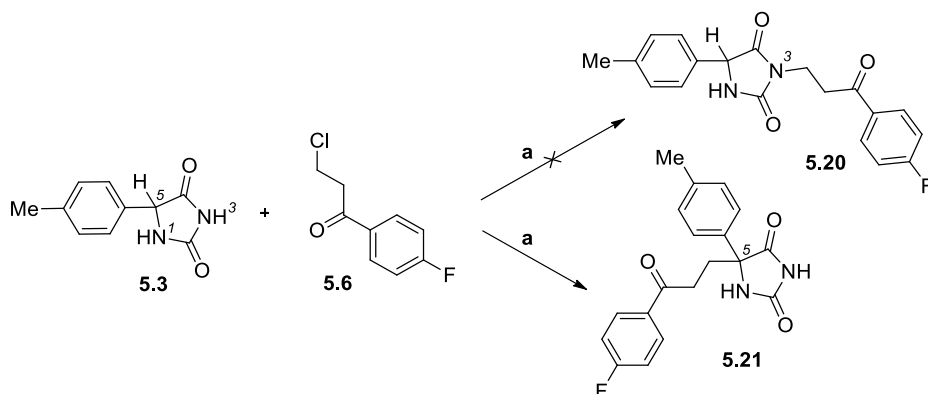
Reagents and conditions: (a) K_2CO_3 or Et_3N, acetone, r.t., 24 hrs

Acylation of the hydantoin **5.3** with the acyl chlorides **5.22** and **5.23** was also performed as shown in Scheme 5.3. In both cases, only the *N-1* acylated products **5.26**, **5.27** were isolated (see Section 5.2 for the NMR assignment details). No desired *N-3* acylated compounds (**5.24**, **5.25**) were detected. The observed regioselectivity could possibly be explained by the expected instability of the *N-3* acylated compounds **5.24**-**5.25**, in which three carbonyl groups would have been attached on the same nitrogen atom. This hypothesis is supported by the finding that an analogous *N-3* acylated compound, (synthesized by a fellow researcher using a different approach) showed to be very prone to hydrolysis.[258]

Scheme 5.3. Acylation of hydantoin 5.3
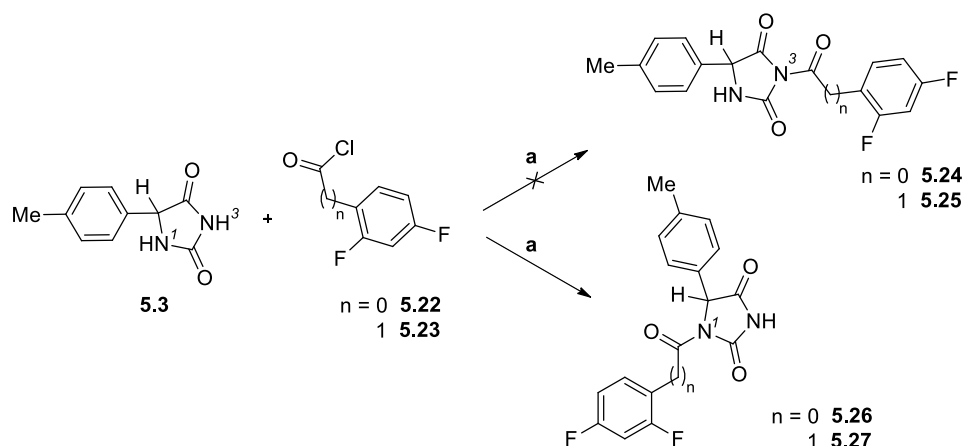
Reagents and conditions: (a) Et$_3$N, DMAP, DCM, r.t., 24 hrs

Two selected direct analogues of the initial hit **4.1** (R$_1$ = CN) with linker variations (**5.30**, **5.31**) were also prepared within this research as shown in Scheme 5.4. The intermediate **5.29**, obtained in two steps from 2,4-difluorophenol, reacted with **5.28** in presence of sodium hydride as a base to provide the final compound **5.30** in an extremely low yield. The alkylation of hydantoin **5.28** with **5.6** resulted in the formation of the desired *N-3* alkylated product **5.31** (in low yield) together with the unexpected *N-1* alkylated side-product **5.32** (Scheme 5.4). The considerable and distinctive difference in the NH chemical shifts of **5.31** and **5.32** was observed in ^{1}H NMR (see more on the alkylation position determination in Section 5.2). Analogous *N-1* alkylated compounds were not isolated previously under similar conditions (*vide supra*).

Scheme 5.4. Preparation of selected 4-CN substituted analogues with linker variation
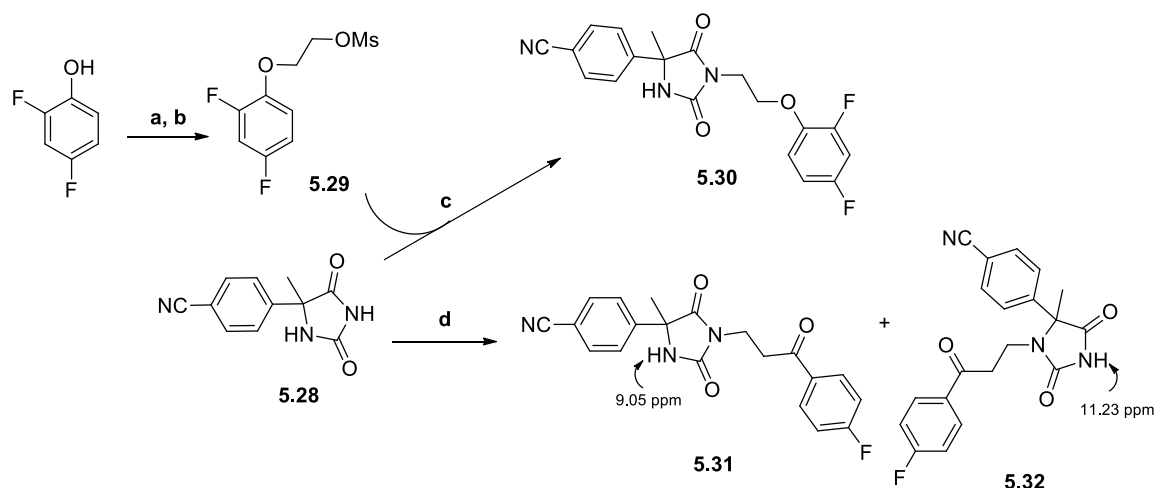
Reagents and conditions: (a) 2-bromoethanol, K$_2$CO$_3$, ACN, MicroWave 100 °C, 2 hrs; (b) MeSO$_2$Cl, Et$_3$N, DCM, 0 °C→r.t., 24 hrs; (c) NaH, DMF, r.t., 72 hrs; (d) **5.6**, Cs$_2$CO$_3$, DMC, r.t., 72 hrs, product ratio 5.31 to 5.32 is approximately 1:3.

5.1.2 Ring A substitution modifications

In this section a number of compounds with substitution pattern variation in the ring A are described in detail. Additional ring A modifications were explored by other OMC team researchers and their synthesis is reported elsewhere.[259] All these analogues were intended to provide in-depth SAR data for this part of the molecule.

It was found that in the majority of cases the late-stage introduction of the ring A modifications was not feasible. Therefore, every new analogue with diversity in ring A required a separate hydantoin core synthesis step, followed but alkylation with an alkyl halide. The adopted two-step synthetic approach is summarized in Scheme 5.5.

Scheme 5.5. Synthesis of compounds with ring A substitution modifications
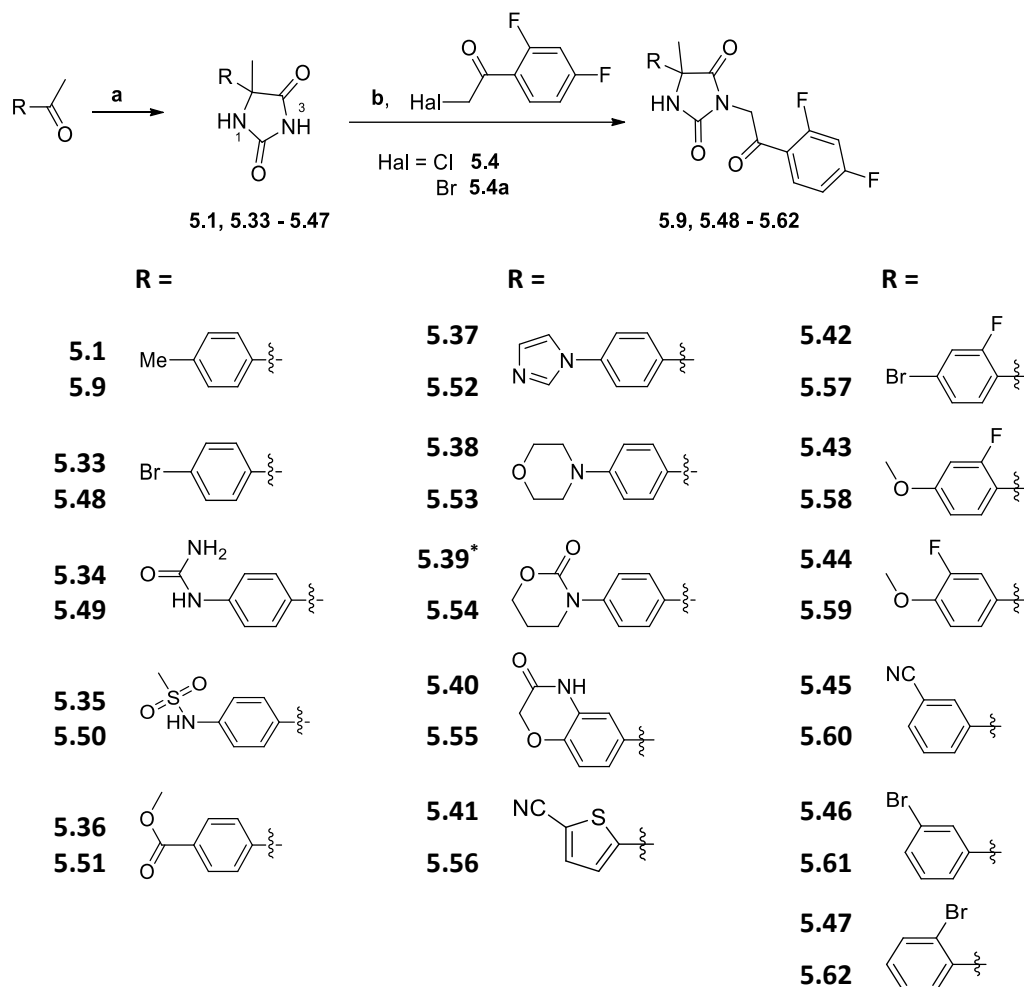
Reagents and conditions: (a) KCN, $(NH_4)_2CO_3$, EtOH-H_2O, MicroWave 70 °C or heating 55 °C, 7-17 hrs; (b) K_2CO_3, DMF or acetone, r.t., 24-48 hrs. *The main reaction product was the hydantoin sodium salt **5.39a**, used also for the alkylation.*

A variety of synthetic approaches towards the hydantoin core preparation is described in the literature, starting from ketones/aldehydes[260–262], amino acids and their derivatives[263–266], unsubstitued hydantoins[267] or domino reactions from carbodiimides[268]. In the presented research, a modification of the Bucherer–Bergs synthesis was exploited, applying conventional heating[260] or microwave irradiation[262]. A reaction of suitably substituted phenylethanones with potassium cyanide and ammonium carbonate provided the corresponding hydantoins **5.1**, **5.33-5.47**.

The precursor ketones were either commercially available or prepared according to literature procedures (see Section 5.5.2 for the experimental details). The hydantoin intermediates were subsequently alkylated with 2-halo-2',4'-difluoroacetophenones **5.4** or **5.4a** in the presence of potassium carbonate as a base[257], resulting in the final *N-3* alkylated compounds (**5.9**, **5.48-5.62**) in good yields (Scheme 5.5). The alkylation position determination is addressed in Section 5.2.

_____

An extensive SAR analysis was performed in the 4-position of the ring A. Compound **5.48** (4-Br) was prepared as a valuable intermediate, used for further substituent introduction via cross-coupling reactions (*vide infra*, Section 6.1.1). The performed modifications included mostly the introduction of various hydrophilic substituents: urea **5.49**, sulfonamide **5.50**, an ester moiety **5.51**, several polar heterocycles **5.52-5.56**, including a fused bicyclic analogue **5.55**. The thiophene ring introduction in place of the phenyl moiety, while preserving the -CN substituent, led to compound **5.56**, a close heterocyclic analogue of the reference hit **4.1**.

Additional fluorine substituents were introduced into the ring A (**5.57-5.59**) in order to assess their influence on compound activity and physicochemical properties. Shifting a few representative substituents from position 4- to 3-/2- resulted in regioisomers **5.60-5.63**. Compound **5.63** was obtained by late-stage palladium-catalyzed coupling reaction from the corresponding bromo-substituted precursor **5.62** according to a described procedure as shown in Scheme 5.6. [269]

Scheme 5.6. Synthesis of 5.63 by a coupling reaction.
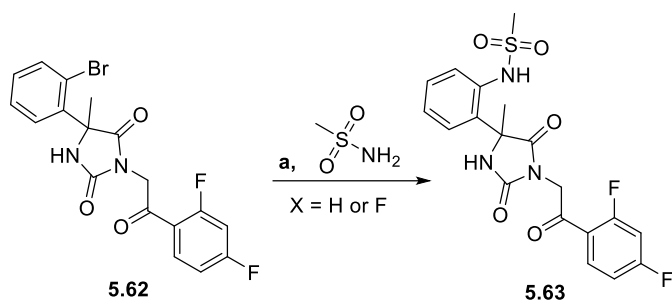
Reagents and conditions: (a) Pd(allyl)Cl]$_2$, *t*-BuXPhos, K$_2$CO$_3$, 2-MeTHF, 80 °C, 2 hrs.

Compounds **5.49**-**5.50**, **5.52** and **5.55** possess in their structure additional nitrogen atoms which could potentially have been reactive in the alkylation step. In fact, in course of **5.50** preparation, complex mixture formation was observed due to an extensive alkylation on the aryl substituted sulfonamide NH in **5.35**, leading to a very low isolated yield (6%) of the desired target product **5.50**. In order to avoid any ambiguity of alkylation position, the full structure assignment of the final products **5.49**-**5.50**, **5.52** and **5.55** was performed by 2D NMR spectroscopy (see Section 5.2).

5.2 Structure Elucidation

Compound **5.10** NMR-assignment is described herein as a characteristic example of the general structure elucidation workflow. The full assignment of ^{1}H and ^{13}C-NMR peaks was performed by 2D NMR (HMQC/HSQC, HMBC), allowing an unambiguous alkylation position determination. In particular, two key cross-peaks of H-1' with C-2 and C-4 detected in the HMBC spectrum were consistent with the *N-3* alkylation product (Figure 5.3A-B). Moreover, the H-1'/C-5 correlation, expected in case of *N-1* alkylation, was not observed.
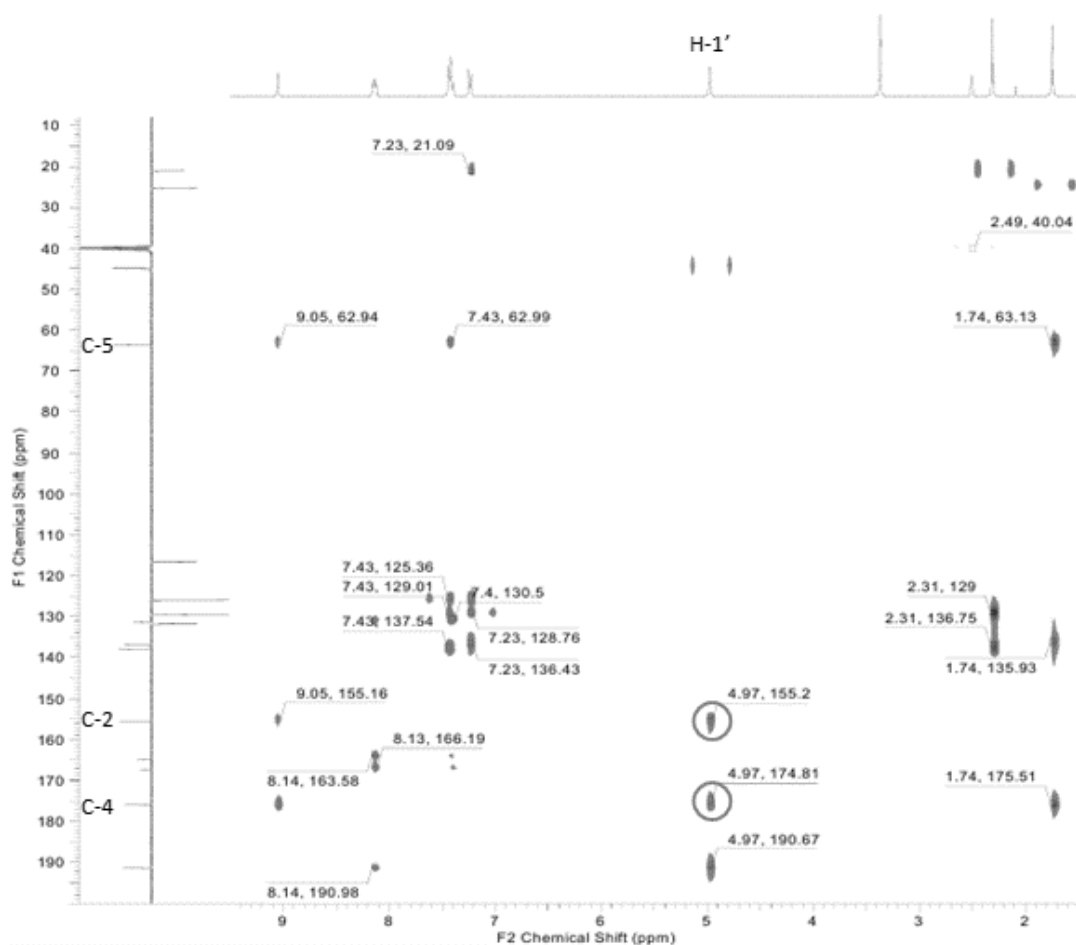
*(A) HMBC spectrum of **5.10**, key correlations are highlighted in red circles*

5.10
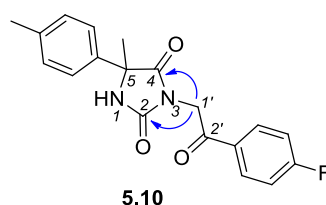
(B) Graphical representation of the relevant HMBC correlations

Figure 5.3 Structure elucidation of 5.10 by means of 2D NMRs

Additionally, ^{1}H NMR of the precursor hydantoin **5.1** showed that both hydantoin amide protons have very different and characteristic chemical shifts: ~8-9 ppm for the amide proton H-1 and ~10-11 ppm in case of H-3 (as shown in Figure 5.4, assigned by 2D NMRs). More acidic OH and NH protons are prone to have higher chemical shifts in ^{1}H NMR due to a deshielding effect, connected with reduced electron density on the nucleus.[270] Hence, the amide proton at N-3 is expected to be more acidic than at N-1 and therefore to be deprotonated first in the presence of a base (potassium carbonate). Moreover, less steric hindrance of N-3 facilitates its alkylation over N-1. This leads to the *N-3* alkylation product formation, in accordance with the obtained experimental results and the literature evidence[257].
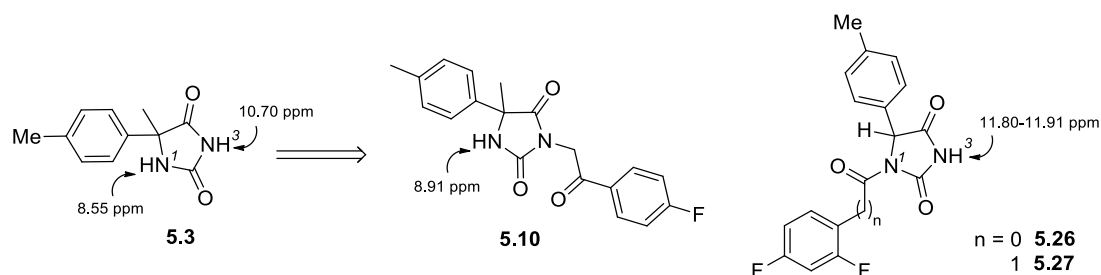
Figure 5.4. ^{1}H NMR shift comparison for amide protons in differently substituted hydantoins

It is worth noting that the chemical shift of the remaining amide proton (H-1) does not change drastically on the hydantoin alkylation, allowing to use its value as an initial indication of the substitution position. For instance, compound **5.10** (Figure 5.4) showed an amide chemical shift of 8.91 ppm, which falls in the expected region for H-1 in case of the *N-3* alkylated products. For a representative example of the NH chemical shifts of the *N-1* vs. *N-3* alkylated products see Scheme 5.4.

In case of acylated products **5.26** and **5.27**, the ^{1}H NMR peak of the amide proton is observed at 11.80 and 11.91 ppm respectively, indicating an undesired *N-1* acylation in both cases (Figure 5.4). And indeed, the *N-1* acylation position was unambiguously proven by HSQC/HMQC and HMBC assignment. The structural assignment was in accordance with results obtained by fellow colleagues.[258]

The ^{1}H NMR of **5.21** showed presence of both amide protons, while no characteristic CH signal was observed. The hydantoin C-5 substitution was proven by 2D NMR.

In case of the final compounds **5.49-5.50**, **5.55**, the correlation of H-1' of the linker CH_2 with both carbonyl groups (C-2 and C-4) was observed in the corresponding HMBC spectra, serving as a proof of the desired *N-3* substitution.
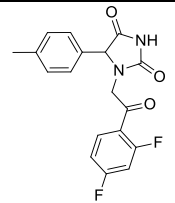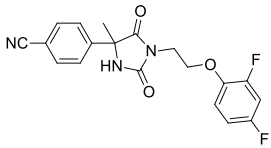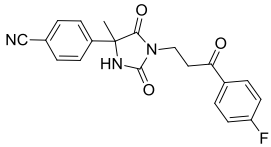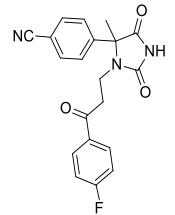
5.3   Results and discussion
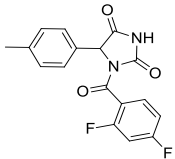
All final compounds were evaluated for their ability to inhibit *Mtb* DprE1 enzymatic activity (pIC$_{50}$-values) and for their ability to inhibit the growth of the *Mtb* H37Rv strain (whole cell MIC-values). In addition, the cytotoxicity in HepG$_2$ cells was evaluated together with two physicochemical parameters: kinetic aqueous solubility (using chemiluminescent nitrogen detection, CLND) and ChromLogD.

5.3.1   Linker modifications

Table 5.1 summarizes the biological evaluation results for the reference compounds with R_1 = 4-Me and their analogues with linker variations (**5.9-5.19**). In addition, the results for the initial hit analogues **5.30**-**5.31** are presented. The unexpected products **5.21**, **5.26**-**5.27**, **5.32** were also evaluated.

Table 5.1. Biological and physicochemical profile of compounds with linker modifications

	Structure	DprE1 pIC$_{50}$[a]	MIC (µM)[b]	Cytotoxicity HepG$_2$ (µM)[c]	Solubility (µM)[d]	Chrom logD[e]
5.9		6.1	80	> 100	213	5.41
5.10		5.2	> 80	> 100	11	5.06
5.11		4.3	> 80	> 100	≥ 395	5.14
5.12		< 4	> 80	> 100	30	5.51
5.13		< 4	> 80	52.7	286	5.39
5.14		< 4	> 80	> 100	343	6.33
5.15		< 4	> 80	77.6	63	5.99
5.16		< 4	> 80	53.9	82	6.11
5.17		< 4	> 80	> 100	< 1	6.55
5.18		< 4	> 80	44.7	48	6.35
5.19		< 4.5	> 80	> 100	283	4.84
5.21		< 4	> 80	> 100	≥ 185	4.37

_____

	Structure	DprE1 pIC$_{50}$[a]	MIC (µM)[b]	Cytotoxicity HepG$_2$ (µM)[c]	Solubility (µM)[d]	Chrom logD[e]
5.26		< 4	> 80	> 100	25	3.69
5.27		< 4	> 80	> 100	71	4.47
5.30		4.4	> 80	> 100	N.D.[f]	N.D.[f]
5.31		4.3	> 80	> 100	≥ 428	4.4
5.32		< 4	> 80	> 100	≥ 424	4.0

[a] MtbDprE1 enzyme inhibition pIC$_{50}$; [b] MIC [µM] against Mycobacterium tuberculosis (H37Rv). Reference: Isoniazid, MIC = 1.8 µM; [c] Cytotoxicity HepG$_2$ IC$_{50}$ [µM]; [d] kinetic aqueous solubility (CLND) [µM]; [e] ChromlogD (pH 7.4); [f] N.D. – not determined

Among the linker modifications performed by other researchers in the OMC team at GSK, the following analogues were evaluated (Figure 5.5):

- analogous compounds to **5.9-5.19** with R$_2$ = Me and R$_1$ = 4-CN, 4-Cl or 4-OMe;
- compounds with a methyl substituted linker methylene group (**5.64**) or with a inker incorporated into a five-membered ring (**5.65**);
- replacement of the keto group by an oxime (**5.66 a-b**), oxetane (**5.67**) or a geminal difluoro group (**5.68**).
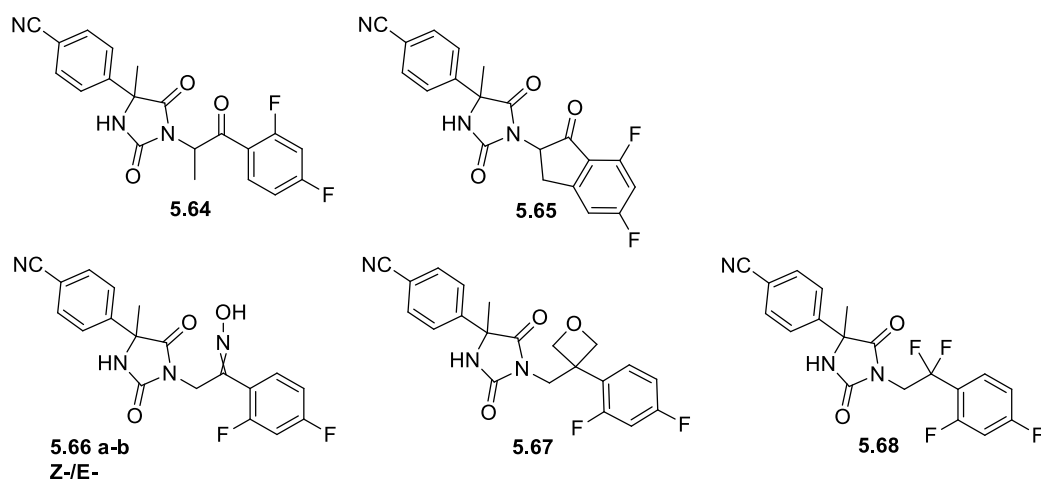
Figure 5.5. Other linker modifications prepared within OMC/DprE1 project

The obtained data demonstrated that most of the described linker modifications resulted in a complete activity loss ($pIC_{50} < 4.5$, MIC ≥ 80 μM). Only compounds **5.64** (Me-substituted linker) and **5.68** (CF_2CH_2-linker) retained some inhibitory activity on DprE1 (pIC_{50} = 5.4 and 5.01 correspondingly), showing no whole-cell activity (MIC ≥ 80 μM) though. Nevertheless, even relatively minor substitution of the methylene with a methyl group in **5.64** led to 40-fold decrease of enzymatic potency.

Additionally, it is worth noting that the replacement of R_2 = Me with *i*-Pr or H with preservation of the original linker in **5.14**-**5.15**, **5.19** caused DprE1 potency loss, suggesting that those changes are not tolerated for the current series. Notably, of all tested compounds only *analogues 5.15-5.16, 5.18 (*with R_2 = *i*-Pr) *together with 5.13* showed any cytotoxicity (HepG₂ IC_{50} < 100 μM). The rest of the tested products demonstrated an absence of detectable cytotoxicity in HepG2 assay (IC_{50} > 100 μM).

Based on the acquired data it was concluded that both the linker length and the presence of the keto group were essential for the series activity. Consequently, in most cases the original linker was preserved during further exploration of this series.

5.3.2 Ring A modifications

The biological and physicochemical evaluation results of the initial hit **4.1** and the analogues with ring A modifications prepared within this research are summarized in Table 5.2. The evaluation results for some selected compounds, prepared by fellow researchers within OMC project, are presented in Table 5.3.

Table 5.2. Biological and physicochemical profile of compounds with ring A modifications

	Structure	DprE1 pIC₅₀[a]	MIC (μM)[b]	Cytotoxicity HepG₂ (μM)[c]	Solubility (μM)[d]	Chrom logD[e]
4.1	NC—⟨ ⟩—ξ-	6.8	8.3	> 100	202	4.54
5.48	Br—⟨ ⟩—ξ-	7.1	20	> 100	4	5.68

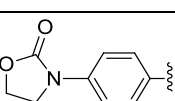|	Structure	DprE1 pIC$_{50}$[a]	MIC (µM)[b]	Cytotoxicity HepG$_2$ (µM)[c]	Solubility (µM)[d]	Chrom logD[e]
5.49		5.3	> 80	> 100	≥ 296	2.71
5.50		7.0	2.5	> 100	≥ 487	3.57
5.51		7.1	12.5	> 100	140	4.84
5.52		6.5	20	> 100	280	3.84
5.53		7.1	10	> 100	277	4.45
5.54		5.3	80	> 100	≥ 486	3.36
5.55		6.8	10	> 100	≥ 369	3.38
5.56		< 4.0	> 80	> 100	≥ 463	4.67
5.57		6.7	30	> 100	17	5.80
5.58		6.2	35	> 100	22	5.04
5.59		5.7	> 80	> 100	147	4.84
5.60		4.4	> 80	> 100	312	4.51
5.61		4.5	80	> 100	68	5.72
5.62		< 4	> 80	> 100	53	5.09

_____
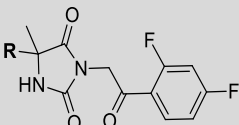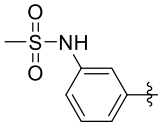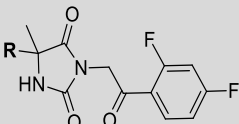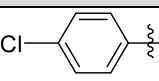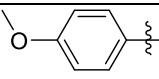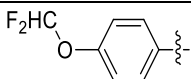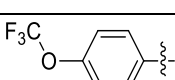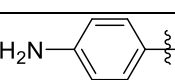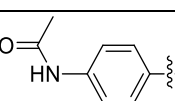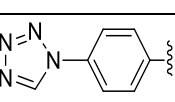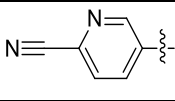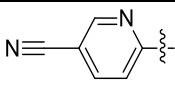
Structure		DprE1 pIC$_{50}$[a]	MIC (µM)[b]	Cytotoxicity HepG$_2$ (µM)[c]	Solubility (µM)[d]	Chrom logD[e]
5.63		4.2	> 80	> 100	≥ 369	3.67

[a] MtbDprE1 enzyme inhibition pIC$_{50}$; [b] MIC [µM] against Mycobacterium tuberculosis (H37Rv). Reference: Isoniazid, MIC = 1.8 µM; [c] Cytotoxicity HepG$_2$ IC$_{50}$ [µM]; [d] kinetic aqueous solubility (CLND) [µM]; [e] ChromlogD (pH 7.4); [f] N.D. – not determined

Table 5.3 Biological and physicochemical profile of compounds prepared by fellow researches in the OMC project

Structure		DprE1 pIC$_{50}$[a]	MIC (µM)[b]	Cytotoxicity HepG$_2$ (µM)[c]	Solubility (µM)[d]	Chrom logD[e]
5.69		6.7	> 40	> 100	17	5.54
5.70		6.7	40	> 100	358	4.78
5.71		7.4	10	> 100	85	5.36
5.72		7.3	35	> 100	4	6.05
5.73		4.1	> 80	> 100	≥ 436	3.38
5.74		5.6	40	> 100	≥ 489	3.28
5.75		6.6	5.6	> 100	359	3.94
5.76		7.3	3.1	> 100	379	3.78
5.77		6.0	20	> 100	≥ 410	3.94
5.78		6.6	10	> 100	≥ 474	3.97

[a] MtbDprE1 enzyme inhibition pIC$_{50}$; [b] MIC [µM] against Mycobacterium tuberculosis (H37Rv). Reference: Isoniazid, MIC = 1.8 µM; [c] Cytotoxicity HepG$_2$ IC$_{50}$ [µM]; [d] kinetic aqueous solubility (CLND) [µM]; [e] ChromlogD (pH 7.4); [f] N.D. – not determined

An important common feature of all the synthesized analogues with ring A modification is the absence of any detectable cytotoxicity in the HepG2 assay (IC_{50} > 100 µM).

Based on the obtained SAR data, it was noted that higher enzymatic potency does not necessarily translate into the whole-cell activity improvement. For example, some of the most potent enzymatic inhibitors (**5.48**, **5.71-5.72**) showed worse whole cell activity (MIC ≥ 10 µM) and demonstrated also a significant increase in lipophilicity (chromlogD ≥ 5.3) accompanied by low solubility.

Nevertheless, some other more hydrophilic analogues, such as sulphonamide **5.50** and tetrazole **5.58**, showed high enzymatic and whole-cell potency and retained good solubility. Moreover, high potency was preserved upon the introduction of some bulkier substituents, such as morpholine **5.53** and tetrazole **5.76**, which suggested that the enzymatic pocket could accommodate further substituent expansion in this part of the molecule.

Overall, introduction of hydrophilic substituents in place of cyano moiety in *para*-position (*4-R*) seemed to be favorable for retaining the DprE1 inhibitory potency (compounds **5.50-5.53, 5.75-5.76**, pIC_{50} = 6.5-7.1), apart from the urea-substituted analogue **5.49**, which demonstrated a notable drop of enzymatic activity (pIC_{50} = 5.3). The sulphonamide analogue **5.50** (4-NHSO$_2$Me) showed an important improvement in the whole-cell activity (MIC = 2.5 µM) in comparison to the initial hit **4.1**. Notably, the products **5.51** and **5.53**, having comparable DprE1-enzyme activity (pIC_{50} = 7.0-7.1) to **5.50**, showed the MIC values of 10-12.5 µM only.

Surprisingly, compound **5.54** showed low DprE1 inhibition potency (pIC_{50} = 5.3) and no whole-cell activity in comparison to its very close analogue **5.75** with a five-membered ring. The latter showed outstanding whole cell activity (MIC = 5.6 µM) accompanied by merely moderate enzymatic potency (pIC_{50} = 6.6). The nature of such a notable difference was not determined.

An enzyme inhibition decrease was observed on introduction of fluorine substituents in position 2- (**5.57-5.58**) and especially 3- (**5.59**) of the ring A in comparison to their analogues **5.48**, **5.70** without fluorine. Shifting some representative substituents from position 4- to 3- or 2- led to the completely inactive compounds **5.60**-**5.63**.

Introduction of a pyridine ring instead of phenyl, while conserving the 4-CN substitution, resulted in compounds **5.77** and **5.78.** These were characterized by a considerable drop in enzymatic activity (pIC_{50} = 6.0 and 6.6, respectively) in comparison with their direct, phenyl analogue **4.1** (pIC_{50} = 7.0). Both compounds, however, preserved moderate MIC values (10-20 µM). This is a promising indication that the phenyl ring A can be exchanged for a hetorocyclic analogue in order to tackle the product's physico-chemical properties. On the other hand, phenyl substitution by a five-membered thiophene ring in **5.56** caused a complete activity loss, implying that this approach of heterocycle introduction may be very limited.

5.4   Conclusions of the first round of Hit-to-Lead optimization

A range of compounds was synthesized within the first round of Hit-to-Lead optimization in an attempt to address some potential liabilities associated with the series and to deliver more potent DprE1 inhibitors.

The presence of cyano-substituent in ring A was shown not to be crucial for series activity. An initial concern about metabolic stability, triggered by the acetophenone moiety present in the linker, was

not proven by the microsomal stability studies (see Section 7.1.4). As all the linker modifications described in this chapter led to complete activity loss, the initial linker was preserved in the further analogues during investigation of other ring A and B modifications in most cases.

A number of compounds with improved whole-cell and enzymatic potencies were prepared applying the ring A substitution variation. The four most active representatives are shown in Figure 5.6.
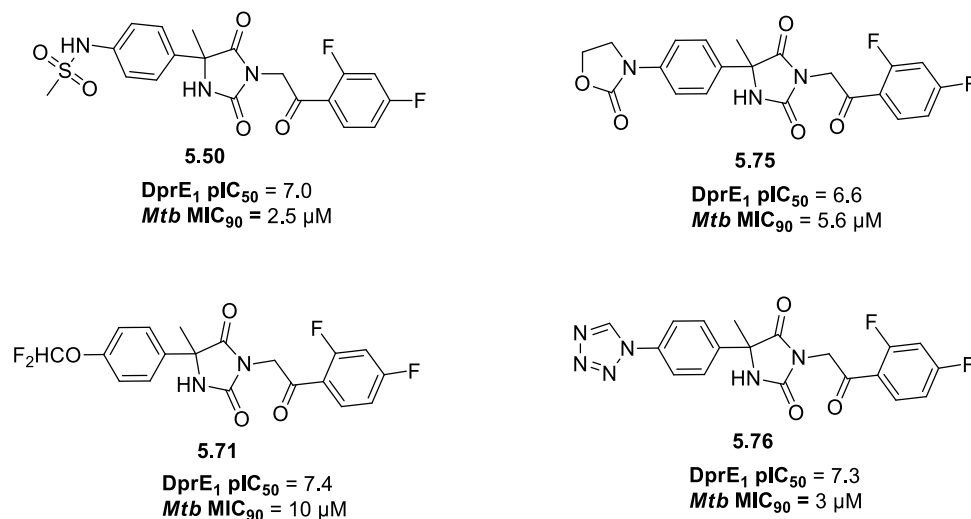

5.50
DprE₁ pIC₅₀ = 7.0
Mtb **MIC₉₀ = 2.5 μM**

5.75
DprE₁ pIC₅₀ = 6.6
Mtb **MIC₉₀ = 5.6 μM**

5.71
DprE₁ pIC₅₀ = 7.4
Mtb **MIC₉₀ = 10 μM**

5.76
DprE₁ pIC₅₀ = 7.3
Mtb **MIC₉₀ = 3 μM**

Figure 5.6. The most potent DprE1 inhibitors from the first round Hit-to-Lead optimization

The sulphonamide (4-NHSO$_2$Me) **5.50** showed approximately 3-fold improvement in whole cell activity over the initial hit **4.1** and slightly higher DprE1 potency. Compounds **5.71** and **5.76** possessed the highest enzymatic inhibitory activity (pIC$_{50}$ = 7.4 and 7.3 respectively) detected in the first round of H2L optimization. However, only analogue **5.76** demonstrated an improved MIC of 3 μM, while **5.71** exhibited only a moderate whole-cell activity of 10 μM. In contrast, product **5.75** showed an unexpectedly good MIC value of 5.6 μM, while having merely a moderate enzymatic inhibitory activity (pIC$_{50}$ = 6.6).

Compounds **4.1**, **5.50** and **5.71** were chosen as new starting points for the second round of Hit-to-Lead optimization. The current research was focused on the sulphonamide sub-series development, based on **5.50**, and its results are reported in Chapter 6. Further exploration of other scaffolds was performed by fellow OMC team members.[258,271]

5.5   Experimental section

All the specifications with respect to reagents, solvents, analytical and structure elucidation techniques and equipment are identical to ones described in detail in the experimental section of Chapter 3 (see Section 3.4.1). In case of microwave radiation-assisted reactions, a Biotage® Initiator+ Microwave Synthesizer was used; the initial absorption was set as 'high' and 2 min of pre-stirring was applied before heating commenced.

The reaction progress was typically monitored by UPLC. The purity of all final compounds, tested on *in vitro* and *in vivo* assays, was 95% or higher (unless stated otherwise), verified by interpretation of ESI-MS (LCMS/UPLC) and ^{1}H NMR data. All the biological and physicochemical evaluation of the final compounds was performed in GSK, the assay description can be found in Chapter 7.2.

_____

5.5.1 General methods

General method A: hydantoin core synthesis. A modified Bucherer-Berg protocol was employed. The appropriate ketone (1.5.0-4.0 mmol, 1.0 eq.), ammonium carbonate $(NH_4)_2CO_3$ (9.0 eq.) and potassium cyanide KCN (1.3 eq.) were dissolved in a mixture of ethanol and water (1:1) (reaction molarity ≈ 0.25-0.4 mol/L). The reaction mixture was heated at 55 °C for 24-48 hrs or irradiated in microwave oven at 70 °C for 3-9 hours. After completion of the reaction, the reaction mixture was cooled down to room temperature and neutralized with dilute hydrochloric acid to pH~7-8. In case of precipitate formation, the product was collected by filtration and washed with water. Otherwise, the solvent was removed under reduced pressure and the residue was diluted with water and extracted with ethyl acetate; the combined organic phases were washed with brine, dried over Na_2SO_4, filtered and evaporated to dryness. In both purification cases, the product was additionally dried in the vacuum oven (40 °C, 0-10 mbr). Typically no additional purification was performed.

General method B: hydantoin core alkylation. A mixture of the appropriate imidazolidine-2,4-dione (0.2-3.7 mmol, 1 eq.) and potassium carbonate K_2CO_3 (1.5-2.0 eq.) was dissolved in DMF or acetone. After 10-20 min, the corresponding alkyl halide **5.4-5.8** was added in slight excess (1.1-1.5 eq.) (reaction molarity ≈ 0.08-0.2 mol/L). The reaction mixture was stirred at room temperature for 20-72 hrs. After the reaction completion, the solvent was removed under reduced pressure and the residue was diluted with saturated ammonium chloride solution and extracted with ethyl acetate. The combined organic phases were washed with brine, dried over Na_2SO_4, filtered and evaporated to dryness. The residue was purified by normal phase column chromatography (gradient *c*-Hex:EtOAc = 100:0 to 10:90, solid loading) or reversed-phase flash column chromatography (gradient water:ACN = 90:10 to 50:50, liquid loading). The fractions containing the desired product were collected and evaporated under reduced pressure. The final product was additionally dried in the vacuum oven (40 °C, 0-10 mbr) or lyophilized.

5.5.2 Chemistry

Compounds **5.4**-**5.8**, **5.22** were commercially available. Intermediate hydantoins **5.2**-**5.3**, **5.28** were available "in house". Final products **5.66-5.80** were prepared within OpenMedChem project by fellow colleagues.
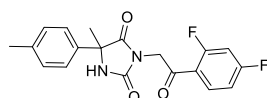
5-Methyl-5-(p-tolyl)imidazolidine-2,4-dione (5.1)
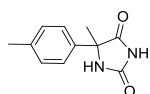
The title compound was prepared according to general method A from 1-(*p*-tolyl)ethanone (500 mg, 3.73 mmol) using microwave irradiation. Yield 57% (455 mg, 2.117 mmol).

¹H NMR (400 MHz, DMSO-*d₆*) δ 10.70 (br. s., 1H), 8.55 (s, 1H), 7.34 (d, *J*=8.34 Hz, 2H), 7.19 (d, *J*=7.83 Hz, 2H), 2.29 (s, 3H), 1.62 (s, 3H). **¹³C NMR** (101 MHz, DMSO-*d₆*) δ 177.1, 156.2, 137.01[*], 137.02[*], 128.9, 125.2, 63.7, 24.9, 20.5. **ESI-MS (A):** *m/z* 203 [M-H]⁻ (R$_t$ = 1.08 min). [*]*These two signals almost overlap in* ¹³C NMR.
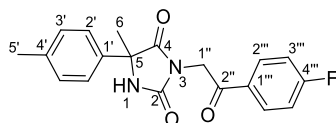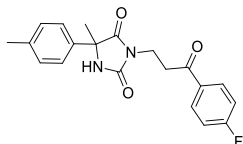
3-(2-(2,4-Difluorophenyl)-2-oxoethyl)-5-methyl-5-(p-tolyl)imidazolidine-2,4-dione (5.9)

_____

The title compound was prepared according to general method B from 5-methyl-5-(*p*-tolyl)imidazolidine-2,4-dione **5.1** (105 mg, 0.514 mmol) and 2-chloro-2',4'-difluoroacetophenone **5.4** (147 mg, 0.771 mmol) in acetone. Yield 74% (144 mg, 0.382 mmol), white amorphous solid, purity ≥ 95%.

¹H NMR (400 MHz, DMSO-*d₆*) δ 9.02 (s, 1H), 8.00 (dt, *J*=6.57, 8.59 Hz, 1H), 7.50 (ddd, *J*=2.40, 9.28, 11.56 Hz, 1H), 7.41 (d, *J*=8.34 Hz, 2H), 7.20-7.32 (m, 3H), 4.79 (d, *J*=2.78 Hz, 2H), 2.31 (s, 3H), 1.73 (s, 3H). **¹³C NMR** (101 MHz, DMSO-*d₆*) δ 189.1 (d, *J*=5.1 Hz), 175.3, 165.7 (dd, *J*=255.4, 12.4 Hz), 162.4 (dd, *J*=257.6, 13.2 Hz), 155.1, 137.3, 136.4, 132.6 (dd, *J*=11.0, 4.4 Hz), 129.0, 125.5, 119.5 (dd, *J*=13.2, 3.7 Hz), 112.8 (dd, *J*=22.0, 3.2 Hz), 105.4 (t, *J*=26.8 Hz), 63.1, 47.1 (d, *J*=10.2 Hz), 24.7, 20.6. **ESI-MS (A):** *m/z* 359 [M+H]⁺ (R$_t$ = 1.26 min).

3-(2-(4-Fluorophenyl)-2-oxoethyl)-5-methyl-5-(p-tolyl)imidazolidine-2,4-dione (5.10)

The title compound was prepared according to general method B from 5-methyl-5-(*p*-tolyl)imidazolidine-2,4-dione **5.1** (60 mg, 0.294 mmol) and 2-bromo-4-fluoroacetophenone **5.5** (96 mg, 0.441 mmol) in acetone. Yield 31% (31.2 mg, 0.092 mmol), white amorphous solid, purity ≥ 95%.

¹H NMR (400 MHz, DMSO-*d₆*) δ 9.05 (s, 1H, NH-1), 8.13 (dd, *J* = 5.65, 8.66 Hz, 2H, CH-2'''), 7.37 - 7.46 (m, 4H, CH-2', CH-3'''), 7.23 (d, *J* = 8.03 Hz, 2H, CH-3'), 4.97 (s, 2H, CH₂-1''), 2.30 (s, 3H, CH₃-5'), 1.74 (s, 3Hm CH₃-6). **¹³C NMR** (101 MHz, DMSO-*d₆*) δ 191.0 (CO-2''), 175.5 (CO-4), 165.6 (d, *J*=253.1 Hz, CF-4'''), 155.3 (CO-2), 137.4 (C$_q$-1'), 136.5 (C$_q$-4'), 131.3 (d, *J*=9.5 Hz, CH-2'''), 130.8 (d, *J*=2.9 Hz, C$_q$-1'''), 129.1 (CH-3'), 125.5 (CH-2'), 116.1 (d, *J*=22.0 Hz, CH-3'''), 63.1 (C$_q$-5), 44.5 (CH₂-1''), 24.8 (CH₃-6), 20.6 (CH₃-5'). **ESI-MS (B):** *m/z* 341 [M+H]⁺ (R$_t$ = 1.65 min).

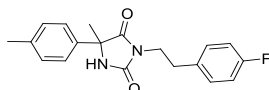### 3-(3-(4-Fluorophenyl)-3-oxopropyl)-5-methyl-5-(p-tolyl)imidazolidine-2,4-dione (5.11)

The title compound was prepared according to general method B from 5-methyl-5-(*p*-tolyl)imidazolidine-2,4-dione **5.1** (60 mg, 0.294 mmol) and 3-chloro-1-(4-fluorophenyl)propan-1-one **5.6** (82 mg, 0.441 mmol) in DMF. Yield 28% (28.7 mg, 0.081 mmol), white amorphous solid, purity ≥ 95%.

¹H NMR (400 MHz, DMSO-*d₆*) δ 8.90 (s, 1H), 8.01 (dd, *J* = 5.52, 8.78 Hz, 2H), 7.28 − 7.39 (m, 4H), 7.19 (d, *J* = 8.03 Hz, 2H), 3.72 (t, *J* = 7.15 Hz, 2H), 3.26 − 3.34 (m, 2H), 2.29 (s, 3H), 1.64 (s, 3H). **¹³C NMR** (101 MHz, DMSO-*d₆*) δ 196.6, 175.3, 165.1 (d, *J*=251.6 Hz), 155.4, 137.2, 136.6, 133.0 (d, *J*=2.9 Hz), 131.0 (d, *J*=9.5 Hz), 129.0, 125.4, 115.7 (d, *J*=21.3 Hz), 62.5, 36.0, 33.9, 24.8, 20.6. **ESI-MS (B):** *m/z* 355 [M+H]⁺, 377 [M+Na]⁺ (R$_t$ = 1.68 min).
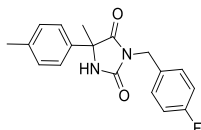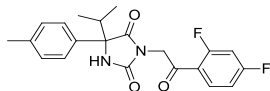
3-(4-Fluorophenethyl)-5-methyl-5-(p-tolyl)imidazolidine-2,4-dione (5.12)

The title compound was prepared according to general method B from 5-methyl-5-(*p*-tolyl)imidazolidine-2,4-dione **5.1** (60 mg, 0.294 mmol) and 1-(2-bromoethyl)-4-fluorobenzene **5.7** (89 mg, 0.441 mmol) in DMF. Yield 17% (16.5 mg, 0.051 mmol), white amorphous solid, purity ≥ 95%.

^{1}H NMR (400 MHz, DMSO-d_6) δ 8.80 (s, 1H), 7.15 - 7.24 (m, 4H), 7.09 - 7.15 (m, 2H), 6.98 - 7.06 (m, 2H), 3.54 - 3.66 (m, 2H), 2.83 (t, *J* = 6.78 Hz, 2H), 2.29 (s, 3H), 1.55 (s, 3H). **^{13}C NMR** (101 MHz, DMSO-d_6) δ 175.2, 160.9 (d, *J*=242.1 Hz), 155.5, 137.2, 136.6, 130.6 (d, *J*=8.1 Hz), 128.9, 125.3, 114.9 (d, *J*=21.3 Hz), 62.4, 39.5*, 32.1, 24.7, 20.6. **ESI-MS (B):** *m/z* 327 [M+H]$^+$ (R_t = 1.71 min). *$^*CH_2$ ^{13}C-signal overlaps with the DMSO signal.*

3-(4-Fluorobenzyl)-5-methyl-5-(p-tolyl)imidazolidine-2,4-dione (5.13)

The title compound was prepared according to general method B from 5-methyl-5-(*p*-tolyl)imidazolidine-2,4-dione **5.1** (60 mg, 0.294 mmol) and 4-fluorobenzyl bromide **5.8** (83 mg, 0.441 mmol) in DMF.Yield 7% (6.3 mg, 0.020 mmol), white amorphous solid, purity ≥ 95%.

^{1}H NMR (400 MHz, DMSO-d_6) δ 9.03 (s, 1H), 7.34 (d, *J* = 8.28 Hz, 2H), 7.23 – 7.29 (m, 2H), 7.11 – 7.22 (m, 4H), 4.53 (s, 2H), 2.28 (s, 3H), 1.67 (s, 3H). **^{13}C NMR** (101 MHz, DMSO-d_6) δ 175.3, 161.4 (d, *J*=242.8 Hz), 155.4, 137.4, 136.5, 133.0 (d, *J*=2.9 Hz), 129.4 (d, *J*=8.1 Hz), 129.1, 125.3, 115.4 (d, *J*=22.0 Hz), 62.8, 40.5, 24.9, 20.6. **ESI-MS (B):** *m/z* 313 [M+H]$^+$ (R_t = 1.68 min).
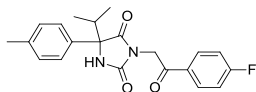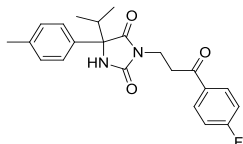
3-(2-(2,4-Difluorophenyl)-2-oxoethyl)-5-isopropyl-5-(p-tolyl)imidazolidine-2,4-dione (5.14)

The title compound was prepared according to general method B from 5-isopropyl-5-(*p*-tolyl)imidazolidine-2,4-dione **5.2** (100 mg, 0.431 mmol) and 2-chloro-2',4'-difluoroacetophenone **5.4** (82 mg, 0.431 mmol) in acetone. Yield 55.0% (96.3 mg, 0.237 mmol), off-white amorphous solid, purity ≥ 95%.

^{1}H NMR (600 MHz, DMSO-d_6) δ 9.10 (s, 1H), 7.93-7.99 (m, 1H), 7.46 (ddd, *J*=2.34, 9.22, 11.27 Hz, 1H), 7.42 (d, *J*=8.20 Hz, 2H), 7.25 (dt, *J*=2.34, 8.35 Hz, 1H), 7.20 (d, *J*=7.91 Hz, 2H), 4.73 (d, *J*=2.05 Hz, 2H), 2.50-2.55 (m, 1H), 2.29 (s, 3H), 0.97 (d, *J*=6.44 Hz, 3H), 0.67 (d, *J*=6.74 Hz, 3H). **^{13}C NMR** (151 MHz, DMSO-d_6) δ 189.0 (d, *J*=4.7 Hz), 174.5, 165.6 (dd, *J*=255.4, 12.8 Hz), 162.3 (dd, *J*=257.7, 13.2 Hz), 155.7, 137.0, 135.3, 132.6 (dd, *J*=10.9, 4.0 Hz), 128.9, 125.4, 119.6 (dd, *J*=12.7, 3.5 Hz), 112.7 (dd, *J*=21.9, 2.3 Hz), 105.4 (t, *J*=26.8 Hz), 70.6, 46.9 (d, *J*=10.6 Hz), 35.0, 20.5, 16.8, 16.4. **ESI-MS (A):** *m/z* 387 [M+H]$^+$ (R_t = 1.28 min).

3-(2-(4-Fluorophenyl)-2-oxoethyl)-5-isopropyl-5-(p-tolyl)imidazolidine-2,4-dione (5.15)

The title compound was prepared according to general method B from 5-isopropyl-5-(*p*-tolyl)imidazolidine-2,4-dione **5.2** (100 mg, 0.431 mmol) and 2-chloro-4'-fluoroacetophenone **5.5** (82 mg, 0.474 mmol) in DMF. Yield 64% (112 mg, 0.274 mmol), off-white amorphous solid, purity ≥ 90%.

_____

¹H NMR (400 MHz, DMSO-d_6) δ 9.19 (s, 1H), 8.13-8.23 (m, 2H), 7.43-7.53 (m, 4H), 7.29 (d, *J*=8.08 Hz, 2H), 4.99 (s, 2H), 2.59-2.65 (m, 1H), 2.37 (s, 3H), 1.07 (d, *J*=6.82 Hz, 3H), 0.76 (d, *J*=7.07 Hz, 3H). **¹³C NMR** (101 MHz, DMSO-d_6) δ 190.8, 174.6, 165.5 (d, *J*=252.5 Hz), 155.9, 137.0, 135.4, 131.2 (d, *J*=9.5 Hz), 130.8 (d, *J*=2.9 Hz), 129.0, 125.4, 116.0 (d, *J*=22.0 Hz), 70.6, 44.3, 35.0, 20.5, 16.8, 16.4. **ESI-MS (A):** *m/z* 369 [M+H]⁺ (R$_t$ = 1.26 min).
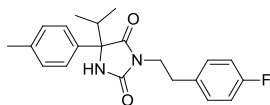
3-(3-(4-Fluorophenyl)-3-oxopropyl)-5-isopropyl-5-(p-tolyl)imidazolidine-2,4-dione (5.16)

The title compound was prepared according to general method B from 5-isopropyl-5-(*p*-tolyl)imidazolidine-2,4-dione **5.2** (100 mg, 0.431 mmol) and 3-chloro-1-(4-fluorophenyl)propan-1-one **5.6** (88 mg, 0.474 mmol) in DMF. Yield 18% (32 mg, 0.079 mmol), off-white amorphous solid, purity ≥ 95%.

¹H NMR (400 MHz, DMSO-d_6) δ 9.06 (s, 1H), 8.00-8.07 (m, 2H), 7.45 (d, *J*=8.34 Hz, 2H), 7.33-7.40 (m, 2H), 7.25 (d, *J*=8.08 Hz, 2H), 3.75 (t, *J*=7.07 Hz, 2H), 3.28-3.37 (m, 2H), 2.47-2.55 (m, 1H), 2.35 (s, 3H), 0.88 (d, *J*=6.57 Hz, 3H), 0.69 (d, *J*=6.82 Hz, 3H). **¹³C NMR** (101 MHz, DMSO-d_6) δ 196.3, 174.6, 165.0 (d, *J*=257.1 Hz), 156.1, 137.0, 135.2, 132.9 (d, *J*=2.2 Hz), 130.9 (d, *J*=9.5 Hz), 128.9, 125.4, 115.7 (d, *J*=22.0 Hz), 69.9, 35.9, 35.2, 33.7, 20.5, 16.5, 16.3. **ESI-MS (A):** *m/z* 383 [M+H]⁺ (R$_t$ = 1.27 min).
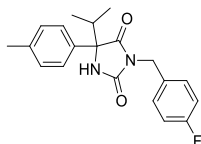
3-(4-Fluorophenethyl)-5-isopropyl-5-(p-tolyl)imidazolidine-2,4-dione (5.17)

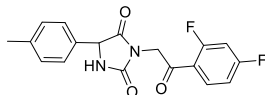

The title compound was prepared according to general method B from 5-isopropyl-5-(*p*-tolyl)imidazolidine-2,4-dione **5.2** (100 mg, 0.431 mmol) and 1-(2-bromoethyl)-4-fluorobenzene **5.7** (96 mg, 0.474 mmol) in DMF. Yield 52% (84 mg, 0.225 mmol), off-white amorphous solid, purity ≥ 95%.

¹H NMR (400 MHz, DMSO-d_6) δ 8.89 (s, 1H), 7.34 (d, *J*=8.34 Hz, 2H), 7.19 (d, *J*=8.08 Hz, 2H), 7.01-7.12 (m, 2H), 6.87-6.98 (m, 2H), 3.46-3.67 (m, 2H), 2.68-2.88 (m, 2H), 2.34-2.47 (m, 1H), 2.30 (s, 3H), 0.70 (d, *J*=6.57 Hz, 3H), 0.60 (d, *J*=6.82 Hz, 3H). **¹³C NMR** (101 MHz, DMSO-d_6) δ 174.5, 160.8 (d, *J*=241.5 Hz), 156.2, 136.9, 135.3, 133.9 (d, *J*=2.9 Hz), 130.4 (d, *J*=8.1 Hz), 128.8, 125.4, 114.8 (d, *J*=21.2 Hz), 69.9, 38.7, 34.8, 32.1, 20.5, 16.4, 16.2. **ESI-MS (A):** *m/z* 353 [M-H]⁻ (R$_t$ = 1.31 min).

3-(4-Fluorobenzyl)-5-isopropyl-5-(p-tolyl)imidazolidine-2,4-dione (5.18)

The title compound was prepared according to general method B from 5-isopropyl-5-(*p*-tolyl)imidazolidine-2,4-dione **5.2** (100 mg, 0.431 mmol) and 4-fluorobenzyl bromide **5.8** (0.059 mL, 0.474 mmol) in DMF. Yield 86% (133 mg, 0.371 mmol), off-white amorphous solid, purity ≥ 95%.

¹H NMR (400 MHz, DMSO-d_6) δ 9.15 (s, 1H), 7.47 (d, *J*=8.34 Hz, 2H), 7.29-7.36 (m, 2H), 7.26 (d, *J*=8.08 Hz, 2H), 7.16-7.24 (m, 2H), 4.50-4.60 (m, 2H), 2.48-2.55 (m, 1H), 2.35 (s, 3H), 0.79 (d, *J*=6.57 Hz, 3H),

_____

0.69 (d, *J*=6.82 Hz, 3H). **¹³C NMR** (101 MHz, DMSO-*d₆*) δ 174.5, 161.4 (d, *J*=243.0 Hz), 156.1, 137.1, 135.1, 132.8 (d, *J*=3.2 Hz), 129.8 (d, *J*=8.8 Hz), 129.0, 125.4, 115.2 (d, *J*=22.0 Hz), 70.1, 40.4, 35.2, 20.5, 16.4, 16.2. **ESI-MS (A):** *m/z* 339 [M-H]⁻ (R$_t$ = 1.29 min).
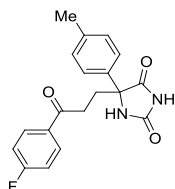
3-(2-(2,4-Difluorophenyl)-2-oxoethyl)-5-(p-tolyl)imidazolidine-2,4-dione (5.19)

The title compound was prepared according to general method B from 5-(*p*-tolyl)imidazolidine-2,4-dione **5.3** (52 mg, 0.273 mmol) and 2-chloro-2′,4′-difluoroacetophenone **4.2** (57.3 mg, 0.301 mmol) in acetone. Yield 16% (16 mg, 0.044 mmol), off-white amorphous solid, purity ≥ 95%.

¹H NMR (400 MHz, DMSO-*d₆*) δ 8.86 (s, 1H), 8.02 (dt, *J*=6.69, 8.53 Hz, 1H), 7.52 (ddd, *J*=2.40, 9.28, 11.56 Hz, 1H), 7.21-7.35 (m, 5H), 5.32 (s, 1H), 4.74-4.90 (m, 2H), 2.32 (s, 3H). **¹³C NMR** (101 MHz, DMSO-*d₆*) δ 189.1 (d, *J*=5.1 Hz), 172.6, 165.7 (dd, *J*=255.4, 13.2 Hz), 162.4 (dd, *J*=257.6, 13.2 Hz), 156.1, 137.8, 132.8, 132.7 (dd, *J*=11.0, 4.4 Hz), 129.2, 127.1, 119.6 (dd, *J*=13.2, 3.7 Hz), 112.8 (dd, *J*=22.0, 3.0 Hz), 105.5 (t, *J*=27.1 Hz), 60.0, 47.2 (d, *J*=11.0 Hz), 20.7. **ESI-MS (A):** *m/z* 345 [M+H]⁺ (R$_t$ = 1.16 min).

5-(3-(4-Fluorophenyl)-3-oxopropyl)-5-(p-tolyl)imidazolidine-2,4-dione (5.21)

The title compound was prepared according to general method B from 5-(*p*-tolyl)imidazolidine-2,4-dione **5.3** (100 mg, 0.526 mmol) and 3-chloro-4′-fluoropropiophenone **5.6** (108 mg, 0.578 mmol) in acetone. Yield 44% (83.6 mg, 0.229 mmol), off-white amorphous solid, purity ≥ 95%.

¹H NMR (400 MHz, DMSO-*d₆*) δ 10.82 (s, 1H), 8.71 (s, 1H), 7.90-7.99 (m, 2H), 7.30-7.43 (m, 4H), 7.21 (d, *J*=8.08 Hz, 2H), 2.97-3.09 (m, 1H), 2.74-2.86 (m, 1H), 2.22-2.42 (m, 5H). **¹³C NMR** (101 MHz, DMSO-*d₆*) δ 197.0, 176.1, 165.0 (d, *J*=251.8 Hz), 156.3, 137.2, 135.5, 133.0 (d, *J*=2.9 Hz), 130.7 (d, *J*=9.5 Hz), 129.1, 125.3, 115.7 (d, *J*=22.0 Hz), 66.6, 32.8, 32.2, 20.5. **ESI-MS (A):** *m/z* 341 [M+H]⁺ (R$_t$ = 1.12 min).

2-(2,4-Difluorophenyl)acetyl chloride (5.23)
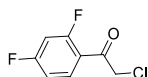
To the stirred solution of 2,4-difluorophenylacetic acid (100 mg, 0.581 mmol) in DCM (0.5 mL) thionyl chloride (0.3 mL, 4.11 mmol) was added dropwise and the reaction mixture was stirred overnight at room temperature. The reaction mixture was evaporated to result in the title compound. The crude product was used directly for the next reaction step.
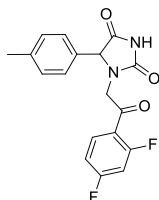
1-(2,4-Difluorobenzoyl)-5-(p-tolyl)imidazolidine-2,4-dione (5.26)
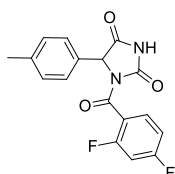
To a stirred solution of 5-(*p*-tolyl)imidazolidine-2,4-dione **5.3** (100 mg, 0.526 mmol), triethylamine (0.147 mL, 1.052 mmol) and 4-(dimethylamino)pyridine (32.1 mg, 0.263 mmol) in dry DCM (0.2 mL) 2,4-difluorobenzoyl chloride **5.22** (0.071 mL, 0.578 mmol) was added dropwise. The resulting mixture was stirred for 24 hrs at room temperature. The reaction mixture was diluted with ethyl acetate and washed with saturated ammonium chloride solution and brine, dried over Na_2SO_4, filtered and evaporated to dryness. The residue was purified by flash column chromatography (gradient *c*-Hex:EtOAc = 80:20 to 20:80, solid loading). The fractions, containing the desired product, were collected and evaporated under reduced pressure. The residue was dried to provide the title compound. Yield 54% (98.8 mg, 0.284 mmol), off-white amorphous solid, purity ≥ 95%.

1H NMR (400 MHz, DMSO-d_6) δ 11.91 (br. s., 1H), 7.68 (dt, *J*=6.57, 8.34 Hz, 1H), 7.44 (ddd, *J*=2.27, 9.41, 10.55 Hz, 1H), 7.34-7.39 (m, 2H), 7.22-7.32 (m, 3H), 5.74 (s, 1H), 2.37 (s, 3H). **13C NMR** (101 MHz, DMSO-d_6) δ 171.3, 163.9 (dd, *J*=250.3, 13.2 Hz), 161.6, 159.7 (dd, *J*=251.0, 13.2 Hz), 153.8, 137.9, 131.4 (dd, *J*=10.2, 4.4 Hz), 131.2, 129.3, 126.7, 120.4 (dd, *J*=15.3, 3.7 Hz), 111.7 (dd, *J*=22.0, 3.7 Hz), 104.1 (t, *J*=26.3 Hz), 63.2, 20.7. **ESI-MS (A):** *m/z* 331 [M+H]+ (R$_t$ = 1.09 min).

### 1-(2-(2,4-Difluorophenyl)acetyl)-5-(p-tolyl)imidazolidine-2,4-dione (5.27)

The title compound was prepared analogously to **5.26** from 5-(*p*-tolyl)imidazolidine-2,4-dione **5.3** (91 mg, 0.478 mmol) and 2-(2,4-difluorophenyl)acetyl chloride **5.23** (100 mg, 0.526 mmol). Yield 12% (20.3 mg, 0.056 mmol), off-white amorphous solid, purity ≥ 95%.

1H NMR (400 MHz, DMSO-d_6) δ 11.80 (br. s., 1H), 7.32 (q, *J*=7.83 Hz, 1H), 7.09-7.23 (m, 5H), 7.01 (t, *J*=8.59 Hz, 1H), 5.46 (s, 1H), 4.17-4.40 (m, 2H), 2.28 (s, 3H). **13C NMR** (101 MHz, DMSO-d_6) δ 170.8, 167.8, 161.5 (dd, *J*=245.2, 12.5 Hz), 160.6 (dd, *J*=247.4, 12.5 Hz), 154.4, 137.7, 133.0 (dd, *J*=9.9, 6.2 Hz), 131.4, 129.2, 126.4, 117.8 (dd, *J*=16.1, 3.7 Hz), 111.0 (dd, *J*=20.7, 3.7 Hz), 103.4 (t, *J*=25.8 Hz), 63.2, 36.0, 20.6. **ESI-MS (A):** *m/z* 345 [M+H]+ (R$_t$ = 1.14 min).

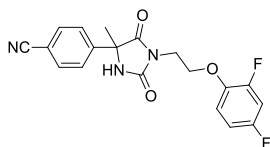### 2-(2,4-Difluorophenoxy)ethyl methanesulfonate (5.29)
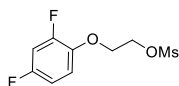
To the stirred solution of 2-(2,4-difluorophenoxy)ethanol (115 mg, 0.660 mmol) and triethylamine (0.184 mL, 1.321 mmol) in DCM (2 mL), methanesulfonyl chloride (0.056 mL, 0.726 mmol) was added dropwise at 0 °C and the reaction mixture was slowly warmed up to room temperature and stirred for 24 hrs. After the solution was evaporated, the residue was dissolved in ethyl acetate and washed with saturated ammonium chloride solution and brine, dried over Na_2SO_4, filtered and evaporated to dryness resulting in the title compound (yield 71 %, 118 mg, 0.468 mmol). The crude product was used diretly for the next reaction step without any further purification.

1H NMR (400 MHz, CDCl$_3$) δ 6.77-7.01 (m, 3H), 4.53-4.63 (m, 2H), 4.25-4.30 (m, 2H), 4.09-4.16 (m, 1H), 3.95-3.99 (m, 1H), 3.81 (t, *J*=5.94 Hz, 1H), 3.69 (s, 1H), 3.13 (s, 3H).

2-(2,4-Difluorophenoxy)ethanol
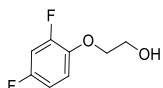
2,4-Difluorophenol (566 µl, 5.93 mmol), 2-bromoethanol (350 µl, 4.94 mmol) and potassium carbonate (1024 mg, 7.41 mmol) were mixed in ACN (5 mL) and irradiated in microwave oven at 100 °C for 2 hours. After the reaction mixture was cooled down to the room temperature, filtered from the inorganic residue and evaporated. The residue was purified by flash column chromatography (gradient *c*-Hex:EtOAc = 100:0 to 80:20, solid loading). The fractions, containing the desired product, were collected, evaporated and dried, resulting in 2-(2,4-difluorophenoxy)ethanol (200 mg, 1.148 mmol, 23.26 % yield) as yellowish oil.

1H NMR (400 MHz, CDCl$_3$) δ 6.96 (dt, J=5.18, 9.16 Hz, 1H), 6.88 (ddd, J=2.91, 8.27, 11.05 Hz, 1H), 6.73-6.83 (m, 1H), 4.09-4.15 (m, 2H), 3.94-4.00 (m, 2H), 1.68-2.16 (m, 1H)

4-(1-(2-(2,4-Difluorophenoxy)ethyl)-4-methyl-2,5-dioxoimidazolidin-4-yl)benzonitrile (5.30)

To a stirred solution of 4-(4-methyl-2,5-dioxoimidazolidin-4-yl)benzonitrile **5.28** (70 mg, 0.325 mmol) in DMF (2 mL) sodium hydride (14.31 mg, 0.358 mmol) was added and the mixture was stirred for 15 min, after a solution of 2-(2,4-difluorophenoxy)ethyl methanesulfonate **5.29** (98 mg, 0.390 mmol) in 1 mL DMF was added dropwise. The resulting mixture was stirred for 72 hrs at room temperature. Complete conversion was not reached. The reaction mixture was diluted with ethyl acetate and washed with saturated ammonium chloride solution and brine, dried over Na$_2$SO$_4$, filtered and evaporated to dryness. The residue was purified by HPLC (gradient: 40-100 acid; liquid loading). The fractions, containing the desired product, were collected and evaporated under reduced pressure. The residue was dried to provide the title compound. Yield 3.5% (5.0 mg, 0.011 mmol), off-white amorphous solid, purity ≥ 85%.

1H NMR[*] (400 MHz, Methanol-*d$_4$*) δ 7.69-7.78 (m, 4H), 7.03 (dt, *J*=5.31, 9.22 Hz, 1H), 6.92 (ddd, *J*=2.91, 8.53, 11.31 Hz, 1H), 6.76-6.84 (m, 1H), 4.22-4.27 (m, 2H), 3.89 (t, *J*=5.43 Hz, 2H), 1.79 (s, 3H). **ESI-MS (A):** *m/z* 370 [M-H]$^-$ (R$_t$ = 1.51 min). [*]*NH signal was not detected, exchangeable.*

### 4-(1-(3-(4-Fluorophenyl)-3-oxopropyl)-4-methyl-2,5-dioxoimidazolidin-4-l)benzonitrile (5.31)
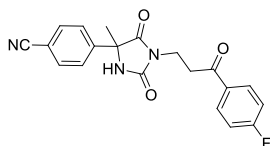
The title compound was prepared according to general method B from 4-(4-methyl-2,5-dioxoimidazolidin-4-yl)benzonitrile **5.28** (100 mg, 0.465 mmol) and 3-chloro-4'-fluoropropiophenone **5.6** (95 mg, 0.511 mmol) in DMF with cesium carbonate (151 mg, 0.465 mmol) as a base. Yield 10% (20.4 mg, 0.047 mmol), off-white amorphous solid, purity ≥ 85%.

1H NMR (400 MHz, DMSO-*d$_6$*) δ 9.04 (s, 1H), 7.95-8.02 (m, 2H), 7.85-7.90 (m, 2H), 7.64-7.70 (m, 2H), 7.26-7.36 (m, 2H), 3.72 (t, *J*=7.07 Hz, 2H), 3.27-3.36 (m, 2H), 1.68 (s, 3H). **13C NMR** (101 MHz, DMSO-

d_6) δ 196.5, 174.2, 165.1 (d, J=251.7 Hz), 155.2, 144.7, 132.9 (d, J=2.9 Hz), 132.4, 130.9 (d, J=9.5 Hz), 126.6, 118.5, 115.7 (d, J=22.0 Hz), 110.9, 62.7, 35.8, 34.1, 25.0. **ESI-MS (A):** *m/z* 366 [M+H]⁺ (R$_t$ = 1.13 min).

4-(3-(3-(4-Fluorophenyl)-3-oxopropyl)-4-methyl-2,5-dioxoimidazolidin-4-l)benzonitrile (5.32)
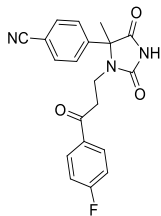
The title compound was obtained as a side produce in the preparation of **5.31**. Yield 31% (55.7 mg, 0.145 mmol), off-white amorphous solid, purity ≥ 95%.

¹H NMR (400 MHz, DMSO-d_6) δ 11.23 (s, 1H), 7.88-7.96 (m, 2H), 7.83 (d, J=8.34 Hz, 2H), 7.53 (d, J=8.59 Hz, 2H), 7.28-7.36 (m, 2H), 3.59-3.70 (m, 1H), 3.33-3.39 (m, 1H), 3.16-3.29 (m, 2H), 1.84 (s, 3H). **¹³C NMR** (101 MHz, DMSO-d_6) δ 196.4, 175.0, 165.0 (d, J=251.8 Hz), 155.9, 142.9, 132.8 (d, J=2.9 Hz), 132.8, 130.8 (d, J=9.5 Hz), 127.3, 118.3, 115.6 (d, J=22.0 Hz), 111.2, 67.6, 37.2, 35.3, 19.7. **ESI-MS (A):** *m/z* 366 [M+H]⁺ (R$_t$ = 1.10 min).

5-(4-Bromophenyl)-5-methylimidazolidine-2,4-dione (5.33)
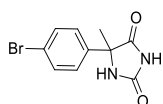
The title compound was prepared according to general method A from 1-(4-bromophenyl)ethanone (3000 mg, 15.07 mmol) using reaction mixture heating. Yield 48% (2065 mg, 7.29 mmol).

¹H NMR (400 MHz, DMSO-d_6) δ 10.82 (br. s., 1H), 8.64 (br. s., 1H), 7.60 (d, J=7.83 Hz, 2H), 7.43 (d, J=7.83 Hz, 2H), 1.64 (s, 3H). **¹³C NMR** (101 MHz, DMSO-d_6) δ 176.5, 156.1, 139.4, 131.4, 127.6, 121.2, 63.6, 25.0. **ESI-MS (A):** *m/z* 267, 269 [M-H]⁻ (R$_t$ = 1.05 min).

1-(4-(4-Methyl-2,5-dioxoimidazolidin-4-yl)phenyl)urea (5.34)
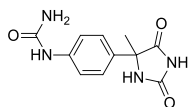
The title compound was prepared according to general method A from a crude mixture containing 1-(4-acetylphenyl)urea (382 mg, 2.144 mmol), using reaction mixture heating. The reaction mixture was evaporated under reduced pressure and the residue was washed with hot ethyl acetate to provide a mixture (363 mg) containing the title compound with an impurity of 1-carbamoyl-1-(4-(4-methyl-2,5-dioxoimidazolidin-4-yl)phenyl)urea. The title compound was not isolated , the crude residue was used for the next reaction step without any further purification.

**ESI-MS (B):** *m/z* 249 [M+H]⁺ (R$_t$ = 0.32 min).

1-(4-Acetylphenyl)urea
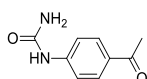
The title compound was prepared analogously to the described procedure.[272] To a solution of 4'-aminoacetophenone (700 mg, 5.18 mmol) in water (2 mL) and glacial acetic acid (1 mL), sodium cyanate (337 mg, 5.18 mmol) in warm water (2 mL) was added slowly under continuous stirring. The mixture was warmed at 50 °C for 2 hrs. Then the reaction mixture was cooled on ice, the crude solid obtained was filtered, dried, and recrystallized from hot water to provide the title compound (~80% purity) with an impurity of 1-(4-acetylphenyl)-1-carbamoylurea. The crude residue was used for the next reaction step without any further purification.

^{1}H NMR (400 MHz, DMSO-d_6) d 9.03 (s, 1H), 7.84 (d, J = 8.78 Hz, 2H), 7.52 (d, J = 8.53 Hz, 2H), 6.08 (br. s., 2H), 2.48 (s, 3H).

N-(4-(4-Methyl-2,5-dioxoimidazolidin-4-yl)phenyl)methanesulfonamide (5.35)
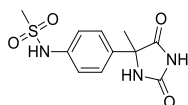
The title compound was prepared according to general method A from *N*-(4-acetylphenyl)methanesulfonamide (800 mg, 3.75 mmol) using microwave irradiation. Yield 57% (635 mg, 2.129 mmol).

^{1}H NMR (400 MHz, DMSO-d_6) δ 10.73 (br. s., 1H), 9.80 (br. s., 1H), 8.56 (s, 1H), 7.37-7.47 (m, 2H), 7.16-7.26 (m, 2H), 2.99 (s, 3H), 1.63 (s, 3H). **^{13}C NMR** (101 MHz, DMSO-d_6) δ 176.9, 156.2, 138.0, 135.2, 126.4, 119.5, 63.5, 39.4, 24.8. **ESI-MS (A):** *m/z* 282 [M-H]$^-$ (R$_t$ = 0.94 min).

Methyl 4-(4-methyl-2,5-dioxoimidazolidin-4-yl)benzoate (5.36)
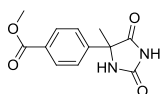
The title compound was prepared according to general method A from methyl 4-acetylbenzoate (500 mg, 2.81 mmol), using microwave irradiation. The extraction was performed, resulting in isolation of a mixture (815 mg) of the title compound (~82% Wt. by NMR) with an impurity of the ethyl 4-(4-methyl-2,5-dioxoimidazolidin-4-yl)benzoate (formed by the re-esterification of the title compound on heating in ethanol with base). The crude residue was used for the next reaction step without any further purification.

^{1}H NMR (400 MHz, DMSO-d_6) δ 10.86 (br. s., 1H), 8.70 (s, 1H), 7.95 - 8.03 (m, 2H), 7.60 - 7.67 (m, 2H), 4.32** (q, J = 7.07 Hz, 0.34H), 3.86* (s, 2.44H), 1.68 (s, 3H), 1.32** (t, J = 7.07 Hz, 0.51H). **This signal corresponds to the methyl group of the title compound, **those signals belong to the undesired minor side product – ethyl ester; other peaks overlap for both compounds.*

5-(4-(1H-imidazol-1-yl)phenyl)-5-methylimidazolidine-2,4-dione (5.37)
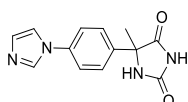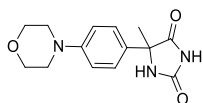

The title compound was prepared according to general method A from 4'-(Imidazol-1-yl)acetophenone (700 mg, 3.76 mmol) using reaction mixture heating. Yield 43% (440 mg, 1.631 mmol).

^{1}H NMR (400 MHz, DMSO-d_6) δ 10.62-10.91 (br. s., 1H), 8.68 (s, 1H), 8.26 (s, 1H), 7.74 (t, J=1.26 Hz, 1H), 7.66-7.71 (m, 2H), 7.57-7.62 (m, 2H), 7.11 (s, 1H), 1.68 (s, 3H). **^{13}C NMR** (101 MHz, DMSO-d_6) δ

176.7, 156.1, 138.4, 136.4, 135.5, 129.9, 126.8, 120.3, 118.0, 63.6, 25.1. **ESI-MS (A):** *m/z* 257 [M+H]$^+$ (R$_t$ = 0.84 min).

5-Methyl-5-(4-morpholinophenyl)imidazolidine-2,4-dione (5.38)

The title compound was prepared according to general method A from 4'-morpholinoacetophenone (500 mg, 2.436 mmol) using microwave irradiation. Yield 35% (250 mg, 0.863 mmol).

^{1}H NMR (400 MHz, DMSO-*d$_6$*) δ 10.65 (s, 1H), 8.48 (s, 1H), 7.29 (d, *J*=8.84 Hz, 2H), 6.94 (d, *J*=9.09 Hz, 2H), 3.64-3.79 (m, 4H), 3.00-3.14 (m, 4H), 1.60 (s, 3H). **^{13}C NMR** (101 MHz, DMSO-*d$_6$*) δ 177.3, 156.2, 150.5, 130.2, 126.0, 114.8, 66.0, 63.4, 48.3, 24.7. **ESI-MS (A):** *m/z* 276 [M+H]$^+$ (R$_t$ = 0.88 min).

5-Methyl-5-(4-(2-oxo-1,3-oxazinan-3-yl)phenyl)imidazolidine-2,4-dione (5.39)
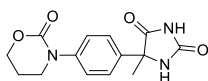
The title compound was prepared according to general method A from 3-(4-acetylphenyl)-1,3-oxazinan-2-one (300 mg, 1.368 mmol) in water (6 mL), DMF (2 mL) and using heating at 70 °C. It was isolated as a minor product on the extraction of the reaction mixture. Yield 3.0% (12 mg, 0.041 mmol), purity ≥ 80%. The major isolated product was the corresponding hydantoin sodium salt **5.39a** (*vide infra*).

^{1}H NMR (400 MHz, DMSO-*d$_6$*) δ 10.81 (br. S., 1H), 8.64 (s, 1H), 7.44 – 7.50 (m, 2H), 7.35 – 7.42 (m, 2H), 4.34 (t, *J* = 5.27 Hz, 2H), 3.65 (t, *J* = 6.02 Hz, 2H), 2.05 – 2.14 (m, 2H), 1.66 (s, 3H). **ESI-MS (C):** *m/z* 290 [M+H]$^+$, 312 [M+Na]$^+$ (R$_t$ = 0.71 min).

Sodium 4-methyl-2,5-dioxo-4-(4-(2-oxo-1,3-oxazinan-3-yl)phenyl)imidazolidin-1-die (5.39a)
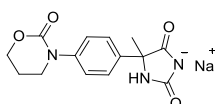
The title compound was formed as the main product in the preparation of **5.39** (*vide supra*). It was isolated as a precipitate on neutralization of the reaction mixture. Yield 50% (212 mg, 0.681 mmol).

^{1}H NMR (400 MHz, DMSO-*d$_6$*) δ 8.64 (s, 1H), 7.47 (d, *J* = 8.28 Hz, 2H), 7.38 (d, *J* = 8.03 Hz, 2H), 4.34 (t, *J* = 4.77 Hz, 2H), 3.65 (t, *J* = 5.65 Hz, 2H), 2.04 - 2.16 (m, 2H), 1.66 (s, 3H). **^{13}C NMR** (101 MHz, DMSO-*d$_6$*) δ 176.9, 156.2, 151.9, 143.0, 137.6, 126.0, 125.8, 66.8, 63.7, 48.1, 24.9, 22.0. **ESI-MS (B):** *m/z* 290 [M+H]$^+$, 312 [M+Na]$^+$ (R$_t$ = 0.93 min) (broadened peak). **ESI-MS (C):** *m/z* 290 [M+H]$^+$, 312 [M+Na]$^+$ (R$_t$ = 0.77 min).

5-Methyl-5-(3-oxo-3,4-dihydro-2H-benzo[b][1,4]oxazin-6-yl)imidazolidine-2,4-dione (5.40)

_____
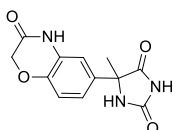
The title compound was prepared according to general method A from 6-acetyl-2*H*-benzo[*b*][1,4]oxazin-3(4*H*)-one (600 mg, 3.14 mmol) using microwave irradiation. Yield 50% (428 mg, 1.556 mmol).

¹H NMR (400 MHz, DMSO-*d₆*) δ 10.59 (br. s, 2H), 8.48 (s, 1H), 6.82-7.00 (m, 3H), 4.47 (s, 2H), 1.52 (s, 3H). **¹³C NMR** (101 MHz, DMSO-*d₆*) δ 176.9, 164.8, 156.2, 142.9, 134.1, 127.2, 120.1, 116.0, 113.0, 66.7, 63.4, 24.7. **ESI-MS (A):** *m/z* 260 [M-H]⁻ (R$_t$ = 0.85 min).

5-(4-Methyl-2,5-dioxoimidazolidin-4-yl)thiophene-2-carbonitrile (5.41)
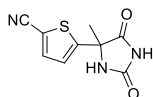
The title compound was prepared according to a modified general method A from 5-acetylthiophene-2-carbonitrile (600 mg, 3.97 mmol), potassium cyanide (271 mg, 4.17 mmol, 1.05 eq.) and ammonium carbonate (2288 mg, 23.81 mmol, 6.0 eq.) in water (5 mL), DMF (5 mL) using heating at 70 °C. Yield 50% (442 mg, 1.998 mmol).

¹H NMR (400 MHz, DMSO-*d₆*) δ 11.12 (s, 1H), 8.99 (s, 1H), 7.91 (d, *J* = 4.02 Hz, 1H), 7.29 (d, *J* = 4.02 Hz, 1H), 1.72 (s, 3H). **¹³C NMR** (101 MHz, DMSO-*d₆*) δ 174.8, 155.9, 152.7, 139.7, 125.9, 114.1, 107.8, 62.9, 25.3. **ESI-MS (B):** *m/z* 220 [M-H]⁻ (R$_t$ = 1.16 min).
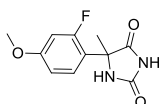
5-(4-Bromo-2-fluorophenyl)-5-methylimidazolidine-2,4-dione (5.42)
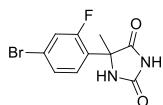
The title compound was prepared according to general method A from 4-Bromo-2-fluoroacetophenone (500 mg, 2.304 mmol), using microwave irradiation. Yield 90% (597 mg, 2.080 mmol), purity ≥ 90%.

¹H NMR (400 MHz, DMSO-*d₆*) δ 10.90 (br. s., 1H), 8.36 (s, 1H), 7.57-7.63 (m, 1H), 7.45-7.52 (m, 2H), 1.70 (s, 3H). **¹³C NMR** (101 MHz, DMSO-*d₆*) δ 176.6, 160.3 (d, *J*=253.2 Hz), 156.2, 130.1 (d, *J*=4.4 Hz), 127.5 (d, *J*=2.9 Hz), 126.1 (d, *J*=11.7 Hz), 122.2 (d, *J*=10.2 Hz), 119.5 (d, *J*=25.6 Hz), 61.1, 23.0. **ESI-MS (A):** *m/z* 285, 287 [M-H]⁻ (R$_t$ = 0.98 min).
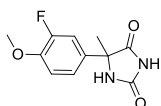
5-(2-Fluoro-4-methoxyphenyl)-5-methylimidazolidine-2,4-dione (5.43)

The title compound was prepared according to general method A from 1-(2-fluoro-4-methoxyphenyl)ethanone (500 mg, 2.97 mmol), using microwave irradiation. Yield 36% (268 mg, 1.069 mmol).

¹H NMR (400 MHz, DMSO-*d₆*) δ 10.78 (s, 1H), 8.25 (s, 1H), 7.40 (t, *J*=9.22 Hz, 1H), 6.76-6.88 (m, 2H), 3.77 (s, 3H), 1.67 (s, 3H). **¹³C NMR** (101 MHz, DMSO-*d₆*) δ 177.3, 160.8 (d, *J*=11.7 Hz), 161.1 (d, *J*=247.3 Hz), 156.2, 128.9 (d, *J*=5.9 Hz), 118.3 (d, *J*=12.4 Hz), 109.7 (d, *J*=2.2 Hz), 102.3 (d, *J*=26.0 Hz), 60.9, 55.7, 23.2. **ESI-MS (A):** *m/z* 237 [M-H]⁻ (R$_t$ = 1.04 min).
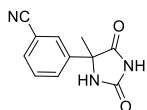
5-(3-Fluoro-4-methoxyphenyl)-5-methylimidazolidine-2,4-dione (5.44)

_____

The title compound was prepared according to general method A from 1-(3-fluoro-4-methoxyphenyl)ethanone (500 mg, 2.97 mmol), using microwave irradiation. Yield 31% (232 mg, 0.925 mmol).

^{1}H NMR (400 MHz, DMSO-d_6) δ 10.67 (br. s., 1H), 8.59 (s, 1H), 7.10-7.32 (m, 3H), 3.83 (s, 3H), 1.61 (s, 3H). **^{13}C NMR** (101 MHz, DMSO-d_6) δ 176.7, 156.1, 151.1 (d, J=243.7 Hz), 146.6 (d, J=10.2 Hz), 132.8 (d, J=5.1 Hz), 121.5 (d, J=3.7 Hz), 113.7 (d, J=2.2 Hz), 113.2 (d, J=19.8 Hz), 63.2 (d, J=1.5 Hz), 56.1, 25.1. **ESI-MS (A):** *m/z* 237 [M-H]$^-$ (R$_t$ = 0.95 min).
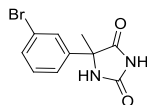
3-(4-Methyl-2,5-dioxoimidazolidin-4-yl)benzonitrile (5.45)

The title compound was prepared according to general method A from 3-acetylbenzonitrile (500 mg, 3.44 mmol), using microwave irradiation. Yield 65% (510 mg, 2.251 mmol).

^{1}H NMR (400 MHz, DMSO-d_6) δ 10.61 (br. s, 1H), 8.60 (s, 1H), 7.82 (s, 1H), 7.74 (dd, J=1.52, 7.83 Hz, 2H), 7.49-7.61 (m, 1H), 1.59 (s, 3H). **^{13}C NMR** (101 MHz, DMSO-d_6) δ 176.2, 156.0, 141.4, 131.7, 130.4, 129.9, 129.1, 118.6, 111.6, 63.6, 25.2. **ESI-MS (A):** *m/z* 214 [M-H]$^-$ (R$_t$ = 0.91 min).

5-(3-Bromophenyl)-5-methylimidazolidine-2,4-dione (5.46)

The title compound was prepared according to general method A from 1-(3-bromophenyl)ethanone (700 mg, 3.52 mmol), using microwave irradiation. Yield 78% (780 mg, 2.75 mmol).

^{1}H NMR (400 MHz, DMSO-d_6) δ 10.85 (br. s., 1H), 8.66 (s, 1H), 7.63 (t, J=1.89 Hz, 1H), 7.46-7.59 (m, 2H), 7.33-7.42 (m, 1H), 1.65 (s, 3H). **^{13}C NMR** (101 MHz, DMSO-d_6) δ 176.4, 156.0, 142.6, 130.7*, 128.0, 124.5, 121.8, 63.5, 25.2. **ESI-MS (A):** *m/z* 267, 269 [M-H]$^-$ (R$_t$ = 1.02 min). **Two ^{13}C peaks from 2 CH group are overlapping (proven by HSQC).*
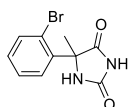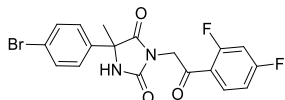
5-(2-Bromophenyl)-5-methylimidazolidine-2,4-dione (5.47)

The title compound was prepared according to general method A from 1-(2-bromophenyl)ethanone (600 mg, 3.01 mmol) in water (6 mL), DMF (2 mL), using heating at 70 °C. Yield 77% (627 mg, 2.33 mmol).

^{1}H NMR (400 MHz, DMSO-d_6) δ 10.92 (br. s., 1H), 8.24 (s, 1H), 7.67 (dt, J = 1.38, 7.09 Hz, 2H), 7.45 (dt, J = 1.25, 7.65 Hz, 1H), 7.33 (dt, J = 1.51, 7.53 Hz, 1H), 1.78 (s, 3H). **^{13}C NMR** (101 MHz, DMSO-d_6) δ 177.1, 156.8, 136.5, 134.6, 130.5, 130.3, 127.7, 122.8, 64.1, 25.5. **ESI-MS (B):** *m/z* 269, 271 [M+H]$^+$ (R$_t$ = 1.15 min).

_____

5-(4-Bromophenyl)-3-(2-(2,4-difluorophenyl)-2-oxoethyl)-5-methylimidazolidine-2,4-dione (5.48)
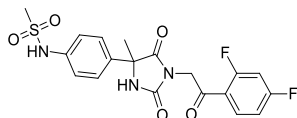

The title compound was prepared according to general method B from 5-(4-bromophenyl)-5-methylimidazolidine-2,4-dione **5.48** (1000 mg, 3.72 mmol) and 2-chloro-2′,4′-difluoroacetophenone **5.4** (1062 mg, 5.57 mmol) in acetone for 20-100 hrs. The reaction has not reach completion, most of the product was obtained in the mixture with the starting hydantoin. Pure product yield 16% (256 mg, 0.605 mmol), white amorphous solid, purity ≥ 95%.

¹H NMR (400 MHz, DMSO-d_6) δ 9.11 (s, 1H), 7.94-8.06 (m, 1H), 7.61-7.68 (m, 2H), 7.46-7.54 (m, 3H), 7.28 (dt, *J*=2.40, 8.40 Hz, 1H), 4.80 (d, *J*=2.78 Hz, 2H), 1.74 (s, 3H). **¹³C NMR** (101 MHz, DMSO-d_6) δ 189.1 (d, *J*=5.1 Hz), 174.8, 165.7 (dd, *J*=255.4, 13.2 Hz), 162.4 (dd, *J*=257.6, 13.2 Hz), 155.0, 138.8, 132.6 (dd, *J*=11.0, 4.4 Hz), 131.4 (s), 127.9, 121.5, 119.5 (dd, *J*=13.2, 3.7 Hz), 112.8 (dd, *J*=22.0, 3.1 Hz), 105.4 (t, *J*=26.6 Hz), 62.9, 47.2 (d, *J*=11.0 Hz), 24.8. **ESI-MS (A):** *m/z* 423, 425 [M+H]⁺ (R$_t$ = 1.23 min).

1-(4-(1-(2-(2,4-Difluorophenyl)-2-oxoethyl)-4-methyl-2,5-dioxoimidazolidin-4-yl)phenyl)urea (5.49)
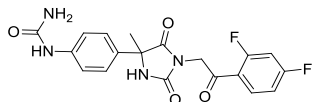
The title compound was prepared according to general method B from the crude mixture containing 1-(4-(4-methyl-2,5-dioxoimidazolidin-4-yl)phenyl)urea **5.49** (80 mg, 0.322 mmol) and 2-bromo-1-(2,4-difluorophenyl)ethanone **5.4a** (68.2 mg, 0.290 mmol, 0.9 eq.) in DMF. Compound **5.49** was used in excess to **5.4a** in order to avoid any potential alkylation of the urea moiety. Yield 22% (28.8 mg, 0.072 mmol), off-white amorphous solid, purity ≥ 95%.

¹H NMR (400 MHz, DMSO-d_6) δ 8.99 (s, 1H), 8.62 (s, 1H), 7.97 - 8.07 (m, 1H), 7.52 (ddd, *J* = 2.51, 9.35, 11.48 Hz, 1H), 7.40 - 7.46 (m, 2H), 7.34 - 7.40 (m, 2H), 7.30 (dt, *J* = 2.26, 8.41 Hz, 1H), 5.88 (s, 2H), 4.80 (d, *J* = 2.26 Hz, 2H), 1.72 (s, 3H). **¹³C NMR** (101 MHz, DMSO-d_6) δ 189.2 (d, *J*=4.4 Hz), 175.5, 165.7 (dd, *J*=255.3, 12.6 Hz), 162.5 (dd, *J*=257.5, 13.2 Hz), 155.9, 155.1, 140.4, 132.7 (dd, *J*=11.0, 4.4 Hz), 131.6, 126.0, 119.6 (dd, *J*=13.2, 3.7 Hz), 117.5, 112.8 (dd, *J*=22.0, 2.9 Hz), 105.5 (t, *J*=26.8 Hz), 63.0, 47.1 (d, *J*=10.3 Hz), 24.4. **ESI-MS (B):** *m/z* 403 [M+H]⁺, 425 [M+Na]⁺ (R$_t$ = 1.42 min).

N-(4-(1-(2-(2,4-Difluorophenyl)-2-oxoethyl)-4-methyl-2,5-dioxoimidazolidin-4-yl)phenyl)methanesulfonamide (5.50)

The title compound was prepared according to general method B from *N*-(4-(4-methyl-2,5-dioxoimidazolidin-4-yl)phenyl)methanesulfonamide **5.35** (50mg, 0.176 mmol) and 2-chloro-2′,4′-difluoroacetophenone **5.4** (37.0 mg, 0.194 mmol) in DMF with cesium carbonate (86 mg, 0.265 mmol) as a base. Yield 6% (4.6 mg, 0.001 mmol), off-white amorphous solid, purity ≥ 95%.

¹H NMR (400 MHz, DMSO-d_6) δ 9.85 (br. s., 1H), 9.02 (s, 1H), 7.93-8.08 (m, 1H), 7.43-7.57 (m, 3H), 7.19-7.33 (m, 3H), 4.73-4.87 (m, 2H), 3.01 (s, 3H), 1.73 (s, 3H). **¹³C NMR** (101 MHz, DMSO-d_6) δ 189.2 (d, *J*=4.4 Hz), 175.2, 165.7 (dd, *J*=255.4, 13.2 Hz), 162.4 (dd, *J*=257.6, 13.2 Hz), 155.1, 138.2, 134.5, 132.6

_____

(dd, *J*=11.0, 3.7 Hz), 126.7, 119.6 (m)[*], 119.5, 112.8 (dd, *J*=22.0, 2.9 Hz), 105.4 (t, *J*=26.7 Hz), 62.9, 47.1 (d, *J*=10.2 Hz), 39.5, 24.7. **ESI-MS (A):** *m/z* 438 [M+H]+ (Rt = 1.13 min). **HRMS** (ESI) *m/z* calcd for $C_{19}H_{17}F_2N_3O_5S$ [M+H]+: 438.0930; found: 438.0952. *The Cq ($^3J_{CF}$) (always present at this chemical shift in analogous compounds overlaps partially with CH signal.*
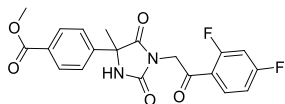
Methyl-4-(1-(2-(2,4-difluorophenyl)-2-oxoethyl)-4-methyl-2,5-dioxoimidazolidin-4-yl)benzoate (5.51)

The title compound was prepared according to general method B from a crude mixture of methyl 4-(4-methyl-2,5-dioxoimidazolidin-4-yl)benzoate **5.36** (110 mg, 0.443 mmol) (with an impurity of the corresponding ethyl-ester) and 2-chloro-2′,4′-difluoroacetophenone **5.4** (127 mg, 0.665 mmol) in DMF. Yield 33% (70.1 mg, 0.148 mmol), off-white amorphous solid, purity ≥ 85%.

1H NMR (400 MHz, DMSO-*d6*) δ 9.18 (s, 1H), 7.94-8.06 (m, 3H), 7.67-7.75 (m, 2H), 7.50 (ddd, *J*=2.40, 9.22, 11.62 Hz, 1H), 7.28 (dt, *J*=2.40, 8.40 Hz, 1H), 4.81 (d, *J*=2.53 Hz, 2H), 3.87 (s, 3H), 1.79 (s, 3H). **13C NMR** (101 MHz, DMSO-*d6*) δ 189.0 (d, *J*=5.1 Hz), 174.6, 165.8, 165.7 (dd, *J*=255.4, 13.2 Hz), 162.4 (dd, *J*=257.8, 13.5 Hz), 155.0, 144.4, 132.6 (dd, *J*=11.0, 3.7 Hz), 129.4, 129.3, 126.1, 119.5 (dd, *J*=13.2, 3.7 Hz), 112.8 (dd, *J*=22.0, 3.6 Hz), 105.4 (t, *J*=26.8 Hz), 63.3, 52.2, 47.2 (d, *J*=10.2 Hz), 25.0. **ESI-MS (A):** *m/z* 403 [M+H]+ (Rt = 1.16 min). **HRMS** (ESI) *m/z* calcd for C20H16F2N2O5 [M+H]+: 425.0919; found: 425.0924.
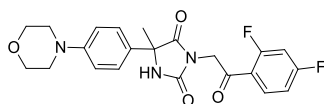
5-(4-(1H-imidazol-1-yl)phenyl)-3-(2-(2,4-difluorophenyl)-2-oxoethyl)-5-methylimidazolidine-2,4-dione (5.52)
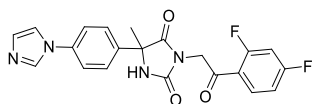
The title compound was prepared according to general method B from 5-(4-(1*H*-imidazol-1-yl)phenyl)-5-methylimidazolidine-2,4-dione **5.37** (100 mg, 0.390 mmol) and 2-chloro-2′,4′-difluoroacetophenone **5.4** (112 mg, 0.585 mmol) in DMF. Yield 57% (95.6 mg, 0.221 mmol), off-white amorphous solid, purity ≥ 95%.

1H NMR (400 MHz, DMSO-*d6*) δ 9.15 (s, 1H), 8.29 (s, 1H), 7.95-8.07 (m, 1H), 7.77 (t, *J*=1.26 Hz, 1H), 7.70-7.75 (m, 2H), 7.65-7.70 (m, 2H), 7.51 (ddd, *J*=2.40, 9.22, 11.62 Hz, 1H), 7.29 (dt, *J*=2.40, 8.40 Hz, 1H), 7.12 (s, 1H), 4.82 (d, *J*=2.53 Hz, 2H), 1.79 (s, 3H). **13C NMR** (101 MHz, DMSO-*d6*) δ 189.1 (d, *J*=5.1 Hz), 175.0, 165.7 (dd, *J*=255.4, 13.2 Hz), 162.4 (dd, *J*=257.6, 13.2 Hz), 155.0, 137.8, 136.6, 135.6, 132.6 (dd, *J*=11.0, 3.6 Hz), 129.9, 127.1, 120.3, 119.5 (dd, *J*=13.2, 3.7 Hz), 118.0, 112.8 (dd, *J*=22.0, 3.2 Hz), 105.4 (t, *J*=26.7 Hz), 63.0, 47.2 (d, *J*=11.0 Hz), 24.9. **ESI-MS (A):** *m/z* 411 [M+H]+ (Rt = 1.15 min). **HRMS** (ESI) *m/z* calcd for $C_{21}H_{16}F_2N_4O_3$ [M+H]+: 433.1083; found: 433.1082.

3-(2-(2,4-Difluorophenyl)-2-oxoethyl)-5-methyl-5-(4-morpholinophenyl)imidazolidine-2,4-dione (5.53)

_____

The title compound was prepared according to general method B from 5-methyl-5-(4-morpholinophenyl)imidazolidine-2,4-dione **5.38** (100 mg, 0.363 mmol) and 2-chloro-2',4'-difluoroacetophenone **5.4** (104 mg, 0.545 mmol) in DMF. Yield 62% (102 mg, 0.226 mmol), off-white amorphous solid, purity ≥ 95%.

¹H NMR (400 MHz, DMSO-d_6) δ 8.95 (s, 1H), 8.00 (dt, J=6.57, 8.59 Hz, 1H), 7.50 (ddd, J=2.40, 9.22, 11.62 Hz, 1H), 7.36 (d, J=8.84 Hz, 2H), 7.29 (dt, J=2.40, 8.40 Hz, 1H), 6.97 (d, J=9.09 Hz, 2H), 4.72-4.85 (m, J=2.53 Hz, 2H), 3.66-3.79 (m, 4H), 3.05-3.15 (m, 4H), 1.71 (s, 3H). **¹³C NMR** (101 MHz, DMSO-d_6) δ 189.2 (d, J=4.4 Hz), 175.5, 165.7 (dd, J=255.9, 13.0 Hz), 162.4 (dd, J=257.7, 13.2 Hz), 155.1, 150.7, 132.6 (dd, J=11.1, 3.7 Hz), 129.5, 126.3, 119.6 (dd, J=13.5, 3.3 Hz), 114.8, 112.8 (dd, J=21.6, 2.8 Hz), 105.4 (t, J=26.9 Hz), 66.0, 62.8, 48.2, 47.1 (d, J=11.0 Hz), 24.6. **ESI-MS (A):** m/z 430 [M+H]⁺ (R_t = 1.14 min). **HRMS** (ESI) m/z calcd for $C_{22}H_{21}F_2N_3O_4$ [M+H]⁺: 452.1392; found: 452.1412.

3-(2-(2,4-Difluorophenyl)-2-oxoethyl)-5-methyl-5-(4-(2-oxo-1,3-oxazinan-3-yl)phenyl)imidazolidine-2,4-dione (5.54)
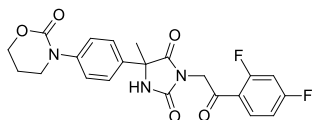
The title compound was prepared according to general method B from sodium 4-methyl-2,5-dioxo-4-(4-(2-oxo-1,3-oxazinan-3-yl)phenyl)imidazolidin-1-ide **5.39a** (76 mg, 0.244 mmol) and 2-bromo-1-(2,4-difluorophenyl)ethanone **5.4a** (57.4 mg, 0.244 mmol) in DMF. Yield 79% (86 mg, 0.194 mmol), white amorphous solid, purity ≥ 95%.

¹H NMR (400 MHz, DMSO-d_6) δ 9.10 (s, 1H), 7.95 – 8.07 (m, 1H), 7.46 – 7.57 (m, 3H), 7.41 (d, J = 8.53 Hz, 2H), 7.29 (dt, J = 2.38, 8.47 Hz, 1H), 4.73 – 4.90 (m, J = 2.26 Hz, 2H), 4.34 (t, J = 5.40 Hz, 2H), 3.66 (t, J = 6.15 Hz, 2H), 2.10 (quin, J = 5.71 Hz, 2H), 1.76 (s, 3H). **¹³C NMR** (101 MHz, DMSO-d_6) δ 189.1 (d, J=5.1 Hz), 175.1, 165.7 (dd, J=255.3, 12.5 Hz), 162.5 (dd, J=258.2, 13.9 Hz), 155.1, 151.9, 143.2, 137.0, 132.7 (dd, J=11.0, 3.7 Hz), 126.1, 126.0, 119.5 (dd, J=13.2, 2.9 Hz), 112.8 (dd, J=22.0, 2.9 Hz), 105.5 (t, J=26.8 Hz), 66.8, 63.1, 48.1, 47.2 (d, J=11.0 Hz), 24.8, 22.0. **ESI-MS (B):** m/z 444 [M+H]⁺, 466 [M+Na]⁺ (R_t = 1.50 min).

3-(2-(2,4-Difluorophenyl)-2-oxoethyl)-5-methyl-5-(3-oxo-3,4-dihydro-2H-benzo[b][1,4]oxazin-6-yl)imidazolidine-2,4-dione (5.55)
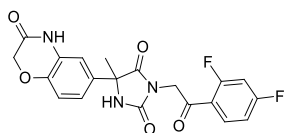
The title compound was prepared according to general method B from 5-methyl-5-(3-oxo-3,4-dihydro-2*H*-benzo[*b*][1,4]oxazin-6-yl)imidazolidine-2,4-dione **5.40** (100 mg, 0.383 mmol) and 2-chloro-2',4'-difluoroacetophenone **5.4** (109 mg, 0.574 mmol) in DMF. Yield 44% (73.6 mg, 0.168 mmol), white amorphous solid, purity ≥ 95%.

¹H NMR (400 MHz, DMSO-d_6) δ 10.75 (br. s., 1H), 9.06 (s, 1H), 7.99 (dt, J=6.82, 8.59 Hz, 1H), 7.50 (ddd, J=2.40, 9.22, 11.62 Hz, 1H), 7.29 (dt, J=2.27, 8.46 Hz, 1H), 7.04-7.14 (m, 2H), 6.97-7.02 (m, 1H), 4.79 (d, J=2.53 Hz, 2H), 4.58 (s, 2H), 1.70 (s, 3H). **¹³C NMR** (101 MHz, DMSO-d_6) δ 189.1 (d, J=4.4 Hz), 175.1, 165.7 (dd, J=255.2, 12.9 Hz), 164.8, 162.4 (dd, J=257.2, 13.9 Hz), 155.0, 143.0, 133.4, 132.6 (dd, J=11.0, 3.9 Hz), 127.2, 120.3, 119.5 (dd, J=13.7, 2.9 Hz), 116.1, 113.2, 112.8 (dd, J=22.0, 2.9 Hz), 105.4 (t, J=27.6

_____

Hz), 66.7, 62.8, 47.1 (d, *J*=10.2 Hz), 25.0. **ESI-MS (A):** *m/z* 416 [M+H]$^+$ (R$_t$ = 1.19 min). **HRMS** (ESI) *m/z* calcd for $C_{20}H_{15}F_2N_3O_5$ [M+H]$^+$: 438.0872; found: 438.0885.

5-(1-(2-(2,4-Difluorophenyl)-2-oxoethyl)-4-methyl-2,5-dioxoimidazolidin-4-yl)thiophene-2-carbonitrile (5.56)
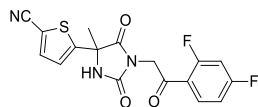
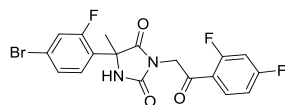The title compound was prepared according to general method B from 5-(4-methyl-2,5-dioxoimidazolidin-4-yl)thiophene-2-carbonitrile **5.41** (100 mg, 0.452 mmol) and 2-bromo-1-(2,4-difluorophenyl)ethanone **5.4a** (159 mg, 0.678 mmol) in DMF. Yield 44% (74.3 mg, 0.198 mmol), off-white amorphous solid, purity ≥ 95%.

^{1}H NMR (400 MHz, DMSO-*d$_6$*) δ 9.49 (br. s., 1H), 8.01 (dt, *J* = 7.03, 8.53 Hz, 1H), 7.96 (d, *J* = 4.02 Hz, 1H), 7.52 (ddd, *J* = 2.26, 9.29, 11.55 Hz, 1H), 7.38 (d, *J* = 3.77 Hz, 1H), 7.30 (dt, *J* = 2.26, 8.41 Hz, 1H), 4.84 (d, *J* = 2.51 Hz, 2H), 1.83 (s, 3H). **^{13}C NMR** (101 MHz, DMSO-*d$_6$*) δ 188.9 (d, *J*=5.1 Hz), 173.1, 165.8 (dd, *J*=255.4, 13.2 Hz), 162.5 (dd, *J*=257.6, 13.2 Hz), 154.8, 152.0, 139.7, 132.7 (dd, *J*=11.8, 3.7 Hz), 126.4, 119.4 (dd, *J*=13.2, 3.7 Hz), 114.0, 112.8 (dd, *J*=22.0, 3.0 Hz), 108.1, 105.5 (t, *J*=26.8 Hz), 62.1, 47.4 (d, *J*=11.0 Hz), 25.4. **ESI-MS (B):** *m/z* 374 [M-H]$^-$ (R$_t$ = 1.60 min).
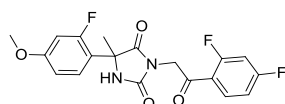
5-(4-Bromo-2-fluorophenyl)-3-(2-(2,4-difluorophenyl)-2-oxoethyl)-5-methylimidazolidine-2,4-dione (5.57)

The title compound was prepared according to general method B from 5-(4-bromo-2-fluorophenyl)-5-methylimidazolidine-2,4-dione **5.42** (200 mg, 0.697 mmol) and 2-bromo-1-(2,4-difluorophenyl)ethanone **5.4a** (246 mg, 1.045 mmol) in acetone. Yield 31% (95 mg, 0.215 mmol), white amorphous solid, purity ≥ 95%.

^{1}H NMR (400 MHz, DMSO-*d$_6$*) δ 8.91 (s, 1H), 8.03 (dt, *J*=6.82, 8.59 Hz, 1H), 7.64 (dd, *J*=1.64, 11.24 Hz, 1H), 7.46-7.58 (m, 3H), 7.30 (dt, *J*=2.40, 8.40 Hz, 1H), 4.86 (d, *J*=2.53 Hz, 2H), 1.82 (s, 3H). **^{13}C NMR** (101 MHz, DMSO-*d$_6$*) δ 189.0 (d, *J*=4.4 Hz), 174.6, 165.7 (dd, *J*=255.4, 13.2 Hz), 162.4 (dd, *J*=257.6, 13.2 Hz), 160.2 (d, *J*=254.0 Hz), 155.0, 132.7 (dd, *J*=11.0, 4.4 Hz), 130.2 (d, *J*=3.7 Hz), 127.6 (d, *J*=3.7 Hz), 125.3 (d, *J*=11.7 Hz), 122.5 (d, *J*=9.5 Hz), 119.7 (d, *J*=25.6 Hz), 119.6 (dd, *J*=13.0, 3.6 Hz), 112.8 (dd, *J*=22.0, 2.9 Hz), 105.4 (t, *J*=26.8 Hz), 60.7, 47.1 (d, *J*=11.0 Hz), 23.4. **ESI-MS (A):** *m/z* 439 [M-H]$^-$ (R$_t$ = 1.23 min).

3-(2-(2,4-Difluorophenyl)-2-oxoethyl)-5-(2-fluoro-4-methoxyphenyl)-5-methylimidazolidine-2,4-dione (5.58)

The title compound was prepared according to general method B from 5-(2-fluoro-4-methoxyphenyl)-5-methylimidazolidine-2,4-dione **5.43** (97 mg, 0.407 mmol) and 2-chloro-2′,4′-difluoroacetophenone **5.4** (116 mg, 0.611 mmol) in acetone. Yield 73% (137 mg, 0.297 mmol), off-white amorphous solid, purity ≥ 95%.

_____

¹H NMR (400 MHz, DMSO-*d₆*) δ 8.81 (s, 1H), 8.03 (dt, *J*=6.82, 8.59 Hz, 1H), 7.42-7.57 (m, 2H), 7.30 (dt, *J*=2.40, 8.40 Hz, 1H), 6.80-6.91 (m, 2H), 4.84 (d, *J*=2.53 Hz, 2H), 3.79 (s, 3H), 1.79 (s, 3H). **¹³C NMR** (101 MHz, DMSO-*d₆*) δ 189.1 (d, *J*=5.1 Hz), 175.3, 165.6 (dd, *J*=255.3, 12.6 Hz), 162.4 (dd, *J*=257.2, 13.2 Hz), 160.9 (d, *J*=11.7 Hz), 161.0 (d, *J*=248.8 Hz), 155.0 (s), 132.6 (dd, *J*=11.0, 3.7 Hz), 129.0 (d, *J*=5.1 Hz), 119.6 (dd, *J*=13.2, 3.7 Hz), 117.5 (d, *J*=11.7 Hz), 112.8 (dd, *J*=22.0, 2.9 Hz), 109.9 (d, *J*=2.2 Hz), 105.4 (t, *J*=26.6 Hz), 102.4 (d, *J*=25.6 Hz), 60.5 , 55.8, 47.0 (d, *J*=10.2 Hz), 23.6. **ESI-MS (A):** *m/z* 393 [M+H]⁺ (R$_t$ = 1.16 min).
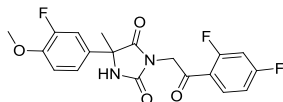
3-(2-(2,4-Difluorophenyl)-2-oxoethyl)-5-(3-fluoro-4-methoxyphenyl)-5-methylimidazolidine-2,4-dione (5.59)

The title compound was prepared according to general method B from 5-(3-fluoro-4-methoxyphenyl)-5-methylimidazolidine-2,4-dione **5.44** (98 mg, 0.411 mmol) and 2-chloro-2',4'-difluoroacetophenone **5.4** (118 mg, 0.617 mmol) in acetone. Yield 38% (65.3 mg, 0.158 mmol), white amorphous solid, purity ≥ 95%.

¹H NMR (400 MHz, DMSO-*d₆*) δ 9.05 (s, 1H), 8.00 (dt, *J*=6.69, 8.53 Hz, 1H), 7.50 (ddd, *J*=2.27, 9.16, 11.56 Hz, 1H), 7.18-7.38 (m, 4H), 4.80 (d, *J*=2.53 Hz, 2H), 3.85 (s, 3H), 1.72 (s, 3H). **¹³C NMR** (101 MHz, DMSO-*d₆*) δ 189.2 (d, *J*=5.1 Hz), 175.0, 165.7 (dd, *J*=255.4, 13.2 Hz), 162.4 (dd, *J*=257.6, 13.2 Hz), 154.9, 151.1 (d, *J*=243.7 Hz), 146.8 (d, *J*=10.6 Hz), 132.6 (dd, *J*=11.0, 3.7 Hz), 132.1 (d, *J*=5.9 Hz), 121.9 (d, *J*=2.9 Hz), 119.5 (dd, *J*=13.2, 3.3 Hz), 113.8 (d, *J*=2.2 Hz), 113.5 (d, *J*=19.8 Hz), 112.8 (dd, *J*=21.8, 3.2 Hz), 105.4 (t, *J*=26.8 Hz), 62.6 (d, *J*=1.5 Hz), 56.1, 47.2 (d, *J*=11.0 Hz), 24.7. **ESI-MS (A):** *m/z* 393 [M+H]⁺ (R$_t$ = 1.16 min).

3-(1-(2-(2,4-Difluorophenyl)-2-oxoethyl)-4-methyl-2,5-dioxoimidazolidin-4-yl)benzonitrile (5.60)
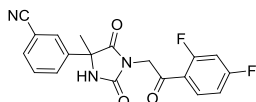
The title compound was prepared according to general method B from 3-(4-methyl-2,5-dioxoimidazolidin-4-yl)benzonitrile **5.45** (100 mg, 0.465 mmol) and 2-chloro-2',4'-difluoroacetophenone **5.4** (133 mg, 0.697 mmol) in DMF. Yield 75% (134.7 mg, 0.346 mmol), off-white amorphous solid, purity ≥ 95%.

¹H NMR (400 MHz, DMSO-*d₆*) δ 9.16 (s, 1H), 7.95-8.05 (m, 2H), 7.85-7.93 (m, 2H), 7.64-7.72 (m, 1H), 7.50 (ddd, *J*=2.40, 9.22, 11.62 Hz, 1H), 7.28 (dt, *J*=2.40, 8.40 Hz, 1H), 4.74-4.89 (m, 2H), 1.79 (s, 3H). **¹³C NMR** (101 MHz, DMSO-*d₆*) δ 189.1 (d, *J*=4.4 Hz), 174.5, 165.7 (dd, *J*=255.7, 12.8 Hz), 162.4 (dd, *J*=257.1, 12.8 Hz), 154.9, 140.9, 132.6 (dd, *J*=11.3, 4.0 Hz), 132.0, 130.6, 129.9, 129.4, 119.4 (dd, *J*=13.1, 3.7 Hz), 118.5, 112.8 (dd, *J*=22.0, 2.9 Hz), 111.6, 105.4 (t, *J*=26.7 Hz), 62.9, 47.3 (d, *J*=11.0 Hz), 24.8. **ESI-MS (A):** *m/z* 370 [M+H]⁺ (R$_t$ = 1.26 min).

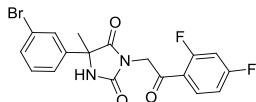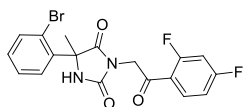### 5-(3-Bromophenyl)-3-(2-(2,4-difluorophenyl)-2-oxoethyl)-5-methylimidazolidine-2,4-dione (5.61)

_____

The title compound was prepared according to general method B from 5-(3-bromophenyl)-5-methylimidazolidine-2,4-dione **5.46** (400 mg, 1.486 mmol) and 2-chloro-2',4'-difluoroacetophenone **5.4** (425 mg, 2.230 mmol) in DMF. Yield 53% (352 mg, 0.790 mmol), off-white amorphous solid, purity ≥ 95%.

¹H NMR (400 MHz, DMSO-*d₆*) δ 9.02-9.08 (m, 1H), 7.86-7.97 (m, 1H), 7.60-7.66 (m, 1H), 7.46-7.52 (m, 2H), 7.38-7.45 (m, 1H), 7.30-7.36 (m, 1H), 7.15-7.23 (m, 1H), 4.68-4.76 (m, 2H), 1.66 (s, 3H). **¹³C NMR** (101 MHz, DMSO-*d₆*) δ 189.1 (d, *J*=5.1 Hz), 174.6, 165.7 (dd, *J*=255.4, 13.2 Hz), 162.4 (dd, *J*=257.6, 13.2 Hz), 154.9, 142.0, 132.6 (dd, *J*=11.0, 3.7 Hz), 131.0, 130.8, 128.4, 124.8, 121.9, 119.5 (dd, *J*=13.2, 3.7 Hz), 112.8 (dd, *J*=21.9, 3.1 Hz), 105.4 (t, *J*=26.7 Hz), 62.9, 47.2 (d, *J*=11.0 Hz), 25.0. **ESI-MS (A):** *m/z* 421, 423 [M-H]⁻ (R$_t$ = 1.24 min).
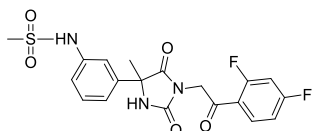
5-(2-Bromophenyl)-3-(2-(2,4-difluorophenyl)-2-oxoethyl)-5-methylimidazolidine-2,4-dione (5.62)

The title compound was prepared according to general method B from 5-(2-bromophenyl)-5-methylimidazolidine-2,4-dione **5.47** (620 mg, 2.304 mmol) and 2-bromo-1-(2,4-difluorophenyl)ethanone **5.4a** (542 mg, 2.304 mmol) in DMF. Yield 47% (462 mg, 1.091 mmol), off-white amorphous solid, purity ≥ 95%.

¹H NMR (400 MHz, DMSO-*d₆*) δ 8.78 (s, 1H), 7.99 - 8.10 (m, 1H), 7.66 - 7.78 (m, 2H), 7.44 - 7.60 (m, 2H), 7.26 - 7.41 (m, 2H), 4.86 (d, *J* = 2.26 Hz, 2H), 1.90 (s, 3H). **¹³C NMR** (101 MHz, DMSO-*d₆*) δ 189.5 (d, *J*=5.1 Hz), 175.0, 165.7 (dd, *J*=255.3, 12.5 Hz), 162.5 (dd, *J*=257.5, 13.2 Hz), 155.6, 135.9, 134.6, 132.7 (dd, *J*=11.5, 4.0 Hz), 130.7, 130.4, 127.8, 122.7, 119.8 (dd, *J*=13.2, 3.7 Hz), 112.8 (dd, *J*=22.0, 2.9 Hz), 105.5 (t, *J*=26.8 Hz), 63.6, 47.0 (d, *J*=10.3 Hz), 25.6. **ESI-MS (A):** *m/z* 423, 425 [M+H]⁺ (R$_t$ = 1.77 min).

N-(3-(1-(2-(2,4-difluorophenyl)-2-oxoethyl)-4-methyl-2,5-dioxoimidazolidin-4-yl)phenyl)methanesulfonamide (5.63)

5-(3-bromophenyl)-3-(2-(2,4-difluorophenyl)-2-oxoethyl)-5-methylimidazolidine-2,4-dione **5.61** (150 mg, 0.354 mmol, 1.0 eq.), methanesulfonamide (40.5 mg, 0.425 mmol, 1.2 eq.), 2-di-tert-butylphosphino-2',4',6'-triisopropylbiphenyl (t-BuXPhos) (6.02 mg, 0.014 mmol, 0.04 eq.), allylpalladium(II) chloride dimer ([Pd(allyl)Cl]₂) (1.297 mg, 3.54 μmol, 0.01 eq.) and potassium carbonate (98 mg, 0.709 mmol, 2.0 eq.) were suspended in dry 2-methyltetrahydrofuran (2-MeTHF) (6 mL), place in the vial, which was evacuated with vacuum and backfilled with nitrogen 3 times. The vial was capped under nitrogen flow and stirred heated at 80 °C for 2 hrs. Then the reaction mixture was cooled to room temperature and diluted with ethyl acetate (20 mL) and 1M hydrochloric acid (20 mL). Subsequently, the acidic layer was extracted with ethyl acetate (2x20 mL). The combined organic layers were filtered through a small celite column, rinsed with ethyl acetate, dried over Na₂SO₄, filtrated and concentrated under reduced pressure. The crude residue was purified by flash column chromatography (gradient *c*-Hex:EtOAc = 100:0 to 10:90, solid loading). The fractions, containing the

_____

desired product, were collected and evaporated under reduced pressure. The residue was dried to provide the title compound. Yield 56% (91 mg, 0.198 mmol), off-white amorphous solid, purity ≥ 95%.

^{1}H NMR (400 MHz, DMSO-d_6) δ 9.86 (s, 1H), 9.10 (s, 1H), 8.00 (dt, *J*=6.69, 8.53 Hz, 1H), 7.51 (ddd, *J*=2.40, 9.28, 11.56 Hz, 1H), 7.35-7.44 (m, 2H), 7.25-7.32 (m, 2H), 7.20 (dd, *J*=1.26, 7.83 Hz, 1H), 4.80 (d, *J*=2.53 Hz, 2H), 3.02 (s, 3H), 1.73 (s, 3H). **^{13}C NMR** (101 MHz, DMSO-d_6) δ 189.0 (d, *J*=4.4 Hz), 174.9, 165.7 (dd, *J*=255.4, 13.0 Hz), 162.4 (dd, *J*=257.6, 13.2 Hz), 155.0, 140.6, 138.6, 132.6 (dd, *J*=11.3, 3.8 Hz), 129.5, 121.0, 119.5 (dd, *J*=13.2, 3.6 Hz), 119.1, 116.8, 112.8 (dd, *J*=21.9, 3.1 Hz), 105.4 (t, *J*=26.6 Hz), 63.1, 47.1 (d, *J*=11.0 Hz), 39.3, 24.9. **ESI-MS (A):** *m/z* 438 [M+H][+] (R$_t$ = 1.06 min).

6. Hydantoins as DprE1 inhibitors: second round of Hit-to-Lead optimization

6.1 Compound design and synthesis

Based on the results obtained in the first round of H2L investigation, most potent compounds were progressed to the second round of optimization. The research described in this chapter covers modifications based on compound **5.50** (4-NHSO$_2$Me, "sulfonamide").

We applied several compound design strategies during the second round of H2L optimization (Figure 6.1). Firstly, a number of variations of the sulfonamide group were explored. The most active sulfonamide-containing compound obtained was chosen as a new reference for a detailed SAR investigation on ring B and additional linker modifications.
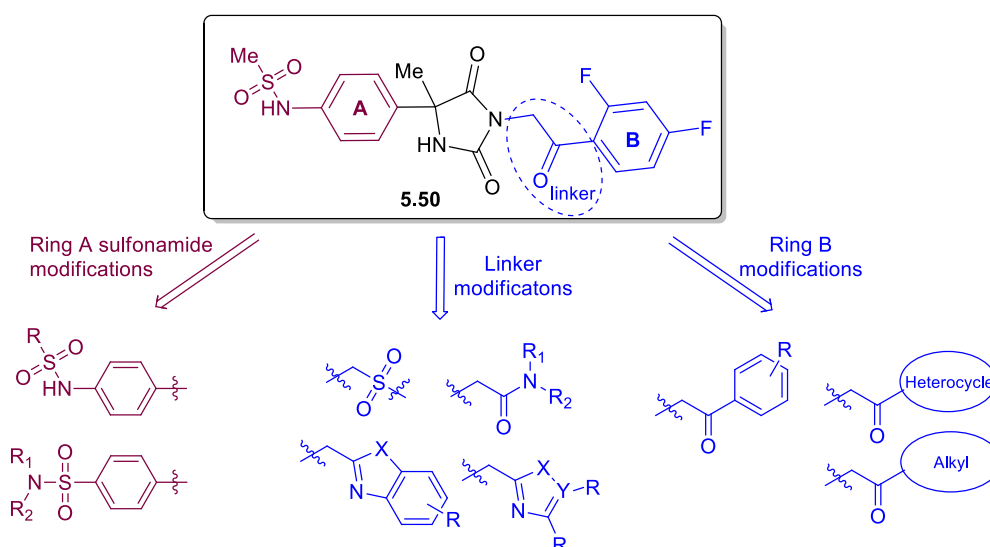
Figure 6.1 Compound design for the second round Hit-to-Lead optimization

The performed modifications described in this chapter include:

- *Ring A sulfonamide modifications:*
  - Substitution pattern variation of **5.50**: 4-NHSO$_2$R synthesis
  - Preparation of the "retro-sulfonamide" (4-SO$_2$NH$_2$)
  - Introduction of amino group substitution in retro-sulfonamide: 4-SO$_2$NR$_1$R$_2$
- *Ring B modifications/substitution:*
  - Aryl substitution variation
  - Introduction of heterocycles and saturated residues in place of the aryl ring B
- *Linker modifications combined with ring B variation*
  - Incorporation of sulfone moiety in the linker
  - Introduction of (benz)oxazoles and related residues as an alternative to the ketone linker
  - Ketone replacement by amide moiety

Around 75 analogues, synthesized and evaluated in the course of the second round of H2L optimization, are presented in this chapter.

_____

6.1.1 Ring A sulfonamide modifications

Differently substituted sulfonamides **6.1-6.3** were obtained in moderate yields from the corresponding bromo-substituted precursor **5.58** by palladium-catalyzed coupling reaction according to a literature procedure (Scheme 6.1).[269] This approach demonstrated several advantages. Foremost, the pre-functionalized hydantoin precursors would have contained in their structure a reactive sulfonamide NH moiety, prone to alkylation. For instance, during sulfonamide **5.50**'s preparation, alkylation of the intermediate hydantoin **5.35** led to *N*-alkylated side product formation (on the –NHSO$_2$Me moiety) leading to low yields and purification issues as described in Section 5.1.2. The new approach allowed us to overcome this issue. Moreover, it provided late-stage functional group variation based on one precursor, which is advantageous for the chemical effort involved as the overall number of synthetic steps for library construction is reduced.

**Scheme 6.1. Synthesis of substituted sulfonamides by the Pd-coupling reaction**
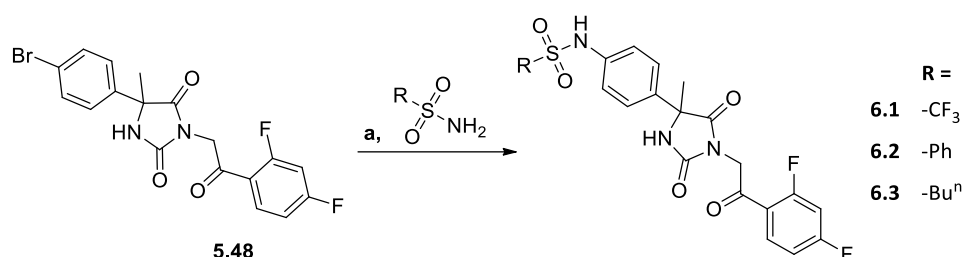
Reagents and conditions: (a) Pd(allyl)Cl]$_2$, t-BuXPhos, K$_2$CO$_3$, 2-MeTHF, 80 °C, 2 hrs.

The 'retro-sulfonamide' **6.9** and its *N*-substituted analogues **6.10-6.13** (4-SO$_2$NR$_1$R$_2$) were synthesized by a straightforward three-step approach (Scheme 6.2). Unfortunately, the last-step differentiation was not possible in this case.

The sulfonamide moiety was introduced by the reaction of 4-acetylbenzenesulfonamide with different amines, followed by modified Bucherer–Bergs synthesis to provide the precursors **6.4-6.8**. The hydantoin intermediates were subsequently alkylated with 2-halo-2',4'-difluoroacetophenones **5.4** or **5.4a** (as in Section 5.1.2) to provide the desired *N*-3 alkylated products **6.9-6.13** in moderate-high yields. To our delight, no indications of *NH*-alkylation of sulfonamide moiety were observed, in contrast to the intermediate **5.35** alkylation, mentioned above. The only exception came with hydantoin **6.8**, bearing the Ph-NH-SO$_2$- moiety like **5.35**, which proved more prone to alkylation leading to a lower isolated yield of the desired product **6.13**.

Scheme 6.2. Synthesis of substituted retro-sulfonamides
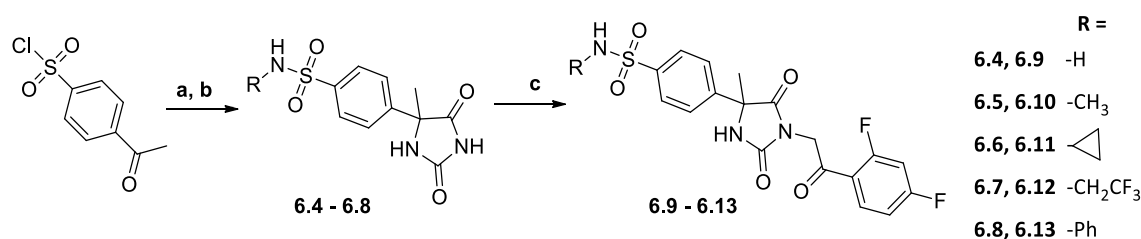
Reagents and conditions: (a) amine·HCl, Et$_3$N or amine with no base, DCM, r.t., 1 hr; (b) KCN, (NH$_4$)$_2$CO$_3$, EtOH-H$_2$O, 70 °C (MW or heating), 7-17 hrs; (c) **5.4** or **5.4a**, K$_2$CO$_3$, acetone, r.t., 24-48 hrs.

According to intermediate biological evaluation results (see Section 6.2.1), benzenesulfonamide derivative **6.9** (4-SO$_2$NH$_2$, "retro-sulfonamide") possessed superior enzymatic and whole-cell potency in comparison to methanesulfonamide **5.50** and was the most potent compound evaluated at that

point. As a result, **6.9** was chosen as a new reference compound for further exploration of the series. Therefore, all ring B and linker modifications presented herein contained the 4-SO$_2$NH$_2$ substituent in the ring.
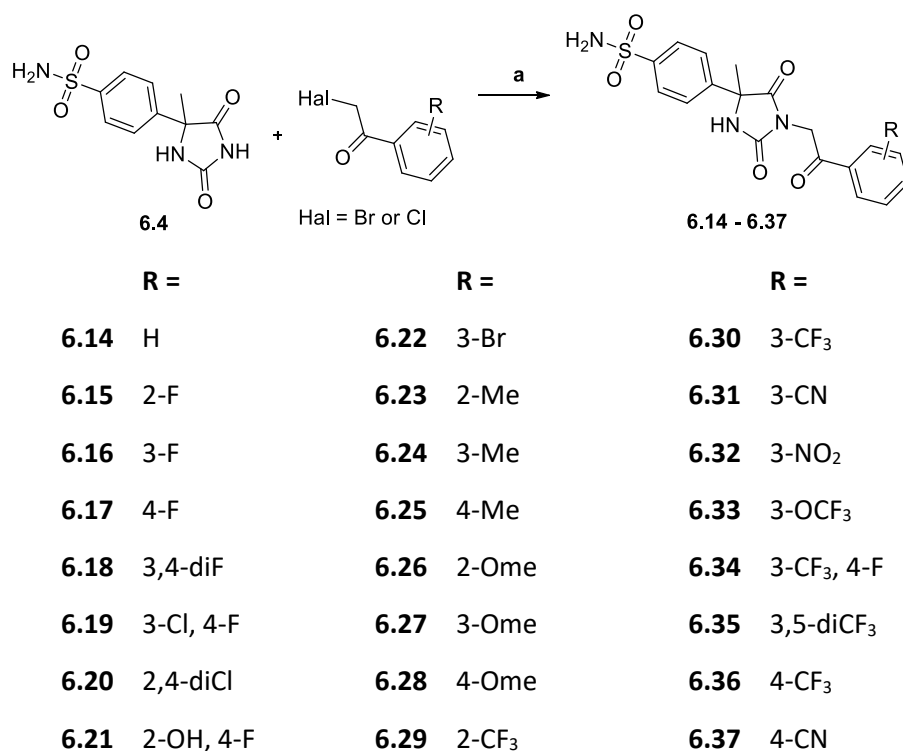
6.1.2 Ring B modifications/removal

A number of ring B substitution variations were introduced in order to deliver thorough SAR data and provide analogues with improved enzymatic and whole-cell potencies. The alkylation of the hydantoin precursor **6.4** with different alkyl halides was quite straightforward, providing the desired products in high to moderate yields. The biological evaluation was performed simultaneously with the synthetic efforts and the obtained results were used as further guidance for the design of additional analogues.

6.1.2.1 Preparation of compounds with a differently substituted ring

The influence of different ring B substituents on product activity and physicochemical profile was examined in compounds **6.14-6.37** (Scheme 6.3).

Scheme 6.3. Synthesis of final compounds with differently substituted ring B

	R =		R =		R =
6.14	H	**6.22**	3-Br	**6.30**	3-CF$_3$
6.15	2-F	**6.23**	2-Me	**6.31**	3-CN
6.16	3-F	**6.24**	3-Me	**6.32**	3-NO$_2$
6.17	4-F	**6.25**	4-Me	**6.33**	3-OCF$_3$
6.18	3,4-diF	**6.26**	2-Ome	**6.34**	3-CF$_3$, 4-F
6.19	3-Cl, 4-F	**6.27**	3-Ome	**6.35**	3,5-diCF$_3$
6.20	2,4-diCl	**6.28**	4-Ome	**6.36**	4-CF$_3$
6.21	2-OH, 4-F	**6.29**	2-CF$_3$	**6.37**	4-CN

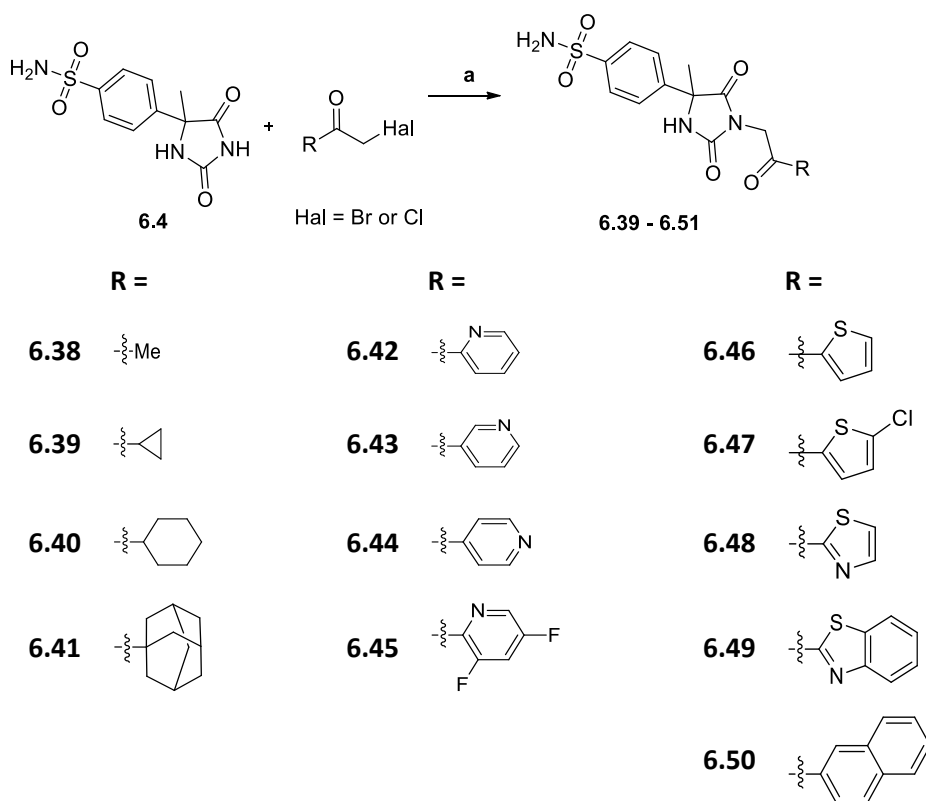Reagents and conditions: (a) K$_2$CO$_3$, acetone or DMF, r.t., 24-48 hrs.

Compound **6.14** contained in its structure an unsubstituted phenyl ring B and was used for activity comparison with analogues containing heterocycles or other substituents on the ring B and lacking fluorine atoms in their structure. In the entities **6.15-6.17,** one of the fluorine atoms was removed and/or shifted in order to provide data on the importance of fluorines in the reference compound **6.9**. A mixed halogen substitution pattern was introduced in products **6.18-6.22**. Compounds **6.23-6.28** possessed an electron-donating group (-Me or -OMe) in different ring positions (*2-, 3- or 4-*), while analogues **6.29-6.37** were used to investigate the electron-withdrawing group influence on compound activity. As compound **6.30** with a 3-CF$_3$-substituent turned out to be very potent in enzymatic and whole-cell assays (see Section 6.2.2.1), additional analogues **6.31-6.33** with an electron-withdrawing

_____

group in the *3*-position were prepared, while compounds **6.34-6.35** represented a mixed substitution pattern, containing a 3-CF$_3$-substituent.

6.1.2.2 Introduction of saturated residues or heterocycles in place of the ring B

The aromatic ring B was exchanged to a simple methyl substituent in **6.38** or a few saturated ring systems in **6.39-6.41** (Scheme 6.4). Moreover, the aryl moiety was substituted by a pyridine ring (**6.42-6.45**), 5-membered heterocycles (**6.46-6.48**) or bicyclic system (**6.49-6.50**) to provide more diverse modifications in this part of the molecule and to improve the physicochemical profile of novel analogues. The product **6.45** represents the closest analogue of the reference compound **6.9**, as it possesses a 2,4-diF substitution pattern on the pyridine ring. Furthermore, the 2-(Benzo[*d*]thiazol-2-yl)-2-oxoethyl moiety, present in the reversible DprE1 inhibitor TCA1, was introduced in **6.49** in an attempt to prepare a hybrid compound. A 2-naphthalene residue was introduced in **6.50** in order to explore if the enzyme-binding site can accommodate bulkier residues with preservation of inhibitor potency.

Scheme 6.4. Synthesis of final compounds with saturated residues or heterocycles in place of ring B

Reagents and conditions: (a) K$_2$CO$_3$, acetone or DMF, r.t., 24-48 hrs.

6.1.3 Linker modifications

This section provides insight on the effect of more fundamental modifications of reference **6.9**, as both linker and ring B were modified in the synthesized analogues.

### 6.1.3.1 Keto-group removal and introduction of sulfone surrogates

Compounds **6.51-6.52** were synthesized as analogues of **6.9** with no carbonyl group in the linker, while preserving its overall length (Scheme 6.5). In particular, product **6.51** possessed a –CH$_2$-CH$_2$– linker, analogously to previously prepared entities **5.12**, **5.17** (*vide supra*, Chapter 5). It was hypothesized that

the presence of a –SONH$_2$ moiety in the ring A, responsible for the high potency of **6.9**, might provide an activity boost in **6.51**.

Compound **6.52** was prepared in order to evaluate the influence of the sulfonyl-substituted linker on product potency in comparison to its closest carbonyl-bearing analogue **6.14**, both containing an unsubstituted phenyl in ring B. It is worth noting that the alkylation of **6.4** with bromomethyl phenyl sulfone (commercially available) was not successful at room temperature, only prolonged heating at 100 °C provided the desired product **6.52** in low yield (~11%).

**Scheme 6.5. Synthesis of final compounds with removed keto-group or a sulfone surrogate.**
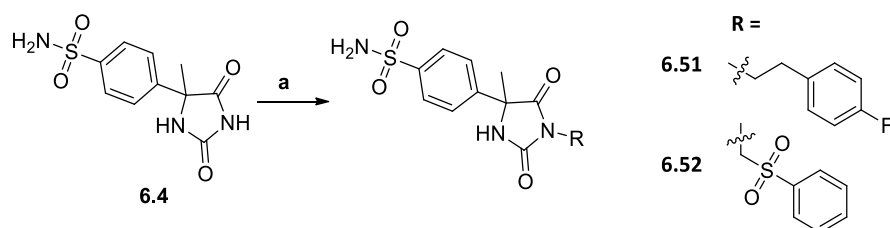
Reagents and conditions: (a) R-Hal, K$_2$CO$_3$, DMF, r.t. or 100 °C, 24-48 hrs.

As compound **6.52** retained moderate activity in the enzymatic assay (DprE1 pIC$_{50}$ = 6.0, see Section 6.2.3.1), we decided to develop a synthetic approach for more analogues with a sulfone moiety in the linker. The designed compounds **6.59-6.61** (Scheme 6.6) included the most promising ring B substitutions identified at that moment (4-F, 3-CF$_3$ and 2,4-diF).

Two synthetic approaches were explored for the preparation of the corresponding precursors **6.56-6.58**. According to literature, these halides can be obtained by direct alkylation of sodium benzenesulfinates (Scheme 6.6, route A).[273] An alternative approach, consisting in the reduction of more commonly accessible sulfonyl chlorides with sodium sulfite (Scheme 6.6, route B) to form the intermediate arylsulfinic acids *in situ*, was also explored based on a literature procedure.[274]

Scheme 6.6. Synthesis of intermediates with sulfone-containing linker and 6.4 alkylation
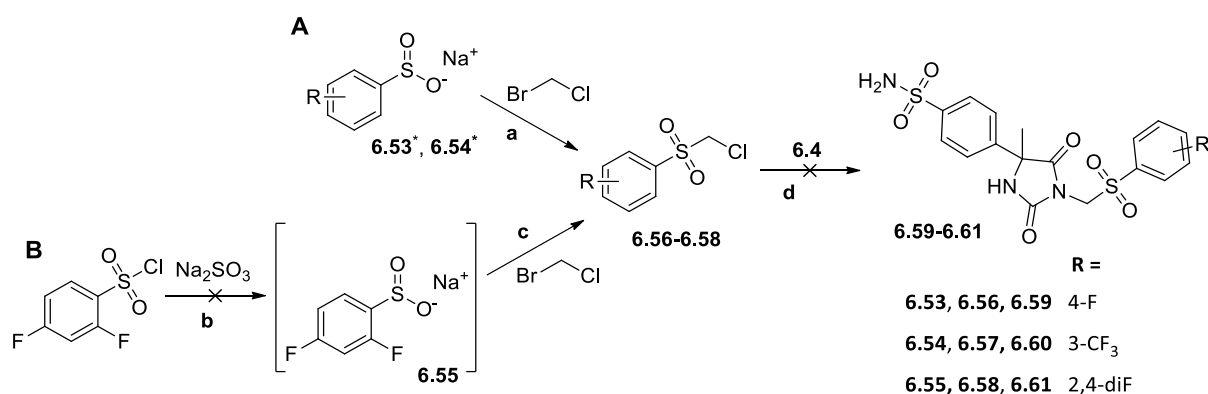
Reagents and conditions: (a) DMSO, 100 °C, 2 hrs; (b) NaHCO$_3$, water or water/DMSO, 100 °C, 1-6 hrs; (c) tetrabutylammonium bromide, 75 °C, 17-24 hrs; (d) K$_2$CO$_3$, DMF, r.t. to 120 °C, 24-48 hrs. *Commercially available*

The intermediates **6.56-6.57**, obtained from available sodium benzenesulfinates (Scheme 6.6 A), were used directly for alkylation of hydantoin **6.4**. Nevertheless, no desired alkylation products **5.59-5.60** were detected under different reaction conditions, including prolonged heating of reaction mixtures up to 120 °C or NaI addition to promote reactivity by halogen exchange.

All attempts to obtain precursor **6.58** failed under tested conditions. The molecular peak corresponding to the *in situ* intermediate **6.55** (Scheme 6.6 B) was not detected by UPLC in all cases, while a molecular peak of 2,4-difluorobenzenesulfonic acid was observed. We hypothesized that the formation of sulfonic acid from the sulfonic chloride in the reaction mixture prevented the desired reduction to sulfinate **6.55**.

The structural identification of intermediates **6.56-6.58** was in general problematic as no molecular ion was detectable by UPLC and their NMR spectra possessed only one additional CH$_2$-group signal in comparison to their precursors **6.53-6.55**.

6.1.3.2 Introduction of (benz)oxazoles and related compounds

A number of analogues containing a hererocyclic counterpart, connected by a CH$_2$-linker to the hydantoin *N*-3 position, were prepared as described in Scheme 6.7. Compounds **6.62-6.75** were obtained by one-step alkylation of **6.4** with corresponding alkyl halides in moderate to high yields.

To begin with, compounds **6.62-6.64**, containing benzoxazole, benzothiazole or *1-*methylbenzimidazole, were prepared based on the assumption that a heteroatom (O, N or S) of the five-membered ring could function as a hydrogen bond acceptor in a similar manner as the carbonyl group in the original acetophenone linker. Quinoline and quinazoline derivatives **6.65-6.66** were prepared relying on the same reasoning.

Scheme 6.7. Synthesis of final compounds with (benz)oxazole and related moieties in place of the ketone linker
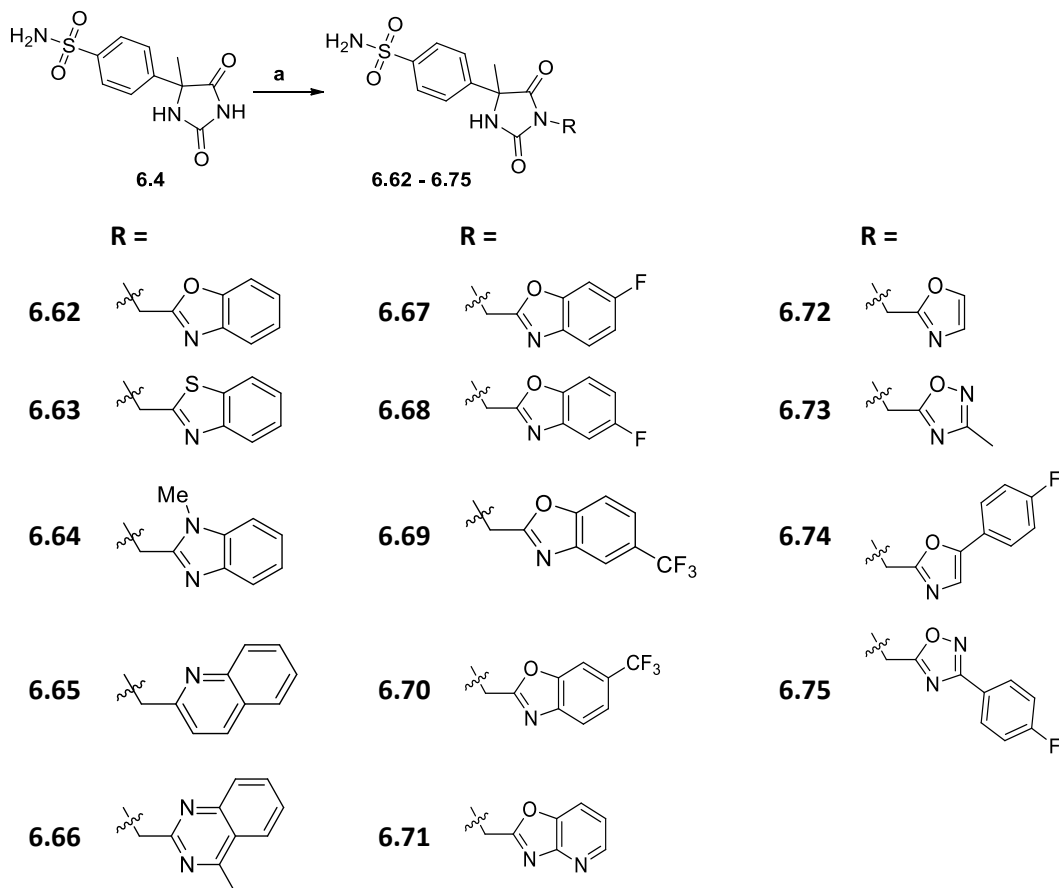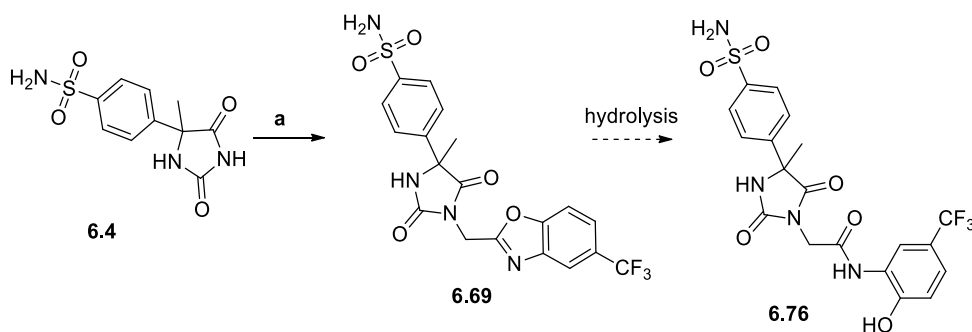

Reagents and conditions: (a) R-Hal, K$_2$CO$_3$, DMF, r.t., 24-48 hrs.

At this stage, benzoxazole- and benzothiazol-containing products (**6.62**-**6.63**) demonstrated the best enzymatic and whole-cell potency during the initial biological evaluation of **6.62-6.66** (see Section 6.2.3.2 for details). In order to obtain a better SAR-understanding of this sub-series, a number of benzoxazole derivatives substituted on the aryl ring (**6.67-6.71**) were synthesized as well. We were particularly interested in analogues substituted with F- (**6.67-6.68**) and CF_3-groups (**6.69-6.70**): several of the most potent parent compounds (containing an acetophenone moiety) also contained these substituents in different positions of the ring B (compounds **6.15-6.17, 6.29-6.30**, Section 6.2.2.1).

Some other related moieties were incorporated in place of the original linker and ring B to provide analogues **6.72-6.75**. In compounds **6.72-6.73,** smaller five-membered oxazole and oxadiazole substituents were introduced in order to assess the importance of a bulkier fused bicyclic system at this position for compound potency. In case of **6.74-6.75,** the corresponding heterocycles were additionally substituted by an aryl ring in order to compare their biological profile with benzoxazole derivatives **6.62, 6.67-6.71**.

In course of the preparation of **6.69**, an unexpected side product **6.76** was isolated (Scheme 6.8). Its structure was proven by 1D and 2D NMR. Most likely, **6.76** was formed from **6.69** by hydrolysis of the oxazole ring during purification by reverse-phase chromatography using water as an eluent. The reaction mechanism or reaction reproducibility were not studied, and no similar side-products were detected during preparation of analogous compounds **6.62**, **6.67**-**6.68** and **6.70-6.71**.

**Scheme 6.8. Formation of 6.76 in course of preparation of 6.69, probably by hydrolysis**

Reagents and conditions: (a) R-Hal, K_2CO_3, DMF, r.t., 24-48 hrs.

6.1.3.3 Compounds containing an amide group as a ketone-replacing moiety.

The keto-function in the original linker was replaced by an amide moiety in products **6.89-6.100**. All amide derivatives were prepared in a two-step synthesis as described in Scheme 6.9. The intermediate alkyl halides **6.77-6.88** were prepared by acylation of the appropriate amines with chloroacetyl chloride. Afterwards, alkylation of hydantoin **6.4** was performed under standard conditions. In a number of cases, the NMR analysis of the final amides **6.89-6.100** was complicated by peak multiplication and broadening due to the presence of multiple diastereomers and amide-bond rotamers.

Scheme 6.9. Synthesis of final compounds with an amide moiety in place of ketone in the linker
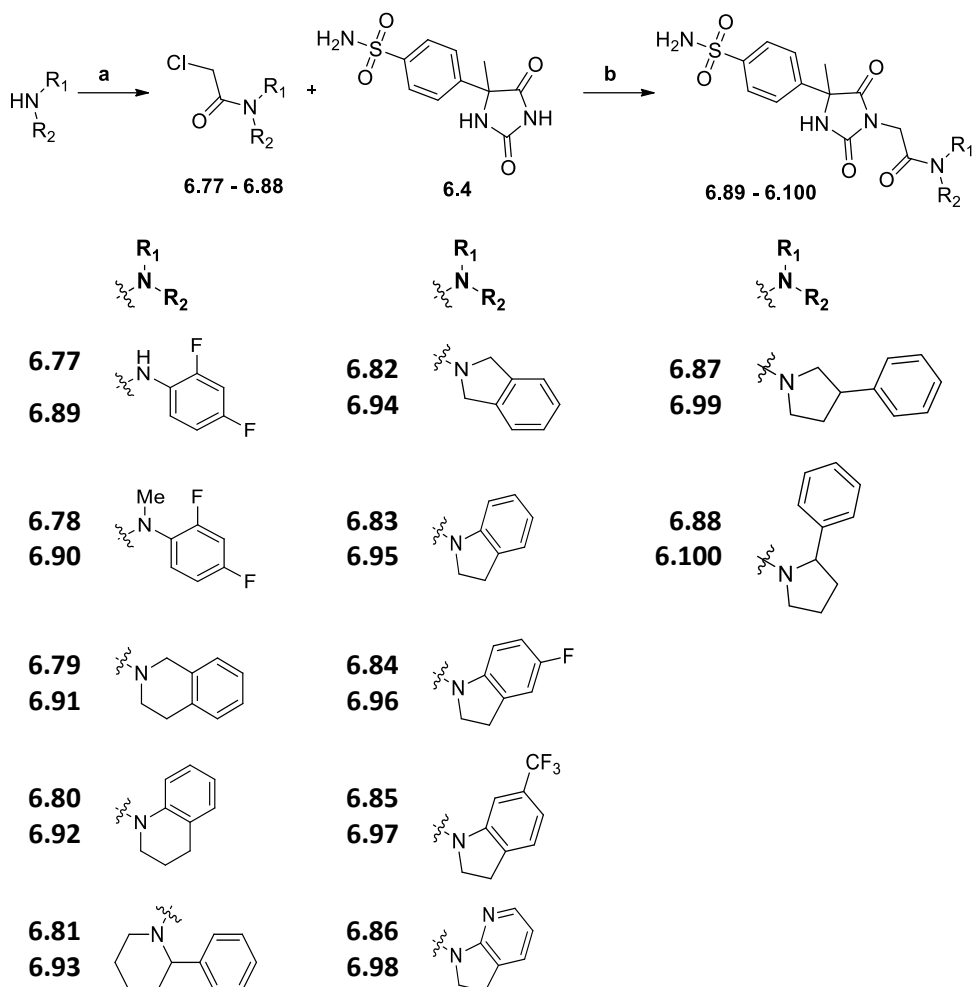
Reagents and conditions: (a) chloroacetyl chloride, Et$_3$N, DCM, 0°C, 17-20 hrs; (b) K$_2$CO$_3$, DMF, r.t., 24-48 hrs.

Compounds **6.89** and **6.90** were prepared as the closest analogues of the reference compound **6.9**, containing a 2,4-diF-substituted ring B but elongating the linker by –*NH*- or –*NMe*– moieties. A few cyclic amides **6.91-6.95** were prepared as well. Their biological evaluation demonstrated that the indoline derivative **6.95** was the most potent representative, retaining very good cellular potency and moderate enzyme inhibitory activity (MIC = 2.5 µM, DprE1 pIC$_{50}$ = 6.0, see Section 6.2.3.3 for more detail). Based on this promising result, some closely related analogues **6.96-6.100** were additionally prepared in order to provide better SAR-understanding and explore the potential of the current amide sub-series. Compounds **6.96-6.98** contained a substituted indoline core, while **6.99** and **6.100** possessed in their structure aryl-substituted pyrrolidines.
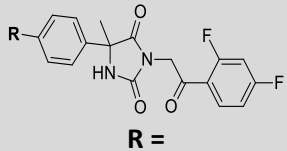
6.2   Results and discussion

All final compounds were evaluated for their ability to inhibit *Mtb* DprE1 enzymatic activity (pIC$_{50}$-values) and for their ability to inhibit the growth of the *Mtb* H37Rv strain (whole cell MIC-values). In addition, the cytotoxicity in HepG$_2$ cells was evaluated together with two physico-chemical parameters: kinetic aqueous solubility (using chemiluminescent nitrogen detection, CLND) and ChromLogD.

6.2.1 Ring A sulfonamide modifications

The biological and physicochemical evaluation results of the reference compound **5.50** and its analogues with the ring A sulfonamide modifications are summarized in Table 6.1.

Table 6.1. Biological and physicochemical profile of compounds with ring A substitution modifications

Structure R =		DprE1 pIC$_{50}$[a]	MIC (μM)[b]	Cytotoxicity HepG$_2$ (μM)[c]	Solubility (μM)[d]	Chrom logD[e]
5.50	-NHSO$_2$-Me	7.0	2.5	> 100	$\geq$ 487	3.57
6.1	-NHSO$_2$-CF$_3$	5.0	> 80	> 100	$\geq$ 372	3.24
6.2	-NHSO$_2$-Ph	6.4	80	100	44	4.90
6.3	-NHSO$_2$-Bu^n	5.4	> 80	100	154	4.96
6.9	-SO$_2$NH$_2$	7.2	0.7	> 100	$\geq$ 486	3.19
6.10	-SO$_2$NH-Me	6.1	20	> 100	$\geq$ 478	3.88
6.11	-SO$_2$NH-cPr	5.7	80	> 100	334	4.48
6.12	-SO$_2$NH-CH$_2$CF$_3$	4.5	> 80	63.1	57	4.78
6.13	-SO$_2$NH-Ph	4.7	> 80	79.4	55	5.03

[a] *Mtb*DprE1 enzyme inhibition pIC$_{50}$; [b] MIC [μM] against *Mycobacterium tuberculosis* (H37Rv). Reference: Isoniazid, MIC = 1.8 μM; [c] Cytotoxicity HepG$_2$ IC$_{50}$ [μM]; [d] kinetic aqueous solubility (CLND) [μM]; [e] ChromlogD (pH 7.4); [f] N.D. – not determined.

Differently substituted sulfonamides **6.1-6.3** demonstrated significant potency decrease in comparison with the methyl-substituted analogue **5.50**. The "retro-sulfonamide" **6.9** resulted in superior DprE1 inhibitory potency and over eight-fold improvement in the whole-cell activity (MIC = 0.6 μM). Remarkably, introduction of any substituent on the "retro-sulfonamide" moiety in compounds **6.10-6.13** was detrimental for their DprE1 inhibitory potency.

A few additional related modifications were introduced by other OMC researchers (Figure 6.2). Those products **6.101-6.103** demonstrated weak to moderate enzyme inhibitory potency (pIC$_{50}$ = 4.9-5.7) together with no activity in the whole-cell assay (MIC $\geq$ 40 μM).
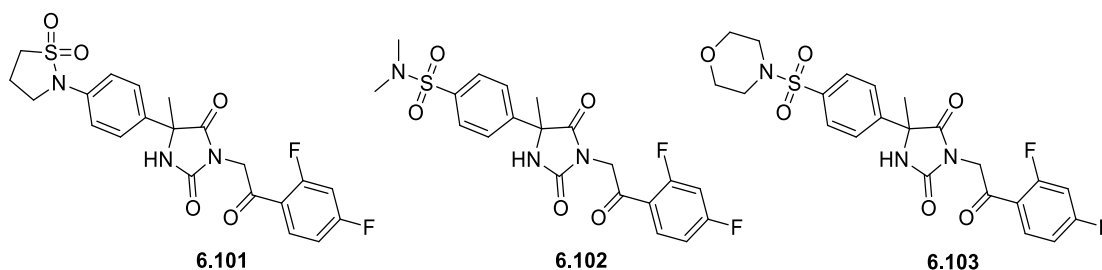

Figure 6.2. Ring A sulfonamide modification prepared by fellow OMC/DprE1 researchers
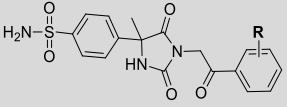
Based on the obtained SAR results, we decided to choose the benzenesulfonamide derivative **6.9** as a new reference compound for exploration of the ring B and linker modifications.

6.2.2 Ring B modifications/removal

6.2.2.1 Preparation of compounds with a differently substituted ring B

Table 6.2 summarizes the biological and physicochemical evaluation results of the new reference **6.9** and its analogues with substitution variation in ring B.

Table 6.2. Biological and physicochemical profile of compounds with ring B substitution modifications

Structure		DprE1 pIC$_{50}$[a]	MIC (μM)[b]	Cytotoxicity HepG$_2$ (μM)[c]	Solubility (μM)[d]	Chrom logD[e]
	R =					
6.9	2,4-diF	7.2	0.7	> 100	≥ 486	3.19
6.14	H	6.6	10	> 100	≥ 415	2.81
6.15	2-F	6.7	2.5	> 100	340	2.94
6.16	3-F	6.8	5.0	> 100	≥ 408	3.08
6.17	4-F	6.8	2.2	> 100	≥ 387	3.03
6.18	3,4-diF	7.2	1.2	> 100	≥ 314	3.34
6.19	3-Cl, 4-F	7.2	1.3	> 100	362	3.82
6.20	2,4-diCl	7.1	7.5	> 100	372	4.11
6.21	2-OH, 4-F	7.2	2.5	> 100	≥ 496	3.12
6.22	3-Br	7.0	1.9	> 100	≥ 347	3.77
6.23	2-Me	7.0	2.5	> 100	≥ 311	3.30
6.24	3-Me	6.7	5.0	> 100	≥ 320	3.36
6.25	4-Me	6.8	10	> 100	351	3.33
6.26	2-OMe	5.6	> 80	> 100	≥ 473	2.98
6.27	3-OMe	6.9	10	> 100	≥ 417	3.00
6.28	4-OMe	6.5	20	> 100	≥ 392	2.86
6.29	2-CF$_3$	7.0	2.5	> 100	≥ 381	3.56
6.30	3-CF$_3$	7.1	0.9	> 100	279	3.96
6.31	3-CN	5.9	40	> 100	≥ 482	2.40
6.32	3-NO$_2$	6.2	20	> 100	132	2.77
6.33	3-OCF$_3$	7.1	0.6	> 100	≥ 438	4.14
6.34	3-CF$_3$, 4-F	7.2	0.6	> 100	≥ 287	4.24
6.35	3,5-diCF$_3$	5.1	> 80	74.6	95	4.90
6.36	4-CF$_3$	6.0	20	65.4	370	4.15
6.37	4-CN	5.3	60	> 100	≥ 411	2.54

[a] *Mtb*DprE1 enzyme inhibition pIC$_{50}$; [b] MIC [μM] against *Mycobacterium tuberculosis* (H37Rv). Reference: Isoniazid, MIC = 1.8 μM; [c] Cytotoxicity HepG$_2$ IC$_{50}$ [μM]; [d] kinetic aqueous solubility (CLND) [μM]; [e] ChromlogD (pH 7.4); [f] N.D. – not determined.

Analogues **6.14-6.17** with one or both fluorine atoms removed demonstrated a notable drop of enzymatic activity (pIC$_{50}$ = 6.6-6.8), while compounds **6.18-6.19** possessing 4-F substitution together with a halogen (Cl or F) in the *3*-position retained high potency (pIC$_{50}$ = 7.2). The introduction of a 2,4-chlorine-subsituted ring B in **6.20** led to approximately eight times weaker whole-cell activity (MIC = 5 μM) than the reference **6.9** (MIC = 0.6 μM), indicating a particular importance of fluorine substituents
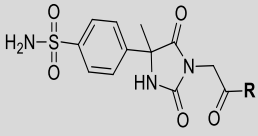
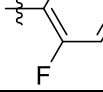for the series' whole-cell activity. Notably, product **6.21** with a 2-hydroxy group instead of fluorine atom resulted in retained enzymatic potency (pIC$_{50}$ = 7.2), but showed a MIC value of only 2.5 µM.

The 3-Br substituted product **6.22** and the compounds **6.23-6.28** with an electron-donating group (-Me or -OMe) demonstrated lower enzymatic and whole-cell potency in comparison with the reference **6.9**. Among the products **6.29-6.37** containing electron-withdrawing substituents, the most potent representatives were the 3-substituted analogues (**6.30** 3-CF$_3$, **6.33** 3-OCF$_3$ and **6.34** 3-CF$_3$, 4-F), which retained sub-micromolar whole-cell potency. The 2-CF$_3$-substitued compound **6.29** possessed the MIC value of 2.5 µM, while all other tested analogues showed even more significant enzymat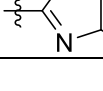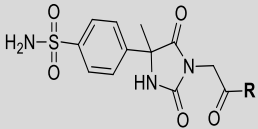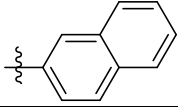ic and whole-cell activity drop. Gratifyingly, all synthesized ring B modified analogues, apart from **6.35-6.36**, demonstrated absence of any detectable cytotoxicity in the HepG2 assay (IC$_{50}$ > 100 µM).

6.2.2.2   Introduction of saturated residues or heterocycles in place of ring B

Table 6.3 contains the biological and physicochemical evaluation results of compounds **6.38-6.50**, containing a saturated residue or a heterocycle moiety in place of ring B.

Table 6.3. Biological and physicochemical profile of compounds with the ring B replaced by a saturated residue or a heterocycle moiety.

	Structure	DprE1 pIC$_{50}$[a]	MIC (µM)[b]	Cytotoxicity HepG$_2$ (µM)[c]	Solubility (µM)[d]	Chrom logD[e]
	R =					
6.38	-Me	4.0	> 80	> 100	≥ 504	0.54
6.39	◁	4.5	> 80	> 100	518	1.51
6.40	cyclohexyl	6.7	7.5	> 100	≥ 317	3.62
6.41	adamantyl	5.9	> 80	> 100	≥ 404	4.87
6.42	pyridinyl	6.4	10	> 100	≥ 405	2.03
6.43	pyridinyl	5.5	> 80	> 100	≥ 298	1.16
6.44	pyridinyl	5.6	80	> 100	≥ 439	1.16
6.45	difluoropyridinyl	7.1	0.6	> 100	≥ 441	2.39
6.46	thiophenyl	6.7	10	> 100	≥ 311	2.35
6.47	chlorothiophenyl	7.0	2.5	> 100	≥ 437	3.52
6.48	thiazolyl	6.2	60	> 100	453	4.90
6.49	benzothiazolyl	6.7	40*	> 97	≥ 339	3.78

Structure	DprE1 pIC$_{50}$[a]	MIC (µM)[b]	Cytotoxicity HepG$_2$ (µM)[c]	Solubility (µM)[d]	Chrom logD[e]
6.50	6.3	10	> 100	167	3.93
[a] *Mtb*DprE1 enzyme inhibition pIC$_{50}$; [b] MIC [µM] against *Mycobacterium tuberculosis* (H37Rv). Reference: Isoniazid, MIC = 1.8 µM; [c] Cytotoxicity HepG$_2$ IC$_{50}$ [µM]; [d] kinetic aqueous solubility (CLND) [µM]; [e] ChromlogD (pH 7.4); [f] N.D. – not determined. *only partial inhibition was reached.					

In compounds **6.38-6.41,** the ring B was replaced by a saturated residue. Methyl- or cyclopropyl-substitued compounds **6.38** and **6.39** showed a complete activity loss, while adamantyl-containing analogue **6.41** retained moderate DprE1 affinity (pIC$_{50}$ = 5.9). Introduction of a cyclohexyl ring in place of the ring B in **6.40,** led to slight improvement in potency over its direct phenyl-substituted analogue **6.14**: pIC$_{50}$–values were 6.7 and 6.6, respectively, and MIC-values 7.5 and 10 µM. This could indicate that appropriately substituted cyclohexyl-containing analogues may provide even higher potency.

Introduction of a pyridine instead of an aryl at this position (**6.42-6.45**) led to an activity drop, only the 2-pyridinyl-based **6.42** retained an activity comparable with its phenyl-substituted reference **6.14.** Therefore, the 2-pyridinyl moiety was combined with di-fluoro substitution pattern of the reference **6.9**, providing its closest heterocyclic analogue **6.45**. The latter retained sub-micromolar whole-cell activity (MIC = 0.6 µM) and DprE1 inhibition activity (pIC$_{50}$ = 7.1).

The 2-thiophenyl-substituted product **6.46** retained enzymatic and whole-cell potency compared to its direct phenyl analogue **6.14**, while addition of a chlorine substituent in position 5- of the thiophene ring in **6.47** led to further potency improvement (pIC$_{50}$ = 7.0, MIC = 2.5 µM). The latter was, however, still inferior to the activity of reference **6.9**. In contrast, introduction of a (benz-)thiazole moiety in **6.48-6.49** was characterized by a significant loss of potency.
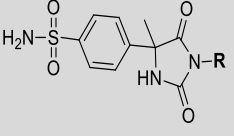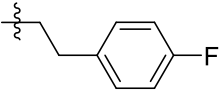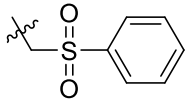
2-naphthalene-containing compound **6.50** showed modest DprE1 inhibition potency, while preserving the same whole-cell activity (MIC = 10 µM) as its phenyl analogue **6.14**, which may suggest that the enzymatic pocket could accommodate further substituent expansion in this part of the molecule.

6.2.3 Linker modifications

6.2.3.1 Keto-group removal, sulfone introduction

The biological and physicochemical evaluation results of compounds **6.51-6.52** are summarized in Table 6.5. The removal of a carbonyl group in the linker led to a complete activity loss in **6.51**, while **6.52** with a sulfonyl-containing linker retained moderate enzymatic potency (pIC$_{50}$ = 6.0).

Table 6.4. Biological and physicochemical profile of compounds 6.51-6.52
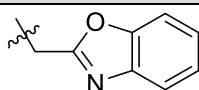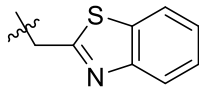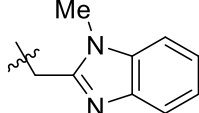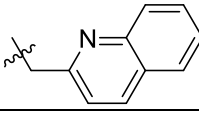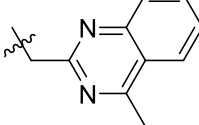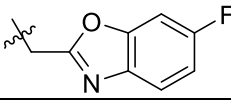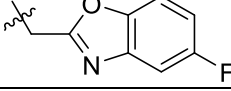
Structure R =	DprE1 pIC$_{50}$[a]	MIC (μM)[b]	Cytotoxicity HepG$_2$ (μM)[c]	Solubility (μM)[d]	Chrom logD[e]
6.51	4.8	> 80	> 100	≥ 476	3.09
6.52	6.0	50	> 100	≥ 386	1.99
[a] *Mtb*DprE1 enzyme inhibition pIC$_{50}$; [b] MIC [μM] against *Mycobacterium tuberculosis* (H37Rv). Reference: Isoniazid, MIC = 1.8 μM; [c] Cytotoxicity HepG$_2$ IC$_{50}$ [μM]; [d] kinetic aqueous solubility (CLND) [μM]; [e] ChromlogD (pH 7.4); [f] N.D. – not determined.					
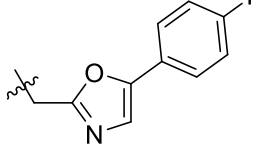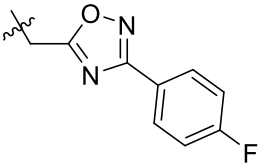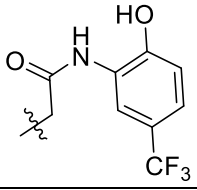
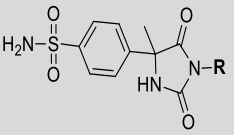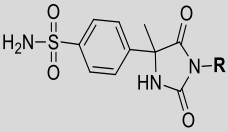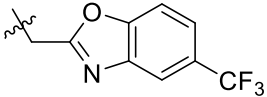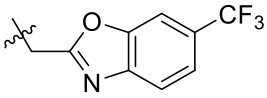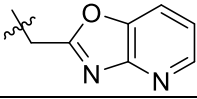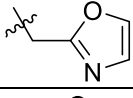### 6.2.3.2   Introduction of (benz)oxazoles and related compounds

The biological and physicochemical evaluation results of analogues containing (benz-)oxazole or related moieties in place of linker and ring B are summarized in Table 6.5.

Table 6.5. Biological and physicochemical profile of compounds substituted with (benz)oxazoles and related moieties

Structure R =	DprE1 pIC$_{50}$[a]	MIC (μM)[b]	Cytotoxicity HepG$_2$ (μM)[c]	Solubility (μM)[d]	Chrom logD[e]
6.62	6.3	15	> 100	≥ 312	2.70
6.63	6.3	10	> 100	33	3.07
6.64	4.6	> 80	> 100	≥ 507	2.16
6.65	5.4	> 80	> 100	< 1	2.83
6.66	5.5	80*	> 100	≥ 312	2.45
6.67	6.8	10	> 100	≥ 496	2.97
6.68	6.2	10	> 100	≥ 477	2.88

Structure R =	DprE1 pIC$_{50}$[a]	MIC (µM)[b]	Cytotoxicity HepG$_2$ (µM)[c]	Solubility (µM)[d]	Chrom logD[e]
6.69	6.6	5	38.4	≥ 357	4.06
6.70	6.3	15	90.3	255	4.08
6.71	4.5	> 80	> 100	≥ 295	1.33
6.72	4.1	> 80	> 100	≥ 503	0.78
6.73	4.0	> 80	> 100	≥ 426	1.31
6.74	5.3	80	> 100	≥ 492	3.30
6.75	5.5	> 80	26.0	≥ 415	3.69
6.76	4.5	> 80	> 100	69	3.00

[a] *Mtb*DprE1 enzyme inhibition pIC$_{50}$; [b] MIC [µM] against *Mycobacterium tuberculosis* (H37Rv). Reference: Isoniazid, MIC = 1.8 µM; [c] Cytotoxicity HepG$_2$ IC$_{50}$ [µM]; [d] kinetic aqueous solubility (CLND) [µM]; [e] ChromlogD (pH 7.4); [f] N.D. – not determined. *only partial inhibition was reached.

Benzoxazole- (**6.62**) and benzothiazole-containing (**6.63**) products possessed the best enzymatic and whole-cell potency within the evaluated sub-series **6.62-6.66**, in which various heterocyclic counterparts were connected by a CH$_2$-linker to the hydantoin's *N*-3 position.

Compounds **6.67-6.70**, comprising a substituted benzoxazole moiety, demonstrated moderate DprE1 inhibition potency (pIC$_{50}$ = 6.2-6.8), accompanied by promising whole cell activity (MIC = 5-15 µM) for analogues with modified linker. Unfortunately, CF$_3$-substituted products **6.69-6.70** exhibited cytotoxicity in HepG2 assay (IC$_{50}$ < 100 µM), indicating a potential liability of this sub-series.

Introduction of oxazolo[4,5-*b*]pyridin-2-ylmethyl moiety in **6.71** or five-membered oxazole and oxadiazole substituents in **6.72-6.75** led to a significant enzyme inhibition decrease (pIC$_{50}$ = 4.0-5.5) and no whole-cell activity (MIC ≥ 80 µM). The unexpected side product **6.76** with amide linker was inactive in the enzymatic and whole-cell assays.
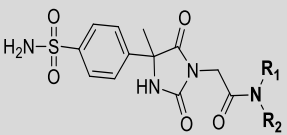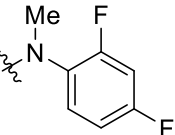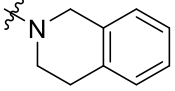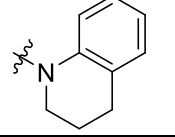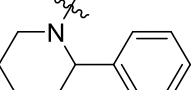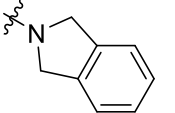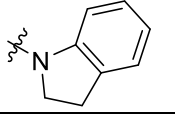
6.2.3.3 Amide as a replacement for ketone
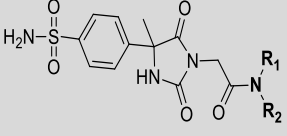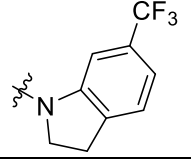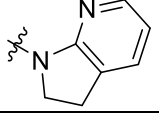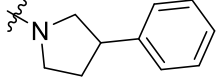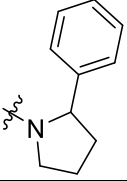
Table 6.6 summarizes the biological and physicochemical evaluation results of compounds with an amide moiety in place of ketone in the linker. In most cases, such a replacement led to a complete activity loss in the whole-cell assay and a significant drop in enzymatic activity (compounds **6.89-6.93**, **6.98-6.100**). The isoindoline analogue **6.94** showed moderate enzymatic potency, but reached only partial inhibition in the whole-cell assay.

Compounds containing an indoline moiety in lieu of an aryl ring B, demonstrated very promising whole cell activity (2.5 µM for **6.95-6.96**, 0.3 µM for **6.97**), accompanied by moderate DprE1-enzymatic inhibition (pIC$_{50}$ = 6.6-7.0). In fact, product **6.97**, containing a 3-CF$_3$ substituted indoline residue, demonstrated twofold improvement of the whole-cell potency over the reference **6.9** despite somewhat lower DprE1 potency.

All analogues with amide linker exhibited no detectable cytotoxicity in the HepG2 assay (IC$_{50}$ > 100 µM). Therefore, preparation of more substituted indolines as well as other related amides could be of interest for further potency improvement within the presented series.

Table 6.6. Biological and physicochemical profile of compounds with an amide moiety in place of ketone in the linker

Structure		DprE1 pIC$_{50}$[a]	MIC (µM)[b]	Cytotoxicity HepG$_2$ (µM)[c]	Solubility (µM)[d]	Chrom logD[e]
6.89		4.5	> 80	> 100	≥ 580	2.58
6.90		5.5	> 80	> 100	≥ 416	2.98
6.91		5.4	> 80	> 100	≥ 384	3.00
6.92		5.2	> 80	> 100	≥ 401	3.25
6.93		6.2	> 80	> 100	≥ 408	3.90
6.94		6.2	20*	> 100	≥ 503	2.56
6.95		6.7	2.5	> 100	77	2.99

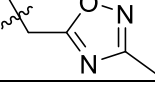| Structure	DprE1 pIC$_{50}$[a]	MIC (µM)[b]	Cytotoxicity HepG$_2$ (µM)[c]	Solubility (µM)[d]	Chrom logD[e]
6.96	6.6	2.5	> 100	≥ 323	3.14
6.97	7.0	0.3	> 100	225	4.10
6.98	5.2	> 80	> 100	≥ 269	2.53
6.99	4.7	> 80	> 100	≥ 289	3.30
6.100	5.2	> 80	> 100	277	3.20

[a] *Mtb*DprE1 enzyme inhibition pIC$_{50}$; [b] MIC [µM] against *Mycobacterium tuberculosis* (H37Rv). Reference: Isoniazid, MIC = 1.8 µM; [c] Cytotoxicity HepG$_2$ IC$_{50}$ [µM]; [d] kinetic aqueous solubility (CLND) [µM]; [e] ChromlogD (pH 7.4); [f] N.D. – not determined.*only partial inhibition was reached.

6.3 Conclusions of the second round of Hit-to-Lead optimization

Several most active representatives obtained during the second round of H2L otimazation are shown in Figure 6.3.

The "retro-sulfonamide" **6.9** (4-SO$_2$NH$_2$) was the most active sulfonamide-based compound obtained and it was chosen as a new reference, therefore the 4-SO$_2$NH$_2$ substituent in the ring A was kept constant during the extensive SAR investigation on ring B and additional linker modifications.
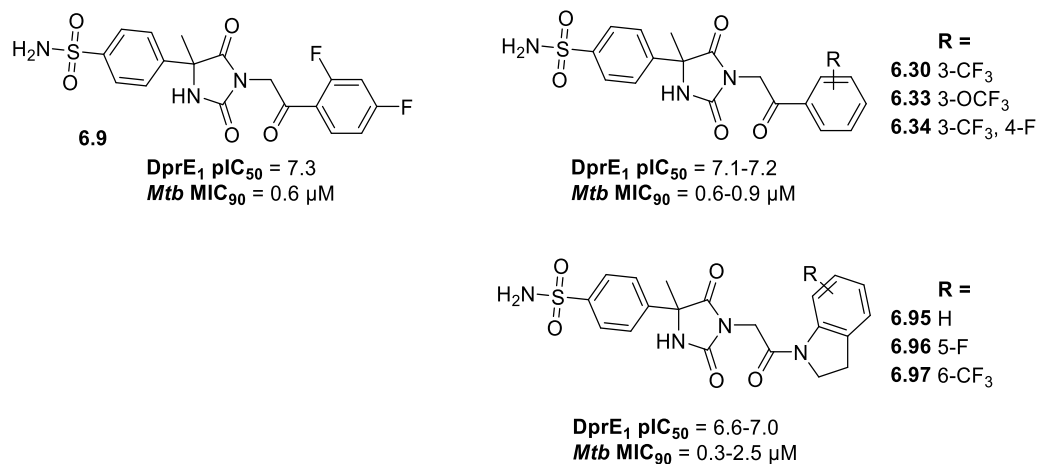
Figure 6.3. The most potent DprE1 inhibitors from the first round Hit-to-Lead optimization

122

Among the compounds with a differently substituted ring B, the most potent representatives were the 3-substituted analogues (**6.30** 3-CF$_3$, **6.33** 3-OCF$_3$ and **6.34** 3-CF$_3$, 4-F), that retained sub-micromolar whole-cell potency.

Several compounds containing an indoline moiety as the ring B, demonstrated very promising whole cell activity (2.5 μM for **6.95-6.96**, 0.3 μM for **6.97**), accompanied by moderate DprE1 enzyme inhibition (pIC$_{50}$ = 6.7-7.0). Therefore, the presence of a keto-group in the linker was shown to be not strictly essential for the activity in the series, in contrast to previous findings.

6.4 Experimental section

All the specifications with respect to reagents, solvents, analytical and structure elucidation techniques and equipment are identical to ones described in detail in the experimental section of Chapter 3 (see Section 3.4.1). In case of microwave radiation-assisted reactions, a Biotage® Initiator+ Microwave Synthesizer was used; the initial absorption was set as 'high' and 2 min of pre–stirring was applied before heating commenced.

The reaction progress was typically monitored by UPLC. The purity of all final compounds, tested on *in vitro* and *in vivo* assays, was 95% or higher (unless stated otherwise), verified by interpretation of ESI-MS (LCMS/UPLC) and ^{1}H NMR data. All the biological and physicochemical evaluation of the final compounds was performed in GSK, the assay description can be found in Chapter 7.2.

6.4.1 General methods

General method A: late stage sulfonamide introduction by a coupling reaction. 5-(4-bromophenyl)-3-(2-(2,4-difluorophenyl)-2-oxoethyl)-5-methylimidazolidine-2,4-dione **5.48** (0.08-0.19 mmol, 1.0 eq.), appropriate sulfonamide (1.2-2.0 eq.), 2-di-*tert*-butylphosphino-2′,4′,6′-triisopropylbiphenyl (t-BuXPhos) (0.04 eq.), allylpalladium(II) chloride dimer ([Pd(allyl)Cl]$_2$) (0.01 eq.) and potassium carbonate (2.0 eq.) were suspended in dry 2-methyltetrahydrofuran (2-MeTHF) (6 mL), place in the vial, which was evacuated with vacuum and backfilled with nitrogen 3 times. The vial was capped under nitrogen flow and stirred heated at 80 °C for 7-48 hrs. Then the reaction mixture was cooled to room temperature, 1M hydrochloric acid solution (20 mL) was added. Subsequently, the aqueous layer was extracted with ethyl acetate (3x20 mL). The combined organic layers were filtered through a small celite column, rinsed with ethyl acetate, dried over Na$_2$SO$_4$, filtrated and concentrated under reduced pressure. The crude residue was purified by normal phase flash column chromatography (gradient *c*-Hex:EtOAc = 100:0 to 10:90, solid loading) and additionally by HPLC (gradient: 40-100 basic/acid) in required. The fractoins, containing the desired product, were collected and evaporated under reduced pressure. The residue was dried to provide the title compound. The product was additionally dried in the vacuum oven (40 °C, 0-10 mbar).

General method B: hydantoin core synthesis. A modified Bucherer-Berg protocol was employed. The appropriate ketone (1.0-6.2 mmol, 1.0 eq.), ammonium carbonate (NH$_4$)$_2$CO$_3$ (9.0 eq.) and potassium cyanide KCN (1.3 eq.) were dissolved in a mixture of ethanol and water (1:1) (reaction molarity ≈ 0.08-0.20 mol/L). The reaction mixture was heated at 55 °C for 24-48 hrs or irradiated in microwave oven at 70 °C for 3-9 hours. After the reaction completion, the reaction mixture was cooled down to room temperature and neutralized with diluted hydrochloric acid to pH~7-8. In case of precipitate formation,

the product was collected by filtration and washed with water. Otherwise, the solvent was removed under reduced pressure and the residue was diluted with water and extracted with ethyl acetate; the combined organic phases were washed with brine, dried over Na_2SO_4, filtered and evaporated to dryness. In both purification cases, the product was additionally dried in the vacuum oven (40 °C, 0-10 mbr). No additional purification was performed.

General method C: hydantoin core alkylation. A mixture of the appropriate imidazolidine-2,4-dione (0.15-0.4 mmol, 1.0 eq.) and potassium carbonate K_2CO_3 (1.5-3.0 eq.) was dissolved in DMF or acetone. After 20 min, the corresponding alkyl halide was added in slight excess (1.05-1.5 eq.) (reaction molarity ≈ 0.04-0.1 mol/L). The reaction mixture was stirred at room temperature for 20-72 hrs. After completion of the reaction, the solvent was removed under reduced pressure and the residue was diluted with saturated ammonium chloride solution and extracted with ethyl acetate. The combined organic phases were washed with brine, dried over Na_2SO_4, filtered and evaporated to dryness. The residue was purified by normal phase column chromatography (gradient *c*-Hex:EtOAc = 100:0 to 10:90, solid loading) or reversed-phase flash column chromatography (gradient water:ACN = 90:10 to 50:50, liquid loading). The fractions, containing the desired product, were collected and evaporated under reduced pressure. The final product was additionally dried in the vacuum oven (40 °C, 0-10 mbr) or lyophilized.

General method D: 2-chloroacetamides synthesis. To a solution of the appropriate amine (1.40-1.80 mmol, 1.0 eq.) and triethylamine (2.0 eq.) in DCM, chloroacetyl chloride (1.10 eq.) in DCM was added dropwise at 0°C (reaction molarity ≈ 0.25-0.50 mol/L). The reaction mixture was left to warm up to room temperature and left stirring overnight. After the reaction completion, the reaction mixture was diluted with ethyl acetate and washed with water. The aqueous layer was extracted with EtOAc twice, the combined organic phases were washed with brine, dried over Na_2SO_4, filtered and evaporated to dryness. The resulting crude mixture containing the title compound was directly used for the next reaction step. No additional purification was performed, the title compound was not isolated; its identity and approximate content in the mixture was monitored by UPLC.

6.4.2 Chemistry

Final products **6.101-6.103** were prepared within OpenMedChem project by fellow colleagues. Compounds **6.53**, **6.54** were commercially available.

N-(4-(1-(2-(2,4-difluorophenyl)-2-oxoethyl)-4-methyl-2,5-dioxoimidazolidin-4-yl)phenyl)-1,1,1-trifluoromethanesulfonamide (6.1)
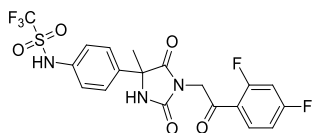
The title compound was prepared according to general method A from 5-(4-bromophenyl)-3-(2-(2,4-difluorophenyl)-2-oxoethyl)-5-methylimidazolidine-2,4-dione **5.48** (35 mg, 0.083 mmol) and trifluoromethanesulfonamide (24.66 mg, 0.165 mmol, 2 eq.). Yield 27% (11 mg, 0.022 mmol), off-white amorphous solid, purity ≥ 95%.

¹H NMR (400 MHz, DMSO-*d₆*) δ 11.99 (br. s., 1H), 9.05 (s, 1H), 8.00 (dt, *J*=6.82, 8.59 Hz, 1H), 7.46-7.58 (m, 3H), 7.22-7.35 (m, 3H), 4.80 (d, *J*=2.53 Hz, 2H), 1.74 (s, 3H). **ESI-MS (A):** *m/z* 490 [M-H]⁻ (R$_t$ = 1.02 min).

N-(4-(1-(2-(2,4-difluorophenyl)-2-oxoethyl)-4-methyl-2,5-dioxoimidazolidin-4-yl)phenyl)benzenesulfonamide (6.2)
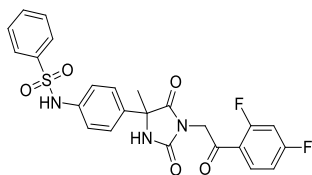
The title compound was prepared according to general method A from 5-(4-bromophenyl)-3-(2-(2,4-difluorophenyl)-2-oxoethyl)-5-methylimidazolidine-2,4-dione **5.48** (80 mg, 0.189 mmol) and benzenesulfonamide (35.7 mg, 0.227 mmol, 1.2 eq.). Yield 31% (31 mg, 0.059 mmol), off-white amorphous solid, purity ≥ 95%.

¹H NMR (400 MHz, DMSO-d_6) δ 10.46 (s, 1H), 8.94 (s, 1H), 7.99 (dt, J=6.82, 8.59 Hz, 1H), 7.77-7.83 (m, 2H), 7.45-7.66 (m, 4H), 7.38 (d, J=8.59 Hz, 2H), 7.28 (dt, J=2.27, 8.46 Hz, 1H), 7.13 (d, J=8.84 Hz, 2H), 4.76 (d, J=2.53 Hz, 2H), 1.67 (s, 3H). **¹³C NMR** (101 MHz, DMSO-d_6) δ 189.1 (d, J=5.1 Hz), 175.1, 165.7 (dd, J=255.6, 12.4 Hz), 162.4 (dd, J=257.6, 11.6 Hz), 155.0, 139.6, 137.5, 134.6, 133.0, 132.6 (dd, J=11.0, 4.2 Hz), 129.3, 126.6*, 119.5 - 119.6 (m), 119.5, 112.8 (dd, J=22.6, 2.6 Hz), 105.4 (t, J=26.6 Hz), 62.8, 47.1 (d, J=11.0 Hz), 24.5. **ESI-MS (A):** m/z 500 [M+H]⁺ (R$_t$ = 1.39 min). *Two peaks possess the identical chemical shift (proven by HSQC).*

N-(4-(1-(2-(2,4-difluorophenyl)-2-oxoethyl)-4-methyl-2,5-dioxoimidazolidin-4-yl)phenyl)butane-1-sulfonamide (6.3)
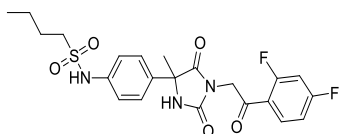
The title compound was prepared according to general method A from 5-(4-bromophenyl)-3-(2-(2,4-difluorophenyl)-2-oxoethyl)-5-methylimidazolidine-2,4-dione **5.48** (80 mg, 0.189 mmol) and butane-1-sulfonamide (38.9 mg, 0.284 mmol, 1.5 eq.). Yield 34% (55 mg, 0.097 mmol), off-white amorphous solid, purity ≥ 95%.

¹H NMR (400 MHz, DMSO-d_6) δ 9.69 (br. s., 1H), 9.01 (s, 1H), 8.01 (dt, J=6.57, 8.59 Hz, 1H), 7.43-7.56 (m, 3H), 7.29 (dt, J=2.40, 8.40 Hz, 1H), 7.23 (d, J=8.84 Hz, 2H), 4.80 (d, J=2.53 Hz, 2H), 3.04-3.14 (m, 2H), 1.73 (s, 3H), 1.58-1.69 (m, 2H), 1.35 (sxt, J=7.43 Hz, 2H), 0.84 (t, J=7.33 Hz, 3H). **¹³C NMR** (101 MHz, DMSO-d_6) δ 189.1 (d, J=4.4 Hz), 175.2, 165.7 (dd, J=255.4, 13.2 Hz), 162.4 (dd, J=257.6, 13.2 Hz), 155.0, 138.2, 134.3, 132.6 (dd, J=11.0, 4.0 Hz), 126.7, 119.5 (dd, J=12.8, 3.2 Hz), 119.1, 112.6 - 113.0 (m), 105.4 (t, J=26.6 Hz), 62.9, 50.5, 47.1 (d, J=10.2 Hz), 25.1, 24.6, 20.6, 13.4. **ESI-MS (A):** m/z 480 [M+H]⁺ (R$_t$ = 1.39 min).

4-(4-Methyl-2,5-dioxoimidazolidin-4-yl)benzenesulfonamide (6.4)
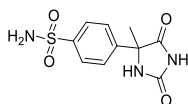
The title compound was prepared according to general method B from 4-acetylbenzenesulfonamide (1230 mg, 6.17 mmol) using microwave irradiation. Yield 70% (1225 mg, 4.32 mmol).

¹H NMR (400 MHz, DMSO-*d₆*) δ 10.87 (br. s., 1H), 8.69 (s, 1H), 7.84 (d, *J*=8.59 Hz, 2H), 7.67 (d, *J*=8.59 Hz, 2H), 7.37 (s, 2H), 1.68 (s, 3H). **¹³C NMR** (101 MHz, DMSO-*d₆*) δ 176.3, 156.1, 143.6, 143.5, 126.0, 125.8, 63.8, 25.0.**ESI-MS (A):** *m/z* 268 [M-H]⁻ (R$_t$ = 0.77 min).

4-Acetylbenzenesulfonamide
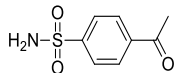
4-Acetylbenzenesulfonyl chloride (600 mg, 2.74 mmol) was slowly added to excess of 0.5 M ammonia solution (27 mL, 13.72 mmol) in dioxane under vigorous stirring. After completion of the reaction, the solvent was removed under reduced pressure and the residue was diluted with ethyl acetate and washed with saturated potassium carbonate solution and brine. The combined organic phases were washed with brine, dried over Na$_2$SO$_4$, filtered and evaporated to dryness. The crude title compound was directly used for the next reaction step. No additional purification was performed. Yield 74% (448 mg, 2.024 mmol).

¹H NMR (400 MHz, DMSO-*d₆*) δ 8.12 (d, J=8.59 Hz, 2H), 7.95 (d, J=8.59 Hz, 2H), 7.54 (s, 2H), 2.63 (s, 3H).

N-methyl-4-(4-methyl-2,5-dioxoimidazolidin-4-yl)benzenesulfonamide (6.5)
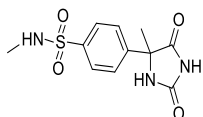
The title compound was prepared according to general method B from 4-acetyl-*N*-methylbenzenesulfonamide (396 mg, 1.857 mmol) using microwave irradiation. Yield 91% (502 mg, 1.683 mmol).

¹H NMR (400 MHz, DMSO-*d₆*) δ 10.89 (s, 1H), 8.70 (s, 1H), 7.78-7.83 (m, 2H), 7.68-7.74 (m, 2H), 7.48 (q, *J*=4.88 Hz, 1H), 2.41 (d, *J*=5.05 Hz, 3H), 1.69 (s, 3H). **¹³C NMR** (101 MHz, DMSO-*d₆*) δ 176.3, 156.1, 144.1, 138.8, 126.9, 126.3, 63.9, 28.6, 25.0. **ESI-MS (A):** *m/z* 282 [M-H]⁻ (R$_t$ = 1.17 min).

4-Acetyl-N-methylbenzenesulfonamide
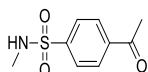
To a mixture of triethylamine (956 μl, 6.86 mmol) and methylamine hydrochloride (463 mg, 6.86 mmol) (in excess) in DCM (5 mL) 4-acetylbenzenesulfonyl chloride (500 mg, 2.287 mmol) was slowly added under vigorous stirring. After completion of the reaction, the solvent was removed under reduced pressure and the residue was diluted with ethyl acetate and washed with saturated potassium carbonate solution and brine. The combined organic phases were washed with brine, dried over Na$_2$SO$_4$, filtered and evaporated to dryness. The crude title compound was directly used for the next reaction step. No additional purification was performed. Yield 81% (396 mg, 1.857 mmol).

¹H NMR (400 MHz, DMSO-*d₆*) δ 8.13-8.17 (m, 2H), 7.91 (d, J=8.59 Hz, 2H), 7.61-7.69 (m, 1H), 2.64 (s, 3H), 2.44 (s, 3H).

N-cyclopropyl-4-(4-methyl-2,5-dioxoimidazolidin-4-yl)benzenesulfonamide (6.6)
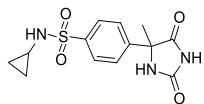
The title compound was prepared according to general method B from 4-acetyl-*N*-cyclopropylbenzenesulfonamide (594 mg, 2.482 mmol) using microwave irradiation. Yield 93% (750 mg, 2.303 mmol).

¹H NMR (400 MHz, DMSO-*d₆*) δ 10.89 (s, 1H), 8.71 (s, 1H), 7.95 (d, *J*=2.53 Hz, 1H), 7.82-7.86 (m, 2H), 7.69-7.74 (m, 2H), 2.03-2.11 (m, 1H), 1.70 (s, 3H), 0.44-0.51 (m, 2H), 0.34-0.42 (m, 2H). **¹³C NMR** (101 MHz, DMSO-*d₆*) δ 176.3, 156.1, 144.2, 139.8, 127.0, 126.3, 63.9, 25.0, 24.1, 5.1*. **ESI-MS (A):** *m/z* 308 [M-H]⁻ (R$_t$ = 0.95 min). *Two CH₂ peaks possess almost identical chemical shift.*

4-Acetyl-N-cyclopropylbenzenesulfonamide
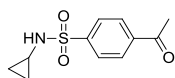
4-Acetylbenzenesulfonyl chloride (600 mg, 2.74 mmol) was slowly added to excess of cyclopropanamine (570 µl, 8.23 mmol) in DCM (5 mL) under vigorous stirring. After the reaction completion, the reaction mixture was diluted with ethyl acetate and washed with hydrochloric acid solution (0.5 M) and brine. The combined organic phases were washed with brine, dried over Na₂SO₄, filtered and evaporated to dryness. The crude title compound was directly used for the next reaction step. No additional purification was performed. Yield 87% (602 mg, 2.390 mmol).

¹H NMR (400 MHz, DMSO-*d₆*) δ 8.13-8.19 (m, 2H), 8.10 (s, 1H), 7.91-7.97 (m, 2H), 2.65 (s, 3H), 2.13 (dt, *J*=3.16, 6.51 Hz, 1H), 0.46-0.53 (m, 2H), 0.35-0.41 (m, 2H).

4-(4-Methyl-2,5-dioxoimidazolidin-4-yl)-N-(2,2,2-trifluoroethyl)benzenesulfonamide (6.7)
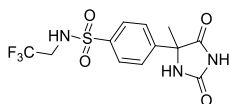
The title compound was prepared according to general method B from 4-acetyl-*N*-(2,2,2-trifluoroethyl)benzenesulfonamide (293 mg, 1.042 mmol) using microwave irradiation. Yield 66% (243 mg, 0.692 mmol), purity > 90%.

¹H NMR (400 MHz, DMSO-*d₆*) δ 10.89 (br. s., 1H), 8.72 (s, 1H), 8.65 (br. s., 1H), 7.83-7.90 (m, 2H), 7.68-7.73 (m, 2H), 3.70 (q, *J*=9.52 Hz, 2H), 1.69 (s, 3H). **¹³C NMR** (101 MHz, DMSO-*d₆*) δ 176.2, 156.1, 144.4, 140.2, 126.6, 126.4, 124.3 (q, *J*=278.8 Hz), 63.9, 43.3 (q, *J*=33.7 Hz), 25.0. **ESI-MS (A):** *m/z* 350 [M-H]⁻ (R$_t$ = 1.19 min).

4-Acetyl-N-(2,2,2-trifluoroethyl)benzenesulfonamide

The title compound was prepared in an analogous way to 4-acetyl-*N*-cyclopropylbenzenesulfonamide from 4-acetylbenzenesulfonyl chloride (600 mg, 2.74 mmol) and 2,2,2-trifluoroethylamine (646 µl, 8.23 mmol). Yield 38% (772 mg, 1.042 mmol).

¹H NMR (400 MHz, DMSO-*d₆*) δ 8.84 (t, J=6.69 Hz, 1H), 8.10-8.16 (m, 2H), 7.92-8.00 (m, 2H), 3.75 (dq, J=6.57, 9.52 Hz, 2H), 2.64 (s, 3H).

_____

4-(4-Methyl-2,5-dioxoimidazolidin-4-yl)-N-phenylbenzenesulfonamide (6.8)
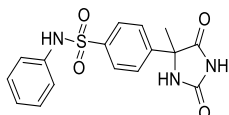
The title compound was prepared according to general method B from 4-acetyl-*N*-phenylbenzenesulfonamide (676 mg, 2.455 mmol) using microwave irradiation. Yield 87% (817 mg, 2.129 mmol), purity > 90%.

^{1}H NMR (400 MHz, DMSO-*d_6*) δ 10.87 (br. s., 1H), 10.34 (br. s., 1H), 8.63 (s, 1H), 7.77-7.83 (m, 2H), 7.62-7.69 (m, 2H), 7.18-7.26 (m, 2H), 7.07-7.14 (m, 2H), 6.98-7.05 (m, 1H), 1.64 (s, 3H). **^{13}C NMR** (101 MHz, DMSO-*d_6*) δ 176.2, 156.0, 144.5, 139.1, 137.6, 129.2, 126.9, 126.4, 124.0, 119.8, 63.8, 24.9. **ESI-MS (A):** *m/z* 344 [M-H]$^-$ (R$_t$ = 1.03 min).

4-Acetyl-N-phenylbenzenesulfonamide
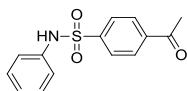
The title compound was prepared in an analogous way to 4-acetyl-*N*-cyclopropylbenzenesulfonamide from 4-acetylbenzenesulfonyl chloride (600 mg, 2.74 mmol) and aniline (0.250 mL, 2.74 mmol). Yield 87% (668 mg, 2.374 mmol).

^{1}H NMR (400 MHz, DMSO-*d_6*) δ 10.45 (s, 1H), 8.05-8.11 (m, 2H), 7.85-7.91 (m, 2H), 7.20-7.27 (m, 2H), 7.07-7.14 (m, 2H), 7.01-7.07 (m, 1H), 2.59 (s, 3H).

4-(1-(2-(2,4-Difluorophenyl)-2-oxoethyl)-4-methyl-2,5-dioxoimidazolidin-4-yl)benzenesulfonamide (6.9)
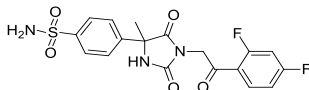
The title compound was prepared according to general method C from 4-(4-methyl-2,5-dioxoimidazolidin-4-yl)benzenesulfonamide **6.4** (200 mg, 0.743 mmol) and 2-chloro-2',4'-difluoroacetophenone (212 mg, 1.114 mmol) in acetone. Yield 53% (176 mg, 0.395 mmol), white amorphous solid, purity ≥ 95%.

^{1}H NMR (400 MHz, DMSO-*d_6*) δ 9.18 (br. s., 1H), 8.00 (dt, *J*=6.82, 8.59 Hz, 1H), 7.85-7.91 (m, 2H), 7.71-7.77 (m, 2H), 7.51 (ddd, *J*=2.40, 9.22, 11.62 Hz, 1H), 7.39 (s, 2H), 7.29 (dt, *J*=2.27, 8.46 Hz, 1H), 4.73-4.89 (m, *J*=2.78 Hz, 2H), 1.79 (s, 3H). **^{13}C NMR** (101 MHz, DMSO-*d_6*) δ 189.0 (d, *J*=4.4 Hz), 174.6, 165.7 (dd, *J*=255.4, 13.3 Hz), 162.5 (dd, *J*=257.6, 13.9 Hz), 155.0, 143.8, 142.9, 132.7 (dd, *J*=11.3, 3.8 Hz), 126.3, 125.9, 119.5 (dd, *J*=13.2, 3.1 Hz), 112.8 (dd, *J*=22.0, 2.9 Hz), 105.4 (t, *J*=26.7 Hz), 63.2, 47.2 (d, *J*=10.2 Hz), 24.9. **ESI-MS (A):** *m/z* 424 [M+H]$^+$ (R$_t$ = 1.05 min). **HRMS** (ESI) *m/z* calcd for C$_{18}$H$_{15}$F$_2$N$_3$O$_5$S [M+H]$^+$: 446.0593; found: 446.0602.

4-(1-(2-(2,4-Difluorophenyl)-2-oxoethyl)-4-methyl-2,5-dioxoimidazolidin-4-yl)-N-methylbenzenesulfonamide (6.10)

_____
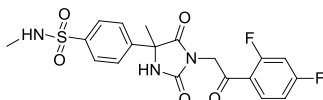
The title compound was prepared according to general method C from *N*-methyl-4-(4-methyl-2,5-dioxoimidazolidin-4-yl)benzenesulfonamide **6.5** (97 mg, 0.342 mmol) and 2-chloro-2',4'-difluoroacetophenone (98 mg, 0.514 mmol) in acetone. Yield 62% (98 mg, 0.213 mmol), white amorphous solid, purity ≥ 95%.

¹H NMR (400 MHz, DMSO-*d₆*) δ 9.18 (br. s., 1H), 8.00 (dt, *J*=6.57, 8.59 Hz, 1H), 7.82-7.86 (m, 2H), 7.75-7.80 (m, 2H), 7.46-7.55 (m, 2H), 7.28 (dt, *J*=2.40, 8.40 Hz, 1H), 4.82 (d, *J*=2.53 Hz, 2H), 2.43 (s, 3H), 1.79 (s, 3H). **¹³C NMR** (101 MHz, DMSO-*d₆*) δ 189.0 (d, *J*=5.1 Hz), 174.5, 165.7 (dd, *J*=255.3, 12.4 Hz), 162.5 (dd, *J*=257.6, 13.2 Hz), 155.0, 143.5, 139.1, 132.7 (dd, *J*=11.3, 4.0 Hz), 126.9, 126.6, 119.5 (dd, *J*=13.2, 2.9 Hz), 112.8 (dd, *J*=22.0, 3.2 Hz), 105.4 (t, *J*=27.1 Hz), 63.2, 47.3 (d, *J*=11.0 Hz), 28.7, 24.9. **ESI-MS (A):** *m/z* 438 [M+H]⁺ (R$_t$ = 1.11 min). **HRMS** (ESI) *m/z* calcd for C$_{19}$H$_{17}$F$_2$N$_3$O$_5$S [M+H]⁺: 460.0749; found: 460.0758.

N-cyclopropyl-4-(1-(2-(2,4-difluorophenyl)-2-oxoethyl)-4-methyl-2,5-dioxoimidazolidin-4-yl)benzenesulfonamide (6.11)
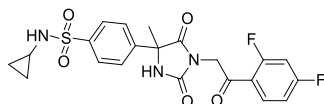
The title compound was prepared according to general method C from *N*-cyclopropyl-4-(4-methyl-2,5-dioxoimidazolidin-4-yl)benzenesulfonamide **6.6** (100 mg, 0.323 mmol) and 2-chloro-2',4'-difluoroacetophenone (92 mg, 0.485 mmol) in acetone. Yield 75% (118 mg, 0.242 mmol), off-white amorphous solid, purity ≥ 90%.

¹H NMR (400 MHz, DMSO-*d₆*) δ 9.19 (s, 1H), 7.95-8.05 (m, 2H), 7.84-7.90 (m, 2H), 7.75-7.82 (m, 2H), 7.50 (ddd, *J*=2.40, 9.28, 11.56 Hz, 1H), 7.28 (dt, *J*=2.40, 8.40 Hz, 1H), 4.82 (d, *J*=2.53 Hz, 2H), 2.09 (m, 1H), 1.80 (s, 3H), 0.44-0.53 (m, 2H), 0.35-0.44 (m, 2H). **¹³C NMR** (101 MHz, DMSO-*d₆*) δ 189.0 (d, *J*=4.4 Hz), 174.5, 165.7 (dd, *J*=255.3, 13.2 Hz), 162.5 (dd, *J*=257.6, 13.2 Hz), 155.0, 143.6, 140.0, 132.6 (dd, *J*=11.0, 4.4 Hz), 127.0, 126.5, 119.5 (dd, *J*=13.2, 3.7 Hz), 112.8 (dd, *J*=22.0, 3.1 Hz), 105.4 (t, *J*=26.8 Hz), 63.2, 47.3 (d, *J*=11.0 Hz), 24.9, 24.1, 5.1. **ESI-MS (A):** *m/z* 464 [M+H]⁺ (R$_t$ = 1.16 min).
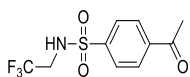
4-(1-(2-(2,4-Difluorophenyl)-2-oxoethyl)-4-methyl-2,5-dioxoimidazolidin-4-yl)-N-(2,2,2-trifluoroethyl)benzenesulfonamide (6.12)

The title compound was prepared according to general method C from 4-(4-methyl-2,5-dioxoimidazolidin-4-yl)-*N*-(2,2,2-trifluoroethyl)benzenesulfonamide **6.7** (100 mg, 0.285 mmol) and 2-bromo-1-(2,4-difluorophenyl)ethanone (100 mg, 0.427 mmol) in acetone. Yield 16% (23.4 mg, 0.046 mmol), off-white amorphous solid, purity ≥ 90%.

¹H NMR* (400 MHz, DMSO-*d₆*) δ 9.20 (s, 1H), 8.68 (s, 1H), 8.00 (dt, *J*=6.57, 8.59 Hz, 1H), 7.88-7.93 (m, 2H), 7.74-7.81 (m, 2H), 7.51 (ddd, *J*=2.40, 9.28, 11.56 Hz, 1H), 7.29 (dt, *J*=2.40, 8.40 Hz, 1H), 4.82 (d, *J*=2.53 Hz, 2H), 3.73 (q, *J*=9.60 Hz, 2H), 1.79 (s, 3H). **¹³C NMR** (101 MHz, DMSO-*d₆*) δ 189.0 (d, *J*=5.2 Hz), 174.5, 165.7 (dd, *J*=255.4, 13.2 Hz), 162.5 (dd, *J*=257.6, 13.2 Hz), 155.0, 143.9, 140.5, 132.6 (dd, *J*=11.0, 3.7 Hz), 126.6**, 124.3 (q, *J*=278.1 Hz), 119.4 (dd, *J*=13.2, 3.7 Hz), 112.8 (dd, *J*=22.0, 3.2 Hz), 105.4 (t, *J*=26.8 Hz), 63.2, 47.3 (d, *J*=10.2 Hz), 43.3 (q, *J*=34.8 Hz), 25.0. **ESI-MS (A):** *m/z* 504 [M-H]⁻ (R$_t$ = 1.14

min). *Alk position is proven by HSQC and HMBC NMR.* **Two peaks possess the identical chemical shift (proven by HSQC).*

4-(1-(2-(2,4-Difluorophenyl)-2-oxoethyl)-4-methyl-2,5-dioxoimidazolidin-4-yl)-N-phenylbenzenesulfonamide (6.13)

The title compound was prepared according to general method C from 4-(4-methyl-2,5-dioxoimidazolidin-4-yl)-*N*-phenylbenzenesulfonamide **6.8** (100 mg, 0.290 mmol) and 2-chloro-2',4'-difluoroacetophenone (83 mg, 0.434 mmol) in acetone. Yield 13% (21 mg, 0.038 mmol), off-white amorphous solid, purity ≥ 95%.

¹H NMR (400 MHz, DMSO-*d₆*) δ 10.38 (s, 1H), 9.11 (s, 1H), 7.99 (dt, *J*=6.57, 8.59 Hz, 1H), 7.80-7.87 (m, 2H), 7.72 (d, *J*=8.59 Hz, 2H), 7.49 (ddd, *J*=2.40, 9.22, 11.62 Hz, 1H), 7.20-7.32 (m, 3H), 7.09-7.15 (m, 2H), 6.98-7.06 (m, 1H), 4.79 (d, *J*=2.53 Hz, 2H), 1.75 (s, 3H). **¹³C NMR** (101 MHz, DMSO-*d₆*) δ 189.0 (d, *J*=4.4 Hz), 174.4,), 165.7 (dd, *J*=255.3, 12.6 Hz), 162.4 (dd, *J*=257.6, 13.2 Hz), 154.9, 143.9, 139.4, 137.6, 132.6 (dd, *J*=11.1, 3.9 Hz), 129.2, 126.9, 126.7, 124.0, 119.7, 119.4 (dd, *J*=13.9, 3.0 Hz), 112.8 (dd, *J*=21.9, 2.9 Hz), 105.4 (t, *J*=27.1 Hz), 63.2, 47.3 (d, *J*=11.7 Hz), 24.8. **ESI-MS (A):** *m/z* 498 [M-H]⁻ (R$_t$ = 1.21 min).

4-(4-Methyl-2,5-dioxo-1-(2-oxo-2-phenylethyl)imidazolidin-4-yl)benzenesulfonamide (6.14)

The title compound was prepared according to general method C from 4-(4-methyl-2,5-dioxoimidazolidin-4-yl)benzenesulfonamide **6.4** (50 mg, 0.186 mmol) and 2-bromo-1-phenylethanone (55.4 mg, 0.279 mmol) in acetone. Yield 50% (36 mg, 0.093 mmol), off-white amorphous solid, purity ≥ 95%.

¹H NMR (400 MHz, DMSO-*d₆*) δ 9.18 (br. s., 1H), 8.02-8.07 (m, 2H), 7.86-7.91 (m, 2H), 7.69-7.78 (m, 3H), 7.55-7.61 (m, 2H), 7.39 (s, 2H), 4.99 (s, 2H), 1.80 (s, 3H). **¹³C NMR** (101 MHz, DMSO-*d₆*) δ 192.1, 174.8, 155.1, 143.8, 143.0, 134.2, 133.9, 129.0, 128.1, 126.3, 125.9, 63.2, 44.6, 24.9. **ESI-MS (A):** *m/z* 386 [M-H]⁻ (R$_t$ = 0.99 min).

4-(1-(2-(2-Fluorophenyl)-2-oxoethyl)-4-methyl-2,5-dioxoimidazolidin-4-yl)benzenesulfonamide (6.15)

The title compound was prepared according to general method C from 4-(4-methyl-2,5-dioxoimidazolidin-4-yl)benzenesulfonamide **6.4** (100 mg, 0.371 mmol) and 2-bromo-1-(2-fluorophenyl)ethanone (121 mg, 0.557 mmol) in acetone. Yield 64% (96 mg, 0.237 mmol), white amorphous solid, purity ≥ 95%.

¹H NMR (400 MHz, DMSO-*d₆*) δ 9.18 (s, 1H), 7.84-7.94 (m, 3H), 7.71-7.80 (m, 3H), 7.32-7.49 (m, 4H), 4.82 (d, *J*=2.53 Hz, 2H), 1.79 (s, 3H). **¹³C NMR** (101 MHz, DMSO-*d₆*) δ 190.3 (d, *J*=4.4 Hz), 174.6, 161.5

(d, J=254.7 Hz), 155.0, 143.8, 142.9, 136.3 (d, J=9.5 Hz), 130.3 (d, J=2.2 Hz), 126.3, 125.9, 125.1 (d, J=2.9 Hz), 122.4 (d, J=13.2 Hz), 117.0 (d, J=22.7 Hz), 63.2, 47.4 (d, J=10.2 Hz), 24.8. **ESI-MS (A):** *m/z* 404 [M-H]⁻ (R$_t$ = 1.23 min).

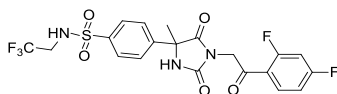### 4-(1-(2-(3-Fluorophenyl)-2-oxoethyl)-4-methyl-2,5-dioxoimidazolidin-4-yl)benzenesulfonamide (6.16)

The title compound was prepared according to general method C from 4-(4-methyl-2,5-dioxoimidazolidin-4-yl)benzenesulfonamide **6.4** (50mg, 0.186 mmol) and 2-bromo-3'-fluoroacetophenone (60.4 mg, 0.279 mmol) in acetone. Yield 45% (34 mg, 0.084 mmol), white amorphous solid, purity ≥ 95%.

¹H NMR (400 MHz, DMSO-d_6) δ 9.19 (s, 1H), 7.81-7.92 (m, 4H), 7.72-7.77 (m, 2H), 7.55-7.67 (m, 2H), 7.39 (s, 2H), 5.01 (s, 2H), 1.80 (s, 3H). **¹³C NMR** (101 MHz, DMSO-d_6) δ 191.4 (d, J=2.4 Hz), 174.7, 162.1 (d, J=245.9 Hz), 155.1, 143.8, 142.9, 136.0 (d, J=6.6 Hz), 131.2 (d, J=7.3 Hz), 126.3, 125.9, 124.4 (d, J=2.9 Hz), 121.2 (d, J=21.2 Hz), 114.8 (d, J=22.7 Hz), 63.2, 44.8, 24.9. **ESI-MS (A):** *m/z* 406 [M+H]⁺ (R$_t$ = 1.0 min).

4-(1-(2-(4-Fluorophenyl)-2-oxoethyl)-4-methyl-2,5-dioxoimidazolidin-4-yl)benzenesulfonamide (6.17)

The title compound was prepared according to general method C from 4-(4-methyl-2,5-dioxoimidazolidin-4-yl)benzenesulfonamide **6.4** (100 mg, 0.371 mmol) and 2-bromo-1-(4-fluorophenyl)ethanone (121 mg, 0.557 mmol) in acetone. Yield 65% (98 mg, 0.242 mmol), white amorphous solid, purity ≥ 95%.

¹H NMR (400 MHz, DMSO-d_6) δ 9.18 (s, 1H), 8.10-8.20 (m, 2H), 7.86-7.92 (m, 2H), 7.72-7.79 (m, 2H), 7.35-7.47 (m, 4H), 4.99 (s, 2H), 1.80 (s, 3H). **¹³C NMR** (101 MHz, DMSO-d_6) δ 190.8, 174.8, 165.5 (d, J=253.2 Hz), 155.1, 143.8, 143.0, 131.3 (d, J=9.5 Hz), 130.7 (d, J=2.9 Hz), 126.3, 125.9, 116.1 (d, J=22.0 Hz), 63.2, 44.6, 24.9. **ESI-MS (A):** *m/z* 404 [M-H]⁻ (R$_t$ = 1.24 min).

4-(1-(2-(3,4-Difluorophenyl)-2-oxoethyl)-4-methyl-2,5-dioxoimidazolidin-4-yl)benzenesulfonamide (6.18)

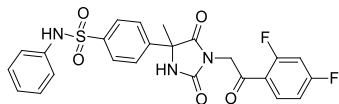

The title compound was prepared according to general method C from 4-(4-methyl-2,5-dioxoimidazolidin-4-yl)benzenesulfonamide **6.4** (75 mg, 0.279 mmol) and 2-bromo-1-(3,4-difluorophenyl)ethanone (98 mg, 0.418 mmol) in DMF. Yield 54% (63.6 mg, 0.150 mmol), white amorphous solid, purity ≥ 95%.

¹H NMR (400 MHz, DMSO-d_6) δ 9.22 (s, 1H), 8.08 - 8.18 (m, 1H), 7.95 (d, J = 6.27 Hz, 1H), 7.88 (d, J = 8.53 Hz, 2H), 7.75 (d, J = 8.53 Hz, 2H), 7.61 - 7.71 (m, 1H), 7.41 (s, 2H), 5.02 (s, 2H), 1.80 (s, 3H). **¹³C**

NMR (101 MHz, DMSO-d_6) δ 190.4, 174.8, 155.1, 153.3 (dd, *J*=255.3, 13.2 Hz), 149.6 (dd, *J*=248.7, 13.2 Hz), 143.8, 143.0, 131.2 - 131.5 (m), 126.3, 126.2 - 126.3 (m), 126.0, 118.3 (d, *J*=17.6 Hz), 117.8 (d, *J*=18.3 Hz), 63.3, 44.7, 24.9. **ESI-MS (B):** *m/z* 424 [M+H]$^+$ (R_t = 1.50 min).
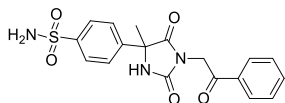
4-(1-(2-(3-Chloro-4-fluorophenyl)-2-oxoethyl)-4-methyl-2,5-dioxoimidazolidin-4-yl)benzenesulfonamide (6.19)

The title compound was prepared according to general method C from 4-(4-methyl-2,5-dioxoimidazolidin-4-yl)benzenesulfonamide **6.4** (50 mg, 0.186 mmol) and 2-bromo-3'-chloro-4'-fluoroacetophenone (70.0 mg, 0.279 mmol) in acetone. Yield 65% (53 mg, 0.120 mmol), off-white amorphous solid, purity ≥ 95%.

¹H NMR (400 MHz, DMSO-d_6) δ 9.16-9.23 (m, 1H), 8.29 (dd, *J*=2.15, 7.20 Hz, 1H), 8.08 (ddd, *J*=2.27, 4.74, 8.65 Hz, 1H), 7.85-7.91 (m, 2H), 7.72-7.78 (m, 2H), 7.64 (t, *J*=8.97 Hz, 1H), 7.40 (s, 2H), 5.03 (s, 2H), 1.80 (s, 3H). **¹³C NMR** (101 MHz, DMSO-d_6) δ 190.4 (s), 174.7 (s), 160.6 (d, *J*=255.4 Hz), 155.0 (s), 143.8 (s), 142.9 (s), 131.7 (d, *J*=3.7 Hz), 131.1 (s), 129.7 (d, *J*=8.8 Hz), 126.3 (s), 125.9 (s), 120.6 (d, *J*=18.3 Hz), 117.6 (d, *J*=22.0 Hz), 63.2 (s), 44.6 (s), 24.9 (s). **ESI-MS (A):** *m/z* 438 [M-H]$^-$ (R_t = 1.06 min).

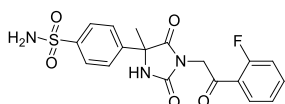### *4-(1-(2-(2,4-Dichlorophenyl)-2-oxoethyl)-4-methyl-2,5-dioxoimidazolidin-4-yl)benzenesulfonamide (6.20)*

The title compound was prepared according to general method C from 4-(4-methyl-2,5-dioxoimidazolidin-4-yl)benzenesulfonamide **6.4** (100 mg, 0.371 mmol) and 2-bromo-2′,4′-dichloroacetophenone (100 mg, 0.371 mmol) in acetone. Yield 53% (100.3 mg, 0.198 mmol), off-white amorphous solid, purity ≥ 95%.

¹H NMR (400 MHz, DMSO-d_6) δ 9.19 (s, 1H), 7.84-7.89 (m, 3H), 7.79 (d, *J*=2.02 Hz, 1H), 7.68-7.72 (m, 2H), 7.60 (dd, *J*=2.02, 8.34 Hz, 1H), 7.39 (s, 2H), 4.84 (s, 2H), 1.76 (s, 3H). **¹³C NMR** (101 MHz, DMSO-d_6) δ 193.4, 174.4, 154.8, 143.8, 142.8, 137.4, 133.4, 132.0, 131.4, 130.5, 127.7, 126.2, 125.9, 63.2, 46.7, 24.9. **ESI-MS (A):** *m/z* 456 [M+H]$^+$ (R_t = 1.14 min). **HRMS** (ESI) *m/z* calcd for $C_{18}H_{15}Cl_2N_3O_5S$ [M+H]$^+$: 478.0002; found: 478.0024.

4-(1-(2-(4-Fluoro-2-hydroxyphenyl)-2-oxoethyl)-4-methyl-2,5-dioxoimidazolidin-4-yl)benzenesulfonamide (6.21)
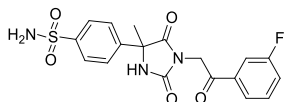

The title compound was prepared according to general method C from 4-(4-methyl-2,5-dioxoimidazolidin-4-yl)benzenesulfonamide **6.4** (100 mg, 0.371 mmol) and 2-(2-bromoacetyl)-5-fluorophenyl pivalate* (130 mg, 0.409 mmol) in DMF. Yield 20% (32 mg, 0.076 mmol), off-white amorphous solid, purity ≥ 95%. **Reagent was prepared in house by a fellow colleague. The pivalate group cleavage was detected under the reaction conditions.*

¹H NMR (400 MHz, DMSO-*d₆*) δ 9.16 (s, 1H), 7.83 - 7.94 (m, 3H), 7.76 (d, *J* = 8.53 Hz, 2H), 7.42 (s, 2H), 6.75 - 6.88 (m, 2H), 4.84 (s, 2H), 1.80 (s, 3H). **¹³C NMR** (101 MHz, DMSO-*d₆*) δ 192.1, 174.8, 166.3 (d, *J*=253.1 Hz), 161.5 (d, *J*=13.2 Hz), 155.3, 143.8, 143.1, 133.0 (d, *J*=12.5 Hz), 126.3, 125.9, 118.0 (d, *J*=2.2 Hz), 107.4 (d, *J*=22.7 Hz), 104.0 (d, *J*=23.5 Hz), 63.2, 47.2, 24.9. **ESI-MS (B):** *m/z* 422 [M+H]⁺ (R$_t$ = 1.45 min).
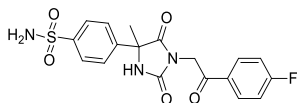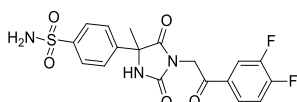
4-(1-(2-(3-Bromophenyl)-2-oxoethyl)-4-methyl-2,5-dioxoimidazolidin-4-yl)benzenesulfonamide (6.22)

The title compound was prepared according to general method C from 4-(4-methyl-2,5-dioxoimidazolidin-4-yl)benzenesulfonamide **6.4** (150 mg, 0.557 mmol) and 2-bromo-1-(3-bromophenyl)ethanone (232 mg, 0.836 mmol) in DMF. Yield 53% (138.6 mg, 0.297 mmol), off-white amorphous solid, purity ≥ 95%.

¹H NMR (400 MHz, DMSO-*d₆*) δ 9.20 (br. S., 1H), 8.19 (s, 1H), 8.03 (d, *J* = 7.78 Hz, 1H), 7.83 − 7.96 (m, 3H), 7.74 (d, *J* = 8.53 Hz, 2H), 7.54 (t, *J* = 7.91 Hz, 1H), 7.41 (br. S., 2H), 5.02 (s, 2H), 1.79 (s, 3H). **¹³C NMR** (101 MHz, DMSO-*d₆*) δ 191.5, 174.7, 155.1, 143.8, 143.0, 136.9, 135.9, 131.2, 130.8, 127.2, 126.3, 126.0, 122.3, 63.3, 44.7, 24.9. **ESI-MS (B):** *m/z* 466, 468 [M+H]⁺ (R$_t$ = 1.58 min).

4-(4-Methyl-2,5-dioxo-1-(2-oxo-2-(o-tolyl)ethyl)imidazolidin-4-yl)benzenesulfonamide (6.23)

The title compound was prepared according to general method C from 4-(4-methyl-2,5-dioxoimidazolidin-4-yl)benzenesulfonamide **6.4** (75 mg, 0.279 mmol) and 2-bromo-1-(o-tolyl)ethanone (89 mg, 0.418 mmol) in DMF. Yield 40% (44.6 mg, 0.111 mmol), white amorphous solid, purity ≥ 95%.

¹H NMR (400 MHz, DMSO-*d₆*) δ 9.10 (s, 1H), 7.76 - 7.84 (m, 3H), 7.63 (d, *J* = 8.53 Hz, 2H), 7.40 - 7.47 (m, 1H), 7.34 (s, 2H), 7.24 - 7.31 (m, 2H), 4.75 (s, 2H), 2.32 (s, 3H), 1.69 (s, 3H). **¹³C NMR** (101 MHz, DMSO-*d₆*) δ 195.8, 174.7 - 174.8 (m), 155.2, 143.8, 143.0, 138.0, 134.4, 132.4, 131.9, 128.9, 126.3, 126.1, 125.9, 63.2, 46.3, 24.9, 20.7. **ESI-MS (B):** *m/z* 402 [M+H]⁺ (R$_t$ = 1.48 min).

4-(4-Methyl-2,5-dioxo-1-(2-oxo-2-(m-tolyl)ethyl)imidazolidin-4-yl)benzenesulfonamide (6.24)
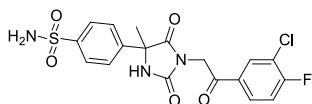

The title compound was prepared according to general method C from 4-(4-methyl-2,5-dioxoimidazolidin-4-yl)benzenesulfonamide **6.4** (60 mg, 0.223 mmol) and 2-bromo-1-(m-tolyl)ethanone (52.2 mg, 0.245 mmol) in DMF. Yield 44% (39 mg, 0.097 mmol), white amorphous solid, purity ≥ 95%.

¹H NMR (400 MHz, DMSO-*d₆*) δ 9.21 (s, 1H), 7.81 − 7.90 (m, 4H), 7.75 (d, *J* = 8.53 Hz, 2H), 7.50 − 7.56 (m, 1H), 7.39 − 7.49 (m, 3H), 4.96 (s, 2H), 2.38 (s, 3H), 1.79 (s, 3H). **¹³C NMR** (101 MHz, DMSO-*d₆*) δ

_____

192.3, 174.9, 155.2, 143.8, 143.0, 138.5, 134.9, 134.0, 128.9, 128.6, 126.4, 126.0, 125.4, 63.3, 44.7, 24.9, 20.9. **ESI-MS (B):** *m/z* 402 [M+H]$^+$ (R$_t$ = 1.54 min).

4-(4-Methyl-2,5-dioxo-1-(2-oxo-2-(p-tolyl)ethyl)imidazolidin-4-yl)benzenesulfonamide (6.25)

The title compound was prepared according to general method C from 4-(4-methyl-2,5-dioxoimidazolidin-4-yl)benzenesulfonamide **6.4** (50 mg, 0.186 mmol) and 2-bromo-1-(*p*-tolyl)ethanone (59.3 mg, 0.279 mmol) in acetone. Yield 38% (28.6 mg, 0.071 mmol), off-white amorphous solid, purity ≥ 95%.

¹H NMR (400 MHz, DMSO-*d₆*) δ 9.19 (s, 1H), 7.95 (d, *J* = 8.28 Hz, 2H), 7.87 - 7.92 (m, 2H), 7.74 - 7.78 (m, 2H), 7.41 (s, 2H), 7.37 - 7.41 (m, 2H), 4.95 (s, 2H), 2.41 (s, 3H), 1.81 (s, 3H). **¹³C NMR** (101 MHz, DMSO-*d₆*) δ 191.5, 174.8, 155.2, 144.9, 143.8, 143.0, 131.5, 129.5, 128.2, 126.3, 125.9, 63.2, 44.5, 24.9, 21.3. **ESI-MS (B):** *m/z* 402 [M+H]$^+$ (R$_t$ = 1.50 min).
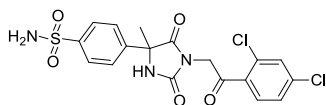
4-(1-(2-(2-Methoxyphenyl)-2-oxoethyl)-4-methyl-2,5-dioxoimidazolidin-4-yl)benzenesulfonamide (6.26)

The title compound was prepared according to general method C from 4-(4-methyl-2,5-dioxoimidazolidin-4-yl)benzenesulfonamide **6.4** (50 mg, 0.186 mmol) and 2-bromo-1-(2-methoxyphenyl)ethanone (63.8 mg, 0.279 mmol) in acetone. Yield 13% (10.2 mg, 0.024 mmol), white amorphous solid, purity ≥ 95%.

¹H NMR (400 MHz, DMSO-*d₆*) δ 9.13 (s, 1H), 7.84 - 7.92 (m, 2H), 7.70 - 7.78 (m, 3H), 7.65 (ddd, *J* = 1.76, 7.15, 8.66 Hz, 1H), 7.40 (s, 2H), 7.24 (d, *J* = 8.28 Hz, 1H), 7.03 - 7.12 (m, 1H), 4.74 (s, 2H), 3.94 (s, 3H), 1.78 (s, 3H). **¹³C NMR** (101 MHz, DMSO-*d₆*) δ 192.3, 174.7, 159.5, 155.3, 143.8, 143.1, 135.5, 130.2, 126.3, 125.9, 123.7, 120.8, 112.8, 63.1, 56.0, 48.4, 24.8. **ESI-MS (B):** *m/z* 418 [M+H]$^+$ (R$_t$ = 1.46 min).
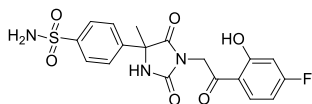
4-(1-(2-(3-Methoxyphenyl)-2-oxoethyl)-4-methyl-2,5-dioxoimidazolidin-4-yl)benzenesulfonamide (6.27)

The title compound was prepared according to general method C from 4-(4-methyl-2,5-dioxoimidazolidin-4-yl)benzenesulfonamide **6.4** (50 mg, 0.186 mmol) and 2-bromo-1-(3-methoxyphenyl)ethanone (63.8 mg, 0.279 mmol) in acetone. Yield 48% (36.8 mg, 0.088 mmol), white amorphous solid, purity ≥ 95%.

¹H NMR (400 MHz, DMSO-*d₆*) δ 9.19 (s, 1H), 7.88 (d, *J* = 8.28 Hz, 2H), 7.75 (d, *J* = 8.53 Hz, 2H), 7.64 (d, *J* = 7.53 Hz, 1H), 7.46 - 7.54 (m, 2H), 7.40 (s, 2H), 7.28 (dd, *J* = 2.13, 8.16 Hz, 1H), 4.98 (s, 2H), 3.83 (s, 3H), 1.80 (s, 3H). **¹³C NMR** (101 MHz, DMSO-*d₆*) δ 192.0, 174.8, 159.5, 155.2, 143.8, 143.0, 135.3, 130.2, 126.3, 125.9, 120.6, 120.4, 112.5, 63.2, 55.4, 44.8, 24.9. **ESI-MS (B):** *m/z* 418 [M+H]$^+$ (R$_t$ = 1.45 min).

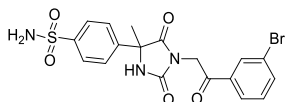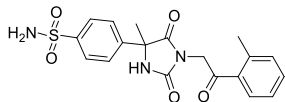### *4-(1-(2-(4-Methoxyphenyl)-2-oxoethyl)-4-methyl-2,5-dioxoimidazolidin-4-yl)benzenesulfonamide (6.28)*
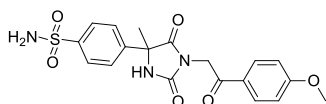
The title compound was prepared according to general method C from 4-(4-methyl-2,5-dioxoimidazolidin-4-yl)benzenesulfonamide **6.4** (50 mg, 0.186 mmol) and 2-bromo-1-(4-methoxyphenyl)ethanone (63.8 mg, 0.279 mmol) in acetone. Yield 32% (25.0 mg, 0.060 mmol), off-white amorphous solid, purity ≥ 95%.

^{1}H NMR (400 MHz, DMSO-d_6) δ 9.16 (s, 1H), 7.98 - 8.06 (m, 2H), 7.85 - 7.91 (m, 2H), 7.72 - 7.79 (m, 2H), 7.40 (br. s., 2H), 7.05 - 7.12 (m, 2H), 4.92 (s, 2H), 3.86 (s, 3H), 1.79 (s, 3H). **^{13}C NMR** (101 MHz, DMSO-d_6) δ 190.2, 174.9, 163.9, 155.3, 143.8, 143.1, 130.5, 126.9, 126.3, 126.0, 114.2, 63.2, 55.7, 44.3, 24.9. **ESI-MS (B):** *m/z* 418 [M+H]$^+$ (R_t = 1.44 min).

4-(4-Methyl-2,5-dioxo-1-(2-oxo-2-(2-(trifluoromethyl)phenyl)ethyl)imidazolidin-4-yl)benzenesulfonamide (6.29)

The title compound was prepared according to general method C from 4-(4-methyl-2,5-dioxoimidazolidin-4-yl)benzenesulfonamide **6.4** (50 mg, 0.186 mmol) and 2-bromo-1-(2-(trifluoromethyl)phenyl)ethanone (74.4 mg, 0.279 mmol) in acetone. Yield 36% (30.4 mg, 0.067 mmol), white amorphous solid, purity ≥ 95%.

^{1}H NMR (400 MHz, DMSO-d_6) δ 9.23 (s, 1H), 7.77 - 7.92 (m, 6H), 7.71 (d, *J* = 8.53 Hz, 2H), 7.40 (s, 2H), 4.82 (s, 2H), 1.78 (s, 3H). **^{13}C NMR*** (101 MHz, DMSO-d_6) δ 196.0, 174.4, 154.8, 143.8, 142.9, 135.7 - 135.8 (m), 132.8, 132.0, 128.4, 127.1 (q, *J*=5.1 Hz), 126.2, 125.9, 123.3 (q, *J*=273.6 Hz), 63.2, 46.8, 25.0. **ESI-MS (B):** *m/z* 456 [M+H]$^+$ (R_t = 1.55 min). **Cq with $^2J_{CF}$ was not detected.*
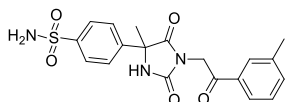
4-(4-Methyl-2,5-dioxo-1-(2-oxo-2-(3-(trifluoromethyl)phenyl)ethyl)imidazolidin-4-yl)benzenesulfonamide (6.30)

The title compound was prepared according to general method C from 4-(4-methyl-2,5-dioxoimidazolidin-4-yl)benzenesulfonamide **6.4** (75 mg, 0.279 mmol) and 2-bromo-1-(3-(trifluoromethyl)phenyl)ethanone (112 mg, 0.418 mmol) in acetone. Yield 19% (24.3 mg, 0.053 mmol), white amorphous solid, purity ≥ 95%.

^{1}H NMR (400 MHz, DMSO-d_6) δ 9.24 (br. s., 1H), 8.29 - 8.40 (m, 2H), 8.10 (d, *J* = 7.78 Hz, 1H), 7.89 (d, *J* = 8.53 Hz, 2H), 7.84 (t, *J* = 7.78 Hz, 1H), 7.76 (d, *J* = 8.53 Hz, 2H), 7.42 (s, 2H), 5.12 (s, 2H), 1.81 (s, 3H). **^{13}C NMR** (101 MHz, DMSO-d_6) δ 191.8, 174.8, 155.1, 143.8, 143.0, 134.7, 132.3, 130.6 (q, *J*=3.7 Hz), 130.4, 129.7 (q, *J*=32.3 Hz), 126.4, 126.0, 124.7 (q, *J*=3.7 Hz), 123.7 (q, *J*=272.9 Hz), 63.3, 44.9, 24.9. **ESI-MS (B):** *m/z* 454 [M-H]$^-$ (R_t = 1.55 min). **ESI-MS (C):** *m/z* 456 [M+H]$^+$ (R_t = 3.31 min).

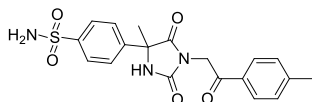### *4-(1-(2-(3-Cyanophenyl)-2-oxoethyl)-4-methyl-2,5-dioxoimidazolidin-4-yl)benzenesulfonamide (6.31)*

The title compound was prepared according to general method C from 4-(4-methyl-2,5-dioxoimidazolidin-4-yl)benzenesulfonamide **6.4** (60 mg, 0.223 mmol) and 3-(2-bromoacetyl)benzonitrile (74.9 mg, 0.334 mmol) in acetone. Yield 36% (32.6 mg, 0.079 mmol), off-white amorphous solid, purity ≥ 95%.

^{1}H NMR (400 MHz, DMSO-d_6) δ 9.24 (s, 1H), 8.55 (s, 1H), 8.31 (d, J = 8.03 Hz, 1H), 8.19 (d, J = 7.78 Hz, 1H), 7.89 (d, J = 8.53 Hz, 2H), 7.72 – 7.83 (m, 3H), 7.43 (s, 2H), 5.09 (s, 2H), 1.81 (s, 3H). **^{13}C NMR** (101 MHz, DMSO-d_6) δ 191.4, 174.8, 155.1, 143.8, 143.0, 137.4, 134.6, 132.5, 132.3, 130.3, 126.3, 126.0, 118.0, 112.2, 63.3, 44.8, 25.0. **ESI-MS (B):** m/z 411 [M-H]$^-$ (R$_t$ = 1.28 min). **ESI-MS (C):** m/z 413 [M+H]$^+$, 435 [M+Na]$^+$ (R$_t$ = 2.71 min).
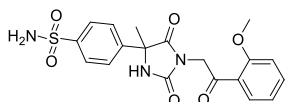
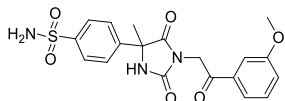### *4-(4-Methyl-1-(2-(3-nitrophenyl)-2-oxoethyl)-2,5-dioxoimidazolidin-4-yl)benzenesulfonamide (6.32)*

The title compound was prepared according to general method C from 4-(4-methyl-2,5-dioxoimidazolidin-4-yl)benzenesulfonamide **6.4** (60 mg, 0.223 mmol) and 3-nitrophenacyl bromide (82 mg, 0.334 mmol) in DMF. Yield 48% (46.2 mg, 0.107 mmol), off-white amorphous solid, purity ≥ 95%.

^{1}H NMR (400 MHz, DMSO-d_6) δ 9.24 (s, 1H), 8.71 (s, 1H), 8.53 (dd, J = 1.51, 8.28 Hz, 1H), 8.47 (d, J = 7.78 Hz, 1H), 7.84 – 7.92 (m, 3H), 7.75 (d, J = 8.53 Hz, 2H), 7.42 (s, 2H), 5.14 (s, 2H), 1.80 (s, 3H). **^{13}C NMR** (101 MHz, DMSO-d_6) δ 191.4, 174.7, 155.1, 148.1, 143.8, 143.0, 135.1, 134.5, 130.8, 128.4, 126.3, 126.0, 122.7, 63.3, 44.9, 24.9. **ESI-MS (B):** m/z 431 [M-H]$^-$ (R$_t$ = 1.38 min).

4-(4-Methyl-2,5-dioxo-1-(2-oxo-2-(3-(trifluoromethoxy)phenyl)ethyl)imidazolidin-4-yl)benzenesulfonamide (6.33)

The title compound was prepared according to general method C from 4-(4-methyl-2,5-dioxoimidazolidin-4-yl)benzenesulfonamide **6.4** (60 mg, 0.223 mmol) and 2-bromo-1-(3-(trifluoromethoxy)phenyl)ethanone (95 mg, 0.334 mmol) in DMF. Yield 24% (25.6 mg, 0.054 mmol), white amorphous solid, purity ≥ 95%.

^{1}H NMR (400 MHz, DMSO-d_6) δ 9.24 (s, 1H), 8.07 - 8.16 (m, 1H), 7.96 (s, 1H), 7.90 (d, J = 8.28 Hz, 2H), 7.72 - 7.80 (m, 4H), 7.43 (s, 2H), 5.07 (s, 2H), 1.81 (s, 3H). **^{13}C NMR** (101 MHz, DMSO-d_6) δ 191.5, 174.8, 155.1, 148.6, 143.8, 143.0, 135.9, 131.4, 127.5, 126.7, 126.3, 126.0, 120.4, 120.0 (q, J=257.6 Hz), 63.3, 44.9, 24.9. **ESI-MS (B):** m/z 472 [M+H]$^+$ (R$_t$ = 1.55 min).

4-(1-(2-(4-Fluoro-3-(trifluoromethyl)phenyl)-2-oxoethyl)-4-methyl-2,5-dioxoimidazolidin-4-yl)benzenesulfonamide (6.34)
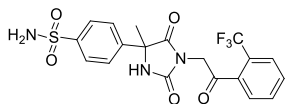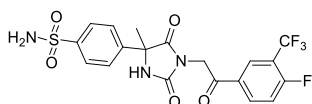
The title compound was prepared according to general method C from 4-(4-methyl-2,5-dioxoimidazolidin-4-yl)benzenesulfonamide **6.4** (60 mg, 0.223 mmol) and 2-bromo-1-(4-fluoro-3-(trifluoromethyl)phenyl)ethanone (95 mg, 0.334 mmol) in DMF. Yield 80% (84.8mg, 0.179 mmol), white amorphous solid, purity ≥ 95%.

¹H NMR (400 MHz, DMSO-*d₆*) δ 9.22 (s, 1H), 8.41 - 8.46 (m, 1H), 8.38 (d, *J* = 6.78 Hz, 1H), 7.89 (d, *J* = 8.53 Hz, 2H), 7.71 - 7.79 (m, 3H), 7.42 (s, 2H), 5.12 (s, 2H), 1.80 (s, 3H). **¹³C NMR** (101 MHz, DMSO-*d₆*) δ 190.6, 174.8, 162.1 (dd, *J*=261.9, 1.5 Hz), 155.1, 143.8, 143.0, 135.8 (d, *J*=10.3 Hz), 130.9 (d, *J*=2.9 Hz), 127.8 - 128.1 (m), 126.3, 126.0, 118.2 (d, *J*=21.2 Hz), 122.1 (q, *J*=272.2 Hz), 117.3 (qd, *J*=33.0, 13.2 Hz), 63.3, 44.8, 24.9. **ESI-MS (B):** *m/z* 472 [M-H]⁻ (R$_t$ = 1.62 min).

4-(1-(2-(3,5-Bis(trifluoromethyl)phenyl)-2-oxoethyl)-4-methyl-2,5-dioxoimidazolidin-4-yl)benzenesulfonamide (6.35)
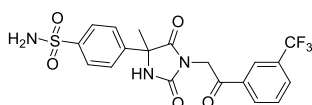

The title compound was prepared according to general method C from 4-(4-methyl-2,5-dioxoimidazolidin-4-yl)benzenesulfonamide **6.4** (60 mg, 0.223 mmol) and 1-(3,5-*bis*(trifluoromethyl)phenyl)-2-bromoethanone (112 mg, 0.334 mmol) in acetone. Yield 38% (44.6 mg, 0.085 mmol), off-white amorphous solid, purity ≥ 95%.

¹H NMR (400 MHz, DMSO-*d₆*) δ 9.26 (s, 1H), 8.63 (s, 2H), 8.50 (s, 1H), 7.90 (d, *J* = 8.53 Hz, 2H), 7.76 (d, *J* = 8.53 Hz, 2H), 7.43 (s, 2H), 5.25 (s, 2H), 1.81 (s, 3H). **¹³C NMR** (101 MHz, DMSO-*d₆*) δ 191.2, 174.7, 155.0, 143.9, 142.9, 135.9, 131.0 (q, *J*=33.7 Hz), 128.8 - 129.2 (m), 127.2 - 127.5 (m), 126.3, 126.0, 122.9 (q, *J*=272.9 Hz), 63.3, 45.1, 24.9. **ESI-MS (B):** *m/z* 522 [M-H]⁻ (R$_t$ = 1.68 min).

4-(4-Methyl-2,5-dioxo-1-(2-oxo-2-(4-(trifluoromethyl)phenyl)ethyl)imidazolidin-4-yl)benzenesulfonamide (6.36)
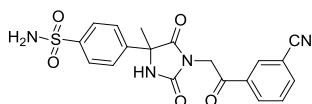

The title compound was prepared according to general method C from 4-(4-methyl-2,5-dioxoimidazolidin-4-yl)benzenesulfonamide **6.4** (50 mg, 0.186 mmol) and 2-bromo-1-(4-(trifluoromethyl)phenyl)ethanone (74.4 mg, 0.279 mmol) in acetone. Yield 54% (46 mg, 0.101 mmol), white amorphous solid, purity ≥ 95%.

¹H NMR (400 MHz, DMSO-*d₆*) δ 9.21 (br. s., 1H), 8.24 (d, *J*=8.08 Hz, 2H), 7.96 (d, *J*=8.34 Hz, 2H), 7.85-7.92 (m, 2H), 7.71-7.79 (m, 2H), 7.40 (br. s., 2H), 5.07 (s, 2H), 1.80 (s, 3H). **¹³C NMR** (101 MHz, DMSO-*d₆*) δ 192.0, 174.7, 155.0, 143.8, 142.9, 137.1, 133.3 (q, *J*=32.2 Hz), 129.1, 126.3, 125.9*, 123.6 (q, *J*=273.0 Hz), 63.3, 44.9, 24.9. **ESI-MS (A):** *m/z* 454 [M-H]⁻ (R$_t$ = 1.09 min). **Two peaks possess the identical chemical shift (proven by HSQC).*

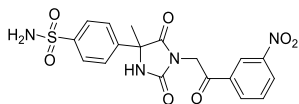### *4-(1-(2-(4-Cyanophenyl)-2-oxoethyl)-4-methyl-2,5-dioxoimidazolidin-4-yl)benzenesulfonamide (6.37)*
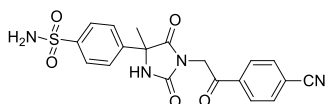
The title compound was prepared according to general method C from 4-(4-methyl-2,5-dioxoimidazolidin-4-yl)benzenesulfonamide **6.4** (50 mg, 0.186 mmol) and 4-(2-bromoacetyl)benzonitrile (62.4 mg, 0.279 mmol) in acetone. Yield 16% (12.3 mg, 0.030 mmol), off-white amorphous solid, purity ≥ 95%.

¹H NMR (400 MHz, DMSO-d_6) δ 9.21 (br. s., 1H), 8.19 (d, *J*=8.59 Hz, 2H), 8.07 (d, *J*=8.59 Hz, 2H), 7.85-7.93 (m, 2H), 7.70-7.80 (m, 2H), 7.40 (br. s., 2H), 5.07 (s, 2H), 1.80 (s, 3H).**¹³C NMR** (101 MHz, DMSO-d_6) δ 192.0, 174.7, 155.0, 143.8, 142.9, 137.0, 133.0, 128.8, 126.3, 125.9, 118.0, 116.1, 63.3, 44.9, 24.9. **ESI-MS (A):** *m/z* 411 [M-H]⁻ (R$_t$ = 0.97 min).

4-(4-Methyl-2,5-dioxo-1-(2-oxopropyl)imidazolidin-4-yl)benzenesulfonamide (6.38)
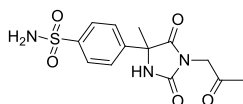
The title compound was prepared according to general method C from 4-(4-methyl-2,5-dioxoimidazolidin-4-yl)benzenesulfonamide **6.4** (75 mg, 0.279 mmol) and chloroacetone (0.033 mL, 0.418 mmol) in acetone. Yield 38% (34 mg, 0.105 mmol), white amorphous solid, purity ≥ 95%.

¹H NMR (400 MHz, DMSO-d_6) δ 9.10 (s, 1H), 7.85 (d, *J* = 8.53 Hz, 2H), 7.70 (d, *J* = 8.53 Hz, 2H), 7.39 (s, 2H), 4.33 (s, 2H), 2.16 (s, 3H), 1.74 (s, 3H). **¹³C NMR** (101 MHz, DMSO-d_6) δ 201.1, 174.6, 155.1, 143.8, 143.0, 126.3, 125.9, 63.1, 47.2, 27.0, 24.8. **ESI-MS (B):** *m/z* 326 [M+H]⁺ (R$_t$ = 0.96 min).

4-(1-(2-Cyclopropyl-2-oxoethyl)-4-methyl-2,5-dioxoimidazolidin-4-yl)benzenesulfonamide (6.39)
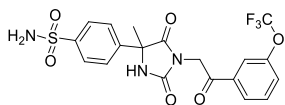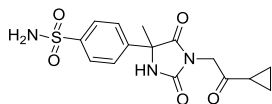

The title compound was prepared according to general method C from 4-(4-methyl-2,5-dioxoimidazolidin-4-yl)benzenesulfonamide **6.4** (75 mg, 0.279 mmol) and 2-bromo-1-cyclopropylethanone (68.1 mg, 0.418 mmol) in acetone. Yield 15% (14.8 mg, 0.042 mmol), white amorphous solid, purity ≥ 95%.

¹H NMR (400 MHz, DMSO-d_6) δ 9.12 (s, 1H), 7.86 (d, *J* = 8.53 Hz, 2H), 7.71 (d, *J* = 8.53 Hz, 2H), 7.40 (s, 2H), 4.48 (s, 2H), 2.11 - 2.20 (m, 1H), 1.75 (s, 3H), 0.95 - 1.04 (m, 2H), 0.84 - 0.93 (m, 2H). **¹³C NMR** (101 MHz, DMSO-d_6) δ 203.0, 174.6, 155.1, 143.8, 143.0, 126.3, 125.9, 63.1, 47.1, 24.8, 18.0, 10.9. **ESI-MS (B):** *m/z* 352 [M+H]⁺ (R$_t$ = 1.18 min).

4-(1-(2-Cyclohexyl-2-oxoethyl)-4-methyl-2,5-dioxoimidazolidin-4-yl)benzenesulfonamide (6.40)
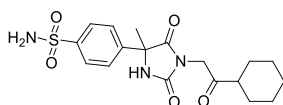
The title compound was prepared according to general method C from 4-(4-methyl-2,5-dioxoimidazolidin-4-yl)benzenesulfonamide **6.4** (90 mg, 0.334 mmol) and 2-bromo-1-

_____

cyclohexylethanone (103 mg, 0.501 mmol) in DMF. Yield 69% (90.3 mg, 0.230 mmol), white amorphous solid, purity ≥ 95%.

¹H NMR (400 MHz, DMSO-d_6) δ 9.10 (s, 1H), 7.86 (d, J = 8.53 Hz, 2H), 7.71 (d, J = 8.53 Hz, 2H), 7.40 (s, 2H), 4.36 (s, 2H), 2.52 - 2.57 (m, 1H), 1.55 - 1.85 (m, 8H), 1.07 - 1.32 (m, 5H). **¹³C NMR** (101MHz, DMSO-d_6): δ = 205.8, 174.6, 155.1, 143.8, 143.1, 126.3, 125.9, 63.1, 47.0, 45.2, 27.7, 25.3, 24.92, 24.86 . **ESI-MS (B):** *m/z* 394 [M+H]⁺ (R$_t$ = 1.56 min).
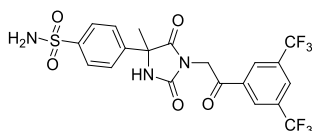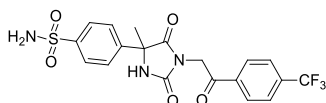
4-(1-(2-(Adamantan-1-yl)-2-oxoethyl)-4-methyl-2,5-dioxoimidazolidin-4-yl)benzenesulfonamide (6.41)

The title compound was prepared according to general method C from 4-(4-methyl-2,5-dioxoimidazolidin-4-yl)benzenesulfonamide **6.4** (75 mg, 0.279 mmol) and 1-(adamantan-1-yl)-2-bromoethanone (107 mg, 0.418 mmol) in DMF. Yield 27% (34.0 mg, 0.076 mmol), white amorphous solid, purity ≥ 95%.

¹H NMR (400 MHz, DMSO-d_6) δ 9.10 (br. s., 1H), 7.86 (d, J = 8.53 Hz, 2H), 7.70 (d, J = 8.53 Hz, 2H), 7.39 (br. s., 2H), 4.40 (s, 2H), 1.99 (br. s., 3H), 1.77 - 1.82 (m, 6H), 1.74 (s, 3H), 1.62 - 1.71 (m, 6H). **¹³C NMR** (101 MHz, DMSO-d_6) δ 206.9, 174.6, 155.1, 143.7, 143.0, 126.3, 125.9, 63.1, 44.8, 42.6, 37.1, 35.8, 27.2, 24.9. **ESI-MS (B):** *m/z* 446 [M+H]⁺ (R$_t$ = 1.70 min).

4-(4-Methyl-2,5-dioxo-1-(2-oxo-2-(pyridin-2-yl)ethyl)imidazolidin-4-yl)benzenesulfonamide (6.42)

The title compound was prepared according to general method C from 4-(4-methyl-2,5-dioxoimidazolidin-4-yl)benzenesulfonamide **6.4** (60 mg, 0.223 mmol) and 2-bromo-1-(pyridin-2-yl)ethanonehydrobromide (94 mg, 0.334 mmol) in DMF. Yield 44% (38.2 mg, 0.098 mmol), white amorphous solid, purity ≥ 95%.

¹H NMR (400 MHz, DMSO-d_6) δ 9.21 (s, 1H), 8.79 (d, J = 4.27 Hz, 1H), 8.04 - 8.11 (m, 1H), 7.97 - 8.01 (m, 1H), 7.89 (d, J = 8.53 Hz, 2H), 7.74 - 7.79 (m, 3H), 7.42 (s, 2H), 5.06 (s, 2H), 1.81 (s, 3H). **¹³C NMR** (101 MHz, DMSO-d_6) δ 193.3, 174.8, 155.2, 150.8, 149.5, 143.8, 143.0, 138.0, 128.8, 126.4, 125.9, 121.9, 63.3, 44.3, 24.9. **ESI-MS (B):** *m/z* 389 [M+H]⁺ (R$_t$ = 1.28 min).

4-(4-Methyl-2,5-dioxo-1-(2-oxo-2-(pyridin-3-yl)ethyl)imidazolidin-4-yl)benzenesulfonamide (6.43)

The title compound was prepared according to general method C from 4-(4-methyl-2,5-dioxoimidazolidin-4-yl)benzenesulfonamide **6.4** (75 mg, 0.279 mmol) and 2-bromo-1-(pyridin-3-yl)ethanone hydrobromide (117 mg, 0.418 mmol) in DMF. Yield 19% (20.1 mg, 0.052 mmol), white amorphous solid, purity ≥ 95%.

_____

¹H NMR (400 MHz, DMSO-d_6) δ 9.18 - 9.28 (m, 2H), 8.87 (dd, J = 1.51, 4.77 Hz, 1H), 8.38 (td, J = 1.88, 8.03 Hz, 1H), 7.90 (d, J = 8.53 Hz, 2H), 7.76 (d, J = 8.53 Hz, 2H), 7.62 (dd, J = 4.89, 7.91 Hz, 1H), 7.43 (s, 2H), 5.08 (s, 2H), 1.81 (s, 3H). **¹³C NMR** (101 MHz, DMSO-d_6) δ 192.1, 174.8, 155.1, 154.4, 149.4, 143.8, 143.0, 135.8, 129.5, 126.4, 126.0, 124.1, 63.3, 44.8, 24.9. **ESI-MS (B):** *m/z* 387 [M-H]⁻ (R_t = 1.08 min). **ESI-MS (C):** *m/z* 389 [M+H]⁺ (R_t = 1.88 min).

4-(4-Methyl-2,5-dioxo-1-(2-oxo-2-(pyridin-4-yl)ethyl)imidazolidin-4-yl)benzenesulfonamide (6.44)

The title compound was prepared according to general method C from 4-(4-methyl-2,5-dioxoimidazolidin-4-yl)benzenesulfonamide **6.4** (75 mg, 0.279 mmol) and 2-bromo-1-(pyridin-4-yl)ethanone hydrobromide (117 mg, 0.418 mmol) in acetone. Yield 12% (13.2 mg, 0.034 mmol), off-white amorphous solid, purity ≥ 90%.

¹H NMR (400 MHz, DMSO-d_6) δ 9.17 (s, 1H), 8.79 (d, J = 6.02 Hz, 2H), 7.79 - 7.85 (m, 4H), 7.67 (d, J = 8.53 Hz, 2H), 7.35 (s, 2H), 4.99 (s, 2H), 1.73 (s, 3H). **¹³C NMR** (101 MHz, DMSO-d_6) δ 193.0, 174.7, 155.0, 151.0, 143.8, 142.9, 139.8, 126.3, 126.0, 121.2, 63.3, 44.9, 24.9. **ESI-MS (B):** *m/z* 387 [M-H]⁻ (R_t = 1.11 min).

4-(1-(2-(3,5-Difluoropyridin-2-yl)-2-oxoethyl)-4-methyl-2,5-dioxoimidazolidin-4-yl)benzenesulfonamide (6.45)

The title compound was prepared according to general method C from 4-(4-methyl-2,5-dioxoimidazolidin-4-yl)benzenesulfonamide **6.4** (75 mg, 0.279 mmol) and 2-bromo-1-(3,5-difluoropyridin-2-yl)ethanone* (65.7 mg, 0.279 mmol) in DMF. Yield 28% (33.2 mg, 0.078 mmol), off-white amorphous solid, purity ≥ 95%. *Reagent was prepared in house by a fellow colleague.*

¹H NMR (400 MHz, DMSO-d_6) δ 9.21 (s, 1H), 8.72 (d, J = 2.26 Hz, 1H), 8.20 (ddd, J = 2.26, 9.04, 11.04 Hz, 1H), 7.89 (d, J = 8.53 Hz, 2H), 7.76 (d, J = 8.53 Hz, 2H), 7.41 (s, 2H), 4.99 (s, 2H), 1.80 (s, 3H). **¹³C NMR** (101 MHz, DMSO-d_6) δ 189.7 (d, J=5.1 Hz), 174.7, 161.3 (dd, J=267.0, 7.3 Hz), 158.5 (dd, J=278.0, 8.1 Hz), 155.1, 143.8, 143.0, 135.9 - 136.2 (m), 134.4 (dd, J=24.2, 5.1 Hz), 126.3, 125.9, 114.6 (t, J=22.0 Hz), 63.2, 44.9, 24.9. **ESI-MS (B):** *m/z* 425 [M+H]⁺ (R_t = 1.28 min).

4-(4-Methyl-2,5-dioxo-1-(2-oxo-2-(thiophen-2-yl)ethyl)imidazolidin-4-yl)benzenesulfonamide (6.46)

The title compound was prepared according to general method C from 4-(4-methyl-2,5-dioxoimidazolidin-4-yl)benzenesulfonamide **6.4** (75 mg, 0.279 mmol) and 2-bromo-1-(thiophen-2-yl)ethanone (86 mg, 0.418 mmol) in DMF. Yield 39% (42.3 mg, 0.108 mmol), white amorphous solid, purity ≥ 95%.

¹H NMR (400 MHz, DMSO-*d₆*) δ 9.21 (s, 1H), 8.17 - 8.21 (m, 1H), 8.12 - 8.16 (m, 1H), 7.89 (d, *J* = 8.53 Hz, 2H), 7.75 (d, *J* = 8.53 Hz, 2H), 7.42 (s, 2H), 7.33 (dd, *J* = 4.02, 4.77 Hz, 1H), 4.94 (s, 2H), 1.80 (s, 3H). **¹³C NMR** (101 MHz, DMSO-*d₆*) δ 185.3, 174.8, 155.1, 143.8, 143.0, 140.1, 136.2, 134.6, 129.1, 126.4, 125.9, 63.2, 44.3, 24.8. **ESI-MS (B):** *m/z* 392 [M-H]⁻ (R$_t$ = 1.36 min).

4-(1-(2-(5-Chlorothiophen-2-yl)-2-oxoethyl)-4-methyl-2,5-dioxoimidazolidin-4-yl)benzenesulfonamide (6.47)

The title compound was prepared according to general method C from 4-(4-methyl-2,5-dioxoimidazolidin-4-yl)benzenesulfonamide **6.4** (60 mg, 0.223 mmol) and 2-chloro-1-(5-chlorothiophen-2-yl)ethanone (47.8 mg, 0.245 mmol) in DMF. Yield 43% (41 mg, 0.096 mmol), off-white amorphous solid, purity ≥ 95%.

¹H NMR (400 MHz, DMSO-*d₆*) δ 9.23 (s, 1H), 8.11 (d, *J* = 4.02 Hz, 1H), 7.88 (d, *J* = 8.53 Hz, 2H), 7.74 (d, *J* = 8.53 Hz, 2H), 7.36 – 7.47 (m, 3H), 4.93 (s, 2H), 1.79 (s, 3H). **¹³C NMR** (101 MHz, DMSO-*d₆*) δ 185.0, 174.8, 155.0, 143.8, 142.9, 139.1, 138.9, 135.1, 129.4, 126.4, 126.0, 63.3, 43.9, 24.8. **ESI-MS (B):** *m/z* 428 [M+H]⁺ (R$_t$ = 1.54 min).

4-(4-Methyl-2,5-dioxo-1-(2-oxo-2-(thiazol-2-yl)ethyl)imidazolidin-4-yl)benzenesulfonamide (6.48)

The title compound was prepared according to general method C from 4-(4-methyl-2,5-dioxoimidazolidin-4-yl)benzenesulfonamide **6.4** (60 mg, 0.223 mmol) and 2-bromo-1-(thiazol-2-yl)ethanone (0.047 mL, 0.334 mmol) in DMF. Yield 24% (21.2 mg, 0.054 mmol), off-white amorphous solid, purity ≥ 95%.

¹H NMR (400 MHz, DMSO-*d₆*) δ 9.24 (s, 1H), 8.35 (d, *J* = 3.01 Hz, 1H), 8.24 (d, *J* = 3.01 Hz, 1H), 7.89 (d, *J* = 8.53 Hz, 2H), 7.75 (d, *J* = 8.53 Hz, 2H), 7.41 (s, 2H), 5.01 (s, 2H), 1.80 (s, 3H). **¹³C NMR** (101 MHz, DMSO-*d₆*) δ 186.0, 174.6, 163.3, 154.9, 145.6, 143.8, 142.9, 129.1, 126.3, 125.9, 63.3, 44.1, 24.8. **ESI-MS (B):** *m/z* 395 [M+H]⁺ (R$_t$ = 1.15 min).
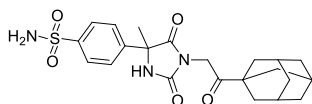
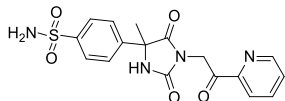### 4-(1-(2-(Benzo[d]thiazol-2-yl)-2-oxoethyl)-4-methyl-2,5-dioxoimidazolidin-4-yl)benzenesulfonamide (6.49)

The title compound was prepared according to general method C from 4-(4-methyl-2,5-dioxoimidazolidin-4-yl)benzenesulfonamide **6.4** (60 mg, 0.223 mmol) and 1-(benzo[*d*]thiazol-2-yl)-2-bromoethanone (57.1 mg, 0.223 mmol) in DMF. Yield 7%* (7.3 mg, 0.016 mmol), off-white amorphous solid, purity ≥ 90%. *Extensive decomposition of alkyl hallide was observed in the reaction mixture, leading to a low isolated yield of the title compound.*

¹H NMR (400 MHz, Acetone-*d₆*) δ 8.26 (ddd, *J* = 2.13, 3.83, 7.09 Hz, 2H), 8.17 (s, 1H), 7.93 – 7.99 (m, 2H), 7.83 – 7.89 (m, 2H), 7.70 (dquin, *J* = 1.38, 7.18 Hz, 2H), 6.67 (s, 2H), 5.15 – 5.28 (m, 2H), 1.94 (s,

3H). **¹H NMR** (400 MHz, DMSO-d_6) δ 9.28 (s, 1H), 8.22 - 8.37 (m, 2H), 7.90 (d, J = 8.53 Hz, 2H), 7.76 (d, J = 8.53 Hz, 2H), 7.66 - 7.74 (m, 2H), 7.43 (s, 2H), 5.16 (s, 2H), 1.81 (s, 3H). **ESI-MS (B):** m/z 445, 446 [M+H]⁺ (R_t = 1.59 min).

4-(4-Methyl-1-(2-(naphthalen-2-yl)-2-oxoethyl)-2,5-dioxoimidazolidin-4-yl)benzenesulfonamide (6.50)

The title compound was prepared according to general method C from 4-(4-methyl-2,5-dioxoimidazolidin-4-yl)benzenesulfonamide **6.4** (60 mg, 0.223 mmol) and 2-bromo-1-(naphthalen-2-yl)ethanone (83 mg, 0.334 mmol) in actone. Yield 63% (61 mg, 0.139 mmo), off-white amorphous solid, purity ≥ 95%.

¹H NMR (400 MHz, DMSO-d_6) δ 9.23 (s, 1H), 8.84 (s, 1H), 8.14 (d, J = 7.78 Hz, 1H), 7.96 - 8.10 (m, 3H), 7.90 (d, J = 8.53 Hz, 2H), 7.79 (d, J = 8.28 Hz, 2H), 7.64 - 7.76 (m, 2H), 7.43 (s, 2H), 5.15 (s, 2H), 1.83 (s, 3H). **¹³C NMR** (101 MHz, DMSO-d_6) δ 192.1, 174.9, 155.3, 143.8, 143.1, 135.4, 132.0, 131.3, 130.6, 129.7, 129.2, 128.7, 127.8, 127.2, 126.4, 126.0, 123.2, 63.3, 44.7, 25.0. **ESI-MS (B):** m/z 438 [M+H]⁺ (R_t = 1.56 min).

4-(1-(4-Fluorophenethyl)-4-methyl-2,5-dioxoimidazolidin-4-yl)benzenesulfonamide (6.51)

The title compound was prepared according to general method C from 4-(4-methyl-2,5-dioxoimidazolidin-4-yl)benzenesulfonamide **6.4** (60 mg, 0.223 mmol) and 1-(2-bromoethyl)-4-fluorobenzene (67.9 mg, 0.334 mmol) in DMF. Yield 92% (80 mg, 0.204 mmol), white amorphous solid, purity ≥ 95%.

¹H NMR (400 MHz, DMSO-d_6) δ 8.95 (br. s., 1H), 7.83 (d, J = 8.53 Hz, 2H), 7.56 (d, J = 8.53 Hz, 2H), 7.40 (br. s., 2H), 7.07 - 7.17 (m, 2H), 6.96 - 7.06 (m, 2H), 3.61 (t, J = 6.90 Hz, 2H), 2.84 (t, J = 6.90 Hz, 2H), 1.61 (s, 3H). **¹³C NMR** (101 MHz, DMSO-d_6) δ 174.5, 161.0 (d, J=242.1 Hz), 155.3, 143.7, 143.1, 134.1 (d, J=2.9 Hz), 130.6 (d, J=8.1 Hz), 126.1, 125.8, 115.0 (d, J=21.3 Hz), 62.5, 39.5*, 32.0, 24.8. **ESI-MS (B):** m/z 392 [M+H]⁺ (R_t = 1.45 min). *One CH₂ ¹³C-signal overlaps with the DMSO signal (proven by HMQC).*
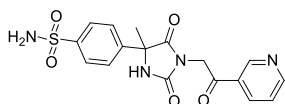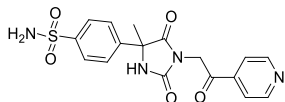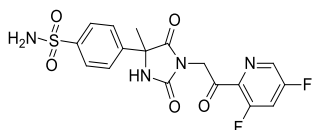
4-(4-Methyl-2,5-dioxo-1-((phenylsulfonyl)methyl)imidazolidin-4-yl)benzenesulfonamide (6.52)

The title compound was prepared according to general method C from 4-(4-methyl-2,5-dioxoimidazolidin-4-yl)benzenesulfonamide **6.4** (40 mg, 0.149 mmol) and ((bromomethyl)sulfonyl)benzene (34.9 mg, 0.149 mmol) in DMF on heating at 100 °C for 18 hrs. Yield 11% (7.1 mg, 0.017 mmol), off-white amorphous solid, purity ≥ 95%.

¹H NMR* (400 MHz, DMSO-d_6) δ 7.87 (d, J = 8.53 Hz, 2H), 7.64 - 7.73 (m, 3H), 7.59 (d, J = 8.53 Hz, 2H), 7.39 - 7.53 (m, 4H), 4.87 - 5.02 (m, 2H), 1.66 (s, 3H). **¹³C NMR** (101 MHz, DMSO-d_6) δ 172.9, 153.0,

144.0, 142.5, 137.4, 134.5, 129.4, 128.3, 126.2, 125.9, 63.1, 58.5, 24.6. **ESI-MS (B):** *m/z* 422 [M-H]⁻ (R$_t$ = 1.26 min). **ESI-MS (C):** *m/z* 424 [M+H]⁺, 446 [M+Na]⁺ (R$_t$ = 2.46 min). **The hydantoin NH was not clearly detected by ¹H NMR; the alkylation position was proven by HMBC results.*

1-((Chloromethyl)sulfonyl)-4-fluorobenzene (6.56)
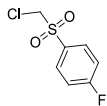
The reaction was performed according to a described procedure.[273] A stirred suspension of sodium 4-fluorobenzenesulfinate (200 mg, 1.098 mmol, 1.0 eq.) in DMSO (1 mL) was treated with chlorobromomethane (0.214 mL, 3.29 mmol, 3.0 eq.). The reaction mixture was heated on stirring at 100°C for 2 hrs. After it was cooled down to room temperature, diluted with EtOAc (15 mL) and washed with water (20 mL). The aqueous phase was extracted with EtOAc (2x20 mL). The organic phase was collected, dried over Na$_2$SO$_4$, filtrated and evaporated under reduced pressure to produce the crude title compound, directly used for the next reaction step. Yield 94% (216 mg, 1.035 mmol).

¹H NMR (400 MHz, DMSO-*d₆*) δ 7.98 - 8.08 (m, 2H), 7.54 - 7.62 (m, 2H), 5.36 (s, 2H). **ESI-MS (B):** *m/z* not detectable (R$_t$ = 1.56 min).

1-((Chloromethyl)sulfonyl)-3-(trifluoromethyl)benzene (6.57)
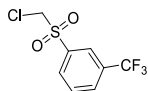
The title compound was prepared in an analogous way to **6.56** from sodium 3-(trifluoromethyl)benzenesulfinate (400 mg, 1.723 mmol). Yield 51% (227 mg, 0.878 mmol), purity > 90%.

¹H NMR (400 MHz, DMSO-*d₆*) δ 8.21 - 8.30 (m, 3H), 7.98 (t, J = 8.03 Hz, 1H), 5.50 (s, 2H). **ESI-MS (B):** *m/z* not detectable (R$_t$ = 1.69 min).

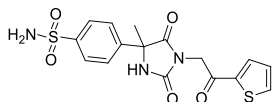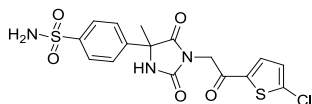### 4-(1-(Benzo[d]oxazol-2-ylmethyl)-4-methyl-2,5-dioxoimidazolidin-4-yl)benzenesulfonamide (6.62)
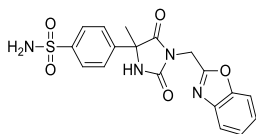
The title compound was prepared according to general method C from 4-(4-methyl-2,5-dioxoimidazolidin-4-yl)benzenesulfonamide **6.4** (75 mg, 0.279 mmol) and 2-(chloromethyl)-1,3-benzoxazole (70.0 mg, 0,418 mmol) in DMF. Yield 27% (29.6 mg, 0.074 mmol), off-white amorphous solid, purity ≥ 95%.

¹H NMR (400 MHz, DMSO-*d₆*) δ 9.23 (br. s., 1H), 7.78 - 7.87 (m, 2H), 7.57 - 7.75 (m, 4H), 7.24 - 7.44 (m, 4H), 4.82 - 4.97 (m, 2H), 1.73 (s, 3H). **¹³C NMR** (101 MHz, DMSO-*d₆*) δ 174.4, 161.1, 154.7, 150.3, 143.9, 142.8, 140.3, 126.4, 126.0, 125.4, 124.8, 119.7, 110.9, 63.3, 35.6, 24.7. **ESI-MS (B):** *m/z* 401 [M+H]⁺ (R$_t$ = 1.41 min).
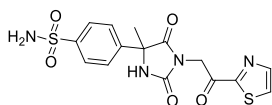
4-(1-(Benzo[d]thiazol-2-ylmethyl)-4-methyl-2,5-dioxoimidazolidin-4-yl)benzenesulfonamide (6.63)
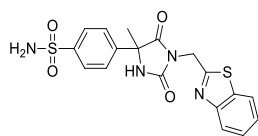
The title compound was prepared according to general method C from 4-(4-methyl-2,5-dioxoimidazolidin-4-yl)benzenesulfonamide **6.4** (90 mg, 0.334 mmol) and 2-(chloromethyl)benzo[*d*]thiazole (92 mg, 0.501 mmol) in DMF. Yield 30% (41.6 mg, 0.100 mmol), white amorphous solid, purity ≥ 95%.

^{1}H NMR (400 MHz, DMSO-*d_6*) δ 9.28 (s, 1H), 8.08 (d, *J* = 7.78 Hz, 1H), 7.94 (d, *J* = 7.78 Hz, 1H), 7.89 (d, *J* = 8.53 Hz, 2H), 7.76 (d, *J* = 8.53 Hz, 2H), 7.48 - 7.56 (m, 1H), 7.36 - 7.47 (m, 3H), 5.04 (s, 2H), 1.81 (s, 3H). **^{13}C NMR** (101MHz, DMSO-*d_6*): δ 174.4, 166.4, 154.8, 152.1, 143.9, 142.8, 134.6, 126.4*, 126.0, 125.4, 122.6, 122.5, 63.2, 40.1, 24.7 . **ESI-MS (B):** *m/z* 417 [M+H]$^+$ (R$_t$ = 1.47 min). *Two peaks possess the identical chemical shift (proven by HSQC).*

4-(4-Methyl-1-((1-methyl-1H-benzo[d]imidazol-2-yl)methyl)-2,5-dioxoimidazolidin-4-yl)benzenesulfonamide (6.64)

The title compound was prepared according to general method C from 4-(4-methyl-2,5-dioxoimidazolidin-4-yl)benzenesulfonamide **6.4** (60 mg, 0.185 mmol) and 2-(chloromethyl)-1-methyl-1H-benzo[*d*]imidazole hydrochloride (60.2 mg, 0.277 mmol) in DMF. Yield 24% (18.1 mg, 0.044 mmol), off-white amorphous solid, purity ≥ 95%.

^{1}H NMR (400 MHz, DMSO-*d_6*) δ 9.15 (s, 1H), 7.80 – 7.92 (m, 4H), 7.54 (d, *J* = 7.78 Hz, 2H), 7.41 (s, 2H), 7.14 – 7.28 (m, 2H), 4.92 (s, 2H), 3.83 (s, 3H), 1.82 (s, 3H). **^{13}C NMR** (101 MHz, DMSO-*d_6*) δ 174.7, 155.2, 149.4, 143.8, 143.1, 141.7, 136.1, 126.6, 125.8, 122.0, 121.5, 118.7, 110.0, 63.1, 34.9, 29.6, 24.5. **ESI-MS (B):** *m/z* 414 [M+H]$^+$ (R$_t$ = 1.11 min).
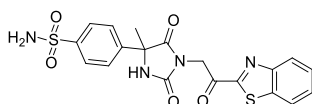
4-(4-Methyl-2,5-dioxo-1-(quinolin-2-ylmethyl)imidazolidin-4-yl)benzenesulfonamide (6.65)
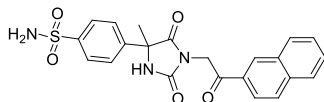

The title compound was prepared according to general method C from 4-(4-methyl-2,5-dioxoimidazolidin-4-yl)benzenesulfonamide **6.4** (60 mg, 0.223 mmol) and 2-(chloromethyl)quinoline hydrochloride (71.6 mg, 0.334 mmol) in DMF. Yield 35% (31.9 mg, 0.078 mmol), off-white amorphous solid, purity ≥ 95%.

^{1}H NMR (400 MHz, DMSO-*d_6*) δ 9.15 (br. S., 1H), 8.36 (d, *J* = 8.53 Hz, 1H), 7.97 (d, *J* = 8.03 Hz, 1H), 7.88 – 7.94 (m, 2H), 7.82 – 7.88 (m, 2H), 7.72 – 7.82 (m, 2H), 7.56 – 7.64 (m, 1H), 7.35 – 7.53 (m, 3H), 4.91 (s, 2H), 1.88 (s, 3H). **^{13}C NMR** (101 MHz, DMSO-*d_6*) δ 175.1, 155.7, 155.3, 146.8, 143.8, 143.3, 136.9, 129.9, 128.3, 127.9, 127.0, 126.6, 126.4, 125.8, 119.4, 63.1, 42.8, 24.7. **ESI-MS (B):** *m/z* 411 [M+H]$^+$ (R$_t$ = 1.38 min).
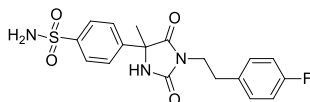
4-(4-Methyl-1-((4-methylquinazolin-2-yl)methyl)-2,5-dioxoimidazolidin-4-yl)benzenesulfonamide (6.66)
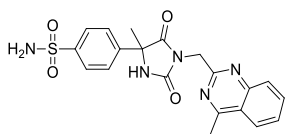
The title compound was prepared according to general method C from 4-(4-methyl-2,5-dioxoimidazolidin-4-yl)benzenesulfonamide **6.4** (60 mg, 0.223 mmol) and 2-(chloromethyl)-4-methylquinazoline (64.4 mg, 0.334 mmol) in DMF. Yield 46% (43.2 mg, 0.102 mmol), off-white amorphous solid, purity ≥ 95%.

¹H NMR (400 MHz, DMSO-*d₆*) δ 9.14 (br. s., 1H), 8.28 (d, *J* = 8.28 Hz, 1H), 7.96 − 8.02 (m, 1H), 7.89 − 7.95 (m, 2H), 7.83 − 7.88 (m, 2H), 7.80 (d, *J* = 8.28 Hz, 1H), 7.73 (t, *J* = 7.65 Hz, 1H), 7.44 (s, 2H), 4.87 (s, 2H), 2.89 (s, 3H), 1.88 (s, 3H). **¹³C NMR** (101 MHz, DMSO-*d₆*) δ 175.0, 169.4, 159.4, 155.6, 148.9, 143.8, 143.3, 134.5, 127.7, 127.6, 126.7, 125.9, 125.8, 122.6, 63.1, 43.1, 24.3, 21.6. **ESI-MS (B):** *m/z* 426 [M+H]⁺ (R$_t$ = 1.36 min).

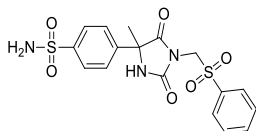### *4-(1-((6-Fluorobenzo[d]oxazol-2-yl)methyl)-4-methyl-2,5-dioxoimidazolidin-4-yl)benzenesulfonamide (6.67)*
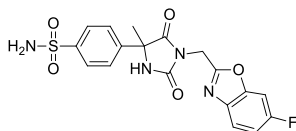
The title compound was prepared according to general method C from 4-(4-methyl-2,5-dioxoimidazolidin-4-yl)benzenesulfonamide **6.4** (75 mg, 0.279 mmol) and 2-(chloromethyl)-6-fluorobenzo[*d*]oxazole (78 mg, 0.418 mmol) in DMF. Yield 74% (86 mg, 0.206 mmol), white amorphous solid, purity ≥ 95%.

¹H NMR (400 MHz, DMSO-*d₆*) δ 9.28 (s, 1H), 7.89 (d, *J* = 8.28 Hz, 2H), 7.69 - 7.79 (m, 4H), 7.41 (s, 2H), 7.20 - 7.31 (m, 1H), 4.93 (s, 2H), 1.79 (s, 3H). **¹³C NMR** (101 MHz, DMSO-*d₆*) δ 174.3, 161.8 (d, *J*=2.9 Hz), 159.9 (d, *J*=242.1 Hz), 154.6, 150.3 (d, *J*=15.4 Hz), 143.9, 142.8, 136.8 (d, *J*=1.5 Hz), 126.4, 126.0, 120.4 (d, *J*=10.3 Hz), 112.6 (d, *J*=25.0 Hz), 99.2 (d, *J*=28.6 Hz), 63.2, 35.5, 24.7. **ESI-MS (B):** *m/z* 419 [M+H]⁺ (R$_t$ = 1.43 min).

4-(1-((5-Fluorobenzo[d]oxazol-2-yl)methyl)-4-methyl-2,5-dioxoimidazolidin-4-yl)benzenesulfonamide (6.68)


The title compound was prepared according to general method C from 4-(4-methyl-2,5-dioxoimidazolidin-4-yl)benzenesulfonamide **6.4** (60 mg, 0.223 mmol) and 2-(chloromethyl)-5-fluorobenzo[*d*]oxazole (43.4 mg, 0.234 mmol) in DMF. Yield 60% (56 mg, 0.134 mmol), white amorphous solid, purity ≥ 95%.

¹H NMR (400 MHz, DMSO-d_6) δ 9.35 (s, 1H), 7.95 (d, *J* = 8.53 Hz, 2H), 7.79 – 7.86 (m, 3H), 7.68 (dd, *J* = 2.51, 8.78 Hz, 1H), 7.47 (s, 2H), 7.33 (dt, *J* = 2.64, 9.35 Hz, 1H), 5.01 (s, 2H), 1.86 (s, 3H). **¹³C NMR** (101 MHz, DMSO-d_6) δ 174.3, 163.1, 159.4 (d, *J*=238.4 Hz), 154.6, 146.8, 143.9, 142.8, 141.2 (d, *J*=13.2 Hz), 126.4, 126.0, 112.9 (d, *J*=26.4 Hz), 111.8 (d, *J*=10.3 Hz), 106.3 (d, *J*=25.8 Hz), 63.3, 35.6, 24.7. **ESI-MS (B):** *m/z* 419 [M+H]⁺ (R$_t$ = 1.41 min).

4-(4-Methyl-2,5-dioxo-1-((5-(trifluoromethyl)benzo[d]oxazol-2-yl)methyl)imidazolidin-4-yl)benzenesulfonamide (6.69)
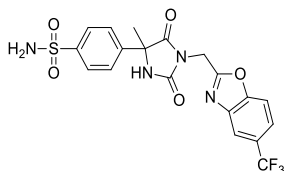
The title compound was prepared according to general method C from 4-(4-methyl-2,5-dioxoimidazolidin-4-yl)benzenesulfonamide **6.4** (60 mg, 0.223 mmol) and 2-(chloromethyl)-5-(trifluoromethyl)benzo[*d*]oxazole (55.1 mg, 0.234 mmol) in DMF. Yield 17% (17.6 mg, 0.038 mmol), off-white amorphous solid, purity ≥ 90%.

¹H NMR (400 MHz, DMSO-d_6) δ 9.30 (s, 1H), 8.18 (s, 1H), 7.97 (d, *J* = 8.53 Hz, 1H), 7.89 (d, *J* = 8.53 Hz, 2H), 7.70 - 7.82 (m, 3H), 7.41 (s, 2H), 5.01 (s, 2H), 1.80 (s, 3H). **¹H NMR** (400 MHz, Acetone-d_6) δ 8.19 (s, 1H), 8.05 (s, 1H), 7.93 – 8.00 (m, 2H), 7.83 – 7.91 (m, 3H), 7.77 (d, *J* = 8.53 Hz, 1H), 6.64 (s, 2H), 5.05 (d, *J* = 2.51 Hz, 2H), 1.94 (s, 3H). **¹³C NMR** (101 MHz, Acetone-d_6) δ 175.1, 164.4, 155.6, 153.9, 145.1, 144.3, 142.2, 127.5, 127.3, 127.7 (q, *J*=32.3 Hz), 123.5 (q, *J*=3.7 Hz), 125.4 (q, *J*=271.5 Hz), 118.4 (q, *J*=4.2 Hz), 112.7, 64.7, 36.5, 25.5. **ESI-MS (B):** *m/z* 469 [M+H]⁺ (R$_t$ = 1.58 min).

N-(2-hydroxy-5-(trifluoromethyl)phenyl)-2-(4-methyl-2,5-dioxo-4-(4-sulfamoylphenyl)imidazolidin-1-yl)acetamide (6.76)
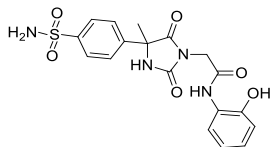
The title compound was isolated as a side-product in the preparation of **6.62**. Most probably, it was formed by hydrolisis of **6.62** in water during purification. Yield 15% (16.1 mg, 0.033 mmol), off-white amorphous solid, purity ≥ 90%.

¹H NMR[*] (400 MHz, DMSO-d_6) δ 9.83 (s, 1H), 9.12 (s, 1H), 8.28 (s, 1H), 7.86 (d, *J* = 8.53 Hz, 2H), 7.73 (d, *J* = 8.53 Hz, 2H), 7.39 (s, 2H), 7.29 (d, *J* = 8.53 Hz, 1H), 7.03 (d, *J* = 8.53 Hz, 1H), 4.33 (s, 2H), 1.76 (s, 3H). **¹H NMR** (400 MHz, Acetone-d_6) δ 9.77 - 9.87 (m, 1H), 9.22 (br. s., 1H), 8.46 (s, 1H), 8.05 (s, 1H), 7.90 - 7.97 (m, 2H), 7.80 - 7.87 (m, 2H), 7.30 (dd, *J* = 1.51, 8.53 Hz, 1H), 7.08 (d, *J* = 8.28 Hz, 1H), 6.62 (s, 2H), 4.52 (d, *J* = 2.51 Hz, 2H), 1.91 (s, 3H). **¹³C NMR**[**] (101 MHz, Acetone-d_6) δ 175.6, 166.6, 156.3, 150.6, 144.9, 144.6, 127.9, 127.4, 127.3, 122.5 (q, *J*=3.7 Hz), 122.2 (q, *J*=32.3 Hz), 118.8 (q, *J*=3.9 Hz), 116.5, 64.5, 42.2[***], 25.7.. **ESI-MS (B):** *m/z* 487 [M+H]⁺ (R$_t$ = 1.48 min). [*]-OH signal was not detected. [**]CF₃ (q, with ¹J$_{CF}$) signal was not detected in ¹³C NMR. [***]Chemical shift of linker CH₂ is characteristic for amides, while in (benz)oxazoles the typical value is 34-37 ppm.

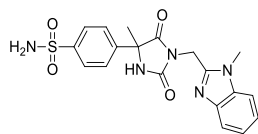### 4-(4-Methyl-2,5-dioxo-1-((6-(trifluoromethyl)benzo[d]oxazol-2-yl)methyl)imidazolidin-4-yl)benzenesulfonamide (6.70)
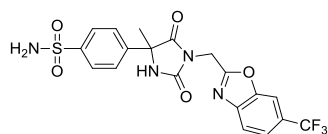
The title compound was prepared according to general method C from 4-(4-methyl-2,5-dioxoimidazolidin-4-yl)benzenesulfonamide **6.4** (60 mg, 0.223 mmol) and 2-(chloromethyl)-6-(trifluoromethyl)benzo[*d*]oxazole (55.1 mg, 0.234 mmol) in DMF. Yield 48% (50.0 mg, 0.107 mmol), white amorphous solid, purity ≥ 90%.

¹H NMR (400 MHz, DMSO-d₆) δ 9.31 (s, 1H), 8.27 (s, 1H), 7.85 - 7.97 (m, 3H), 7.72 - 7.80 (m, 3H), 7.41 (s, 2H), 4.93 - 5.12 (m, 2H), 1.81 (s, 3H). **¹³C NMR** (101 MHz, DMSO-*d₆*) δ 174.3, 164.2, 154.6, 149.9, 143.9, 143.4, 142.7, 126.4, 126.0, 125.9 (q, *J*=32.3 Hz), 124.2 (q, *J*=272.9 Hz), 122.0 (q, *J*=3.7 Hz), 120.7, 109.1 (q, *J*=3.7 Hz), 63.3, 35.7, 24.8. **ESI-MS(B):** *m/z* 469 [M+H]⁺ (Rₜ = 1.61 min).

4-(4-Methyl-1-(oxazolo[4,5-b]pyridin-2-ylmethyl)-2,5-dioxoimidazolidin-4-yl)benzenesulfonamide (6.71)
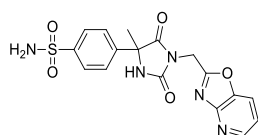
The title compound was prepared according to general method C from 4-(4-methyl-2,5-dioxoimidazolidin-4-yl)benzenesulfonamide **6.4** (60 mg, 0.223 mmol) and 2-(chloromethyl)oxazolo[4,5-*b*]pyridine (56.3 mg, 0.334 mmol) in DMF. Yield 52% (46.8 mg, 0.117 mmol), white amorphous solid, purity ≥ 95%.

¹H NMR (400 MHz, DMSO-*d₆*) δ 9.32 (s, 1H), 8.52 (dd, *J* = 1.25, 4.77 Hz, 1H), 8.20 (dd, *J* = 1.38, 8.16 Hz, 1H), 7.89 (d, *J* = 8.53 Hz, 2H), 7.77 (d, *J* = 8.53 Hz, 2H), 7.38 - 7.48 (m, 3H), 4.94 - 5.09 (m, 2H), 1.81 (s, 3H). **¹³C NMR** (101 MHz, DMSO-*d₆*) δ 174.3, 164.4, 154.6, 154.4, 146.4, 143.9, 142.8, 142.7, 126.4, 126.0, 120.9, 119.3, 63.3, 35.8, 24.8. **ESI-MS (B):** 402 [M+H]⁺ (Rₜ = 1.19 min). **ESI-MS (C):** 402 [M+H]⁺, 424 [M+Na]⁺ (Rₜ = 2.17 min).

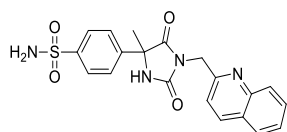### 4-(4-Methyl-1-(oxazol-2-ylmethyl)-2,5-dioxoimidazolidin-4-yl)benzenesulfonamide (6.72)
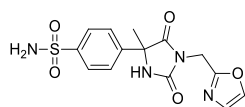
The title compound was prepared according to general method C from 4-(4-methyl-2,5-dioxoimidazolidin-4-yl)benzenesulfonamide **6.4** (75 mg, 0.279 mmol) and 2-(chloromethyl)oxazole (49.1 mg, 0.418 mmol) in DMF. Yield 53% (52 mg, 0.148 mmol), off-white amorphous solid, purity ≥ 95%.

¹H NMR (400 MHz, DMSO-*d₆*) δ 9.23 (s, 1H), 8.08 (s, 1H), 7.87 (d, *J* = 8.53 Hz, 2H), 7.72 (d, *J* = 8.53 Hz, 2H), 7.41 (s, 2H), 7.17 (s, 1H), 4.67 - 4.79 (m, 2H), 1.76 (s, 3H). **¹³C NMR** (101 MHz, DMSO-*d₆*) δ 174.2, 158.4, 154.7, 143.8, 142.9, 140.3, 127.2, 126.3, 126.0, 63.1, 35.1, 24.9. **ESI-MS (B):** *m/z* 351 [M+H]⁺ (Rₜ = 1.07 min).

4-(4-Methyl-1-((3-methyl-1,2,4-oxadiazol-5-yl)methyl)-2,5-dioxoimidazolidin-4-yl)benzenesulfonamide (6.73)
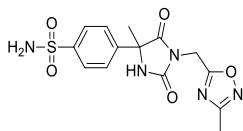
The title compound was prepared according to general method C from 4-(4-methyl-2,5-dioxoimidazolidin-4-yl)benzenesulfonamide **6.4** (60 mg, 0.223 mmol) and 5-(chloromethyl)-3-methyl-1,2,4-oxadiazole (44.3 mg, 0.334 mmol) in DMF. Yield 48% (38.7 mg, 0.106 mmol), off-white amorphous solid, purity ≥ 95%.

**¹H NMR (**400 MHz, DMSO-*d₆*) δ 9.29 (s, 1H), 7.87 (d, *J* = 8.53 Hz, 2H), 7.71 (d, *J* = 8.53 Hz, 2H), 7.40 (s, 2H), 4.91 (s, 2H), 2.31 (s, 3H), 1.77 (s, 3H). **¹³C NMR** (101 MHz, DMSO-*d₆*) δ 174.3, 174.1, 167.1, 154.3, 143.9, 142.6, 126.3, 126.0, 63.3, 34.0, 24.7, 11.0. **ESI-MS (B):** *m/z* 366 [M+H]⁺ (R$_t$ = 1.18 min).

4-(1-((5-(4-Fluorophenyl)oxazol-2-yl)methyl)-4-methyl-2,5-dioxoimidazolidin-4-yl)benzenesulfonamide (6.74)
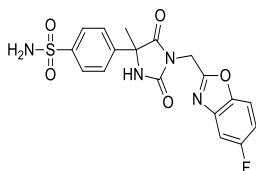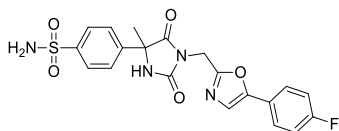

The title compound was prepared according to general method C from 4-(4-methyl-2,5-dioxoimidazolidin-4-yl)benzenesulfonamide **6.4** (60 mg, 0.223 mmol) and 2-(chloromethyl)-5-(4-fluorophenyl)oxazole (70.7 mg, 0.334 mmol) in DMF. Yield 32% (32 mg, 0.072 mmol), white amorphous solid, purity ≥ 95%.

¹H NMR (400 MHz, DMSO-*d₆*) δ 9.20 (s, 1H), 7.81 (d, *J* = 8.53 Hz, 2H), 7.68 (d, *J* = 8.53 Hz, 2H), 7.48 – 7.58 (m, 3H), 7.36 (s, 2H), 7.25 (t, *J* = 8.91 Hz, 2H), 4.73 (s, 2H), 1.72 (s, 3H). **¹³C NMR** (101 MHz, DMSO-*d₆*) δ 174.3, 162.0 (d, *J*=246.5 Hz), 157.9, 154.6, 150.1, 143.9, 142.9, 126.3, 126.0 (d, *J*=8.8 Hz), 126.0, 123.8 (d, *J*=2.9 Hz), 122.6, 116.2 (d, *J*=22.0 Hz), 63.2, 35.2, 24.7. **ESI-MS (B):** *m/z* 445 [M+H]⁺ (R$_t$ = 1.46 min).

4-(1-((3-(4-Fluorophenyl)-1,2,4-oxadiazol-5-yl)methyl)-4-methyl-2,5-dioxoimidazolidin-4-yl)benzenesulfonamide (6.75)

The title compound was prepared according to general method C from 4-(4-methyl-2,5-dioxoimidazolidin-4-yl)benzenesulfonamide **6.4** (60 mg, 0.223 mmol) and 5-(chloromethyl)-3-(4-fluorophenyl)-1,2,4-oxadiazole (71.1 mg, 0.334 mmol) in DMF. Yield 83% (82 mg, 0.184 mmol), off-white amorphous solid, purity ≥ 95%.

¹H NMR (400 MHz, DMSO-*d₆*) δ 9.36 (s, 1H), 7.94 – 8.02 (m, 2H), 7.90 (d, *J* = 8.53 Hz, 2H), 7.76 (d, *J* = 8.53 Hz, 2H), 7.39 – 7.48 (m, 4H), 5.06 (s, 2H), 1.82 (s, 3H). **¹³C NMR** (101 MHz, DMSO-*d₆*) δ 175.3, 174.1, 166.8, 164.1 (d, *J*=249.4 Hz), 154.4, 144.0, 142.7, 129.6 (d, *J*=8.8 Hz), 126.4, 126.0, 122.2 (d, *J*=2.9 Hz), 116.6 (d, *J*=22.0 Hz), 63.4, 34.3, 24.5. **ESI-MS (B):** *m/z* 446 [M+H]⁺ (R$_t$ = 1.51 min).

2-Chloro-N-(2,4-difluorophenyl)acetamide (6.77)

148
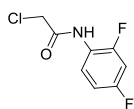
The crude mixture (232 mg) containing the title compound was prepared according to general method D from 2,4-Difluoroaniline (0.15 mL, 1.473 mmol).

ESI-MS (B): *m/z* 206 [M+H]$^+$ (R$_t$ = 1.42 min).

2-Chloro-N-(2,4-difluorophenyl)-N-methylacetamide (6.78)
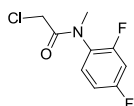
The crude mixture (218 mg) containing the title compound was prepared according to general method D from 2,4-difluoro-*N*-methylaniline (200 mg, 1.397 mmol).

ESI-MS (B): *m/z* 220 [M+H]$^+$ (R$_t$ = 1.49 min).

2-Chloro-1-(3,4-dihydroisoquinolin-2(1H)-yl)ethanone (6.79)
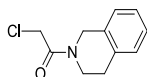
The crude mixture (271 mg) containing the title compound was prepared according to general method D from 1,2,3,4-tetrahydro-isoquinoline (200 mg, 1.502 mmol).

ESI-MS (B): *m/z* 210 [M+H]$^+$ (R$_t$ = 1.54 min).

2-Chloro-1-(3,4-dihydroquinolin-1(2H)-yl)ethanone (6.80)
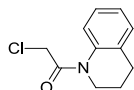
The crude mixture (229 mg) containing the title compound was prepared according to general method D from 1,2,3,4-tetrahydroquinoline (0.189 mL, 1.502 mmol).

ESI-MS (B): *m/z* 210 [M+H]$^+$ (R$_t$ = 1.53 min).

2-Chloro-1-(2-phenylpiperidin-1-yl)ethanone (6.81)
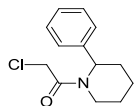
The crude mixture (189 mg) containing the title compound was prepared according to general method D from 2-phenylpiperidine (200 mg, 1.240 mmol).

ESI-MS (B): *m/z* 238 [M+H]$^+$ (R$_t$ = 1.70 min).

2-Chloro-1-(isoindolin-2-yl)ethanone (6.82)
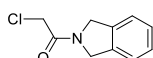
The crude mixture (217 mg) containing the title compound was prepared according to general method D from isoindoline (0.190 mL, 1.678 mmol).

ESI-MS (B): *m/z* 196 [M+H]$^+$ (R$_t$ = 1.35 min).

2-Chloro-1-(indolin-1-yl)ethanone (6.83)
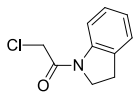
The crude mixture (291 mg) containing the title compound was prepared according to general method D from indoline (0.20 mL, 1.784 mmol).

ESI-MS (B): *m/z* 196 [M+H]$^+$ (R$_t$ = 1.51 min).

2-Chloro-1-(5-fluoroindolin-1-yl)ethanone (6.84)
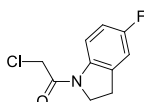
The title compound was prepared according to general method D from 5-fluoroindoline (200 mg, 1.458 mmol). Yield 96% (299 mg, 1.400 mmol), purity > 90%.

^{1}H NMR (400 MHz, DMSO-d$_6$) δ 8.02 (dd, *J* = 5.02, 8.78 Hz, 1H), 7.14 (d, *J* = 6.27 Hz, 1H), 7.01 (dt, *J* = 2.64, 9.10 Hz, 1H), 4.53 (s, 2H), 4.15 (t, *J* = 8.53 Hz, 2H), 3.18 (t, *J* = 8.41 Hz, 2H). **^{13}C NMR** (101 MHz, DMSO-*d$_6$*) δ 163.9, 158.6 (d, *J*=239.9 Hz), 139.0 (d, *J*=2.2 Hz), 134.4 (d, *J*=8.8 Hz), 116.7 (d, *J*=8.1 Hz), 113.2 (d, *J*=22.7 Hz), 112.3 (d, *J*=22.7 Hz), 47.3, 43.7, 27.5. **ESI-MS(B):** *m/z* 214 [M+H]$^+$ (R$_t$ = 1.52 min).

2-Chloro-1-(6-(trifluoromethyl)indolin-1-yl)ethanone (6.85)
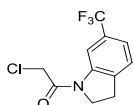
The title compound was prepared according to general method D from 6-(trifluoromethyl)indoline (250 mg, 1.336 mmol). Yield 93% (328 mg, 1.244 mmol).

^{1}H NMR (400 MHz, DMSO-d$_6$) δ 8.32 (s, 1H), 7.45 - 7.53 (m, 1H), 7.37 - 7.44 (m, 1H), 4.58 (s, 2H), 4.20 (t, *J* = 8.53 Hz, 2H), 3.26 (t, *J* = 8.53 Hz, 2H). **^{13}C NMR** (101 MHz, DMSO-*d$_6$*) δ 165.0, 143.2, 137.0, 127.8 (q, *J*=31.6 Hz), 125.8, 124.3 (q, *J*=272.9 Hz), 120.8 (q, *J*=4.0 Hz), 111.9 (q, *J*=3.9 Hz), 47.3, 43.8, 27.5. **ESI-MS(B):** *m/z* 264 [M+H]$^+$ (R$_t$ = 1.68 min).

2-Chloro-1-(2,3-dihydro-1H-pyrrolo[2,3-b]pyridin-1-yl)ethanone (6.86)
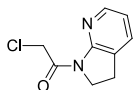
The title compound was prepared according to general method D from 2,3-dihydro-*1H*-pyrrolo[*2,3-b*]pyridine (200 mg, 1.665 mmol). Yield 61% (199 mg, 1.012 mmol), purity > 90%.

^{1}H NMR (400 MHz, DMSO-d$_6$) δ 8.13 (d, *J* = 4.27 Hz, 1H), 7.68 (dd, *J* = 1.25, 7.28 Hz, 1H), 7.03 (dd, *J* = 5.02, 7.28 Hz, 1H), 5.02 (s, 2H), 4.00 (t, *J* = 8.53 Hz, 2H), 3.09 (t, *J* = 8.53 Hz, 2H). **^{13}C NMR** (101 MHz, DMSO-d$_6$) δ 164.5, 154.9, 145.7, 134.3, 126.3, 118.6, 45.7, 44.6, 23.8. **ESI-MS (B):** *m/z* 197 [M+H]$^+$ (R$_t$ = 1.31 min).

2-Chloro-1-(3-phenylpyrrolidin-1-yl)ethanone (6.87)
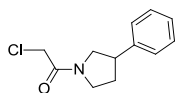
The crude mixture (194 mg) containing the title compound was prepared according to general method D from 3-phenylpyrrolidine (200 mg, 1.359 mmol).

ESI-MS (B): *m/z* 224 [M+H]$^+$ (R$_t$ = 1.59 min).

2-Chloro-1-(2-phenylpyrrolidin-1-yl)ethanone (6.88)
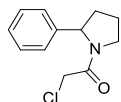
The crude mixture (212 mg) containing the title compound was prepared according to general method D from 2-phenylpyrrolidine (200 mg, 1.359 mmol).

ESI-MS (B): *m/z* 224 [M+H]$^+$ (R$_t$ = 1.54 min).

N-(2,4-difluorophenyl)-2-(4-methyl-2,5-dioxo-4-(4-sulfamoylphenyl)imidazolidin-1-yl)acetamide (6.89)
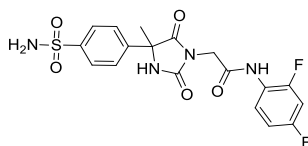
The title compound was prepared according to general method C from 4-(4-methyl-2,5-dioxoimidazolidin-4-yl)benzenesulfonamide **6.4** (60 mg, 0.223 mmol) and a crude mixture (92 mg) containing 2-chloro-N-(2,4-difluorophenyl)acetamide **6.77** (in excess) in DMF. Yield 47% (45.6 mg, 0.104 mmol), off-white amorphous solid, purity ≥ 95%.

¹H NMR* (400 MHz, DMSO-*d$_6$*) δ 10.16 (br. s., 1H), 9.10 (br. s., 1H), 7.78 – 7.89 (m, 3H), 7.72 (d, *J* = 8.53 Hz, 2H), 7.28 – 7.43 (m, 3H), 7.00 – 7.10 (m, 1H), 4.28 (s, 2H), 1.75 (s, 3H). **¹³C NMR** (101 MHz, DMSO-*d$_6$*) δ 174.7, 165.2, 158.5 (dd, *J*=243.6, 11.7 Hz), 155.2, 153.6 (dd, *J*=246.5, 13.2 Hz), 143.7, 143.0, 126.4, 125.9, 125.1 (dd, *J*=9.5, 2.2 Hz), 122.1 (dd, *J*=11.7, 3.7 Hz), 111.2 (dd, *J*=21.3, 3.7 Hz), 104.2 (dd, *J*=26.6, 24.2 Hz), 63.0, 40.6, 24.7. **ESI-MS (B):** *m/z* 439 [M+H]$^+$, 461 [M+Na]$^+$ (R$_t$ = 1.40 min). **Alkylation position was proven by 2DNMRs.*

N-(2,4-difluorophenyl)-N-methyl-2-(4-methyl-2,5-dioxo-4-(4-sulfamoylphenyl)imidazolidin-1-yl)acetamide (6.90)
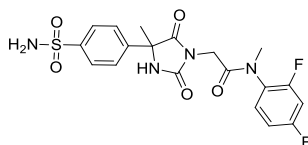
The title compound was prepared according to general method C from 4-(4-methyl-2,5-dioxoimidazolidin-4-yl)benzenesulfonamide **6.4** (60 mg, 0.223 mmol) and a crude mixture (59 mg) containing 2-chloro-N-(2,4-difluorophenyl)-N-methylacetamide **6.78** (in excess) in DMF. Yield 52% (52.6 mg, 0.116 mmol), off-white amorphous solid, purity ≥ 95%.

¹H NMR* (400 MHz, DMSO-*d$_6$*) δ 9.07 (br. s., 1H), 7.85 (d, *J* = 8.28 Hz, 2H), 7.66 - 7.77 (m, 2.8H), 7.49 - 7.61 (m, 0.8H), 7.31 - 7.47 (m, 2.4H), 7.22 - 7.30 (m, 0.8H), 7.13 (m, 0.2H), 4.52 (s, 0.4H), 3.84 - 3.97 (m,

0.8H), 3.69 - 3.81 (m, 0.8H), 3.36 (s, 0.6H), 3.12 (s, 2.4H), 1.69 - 1.76 (m, 3H). **^{1}H NMR**** (400 MHz, DMSO-d_6 with D_2O) δ 7.83 (d, *J* = 8.53 Hz, 2H), 7.61 - 7.72 (m, 2.8H), 7.45 - 7.53 (m, 0.8H), 7.35 - 7.43 (m, 0.2H), 7.27 - 7.35 (m, 0.2H), 7.17 - 7.27 (m, 0.8H), 7.06 - 7.16 (m, 0.2H), 4.49 (s, 0.4H), 3.82 - 3.95 (m, 0.8H), 3.67 - 3.79 (m, 0.8H), 3.32 (s, 0.6H), 3.09 (s, 2.4H), 1.64 - 1.77 (m, 3H). **^{13}C NMR***** (101 MHz, DMSO-d_6) δ 174.9, 165.9, 162.1 (dd, *J*=249.1, 12.5 Hz), 157.9 (dd, *J*=249.8, 13.2 Hz), 155.3, 143.8, 143.3, 131.7 (d, *J*=9.5 Hz), 126.7, 126.1, 125.8 - 126.1 (m), 113.1 - 113.5 (m), 105.5 - 106.3 (m), 63.2, 39.5, 36.7, 24.7. **ESI-MS (B):** *m/z* 453 [M+H]$^+$, 475 [M+Na]$^+$ (R_t = 1.50 min). **Two amide rotamers were observed (in approx. proportion 0.8/0.2); hydantoin NH was not clearly detected. **Addition of D_2O simplified the spectrum and allowed the aromatic protons integration. ***Signals of the minor amide rotamer were not detected clearly in ^{13}C NMR. The chemical shift of some peaks was confirmed by 2DNMRs.*
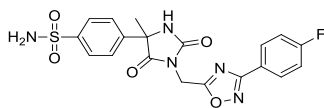
4-(1-(2-(3,4-Dihydroisoquinolin-2(1H)-yl)-2-oxoethyl)-4-methyl-2,5-dioxoimidazolidin-4-yl)benzenesulfonamide (6.91)

The title compound was prepared according to general method C from 4-(4-methyl-2,5-dioxoimidazolidin-4-yl)benzenesulfonamide **6.4** (60 mg, 0.223 mmol) and a crude mixture (93 mg) containing 2-chloro-1-(3,4-dihydroisoquinolin-2(*1H*)-yl)ethanone **6.79** (in excess) in DMF. Yield 44% (43 mg, 0.097 mmol), off-white amorphous solid, purity ≥ 95%.

^{1}H NMR* (400 MHz, DMSO-d_6) δ 9.07 (s, 1H), 7.81 - 7.89 (m, 2H), 7.73 (dd, *J* = 1.63, 8.41 Hz, 2H), 7.40 (s, 2H), 7.15 - 7.24 (m, 4H), 4.72 (s, 0.8H), 4.57 (s, 1.2H), 4.34-4.42 (m, 2H), 3.72 (t, *J* = 5.90 Hz, 1.2H), 3.64 (t, *J* = 5.90 Hz, 0.8H), 2.89 (t, *J* = 5.90 Hz, 1.2H), 2.77 (t, *J* = 5.77 Hz, 0.8H), 1.75 (s, 3H). **^{13}C NMR**** (101 MHz, DMSO-d_6) δ 175.0, 164.4, 164.4, 155.4, 143.7, 143.2, 134.6, 134.4, 133.2, 132.8, 128.6, 128.4, 126.6, 126.6, 126.4, 126.4, 126.3, 126.2, 125.8, 63.0, 45.2, 43.9, 41.7, 39.5, 28.4, 27.8, 24.8, 24.7. **ESI-MS (B):** *m/z* 443 [M+H]$^+$ (R_t = 1.40 min). **Two amide rotamers were observed (in approx. proportion 0.6/0.4). **Due to two rotamers presence, some signals are detected at different chemical shifts for different rotamers. Additional peaks are detected by HMQC, overlapping with DMSO-d_6 signal.*

4-(1-(2-(3,4-Dihydroquinolin-1(2H)-yl)-2-oxoethyl)-4-methyl-2,5-dioxoimidazolidin-4-yl)benzenesulfonamide (6.92)

The title compound was prepared according to general method C from 4-(4-methyl-2,5-dioxoimidazolidin-4-yl)benzenesulfonamide **6.4** (90 mg, 0.277 mmol) and a crude mixture (116 mg) containing 2-chloro-1-(3,4-dihydroquinolin-1(*2H*)-yl)ethanone **6.80** (in excess) in DMF. Yield 49% (60.3 mg, 0.136 mmol), off-white amorphous solid, purity ≥ 95%.

^{1}H NMR* (400 MHz, DMSO-d_6) δ 9.06 (br. s., 1H), 7.85 (d, *J* = 8.53 Hz, 2H), 7.71 (d, *J* = 8.53 Hz, 2H), 7.53 - 7.61 (br. m., 1H), 7.39 (br. s., 2H), 7.05 - 7.25 (m, 3H), 4.85 (br. s., 1H), 4.39 (br. s., 1H), 3.72 (d, *J* = 4.52 Hz, 2H), 2.72 (t, *J* = 5.90 Hz, 2H), 1.88 (t, *J* = 6.15 Hz, 2H), 1.73 (s, 3H). *One aromatic CH proton led to a very weak ^{1}H NMR signal.* **^{1}H NMR$^{*,#}$** (400 MHz, Acetone-d_6) δ 7.91 (d, *J* = 8.53 Hz, 3H), 7.77 - 7.86 (m, 2H), 7.59 (br. s., 1H), 7.07 - 7.29 (m, 3H), 6.62 (s, 2H), 4.82 (s, 1H), 4.41 (br. s., 2H), 3.71 - 3.88 (m,

2H), 2.73 - 2.83 (m, 2H), 1.93 - 2.01 (m, 2H), 1.86 (s, 3H). **^{13}C NMR**[*] (101 MHz, Acetone-d_6) δ 175.6, 166.2, 156.4, 144.9, 144.8, 139.2, 129.7, 127.5, 127.2, 125.4, 64.4, 62.9, 41.4, 27.4, 25.6, 24.6. **ESI-MS (B):** *m/z* 443 [M+H]$^+$ (R$_t$ = 1.44 min). [*]*Due to two rotamers presence, some signals were doubled in ^{1}H and ^{13}C NMR and detected at different chemical shifts for different rotamers, some signals were observed very broaden.*[#]*One aromatic CH proton led to a very weak ^{1}H NMR signal.*

4-(4-Methyl-2,5-dioxo-1-(2-oxo-2-(2-phenylpiperidin-1-yl)ethyl)imidazolidin-4-yl)benzenesulfonamide (6.93)
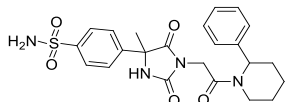
The title compound was prepared according to general method C from 4-(4-methyl-2,5-dioxoimidazolidin-4-yl)benzenesulfonamide **6.4** (60 mg, 0.223 mmol) and a crude mixture (64 mg) containing 2-chloro-1-(2-phenylpiperidin-1-yl)ethanone **6.81** (in excess) in DMF. Yield 27% (27.8 mg, 0.059 mmol), off-white amorphous solid, purity ≥ 90%.

^{1}H NMR[*] (400 MHz, Acetone-d_6) δ 7.88 - 7.98 (m, 3H), 7.81 - 7.87 (m, 2H), 7.19 - 7.48 (m, 5H), 6.54 - 6.69 (m, 2H), 5.82 (br. s., 0.5H), 5.32 (br. s., 0.3H), 4.34 - 4.63 (m, 1.8H), 4.07 - 4.24 (m, 0.3H), 3.81 - 3.97 (m, 0.5H), 2.99 - 3.14 (m, 0.5H), 2.84 (s, 0.2H), 2.61 (br. s., 0.3H), 2.47 (br. s., 1H), 1.87 (m, 3.6H), 1.33 - 1.73 (m, 4H). **ESI-MS (B):** *m/z* 471 [M+H]$^+$, 493 [M+Na]$^+$ (R$_t$ = 1.57 min). [*]*Peaks were broaden and multiplied due to the the diastereomers and rotamers presence.*

4-(1-(2-(Isoindolin-2-yl)-2-oxoethyl)-4-methyl-2,5-dioxoimidazolidin-4-yl)benzenesulfonamide (6.94)
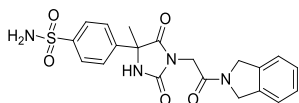
The title compound was prepared according to general method C from 4-(4-methyl-2,5-dioxoimidazolidin-4-yl)benzenesulfonamide **6.4** (90 mg, 0.277 mmol) and a crude mixture (109 mg) containing 2-chloro-1-(isoindolin-2-yl)ethanone **6.82** (in excess) in DMF. Yield 37% (44.2 mg, 0.103 mmol), off-white amorphous solid, purity ≥ 95%.

^{1}H NMR (400 MHz, DMSO-d_6) δ 9.08 (s, 1H), 7.86 (d, *J* = 8.53 Hz, 2H), 7.75 (d, *J* = 8.53 Hz, 2H), 7.26 – 7.45 (m, 6H), 4.95 (s, 2H), 4.65 (s, 2H), 4.34 (s, 2H), 1.77 (s, 3H). **^{13}C NMR** (101 MHz, DMSO-d_6) δ 174.9, 164.3, 155.3, 143.7, 143.2, 136.5, 135.6, 127.51, 127.48, 126.4, 125.8, 123.1, 122.8, 63.0, 52.0, 50.9, 39.8, 24.7. **ESI-MS (B):** *m/z* 429 [M+H]$^+$ (R$_t$ = 1.41 min).

4-(1-(2-(Indolin-1-yl)-2-oxoethyl)-4-methyl-2,5-dioxoimidazolidin-4-yl)benzenesulfonamide (6.95)
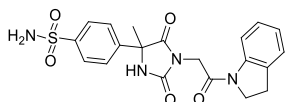
The title compound was prepared according to general method C from 4-(4-methyl-2,5-dioxoimidazolidin-4-yl)benzenesulfonamide **6.4** (60 mg, 0.223 mmol) and a crude mixture (87 mg) containing 2-chloro-1-(indolin-1-yl)ethanone **6.83** (in excess) in DMF. Yield 55% (52.9 mg, 0.123 mmol), off-white amorphous solid, purity ≥ 95%.

^{1}H NMR (400 MHz, DMSO-d_6) δ 9.12 (s, 1H), 7.95 (d, *J* = 8.03 Hz, 1H), 7.88 (d, *J* = 8.53 Hz, 2H), 7.76 (d, *J* = 8.28 Hz, 2H), 7.40 (s, 2H), 7.27 (d, *J* = 7.28 Hz, 1H), 7.15 (t, *J* = 7.65 Hz, 1H), 6.99 - 7.05 (m, 1H), 4.40

(s, 2H), 4.20 (t, *J* = 8.41 Hz, 2H), 3.19 (t, *J* = 8.28 Hz, 2H), 1.78 (s, 3H). **¹³C NMR** (101 MHz, DMSO-*d₆*) δ 174.9, 163.9, 155.3, 143.7, 143.1, 142.4, 131.7, 127.1, 126.4, 125.9, 125.0, 123.8, 115.8, 63.1, 46.3, 40.7, 27.6, 24.9. **ESI-MS (B):** *m/z* 429 [M+H]⁺, 451 [M+Na]⁺ (R$_t$ = 1.45 min).

4-(1-(2-(5-Fluoroindolin-1-yl)-2-oxoethyl)-4-methyl-2,5-dioxoimidazolidin-4-yl)benzenesulfonamide (6.96)
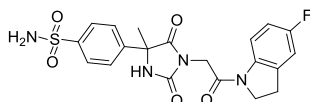
The title compound was prepared according to general method C from 4-(4-methyl-2,5-dioxoimidazolidin-4-yl)benzenesulfonamide **6.4** (50 mg, 0.186 mmol) and 2-chloro-1-(5-fluoroindolin-1-yl)ethanone **6.84** (59.5 mg, 0.279 mmol) in DMF. Yield 43% (36.0mg, 0.081 mmol), white amorphous solid, purity ≥ 95%.

¹H NMR (400 MHz, DMSO-*d₆*) δ 9.13 (s, 1H), 7.94 (dd, *J* = 4.89, 8.91 Hz, 1H), 7.88 (d, *J* = 8.53 Hz, 2H), 7.75 (d, *J* = 8.53 Hz, 2H), 7.41 (s, 2H), 7.14 (dd, *J* = 2.13, 8.41 Hz, 1H), 6.97 (dt, *J* = 2.51, 9.04 Hz, 1H), 4.40 (s, 2H), 4.23 (t, *J* = 8.41 Hz, 2H), 3.19 (t, *J* = 8.28 Hz, 2H), 1.78 (s, 3H). **¹³C NMR** (101 MHz, DMSO-*d₆*) δ 174.9, 163.7, 158.7 (d, *J*=239.2 Hz), 155.3, 143.8, 143.1, 138.9, 134.3 (d, *J*=8.8 Hz), 126.4, 125.9, 116.6 (d, *J*=8.1 Hz), 113.2 (d, *J*=22.7 Hz), 112.3 (d, *J*=24.3 Hz), 63.1, 46.7, 40.6, 27.6, 24.9. **ESI-MS(B):** *m/z* 447 [M+H]⁺ (R$_t$ = 1.43 min).

4-(4-Methyl-2,5-dioxo-1-(2-oxo-2-(6-(trifluoromethyl)indolin-1-yl)ethyl)imidazolidin-4-yl)benzenesulfonamide (6.97)
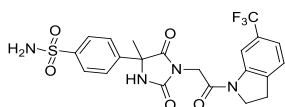
The title compound was prepared according to general method C from 4-(4-methyl-2,5-dioxoimidazolidin-4-yl)benzenesulfonamide **6.4** (50 mg, 0.186 mmol) and 2-chloro-1-(6-(trifluoromethyl)indolin-1-yl)ethanone **6.85** (73.4 mg, 0.279 mmol) in DMF. Yield 42% (39.0 mg, 0.079 mmol), white amorphous solid, purity ≥ 95%.

¹H NMR (400 MHz, DMSO-*d₆*) δ 9.17 (s, 1H), 8.22 (s, 1H), 7.88 (d, *J* = 8.53 Hz, 2H), 7.75 (d, *J* = 8.53 Hz, 2H), 7.49 (d, *J* = 7.78 Hz, 1H), 7.35 - 7.44 (m, 3H), 4.45 (s, 2H), 4.29 (t, *J* = 8.41 Hz, 2H), 3.28 (t, *J* = 8.16 Hz, 2H), 1.79 (s, 3H). **¹³C NMR** (101 MHz, DMSO-*d₆*) δ 174.8 (s), 164.9 (s), 155.2 (s), 143.8 (s), 143.1* (s), 137.0 (s), 127.8 (q, *J*=31.6 Hz), 126.4 (s), 126.0 (s), 125.8 (s), 120.8 (q, *J*=3.7 Hz), 124.3 (q, *J*=272.2 Hz), 111.8 (q, *J*=3.7 Hz), 63.2 (s), 46.8 (s), 40.7 (s), 27.6 (s), 25.0 (s). **ESI-MS(B):** *m/z* 497 [M+H]⁺ (R$_t$ = 1.58 min). *Two different Cq signals overlap, proven by 2D NMRs.

4-(1-(2-(2,3-Dihydro-1H-pyrrolo[2,3-b]pyridin-1-yl)-2-oxoethyl)-4-methyl-2,5-dioxoimidazolidin-4-yl)benzenesulfonamide (6.98)
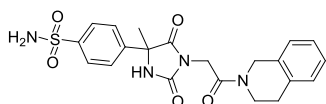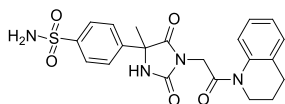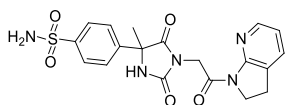

The title compound was prepared according to general method C from 4-(4-methyl-2,5-dioxoimidazolidin-4-yl)benzenesulfonamide **6.4** (60 mg, 0.223 mmol) and 2,3-dihydro-*1H*-pyrrolo[2,3-

b]pyridine-1-carbonyl chloride **6.86** (40.7 mg, 0.223 mmol) in DMF. Yield 21% (20.1 mg, 0.047 mmol), white amorphous solid, purity ≥ 95%.

¹H NMR (400 MHz, DMSO-d_6) δ 9.03 (br. s., 1H), 8.06 (d, J = 4.52 Hz, 1H), 7.80 (d, J = 8.53 Hz, 2H), 7.67 (d, J = 8.53 Hz, 2H), 7.61 - 7.65 (m, 1H), 7.33 (s, 2H), 6.98 (dd, J = 5.14, 7.40 Hz, 1H), 4.70 - 4.82 (m, 2H), 3.90 (t, J = 8.53 Hz, 2H), 3.04 (t, J = 8.41 Hz, 2H), 1.71 (s, 3H). **¹³C NMR** (101 MHz, DMSO-d_6) δ 174.8, 164.6, 155.3, 155.2, 145.7, 143.7, 143.1, 134.3, 126.4, 126.4, 125.9, 118.7, 63.1, 45.4, 42.6, 24.6, 24.0. **ESI-MS (B):** 430 [M+H]⁺ (R$_t$ = 1.35 min).

4-(4-Methyl-2,5-dioxo-1-(2-oxo-2-(3-phenylpyrrolidin-1-yl)ethyl)imidazolidin-4-yl)benzenesulfonamide (6.99)
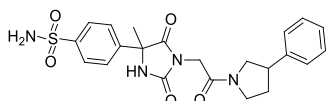
The title compound was prepared according to general method C from 4-(4-methyl-2,5-dioxoimidazolidin-4-yl)benzenesulfonamide **6.4** (60 mg, 0.223 mmol) and a crude mixture (75 mg) containing 2-chloro-1-(3-phenylpyrrolidin-1-yl)ethanone **6.87** (in excess) in DMF. Yield 31% (31.0 mg, 0.068 mmol), white amorphous solid, purity ≥ 95%.

¹H NMR[*] (400 MHz, DMSO-d_6) δ 7.85 (d, J = 8.53 Hz, 2H), 7.73 (d, J = 8.53 Hz, 2H), 7.20 - 7.38 (m, 5.5H), 4.22 - 4.33 (m, 1H), 4.10 - 4.22 (m, 1H), 3.96 - 4.05 (m, 0.5H), 3.80 - 3.90 (m, 0.5H), 3.72 - 3.79 (m, 0.5H), 3.52 - 3.66 (m, 1H), 3.43 (m, 1H), 3.14 - 3.25 (m, 0.5H), 2.32 (m, 0.5H), 2.20 (m, 0.5H), 1.86 - 2.12 (m, 1H), 1.75 (s, 3H). **ESI-MS (B):** 457 [M+H]⁺ (R$_t$ = 1.53 min). *Two amide rotamers were observed (in approx. proportion 0.5/0.5). NH signals were not clearly detected.*

4-(4-Methyl-2,5-dioxo-1-(2-oxo-2-(2-phenylpyrrolidin-1-yl)ethyl)imidazolidin-4-yl)benzenesulfonamide (6.100)
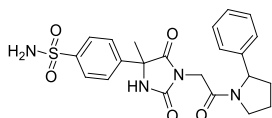
The title compound was prepared according to general method C from 4-(4-methyl-2,5-dioxoimidazolidin-4-yl)benzenesulfonamide **6.4** (60 mg, 0.223 mmol) and and a crude mixture (75 mg) containing 2-chloro-1-(2-phenylpyrrolidin-1-yl)ethanone **6.88** (in excess) in DMF. Yield 17% (17.3 mg, 0.038 mmol), white amorphous solid, purity ≥ 95%.

¹H NMR[*] (400 MHz, DMSO-d_6) δ 9.01 (s, 1H, 0.52H), 8.96 (s, 1H, 0.48H), 7.76 - 7.87 (m, 2H), 7.62 - 7.72 (m, 2H), 7.09 - 7.42 (m, 7H), 5.21 (d, J = 7.28 Hz, 0.48H), 5.03 (t, J = 6.02 Hz, 0.52H), 4.31 - 4.43 (m, 0.52H), 4.20 - 4.31 (m, 1H), 3.86 (m, 0.48H), 3.57 - 3.70 (m, 1H), 3.47 - 3.57 (m, 0.48), 3.41 (m, 0.52H), 2.31 - 2.44 (m, 0.52H), 2.15 - 2.29 (m, 0.48H), 1.75 - 1.96 (m, 2.48H), 1.64 - 1.74 (m, 3.52H). **ESI-MS (B):** 457 [M+H]⁺ (R$_t$ = 1.50 min). *Two amide rotamers were observed (in approx. proportion 0.52/0.48).*

_____

7. Biological evaluation

All the biological and physicochemical evaluation of the final compounds was performed within GSK. Section 7.1 describes the extensive biological profiling of the hydantoin family as DprE1 inhibitors. The description of all the performed biological and physicochemical assays is provided in Section 7.2.

7.1 Hydantoins as DprE1 inhibitors: extensive biological evaluation
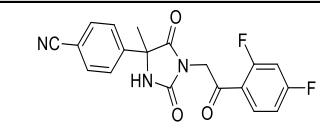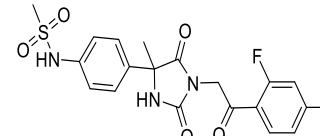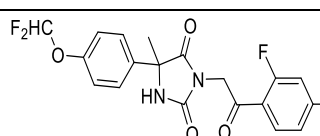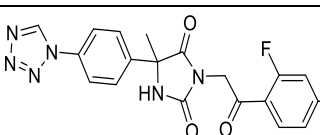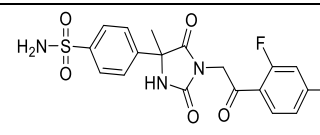
The described results were obtained within the OpenMedChem project in course of the Hit-to-Lead optimization program. The following discussion is based to large extent on the published manuscripts.[252,253]
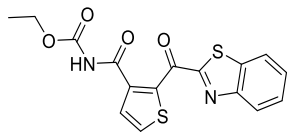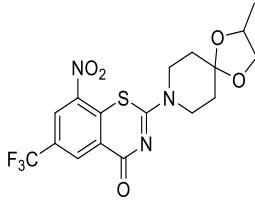
7.1.1 Validation of the mode action via overexpression of DprE1

Although the existing enzymatic and whole cell data seem to indicate that the hydantoin series acts on Mycobacteria by inhibiting the DprE1 enzyme, we were interested whether the whole-cell potency depended exclusively on that interaction or whether there were additional contributions from alternative modes of action.

Hence, a few potent hydantoin analogues (**4.1**, **5.50**, **5.71**, **5.76**, **6.9**) were selected for MIC determination against *M. tuberculosis* strain engineered to overexpress the DprE1 protein. The obtained results are summarized in Table 7.1. Higher expression of the target enzyme caused resistance to all tested compounds with a more than 8-fold shift in the MIC values relative to the wild type strain. These results are in agreement with data from the other known DprE1 inhibitors, both reversible (TCA1)[235] and irreversible (BTZ043).[275] Therefore, inhibition of DprE1 was confirmed as the only major mechanism responsible for antimycobacterial activity of the hydantoin series.

Table 7.1. MIC against *Mtb* overexpressing DprE1

	Structure	MIC_{WT} $(\mu M)^{[a]}$	MIC_{OE} $(\mu M)^{[b]}$	$MIC_{OE}/$ MIC_{WT} [c]
4.1		8.3	125	15
5.50		2.5	> 80	> 32
5.71		10	> 80	> 8
5.76		3.1	> 80	> 25
6.9		2.5	> 80	> 32

_____

	Structure	MIC$_{WT}$ (µM)[a]	MIC$_{OE}$ (µM)[b]	MIC$_{OE}$/ MIC$_{WT}$ [c]
TCA1		0.5	100	200
BTZ043		< 0.6	> 16	> 26

[a] MIC [µM] against wild type *Mycobacterium tuberculosis* (H37Rv). Reference: Isoniazid, MIC = 1.8 µM; [b] MIC [µM] against *Mycobacterium tuberculosis* overexpressing DprE1; [c] Ratio of MIC values against the DprE1-overexpressing strain and the wild type strain.

7.1.2 Hydantoins are reversible DprE1 inhibitors

The initial hit **4.1** contains potentially reactive groups, such as the carbonitrile substituent on ring A and the aromatic ketone in the linker. Thus, we were concerned with possible covalent interaction of the compound with the target protein. In order to assess the mechanism of inhibition, the rates of reaction catalysed by DprE1 were monitored in the presence of varying amounts of the inhibitor **4.1**. The obtained results are presented in Figure 7.1.
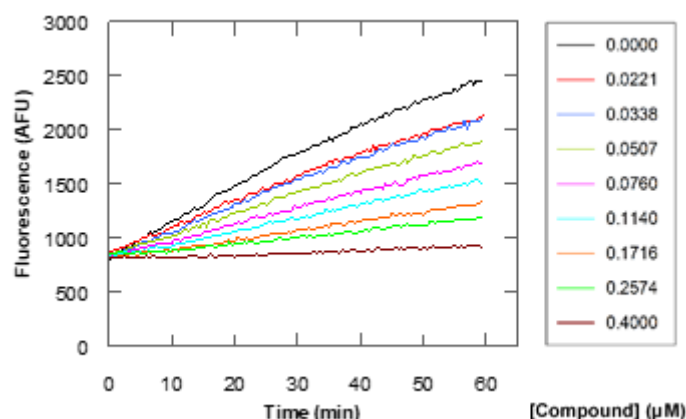
Figure 7.1. DprE1-catalyzed reaction progress in presence of varying concentrations of 4.1

Irreversible covalent inhibition leads to gradual depletion of the active enzyme and hence a decrease of reaction rate over time. As Figure 7.1 shows, almost perfectly linear increase of the product's concentration was maintained throughout a period of 60 minutes with no apparent time-dependent inhibition. Increasing concentration of the inhibitor did not lead to loss of this linearity, suggesting that **4.1** is not a suicide inhibitor and binds to the enzyme in a reversible manner.

7.1.3 Enantiomer activity

In order to provide better understanding if one or both of the hydantoin enantiomers contributed to the series potency, the enantiomers of the initial hit **4.1** and the new reference **6.9** were separated by chiral HPLC and tested (Scheme 7.1). It was found that only the *R-i*somers contributed to both the enzymatic and whole-cell potency (Table 7.2). Possessing this information, all other analogues were synthesized and evaluated as racemates for procedural simplicity.

_____

Scheme 7.1. Enantiomer separation via chiral HPLC of 4.1 and 6.9.

R =
4.1 -CN
6.9 -SO$_2$NH$_2$
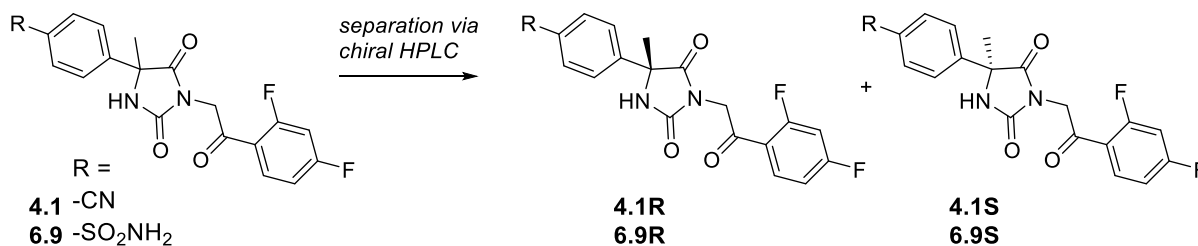
Table 7.2. Biological and physicochemical profile of 4.1, 6.9 and their enantiomers
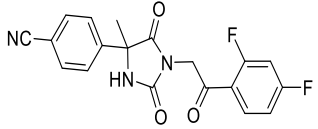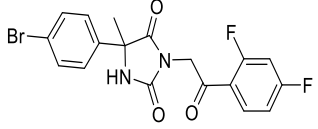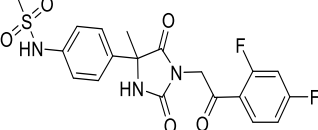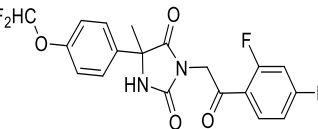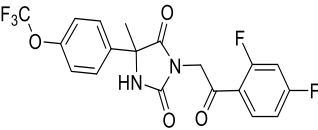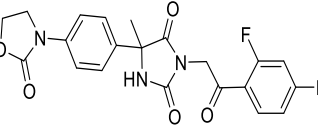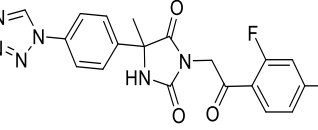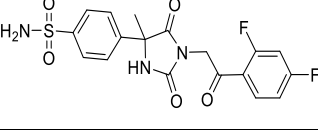
	Structure	DprE1 pIC$_{50}$[a]	MIC (μM)[b]	Cytotoxicity HepG$_2$ (μM)[c]	Solubility (μM)[d]	Chrom logD[e]
4.1		6.8	8.3	> 100	202	4.54
4.1R		7.2	6.7	> 100	355	4.51
4.1S		4.2	> 80	> 100	344	4.51
6.9		7.2	0.7	> 100	≥ 486	3.19
6.9R		7.5	0.78	> 100	≥ 344	3.17
6.9S		5.1	> 80	> 100	≥ 379	3.17

[a] MtbDprE1 enzyme inhibition pIC$_{50}$; [b] MIC [μM] against Mycobacterium tuberculosis (H37Rv). Reference: Isoniazid, MIC = 1.8 μM; [c] Cytotoxicity HepG$_2$ IC$_{50}$ [μM]; [d] kinetic aqueous solubility (CLND) [μM]; [e] ChromlogD (pH 7.4); [f] N.D. – not determined

7.1.4 Metabolic stability

The results of the *in vitro* metabolic stability evaluation of several potent analogues are summarized in Table 7.3. All the tested compounds possessed satisfactory metabolic stability. Most of them demonstrated intrinsic clearance values below 3 mL/min/g in mouse microsomes and lower than 0.4 mL/min/g in human microsomes. Moreover, all potent compounds resulted in an improved microsomal stability over the original hit **4.1**.

Table 7.3. Metabolic stability evaluation results in mouse and human microsomes

	Structure	Mouse Cl_{int} (mL/min/g)	Human Cl_{int} (mL/min/g)
4.1		3.52	0.49
5.48		1.48	< 0.40
5.50		3.29	0.47
5.71		1.78	< 0.40
5.72		1.59	< 0.40
5.75		3.54	< 0.40
5.76		2.44	< 0.40
6.9		2.67	< 0.40

7.1.5 hERG inhibition: cardio toxicity

Even though the hydantoin core in the initial hit **4.1** can be found in marketed drugs and was attractive to us from the synthetic perspective, the presence of this heterocycle has been previously linked to some undesired side-effects, such as the congenital hydantoin syndrome or inhibition of the hERG potassium channel.[276–279]

hERG (Human ether-a-go-go-related gene) is a gene that codes for a protein $K_v11.1$, the alpha subunit of a potassium ion channel. This ion channel, often referred as "hERG" itself, contributes to the electrical activity of the heart that coordinates the heart's beating. hERG potassium channels are essential for normal electrical activity in the heart, and when its ability to conduct electrical current across the cell membrane is inhibited or compromised by either genetic defects or adverse drug
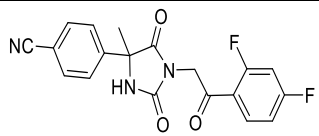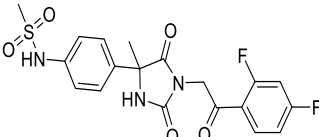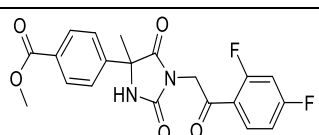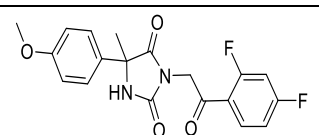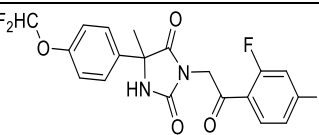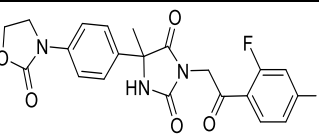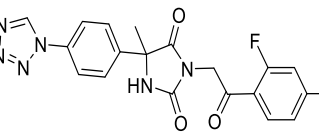
effects, this could lead to a potentially fatal disorder that predisposes individuals to life-threatening arrhythmias.[280,281]

Some drug candidates possess the tendency to inhibit hERG, creating an associated risk of sudden death as a side effect, which is a common reason for drug failure in preclinical safety trials. As cardiovascular risks were considered a major liability for further progression of the series, avoiding the hERG inhibition was crucial during the development of the hydantoin family.

In fact, as shown in Table 7.4, the initial hit **4.1** together with its difluoromethoxy **5.71** and tetrazole **5.76** analogues demonstrated measurable inhibition of the hERG potassium channel. In contrast, their close analogues **5.51**, **5.70**, **5.75**, **6.9** did not inhibit hERG (IC$_{50}$ > 50 μM).

Several potent "retro-sulfonamide" derivatives (4-SO$_2$NH$_2$ substituted on ring A) with various ring B and/or linker substituents were chosen for their hERG evaluation. Notably, essentially all of them showed no appreciable hERG inhibition (Table 7.4). The only exception was CF$_3$-substituted benzoxazole compound **6.69**, which showed both hERG and HepG$_2$ inhibition (see also Section 6.2.3.2), while its close F-substituted analogue **6.67** did not inhibit either hERG or HepG$_2$.

Table 7.4. hERG inhibion of selected potent analogues

	Structure	hERG IC$_{50}$ (μM)[b]
4.1		25
5.50		40
5.51		> 50
5.70		> 50
5.71		5
5.75		> 50
5.76		6

_____

	Structure	hERG IC$_{50}$ (µM)[b]
6.9		> 50
6.21		> 50
6.30		> 50
6.33		> 50
6.40		> 50
6.45		> 50
6.47		> 50
6.67		> 50
6.69		25
6.95		> 50

The obtained results suggest that potential cardiotoxicity is not inherent to the series but rather is dependent on the substituents on rings A and B. Therefore, while the activity against the hERG potassium channel should be monitored for all promising analogues, the hydantoin core itself is not considered a major concern for further development of this compound series.

7.1.6 *Intracellular activity*

Mycobacterium tuberculosis is an intracellular pathogen and survives within macrophages. Therefore, we were interested in the ability of the hydantoin series to inhibit the growth of bacilli in such environments. Several selected potent analogues were tested for their activity in an intracellular model of *M. tuberculosis* infection of human THP-1 macrophages, and the obtained results are summarized in Table 7.5.

Table 7.5. Activity of selected potent hydantoin analogues in an intracellular macrophage infection model

	Structure	MIC (µM)[a]	Intracellular IC$_{50}$ (µM)[b]	Intracellular IC$_{90}$ (µM)[b]
4.1		8.3	1.00	4.0
4.1R		6.7	0.40	1.3
5.50		2.5	0.44	31.6
5.71		10	0.74	N.D[c]
5.75		5.6	0.85	20.0
5.76		3.1	0.13	N.D[c]
6.9		0.9	0.30	N.D[c]

[a] MIC [µM] against Mycobacterium tuberculosis (H37Rv); [b] IC$_{50}$ [µM] and IC$_{90}$ [µM] against *Mycobacterium tuberculosis* (H37Rv) in infected Human THP-1 macrophages; [c] Not Determined as maximum inhibition was 84-88%

The direct comparison of the whole cell potency *in vitro* (MIC) and the intracellular IC$_{50}$ or IC$_{90}$ values was not feasible due to different readouts and calculation methods employed in the corresponding assays. On the other hand, a qualitative comparison between those values and trends observed may provide some insight on the macrophage penetration abilities of the tested compounds.

In general, the representatives of the investigated series exhibited good activity in a macrophage infection model. The obtained results suggested that the intracellular activities overall followed the

trend of the corresponding MIC values. However, the actual intracellular potency was found to be compound-dependent and not directly translatable from the standard MIC values as some additional factors might have an impact on the compound's potency in an intracellular setting.

7.1.7 In vivo: therapeutic efficiency

The two most potent compounds at the time (**5.76** and **6.9**) were selected for *in vivo* studies in an acute murine model of intratracheal TB infection. The therapeutic efficacy of the compounds against *M. tuberculosis* (H37Rv) was estimated using the standard acute assay. The obtained results are summarized in Figure 7.2 and Table 7.6. No adverse clinical signs were observed in any animal.
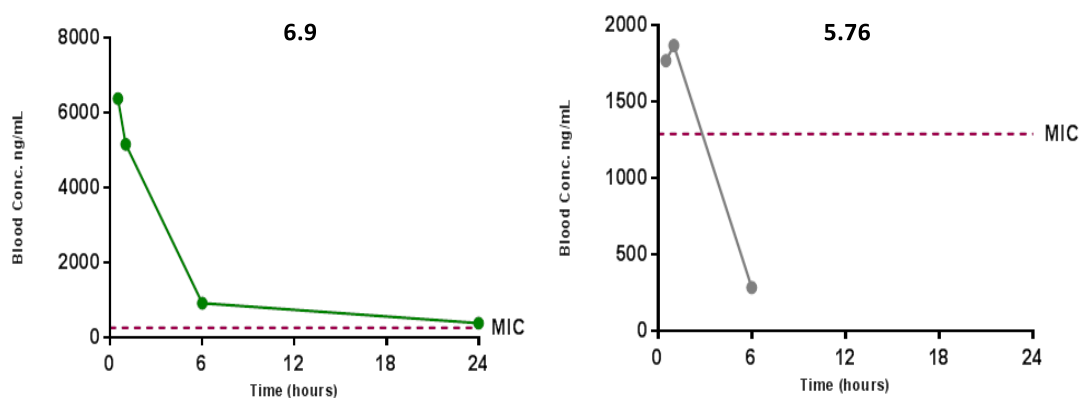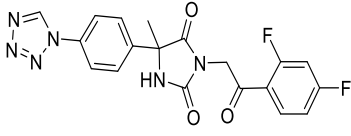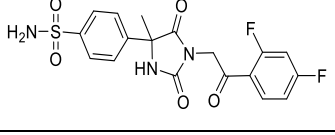
Figure 7.2. Blood exposure levels for 6.9 and 5.76

Hydantoin **6.9** possessed good blood exposure with concentrations above its MIC value up to 24 hrs after oral administration (Figure 7.1). However, in case of **5.76** low exposure levels were obtained (concentrations above the MIC were maintained for less than 6 hours).

As expected based on the lower exposure, **5.76** was inactive and no efficacy in bacterial load reduction was observed compared to the untreated control group. In contrast, **6.9** showed a statistcally significant difference in the lung CFUs of treated mice when compared to untreated mice (Table 7.6).

Table 7.6. Compound dose, the lung microorganism burden (log10 CFUs/lungs) and its difference with respect to untreated controls (Day 9 after infection) for tested compounds and Moxifloxacin as a reference standard.

	Structure	Target dose (mg/kg) [a]	logCFUs /mouse (lungs)[b]	Difference to untreated mice (logCFU)
5.76		170	7.2	0.2
6.9		200	6.9	0.5[c]
Moxifloxacin *(reference)*		100	3.3	4.1[c]
[a] oral administration in a once a day schedule for 4 consecutive days starting five days after the infection; [b] CFU number in lungs of untreated mice: 7.4 logCFU; [c] The value was considered statistically significant.				

_____

Although the *in vivo* activity of **6.9** was modest in comparison to the reference moxifloxacin, the obtained results prove that the hydantoin series is capable of achieving a statistically significant effect in an acute murine model, providing the desired *in vivo* proof of concept for the series.

7.1.8 General antimicrobial activity profile: series selectivity

Antitubercular therapy requires long-term drug administration, and activity against other bacterial species could cause unwanted killing of microbiome and potentially lead to the development and spread of drug resistance. Therefore, microbial selectivity should be be considered as an important factor in development of an antibiotic series.

For further series characterization, its spectrum of activity against other bacteria was investigated. MIC values against a panel of medically relevant strains of gram-positive and gram-negative bacteria were determined for the hit **4.1** and its potent analogues **5.50**, **5.75** and **6.9** (Table 7.7). No appreciable inhibition of growth (MIC ≥ 128 µM) was found in any of the experiments. These results indicate that the investigated series is selective for mycobacteria versus Gram-positive and Gram-negative bacteria.

Table 7.7. Activity of selected analogues against a panel of clinically relevant bacteria

Bacteria strain	MIC (µM)				
	4.1	**5.50**	**5.75**	**6.9**	**Ceftazidime**
A. baumannii 1484749	> 128	> 128	> 128	> 128	> 16
A. baumannii BM4454	> 128	> 128	> 128	> 128	4
A. baumannii BM4652	> 128	> 128	> 128	> 128	1
A. baumannii ATCC 19606-1 LpxC-	> 128	> 128	> 128	> 128	0.25
E. coli 1162222	> 128	> 128	> 128	> 128	1
E. coli 7623	> 128	> 128	> 128	> 128	0.125
E. coli 7623 TolC-	> 128	> 128	> 128	> 128	0.25
E. coli Top 10 TolC- Parent	n.d.	> 128	> 128	> 128	0.25
E. cloacae X4422	> 128	> 128	> 128	> 128	0.5
H. influenzae H128	> 128	> 128	128	128	0.03
H. influenzae H128 Acr A-	> 128	128	128	128	0.03
K. pneumoniae 1511191	> 128	> 128	> 128	> 128	4
K. pneumoniae 1161486	> 128	> 128	> 128	> 128	0.25
K. pneumoniae 1161486a	> 128	> 128	> 128	> 128	0.125
P. aeruginosa 394303	> 128	> 128	> 128	> 128	4
P. aeruginosa PAO1 (MV)	> 128	> 128	> 128	> 128	1
P. aeruginosa PAO322	> 128	> 128	> 128	> 128	0.5
S. aureus WCUH29	> 128	> 128	> 128	> 128	> 16

Bacteria strain	MIC (µM)				
	4.1	5.50	5.75	6.9	Ceftazidime
S. pneumoniae ERY2	> 128	> 128	> 128	> 128	0.125
S. pyogenes 1308007P	> 128	> 128	> 128	> 128	0.125

7.2   Biological assay description

7.2.1   Strain and growth conditions

M. tuberculosis H37Rv (ATC25618) wild-type was grown in Middlebrook 7H9-ADC broth (Difco) supplemented with 0.05% Tween 80 and on 7H10-OADC or 7H11-OADC agar (Difco) at 37 °C. Isoniazid and hygromycin were purchased from Sigma-Aldrich. When required, hygromycin (50 µg/ml) was added to the culture medium.

7.2.2   MIC determination

Minimum Inhibitory Concentration (MIC) determination assay against *M. tuberculosis* H37Rv was performed using a Resazurin reduction assay with fluorescent readout as described previously.[282] Isoniazid (INH) was used as a positive control with MIC = 1.8 µM and Rifampicin was used as a no-growth control.

In particular, the MIC measurement was performed in 96-well flat-bottom, polystyrene microtiter plates in a final volume of 200 µL. Ten two-fold drug dilutions in neat DMSO were performed. Middlebrook 7H9 (Difco) was used as medium. Isoniazid (Sigma Aldrich) was used as a positive control with two-fold dilutions of isoniazid starting at 4 µg/mL placed at row 11 of the plate layout and rifampicin (Sigma Aldrich) was used as no-growth control at concentration of 1 µM, placed at G-12 and H-12 wells. The inoculum (200 µL) was added to the entire plate. All plates were placed in a sealed box to prevent drying out of the peripheral wells and incubated at 37 °C without shaking for six days. A Resazurin solution was prepared by dissolving one tablet of resazurin (Resazurin Tablets for Milk Testing; Ref 330884Y' VWR International Ltd) in 30 mL of sterile PBS (phosphate buffered saline). Of this solution, 25 µL were added to each well. Fluorescence was measured (Spectramax M5 Molecular Devices, Excitation 530nm, Emission 590 nm) after 48 hours to determine the MIC value.

Data provided were the average of 2 experimental replicates, according to the standards of the industrial partner (GSK). Furthermore, MIC-values are typically not reported with an error/SD (unlike IC_{50} values). Standard practice is to consider that the error in the assay is on average ±1 dilution factor. In the reported work, two-fold dilution steps (1:2) are used between the assayed compound concentrations. This implies that, for example, MIC values of 2 and 4 µM should be considered equivalent.

7.2.3   HepG2 cytotoxicity assay

The HepG2 cytotoxicity assay was performed as previously described in literature.[282]

HepG2 cells were cultured using Eagle's Minimum Essential Medium (MEM) supplemented with 10 % heat-inactivated fetal bovine serum (FBS), 1 % Non-Essential Amino Acid (NEAA) supplement and 1% penicillin/streptomycin. Prior to addition of the cell suspension, 250 nL of test compounds per well were pre-dispensed in tissue culture treated black clear-bottomed 384-well plates (Greiner, cat. #

781091) with an Echo 555 instrument. After that, 25 µL of HepG2 (ATCC HB-8065) cells (~3000 cells/well) grown to confluency in Eagle's MEM supplemented with 10% heat-inactivated FBS, 1% NEAA and 1% Pencillin/Streptomycin were added to each well with the reagent dispenser. Plates were allowed to incubate at 37 °C with 20% O2 and 5% CO2 for 48 h. After the incubation period (48 h), the plates were equilibrated to room temperature before proceeding to develop the luminescent signal. ATP levels measured with CellTiter Glo kit (Promega) were used as cell viability read-out. 25 µL of CellTiter Glo substrate dissolved in the buffer was added to each well. Plates were incubated at room temperature for 10 minutes for stabilization of luminescence signal and read on View Lux with excitation and emission filters of 613 and 655 nm, respectively.

7.2.4 Kinetic aqueous solubility (CLND)

The kinetic solubility assay was performed as previously described in literature.[9]

5 µL of 10 mM DMSO stock solution diluted to 100 µL with pH 7.4 phosphate buffered saline, equilibrated for 1 hour at room temperature, filtered through Millipore Multiscreen HTS-PCF filter plates (MSSL BPC). The filtrate was quantified by suitably calibrated flow injection Chemi-Luminescent Nitrogen Detection. The standard error of the CLND solubility determination is ±30 µM, the upper limit of the solubility is 500 µM when working from 10 mM DMSO stock solution.

7.2.5 Hydrophobicity (chromlogD pH7.4)

Determination of chrom log D values at pH = 7.4 was performed as previously described in literature.[9]

The chromatographic hydrophobicity index (CHI) values were measured using a reversed phase HPLC column (50 × 2 mm, 3 µm, Gemini NX C18, Phenomenex, UK) with fast acetonitrile gradient at starting mobile phase of pH = 7.4 as described.3 CHI values were derived directly from the gradient retention time by using a calibration line obtained for standard compounds. The CHI value approximates to the volume % organic concentration when the compound eluted. CHI was linearly transformed into ChromlogD by least-square fitting of experimental CHI values to calculated clogP values using the following formula: ChromlogD = 0.0857 × CHI − 2.0

The average error of the assay was ± 3 CHI unit or ± 0.25 ChromlogD.

7.2.6 DHFR enzymatic inhibition

The DHFR enzymatic inhibition assay was performed as previously described in literature.[283]

The assay contained 0.2 mM NADPH, 10 µM DHF, 8.9 mM ß-mercaptoethanol, 150 mM KCl, 40.7 mM sodium phosphate at pH 7.4 and 125 ng/mL *Mtb* DHFR in a 50 µL volume. Absorbance of NADPH was measured at 340 nm in a 384-well SpectraMax M2 microplate reader (Molecular Devices, Sunnyvale, CA). Activity was calculated as the rate of change in absorbance at 340 nm.

7.2.7 DprE1 enzymatic inhibition, time-dependent DprE1 inhibition and DprE1 overexpressing strain

Expression and purification of Mt-DprE1 and cloning of Mt-DprE1 were performed as described by Batt et al.[284] Enzymatic data were generated using a modified version of the assay described in that report. The new protocol is in the process of being submitted for publication. DprE1 mutants were generated by recombineering as previously described by Thulasi *et al.* in 2016.[285]

Oxidation of farnesylphosphoryl-β-D-ribose (FPR) to farnesylphosphoryl-β-D-2'-keto-erythro-pentafuranose (FPX) by DprE1 enzyme results in the formation of a two-electron reduced flavin

intermediate (FADH2). To complete the catalytic cycle, the FADH2 has to be reoxidized to FAD. In the present assay, this can be accomplished by resazurin, which upon reduction generates the highly fluorescent product resorufin. Reactions were monitored by following an increase in fluorescence intensity (λex = 530 nm, λem = 595 nm) associated with the formation of resorufin. Assays were carried out in black 384-well low-volume microplates (Greiner Bio-one, Stonehouse, UK; catalog no. 78076) and contained 50 mM Hepes, pH 7.5, 100 mM NaCl, 1.5% (v/v) DMSO, 100 µM Tween-20, 2 µM FAD, and 50 µM resazurin, with variable concentrations of FPR and DprE1 in a total reaction volume of 10 µL. Measurements were made using a Tecan Safire2 instrument (Tecan Group Ltd., Seestrasse, Switzerland). Enzymatic rates in arbitrary fluorescence units per unit time were converted to quantity of product formed per unit time using a resorufin standard curve.

7.2.8   Intracellular IC$_{50}$ determination

The assays were performed as described previously[282] using Human THP-1 macrophages differentiated with PMA.

Human THP-1 (Human acute monocytic leukemia cell line, ATCC number TIB-202) macrophages differentiated with PMA (phorbol myristate acetate) was used as a model to study the intracellular stages of M. tuberculosis. The assay determines the effect of the compounds on mycobacteria growing inside phagocytes by determining luciferase activity per well, which is related to the number of living bacteria.

Protocol Steps: (a) Bacterial culture and single cell suspension protocol. A single cell suspension of M. tuberculosis H37Rv pATB45luc was prepared prior to infection. 25 mL of bacterial culture grown to log phase was centrifuged at 2800 g for 10 min. After removal of the supernatant, cell clumps were dispersed by vigorously shaking with sterile glass 3 mm beads (Sigma) for 2 min. Dispersed cells were then resuspended in 10 mL of Roswell Park Memorial Institute medium (RPMI medium) and left to decant for 5 min at room temperature. Cells were then centrifuged at 400 g for 5 min. Supernatant was collected and its optical density at 600 nm (OD600) was measured. OD mL^{-1} was converted to colony-forming unit (CFU) mL^{-1} considering that 0.125 OD is equal to 107 CFU mL^{-1}.

(b) THP-1 cell preparation and infection with M. tuberculosis. THP-1 cells were maintained in suspension with RPMI-1640 media (Sigma) containing 10% fetal bovine serum (Gibco), 1 mM of Pyruvate (Sigma), 2 mM of L-Glutamine (Sigma), and incubated at 37 °C with 5% CO2. THP-1 cells were routinely subcultured every 3 days at a cell density of 105 cells/mL. THP-1 cells were simultaneously differentiated with phorbol myristate acetate (PMA, 40 ng mL-1, Sigma) and infected with a single cell suspension of M. tuberculosis H37Rv-pATB45luc in a roller bottle at a MOI of 1:1. Cells were put in a roller bottle apparatus for 4 hours at 37 °C at 1.5 rpm. After this step of incubation, infected cells were washed four times by centrifugation at 400 g for 5 min and resuspended in fresh RPMI medium to remove extracellular bacilli. In the last wash, infected cells were resuspended in RPMI medium supplemented with 10% fetal bovine serum (Gibco), 2 mM L-

glutamine and pyruvate at a concentration of 2 x 105 cells/mL. 50 µl of this cell suspension (typically 10000 cells per well) were dispensed into the wells of 384-well plates (white, flat bottom, Greiner).

(c) Incubation of infected THP-1 cells with tested compounds. Prior to addition of the infected cell suspension, the compounds (250 nL/well) were dispensed into the plates with an Echo liquid handler. The maximum DMSO concentration is 0.5%. Plates were allowed to incubate at 37 °C at 80% relative humidity for 4 days. Luciferase activity, proportional to bacterial load, was determined by using

BrightGlo™ Luciferase Assay System (Promega, Madison, WI) according to the manufacturer's protocol. Resultant luminescence was measured in an Envision Multilabel Plate Reader (PerkinElmer) using the 384-plate Ultra Sensitive luminescence mode, with a measurement time of 200 ms per well. Results were processed by using an Excel spreadsheet and Grafit software. IC_{50} and IC_{90} values were calculated from the dose-response curves by non-linear regression analysis.

7.2.9 Microsomal fraction stability assays

The Microsomal fraction stability asssays were performed as described previously.[282] The human biological samples were sourced ethically and their research use was in accord with the terms of the informed consents.

Pooled murine liver microsomes were purchased from Xenotech. Microsomes (final protein concentration 0.5 mg/mL), MgCl2 (final concentration 5 mM) and test compound (final substrate concentration 0.5 µM; final DMSO concentration 0.5 %) in 0.1 M phosphate buffer pH 7.4 were pre-incubated at 37 °C prior to the addition of NADPH (final concentration 1 mM) to initiate the reaction. The final incubation volume was 600 µL. All incubations were performed singularly for each test compound. Each compound was incubated for 30 minutes and samples (90 µL) of incubate were taken at 0, 5, 10, 20 and 30 minutes. The reactions were stopped by the addition of sample to 200 µL of acetonitrile:methanol (3:1) containing an internal standard. The terminated samples were centrifuged at 3700 rpm for 15 minutes at 4 °C to precipitate the protein. Quantitative analysis: following protein precipitation, the samples were analyzed using specific LC-MS/MS conditions. Data analysis: from a plot of ln peak area ratio (compound peak area/internal standard peak area) against time, the gradient of the line was determined. Subsequently, half-life and intrinsic clearance were calculated using the equations below:

$$\textbf{Elimination rate constant } (k) = (-\text{gradient})$$

$$\textbf{Half life } (t_{1/2})(\min) = \frac{0.693}{k}$$

$$\textbf{Intrinsic Clearance } (\text{Clint}) \, (\text{mL/min/g}) =$$

$$\frac{0.693}{t_{1/2}} \times \frac{\text{mL of incubation}}{\text{(mg microsomal protein)}} \times \frac{\text{(mg microsmal protein)}}{\text{(g liver)}}$$

7.2.10 hERG Inhibition Determination assay

Inhibition of the hERG potassium channel was determined using in vitro IonWorks patch-clamp electrophysiology as decribed in literature.[286] These assays were performed at the PTS (Platform Technology Science) Department in GSK Stevenage.

HERG channels were stably expressed in CHO-K1 or HEK293 cells. Cryo-preserved cells were used in all experiments. Frozen cells were stored in a liquid nitrogen freezer and quickly thawed in Dulbecco's modified Eagle medium F-12 supplemented with 10% fetal bovine serum before plating into tissue culture vessels. Cells were cultured at 37 °C, 5% CO_2 for 2–4 h and then placed at 30 °C, 5% CO_2 for 24–96 h prior to recording hERG currents. For QPatch recordings, CHO-K1 cells were cultured in Iscove's DMEM supplemented with 10% non-heat inactivated fetal bovine serum, 2% HT supplement, 100 units/mL penicillin, 0.1 mg/mL streptomycin, 0.1 mM non-essential amino acids, and 0.4 mg/mL geneticin. Culturing the cells at 30 °C increases functional expression of hERG channels. All cell culture reagents were from Invitrogen.

Prior to recording hERG currents, culture medium was replaced with external solution and the culture dish was placed onto the microscope stage of a patch clamp set up. All recordings were made in the perforated patch clamp mode with internal solution containing 0.1 mg/mL amphotericin. After giga-seal formation, access resistance (R_a) was monitored and current recordings were not started until R_a reached values below 20 MΩ. Currents were filtered at 5 kHz with an Axopatch 200B patch clamp amplifier (Molecular Devices, Sunnyvale, CA). Current recordings were digitized with a Digidata 1320 interface under the control of the pCLAMP10 software (Molecular Devices, Sunnyvale, CA). All recordings were made at room temperature.

7.2.11 Vibrational Circular Dichroism

VCD analysis and assignment was performed according to an analogous protocol published previously.[287]

VCD spectra were acquired using a BioTools Dual-PEM ChiralIR™ FT-VCD spectrometer operating at 4 cm^{-1} resolution, with modulators calibrated at 1400 cm^{-1} and retardations set at PEM1 = 0.250 λ, PEM2 = 0.260 λ. A total of 18720 scans were accumulated for each VCD measurement. Spectra were acquired using an International Crystal Laboratories sealed transmission cell with BaF$_2$ windows and 100 micron pathlength. Samples were dissolved in CDCl$_3$ at 0.2-M concentration. The baseline artifact inherent in experimental VCD spectra was removed by the half-difference correction method:

VCD$_{corr'd}$ (**1**) = [(VCD$_1$ − VCD$_{1b}$)/2]; VCD$_{corr'd}$ (**1b**) = [(VCD$_{1b}$ − VCD$_1$)/2].

Spectra were calculated for each conformation using the B3LYP/DGDZVP computational method. VCD spectra were synthesized using Gibbs free energies and Boltzmann statistics. The calculated line spectra were fitted with Lorentzian band shapes using an 8 cm^{-1} resolution factor (hwhh) and a uniform scaling factor of 0.975. The level of confidence in the VCD assignments was estimated using CompareVOA™ (BioTools, Inc.; Jupiter, Fla. USA), an algorithm that uses overlap integrals to quantify the agreement between calculated and observed VCD spectra.

7.2.12 General antimicrobial activity assay

Whole-cell antimicrobial activity was determined by broth microdilution using the Clinical and Laboratory Standards Institute (CLSI) recommended procedure, Document M7-A7, "Methods for Dilution Susceptibility Tests for Bacteria that Grow Aerobically." Selected compounds were evaluated against a panel of Gram-positive and Gram-negative organisms, including *Acinetobacter baumannii, Escherichia coli*, *Enterobacter cloacae, Haemophilus influenzae*, *Klebsiella pneumoniae*, *Pseudomonas aeruginosa, Staphylococcus aureus*, *Streptococcus pneumoniae,* and *Streptococcus pyogenes*. Minimum inhibitory concentration (MIC) values were determined as the lowest concentration of compound producing > 80 or 90 % decrease in fluorescence observed.

7.2.13 Therapeutic efficacy

All animal studies were ethically reviewed and carried out in accordance with European Directive 2010/63/EU and the GSK Policy on the Care, Welfare and Treatment of Animals. Specific pathogen-free, 8-10 week-old female C57BL/6 mice were purchased from Harlan Laboratories and were allowed to acclimate for one week. Mice were infected intratracheally with 100.000 CFU/mouse (*M. tuberculosis* H37Rv strain). Compounds were orally administered for four consecutive days, starting from day 5 after infection. Lungs were harvested on day 9, 24 hours after the last compound administration. All lung lobes were aseptically removed, homogenized and frozen. Homogenates were

plated in 10% OADC-7H11 medium supplemented with activated charcoal (0.4%) to avoid product carry over, and incubated for 18 days at 37 °C. No adverse clinical signs were observed in any animal. Blood samples were obtained at different time points from the infected mice to measure the levels of the tested compounds.

The number of CFU/mouse measured for each mouse and the differences in the lung microorganism burden (log10 CFUs/lungs) obtained in the treated mice with respect to untreated controls (Day 9 after infection) were calculated. CFU number in lungs of untreated mice: 7.4 logCFU. This value is included in the interval mean ± 2 SD of the values of the last experiments. Quality controls: In this experiment, Moxifloxacin (100 mg/kg) was administered for four consecutive days starting from day 5 after infection as an inter-assay control. It reduced 4.1 logCFU the bacterial lung number in comparison with the untreated mice (7.4 logCFU). This quality control value is included in the accepted interval.

_____

8. Conclusions and outlook

8.1 Conclusions

The primary goal of this research was hit exploration and hit-to-lead optimization of two novel chemical series in order to provide potent and selective compounds against *M. tuberculosis*. The initial hits that formed the starting point of the research were identified during HTS campaigns performed by GSK.

The first compound family, identified in the whole-cell HTS campaign against *M. bovis* with hit confirmation in *M. tuberculosis*, was proven to inhibit the *Mtb*DHFR enzyme. The initial hits demonstrated very good whole-cell and enzymatic potency, coupled however with significant human-cell toxicity. A scaffold hopping approach was then applied in order to overcome toxicity and selectivity issues while preserving the crucial pharmacophore. Unfortunately, the obtained analogues showed no cellular or DHFR inhibition activity. Therefore, this line of research was discontinued.

A target-based high-throughput screening (HTS) campaign revealed a novel hydantoin-based family of potent DprE1 inhibitors. The follow-up hit-to-lead optimization program was performed in two rounds producing an extensive SAR around the initial hit. A number of highly active DprE1 inhibitors with sub-micromolar cellular potencies and balanced physicochemical profiles were delivered. Moreover, the discussed series showed no cytotoxicity and was found selective against mycobacteria. The proof-of-concept of *in vivo* activity was demonstrated.

8.2 DHFR inhibitors: outlook

Recently, Tawari *et al*. reported the synthesis and evaluation of several diaminotriazines (Figure 8.1 B), structurally related to compounds **3.16-3.17**, discussed in section 3.1.4.3 (Figure 8.1 A). Those compounds were prepared based on virtual screening results and structure-based drug design.[288]
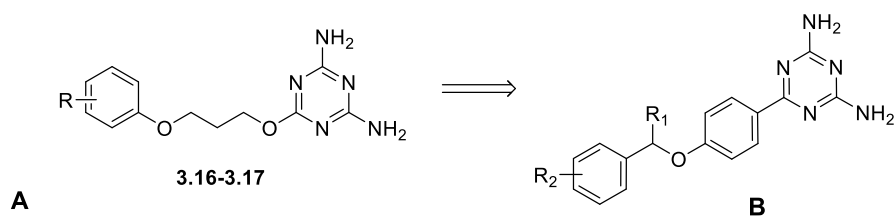
Figure 8.1. Diaminotriazines – (A) inactive synthesized analogues vs. (B) active and selective series against *Mtb* DHFR, reported in the literature[288]

The reported series is structurally related to a known on-target DHFR inhibitor trimethoprim and demonstrated broadly comparable MICs and DHFR-affinities with the latter. Some representatives showed low-micromolar whole-cell activity against *Mtb* H37Rv (MIC = 1.5-2 µM) along with low cytotoxicity (CC$_{50}$ VERO cell line > 300 µM).

These results could provide a valuable starting point for further investigation of DHFR inhibitors with an aromatic heterocyclic core in search of novel anti-tuberculosis agents. In particular, the preparation of analogous pyrimidine-2,4-diamine derivatives (Figure 8.2 A) or the introduction of a saturated ring into the linker (Figure 8.2 B) could be interesting modifications for further series development (Figure 8.2, A and B respectively).
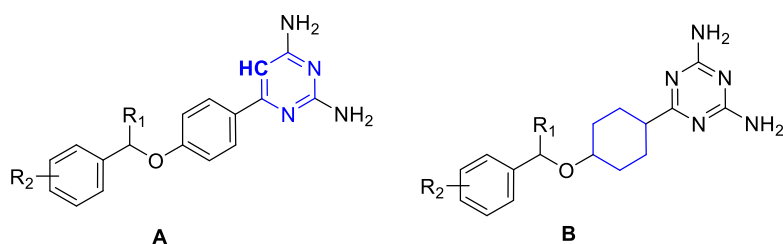
Figure 8.2. Proposed modifications of DHFR inhibitors series (highlighted in blue)

8.3 Hydantoins as DprE1 inhibitors: outlook

Although an extensive SAR around the hydantoin DprE1 inhibitors has been performed within the OpenMedChem project, there are still several different strategies that can be exploited in order to provide a stronger hydantoin-based lead against *M.tuberculosis*, including:

- Further refinement of the SAR
- Docking studies to provide a starting point for the rational structure-based compound design

A particularly competitive landscape in this filed should also be taken into account as several potent DprE1 inhibitors have recently entered in phases I-II of clinical development. Therefore, currently available data, while being encouraging, indicate that additional research, mainly focusing on the improvement of ADME and *in vivo* efficacy responses, is required before preclinical development for this class of compounds can be considered successful.

8.3.1 Additional SAR research

Delivery of several highly potent and structurally diverse compounds is desirable to assess the development potential of this class of molecules. The most potent and promising compound sub-series to-date is represented by sulfonamide **6.9** and its likes (**6.30**, **6.33, 6.97**). Its further optimization in terms of potency enhancement could include the introduction of various modifications in the linker region and the ring (as shown in Figure 8.3).

Direct or hetero-atom linked introduction of heterocyclic substituents at the 3-position of the ring B (Figure 8.3 A) could potentially offer better inhibitors, as it was shown that even bulkier groups in this position retain activity (**6.30** 3-CF_3 and **6.33** 3-OCF_3). Moreover, changing the nature of the substituent could allow fine-tuning of the overall physicochemical compound profile.

A limited number of analogues comprising linker modifications, in which the acetophenone moiety was replaced by a different, non-ketone containing functionality, were shown to retain enzymatic and whole-cell activity (*vide supra*, Section 6.2.3). Additional medicinal chemistry efforts could concentrate on the further development of those compound sub-series.

The representatives **6.95-6.97** containing an indoline moiety in place of the aryl ring B demonstrated highly promising whole-cell activity (2.5 µM for **6.95-6.96**, 0.3 µM for **6.97**), accompanied by moderate DprE1 inhibition (pIC_{50} = 6.6-7.0). Therefore, the preparation of more substituted indolines, as well as other related amides (Figure 8.3 B), could be of interest for further potency improvement.

The introduction of a sulfone group in place of the ketone (compound **6.52**) provided a moderately active compound with pIC_{50} = 6.0, while the corresponding keto-analogue **6.14** with an identical ring substitution pattern possessed a pIC_{50} = 6.6. Logical follow-up compounds could consist of analogues,

containing both the sulfone linker and a ring B substitution pattern present in the most potent DprE1 inhibitors (Figure 8.3 C).

The introduction of a saturated cyclohexyl ring in place of the aryl-type ring B in **6.40** led to a slight improvement in potency over its phenyl-substituted analogue **6.14**. As a result, the synthesis of more analogues containing substituted cyclohexyl moieties (Figure 8.3 D) could potentially deliver potent and promising compounds, although the synthetic approach to the necessary precursors may not be trivial.
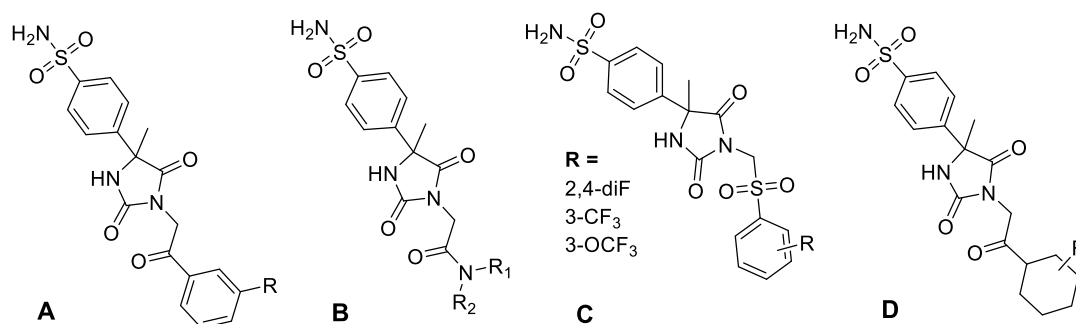
Figure 8.3. Potential further modifications for hydantoin-based DprE1 inhibitors

8.3.2   Docking studies

Cross-resistance of the initial hit **4.1** against a mutant H37Rv-strain resistant to TCA1 analogues (a published, structurally distinct class of DprE1 inhibitors) was detected.[259] This suggested binding of the hydantoin-based inhibitors in the same part of DprE1's active center as TCA1, and possibly interactions with similar key residues in the enzyme. In search of additional guidance for further chemical efforts, some preliminary docking studies of hydantoin representatives on a crystal structure of the *Mtb* DprE1 protein, cocrystallised with the TCA1 ligand, have been initiated within OpenMedChem.[271]

A crystal structure of the *Mtb* DprE1 protein co-crystallized with one of the hydantoin-based inhibitors could allow the identification of the binding pocket of the series and provide far more precise data for future docking studies. No such crystal structure has been obtained to date. Therefore, investing research effort into co-crystallization of the most potent hydantoin analogues with the *Mtb*DprE1 enzyme could give another boost to the project, and allow the application of obtained docking results for the rational design of new analogues.

176

9. Summary

9.1 Introduction

Tuberculosis (TB) remains a global health threat, accounting for more than 9 million new cases per year and 1.5 million deaths.[6] The emergence of multi- (MDR) and extensively-drug resistant (XDR) *Mycobacterium tuberculosis* strains as well as HIV comorbidity, fuel the TB epidemic resurgence.

This leads to an acute need for the discovery and development of new antitubercular agents that would preferably possess novel modes of action and treat drug-resistant forms of the disease. A considerable effort is concentrated, therefore, on the investigation of new biological targets and the development of drugs that would interact with them.

The presented research was performed within the OpenMedChem EID-ITN project (FP7) between the University of Antwerp and GlaxoSmithKline (GSK) with a focus on early hit-to-lead anti-tubercular drug development. It was concentrated on hit exploration and hit-to-lead optimization of two novel chemical series in order to provide potent and selective compounds against *M. tuberculosis*. Hits that were identified during two different HTS campaigns performed by GSK formed the starting point for the research.[171,284]

The dihydro-2,4-diamino-1,3,5-triazine cluster was identified during a whole-cell phenotypic high throughput screening (HTS) campaign against *Mycobacterium bovis* BCG with hit confirmation in the *M. tuberculosis* H37Rv strain.[171] This chemical family was selected for further investigation within the presented research, summarized in Section 9.2.

Flavo-enzyme deca-prenylphosphoryl-beta-D-ribose 2-epimerase (DprE$_1$) is essential for mycobacterial cell wall biosynthesis and was already validated as a promising drug target in *M.tuberculosis*.[247,249] Recently, GSK performed a target-based high-throughput screening (HTS) campaign in search of novel DprE$_1$ inhibitors, leading to the discovery of a novel hydantoin-based family of antimycobacterials as a promising hit series (described in Section 9.3).

9.2 DHFR inhibitors: exploration and scaffold hopping

The initial hits identified in the whole-cell phenotypic HTS campaign possessed in their structure the 2,4-diamino-1,3-diaza pharmacophore, reported to be crucial for DHFR inhibition activity in different organisms. Later on, the series was proven to inhibit *Mtb*DHFR. In the course of this exploration, the modifications were focused on (1) preparation of close analogues of the initial hits; (2) scaffold hopping approach (Figure 9.1, A and B respectively).
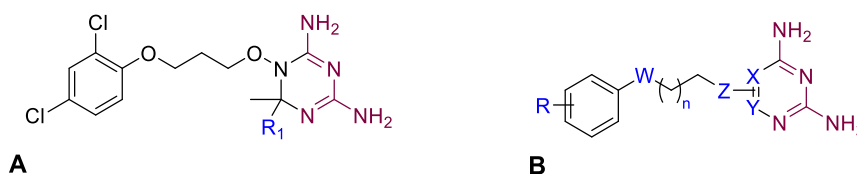
(A) Structure of the initial hit analogues, (B) Scaffold hopping: general compound structure indicating the crucial 2,4-diamino-1,3-diaza pharmacophore (magenta) and the structural features that were modified during this project (blue).

Figure 9.1. Modifications performed in a search for DHFR inhibitors

The synthesis of direct analogues of the initial hits proved to be highly challenging: reproducibility and structure elucidation issues ultimately contributed to our decision to shift attention to synthetically

more accessible classes of structurally related compounds. In the course of the biological evaluation, all the dihydrotriazine-bearing compounds displayed micromolar anti-mycobacterial potencies along with exceptionally high human cytotoxicity in the HepG2 assay ($IC_{50} < 0.01$ μM), probably related to a lack of compound selectivity between *M. tuberculosis* and human DHFR enzymes. Additionally, the limited solubility and membrane permeability of those compounds indicated a higher risk of poor bioavailability.

As the demonstrated physicochemical and cytotoxicity issues might be intrinsically related to the biopharmaceutical properties of the dihydrotriazine ring itself, a scaffold hopping approach was investigated (Figure 9.1 B). The 2,4-diamino-1,3-diaza pharmacophore, crucial for DHFR inhibition, was preserved in all new analogues, while aromatic heterocycles were preferred as they could have improved permeability compared to non-aromatic dihydrotriazines.

In total, 21 structurally diverse pyrimidine and triazine derivatives with variations in 1) linker length and nature and 2) aryl substitution pattern, were synthesized and evaluated. Unfortunately, all the compounds that were prepared by the scaffold hopping approach turned out to be completely inactive in enzymatic and whole-cell assays, which may indicate particular importance of the unsaturated 1,6-dihydro-1,3,5-triazine-2,4-diamine core for potent *Mtb* DHFR inhibition.

Several structurally-related diaminotriazines with low-micromolar whole-cell activity against *Mtb* H37Rv were recently reported by Tawari *et al.*[288] These results could provide a valuable starting point for further investigation of DHFR inhibitors with an aromatic heterocyclic core in search of novel anti-tuberculosis agents.

9.3   Hydantoins as DprE1 inhibitors: Identification and SAR exploration

Overall, the initial hydantoin hit **4.1**, being a potent DprE1 inhibitor, demonstrated an encouraging hit profile with no detectable cytotoxicity in HepG$_2$ assay coupled with satisfactory solubility and lipophilicity (Figure 9.2). The project objectives included:

- preparation of novel hydantoin-based DprE1 inhibitors with enhanced potency in enzymatic and whole-cell assays and balanced physicochemical profile;
- removal of potential structural liabilities
- obtain *in vivo* proof of concept for the series

In order to reach the established project objectives, the hit-to-lead (H2L) optimization process was divided into two rounds.

9.3.1   First round of Hit-to-Lead optimization

In the first round of hit-to-lead (H2L) optimization, the potential liabilities of the initial hit **4.1** (the acetophenone fragment and the carbonitrile group) were addressed together with the exploration of a wider chemical space around it in order to collect primary SAR information. The introduced modification included: (1) modifications of the linker; (2) side chain variation; (3) ring A modifications.

A total of around 100 compounds with these modification types were synthesized and evaluated under the OpenMedChem project, including around 30 of these analogues described in this thesis. Figure 9.2 summarizes the SAR conclusions, obtained in the first round of Hit-to-Lead optimization.

_____
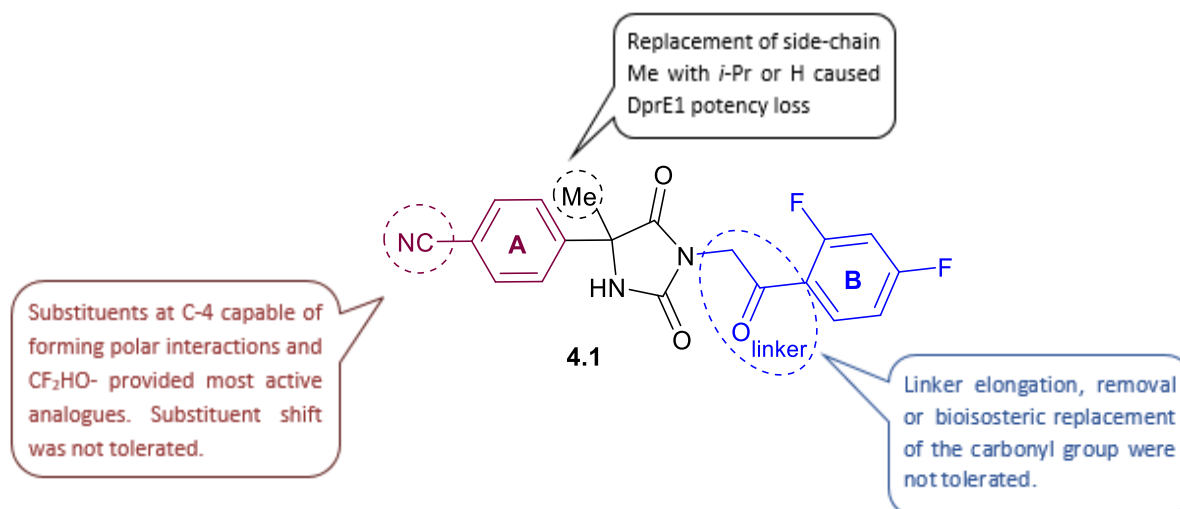
Figure 9.2. The first round of H2L optimization: SAR conclusions

An initial concern about metabolic stability, triggered by the acetophenone moiety present in the linker, proved insignificant after microsomal stability studies. As all the introduced linker modifications resulted in a complete activity loss, the original linker was preserved in further analogues that contained ring A and/or ring B modifications. The replacement of the side-chain Me with *i*-Pr or H with preservation of the original linker and ring B caused DprE1 potency loss, suggesting that those changes were not tolerated for the current series.

A number of compounds with improved whole-cell and enzymatic potencies were identified among compounds with a varied ring A substitution pattern. In general, the introduction of hydrophilic substituents in place of the cyano moiety in *para*-position of ring A seemed to be favorable for retaining the DprE1 inhibitory potency. A sulfonamide moiety (4-NHSO$_2$Me) **5.50** showed a more than 3-fold improvement in whole-cell activity over the initial hit **4.1** and slightly higher DprE1 potency. Compound **5.71** possessed the highest enzymatic inhibitory activity (pIC$_{50}$ = 7.4) detected in the first round of H2L optimization, exhibiting only a moderate whole-cell activity of 10 µM though (Figure 9.3). Compounds **4.1**, **5.50,** and **5.71** were chosen as new starting points for the second round of Hit-to-Lead optimization.
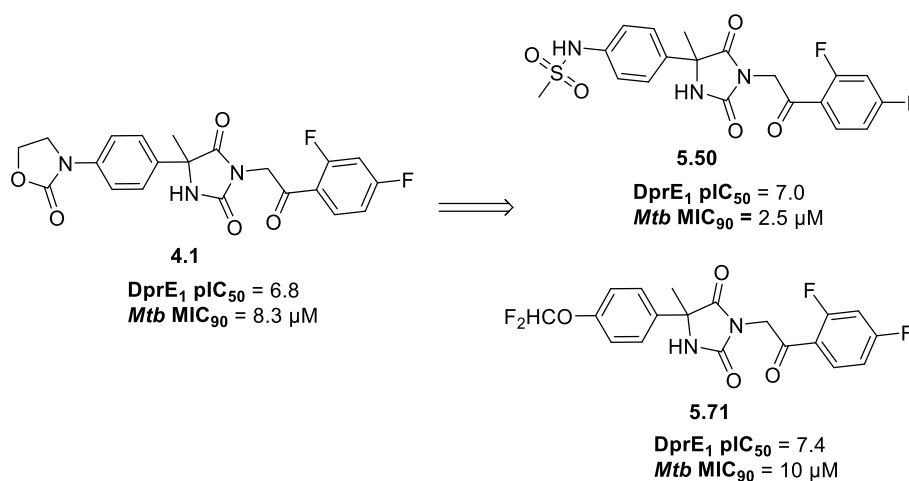
Figure 9.3. Most active compounds chosen as new starting points for the second round of H2L optimization

9.3.2 Second round of Hit-to-Lead optimization

Around 75 analogues, based on the compound **5.50** (4-NHSO$_2$Me, "sulfonamide"), were synthesized and evaluated in the course of the second round of H2L optimization. The most promising representatives are summarized in Figure 9.4.

DprE$_1$ pIC$_{50}$ = 7.0
***Mtb* MIC$_{90}$ = 2.5 µM** (5.50)

DprE$_1$ pIC$_{50}$ = 7.3
***Mtb* MIC$_{90}$ = 0.6 µM** (6.9)

R =
6.30 3-CF$_3$
6.33 3-OCF$_3$
6.34 3-CF$_3$, 4-F

DprE$_1$ pIC$_{50}$ = 7.1-7.2
***Mtb* MIC$_{90}$ = 0.6-0.9 µM**

6.40

DprE$_1$ pIC$_{50}$ = 6.7
***Mtb* MIC$_{90}$ = 7.5 µM**

R =
6.95 H
6.96 5-F
6.97 6-CF$_3$

DprE$_1$ pIC$_{50}$ = 6.6-7.0
***Mtb* MIC$_{90}$ = 0.3-2.5 µM**
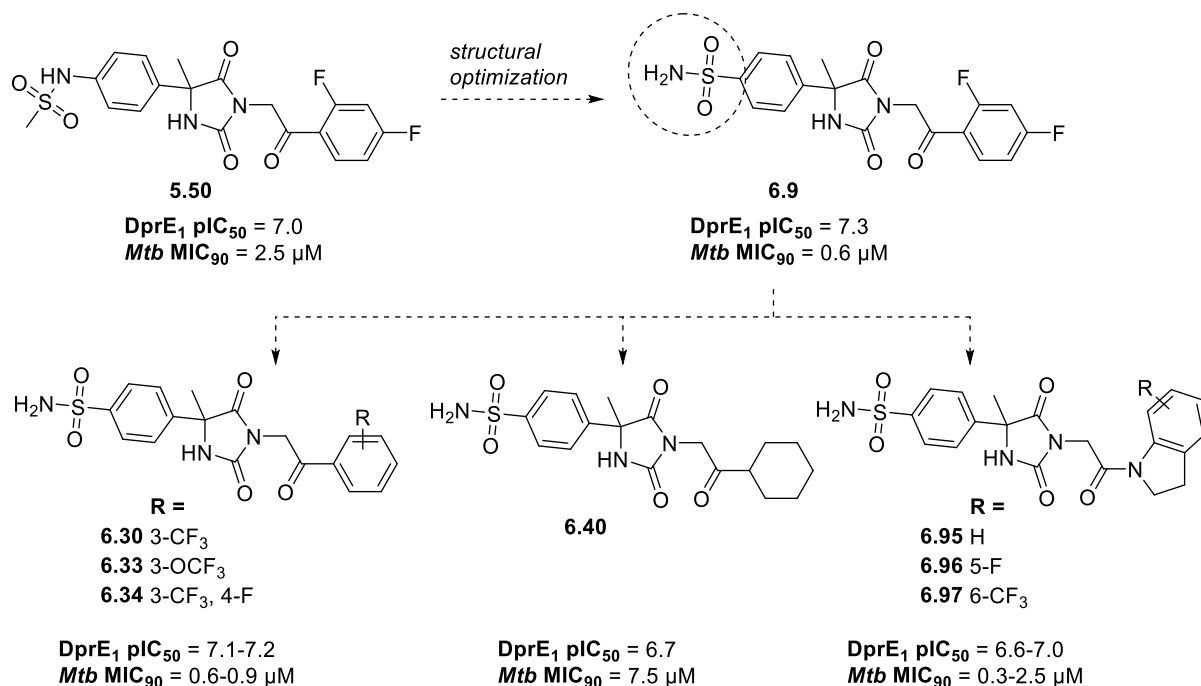
Figure 9.4. Second round of H2L optimization: most outstanding representatives

First, sulfonamide moiety modifications were explored. The most active sulfonamide-based compound obtained turned out to be the "retro-sulfonamide" **6.9** (4-SO$_2$NH$_2$) that possessed very high enzymatic inhibitory activity (pIC$_{50}$ = 7.3) together with sub-micromolar whole-cell potency (MIC = 0.6 µM). Consequently, compound **6.9** was chosen as the new reference compound, and the 4-SO$_2$NH$_2$ substituent in the ring A was kept constant during the extensive SAR investigation on the ring B and additional linker modifications.

Among the compounds with a differently substituted ring B, the most potent representatives were the 3-substituted analogues (**6.30** 3-CF$_3$, **6.33** 3-OCF$_3$, and **6.34** 3-CF$_3$, 4-F), that retained sub-micromolar whole-cell potency. All other substitutions explored, led to an enzymatic and whole-cell activity drop. Introduction of a saturated cyclohexyl ring as the ring B in **6.40** led to a slight improvement in potency over its phenyl-substituted analogue **6.14**, indicating a possibility that substituted cyclohexyl analogues may provide even higher potency.

A number of substituted benzoxazoles, amides, and an arylsulfone were introduced in place of the acetophenone moiety in **6.9**, delivering several analogues with partially retained enzymatic and whole-cell potency. Therefore, the presence of a keto-group in the linker was shown to be not strictly essential for the activity in the series, in contrast to previous findings. Unfortunately, a few substituted benzoxazole derivatives exhibited some cytotoxicity in the HepG$_2$ assay (IC$_{50}$ < 100 µM), together with a moderate MIC of 5-15 µM, indicating a potential liability of this sub-series. Several compounds containing an indoline moiety as the ring B, demonstrated very promising whole-cell activity (2.5 µM for **6.95-6.96**, 0.3 µM for **6.97**), accompanied by moderate DprE1 enzyme inhibition (pIC$_{50}$ = 6.7-7.0).

The introduction of various substituted indolines, as well as other related amides, could, therefore, be of interest for further potency improvement.

9.3.3   Further biological evaluation of the series

Several potent hydantoin analogues were selected for further extensive biological profiling.

Higher expression of the target enzyme caused resistance to all tested compounds with a more than 5-fold shift in the MIC values relative to the wild type strain, confirming inhibition of DprE1 as the only major mechanism responsible for the antimycobacterial activity of this compound series. The rates of the reaction catalyzed by DprE1 were monitored in the presence of varying amounts of the inhibitor to assess the inhibition mechanism, indicating that **4.1** is not a suicide inhibitor and binds to the enzyme reversibly.

MIC values, determined for four compound analogues against a panel of medically relevant strains of gram-positive and gram-negative bacteria, showed no appreciable inhibition of growth. These results indicate that the investigated series selectively inhibits *M. tuberculosis* and possibly other Mycobacteria.

No intrinsic cytotoxicity (HepG$_2$) was found to be associated with the studied hydantoin family. Although hERG inhibition was detected initially for some analogues, it was proven that it is not an inherent issue of the series, and the most active analogues demonstrated no appreciable inhibition. All the tested compounds possessed satisfactory metabolic stability in the i*n vitro* intrinsic clearance evaluation in mouse and human microsomes.

Several hydantoin-based representatives were potent in an intracellular model of *M. tuberculosis* infection of human macrophages; however, the actual intracellular potency was found to be compound-dependent and not directly correlated with the standard MIC-values.

Hydantoin **6.9** demonstrated statistically significant efficacy in an acute murine model of intratracheal infection, providing *in vivo* proof of concept for the series.

9.3.4   Hydantoins as DprE1 inhibitors: outlook

An extensive SAR exploration around the hydantoin DprE1 inhibitors has been performed within the OpenMedChem project, resulting in several highly active DprE$_1$ inhibitors (pIC$_{50}$ = 7.0-7.3) with sub-micromolar cellular potencies, balanced physicochemical profiles and no cytotoxic effects in the HepG2 assay.

Notwithstanding, further improvement of the whole-cell and enzymatic potency together with *in vivo* efficacy enhancement are desirable for further development of the current series as potent antimycobacterial drugs. There are several different strategies that could be exploited, including further refinement of the SAR and/or docking studies to provide a starting point for the rational structure-based compound design.

_____

_____

10.Samenvatting

10.1 Inleiding

Tuberculose (tbc) blijft wereldwijd een belangrijke bedreiging voor de volksgezondheid: er zijn meer dan 9 miljoen nieuwe gevallen per jaar en 1,5 miljoen sterfgevallen.[6] De opkomst van multi- (MDR) en extensief-medicijnresistente (XDR) *M. tuberculosis*-stammen en hiv-comorbiditeit zorgen voor een heropleving van de tbc-epidemie.

Dit leidt tot een acute behoefte aan nieuwe antituberculaire middelen met, bij voorkeur, nieuwe werkingsmechanismen en het potentieel om geneesmiddelresistente vormen van de ziekte te behandelen. Een aanzienlijke inspanning gaat daarom naar het onderzoek van nieuwe biologische doelwitten en de ontwikkeling van geneesmiddelen die daarmee zouden kunnen interageren. Dit onderzoek werd uitgevoerd binnen het OpenMedChem EID-ITN project (FP7) tussen de Universiteit Antwerpen en GlaxoSmithKline (GSK) met focus op vroege hit-to-lead ontwikkeling van anti-tuberculaire geneesmiddelen. Het werk concentreerde zich meerbepaald op hit-exploratie en hit-to-lead-optimalisatie van twee nieuwe chemische families/clusters die werden geïdentificeerd tijdens twee verschillende *High-Throughput Screening* (HTS-) campagnes, uitgevoerd door GSK.[171,284]

De dihydro-2,4-diamino-1,3,5-triazine-cluster werd geïdentificeerd tijdens een whole-cell fenotypische high-throughput screening (HTS) -campagne tegen *M. bovis BCG* met hitbevestiging in de *M. tuberculosis H37Rv*-stam.[171] 2 Deze chemische familie werd geselecteerd voor verder onderzoek. De bekomen resultaten worden samengevat in sectie 10.2 van dit hoofdstuk.

Het flavo-enzym deca-prenylfosforyl-beta-D-ribose 2-epimerase (DprE1) is essentieel voor biosynthese van de mycobacteriële celwand en werd al gevalideerd als een veelbelovend doelwit in *M.tuberculosis*.[247,249] Een *target-based HTS* campagne van GSK met de bedoeling om nieuwe DprE1-remmers te identificeren, leidde tot de ontdekking van een veelbelovende familie hydantoïnes. Onderzoeksresultaten behaald met deze klasse van verbinding worden beschreven in sectie 10.3.

10.2 DHFR inhibitors: Structurele exploratie en 'scaffold hopping'

Uit de hits van een *whole-cell phenotypical HTS*-campagne werd een groep moleculen geselecteerd met een 2,4-diamino-1,3-diaza-farmacofoor. Deze is gekend als een cruciaal structureel onderdeel van dihydrofolaat (DHFR)-remmers. Ook voor deze set verbindingen kon later worden aangetoond dat zij mycobaterieel DHFR remden. Bij de structurele exploratie van deze moleculen waren de modificaties gericht op de bereiding van (1) analogen met eenzelfde basisarchitectuur als de initiële hits; en (2) van analogen met een gewijzigde centrale 'scaffold' (weergegeven in respectievelijk Figuur 1, A en B).
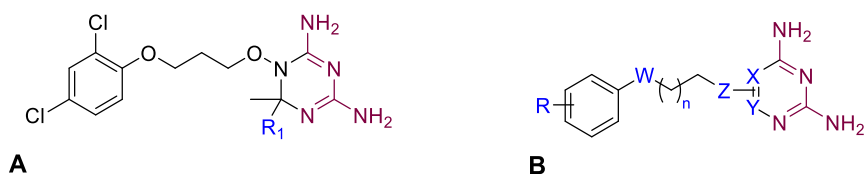
Generische structuur van (A) analogen van de initiële hits en (B) 'Scaffold hopping' analogen. In deze structuren werd de cruciale 2,4-diamino-1,3-diaza farmacofoor aangeduid in magenta en de structurele modificaties die werden doorgevoerd in blauw.

Figuur 10.1 Modificaties uitgevoerd op HTS-hits.

De synthese van directe analogen van de initiële hits bleek zeer uitdagend: de beperkte reproduceerbaarheid van de syntheses en problemen met structuuropheldering droegen bij tot de beslissing om de aandacht te verleggen naar synthetisch meer toegankelijke klassen van verbindingen. Tijdens de biologische evaluatie vertoonden alle dihydrotriazine-gebaseerde moleculen micromolaire anti-mycobacteriële potentie samen met uitzonderlijk hoge menselijke cytotoxiciteit in de HepG2-test (IC$_{50}$<0,01 µM), waarschijnlijk gerelateerd aan een gebrekkige selectiviteit tussen mycobacterieel en menselijk DHFR. Bovendien duidden de beperkte oplosbaarheid en membraanpermeabiliteit van die verbindingen op een hoger risico op slechte biologische beschikbaarheid.

Omdat deze fysico-chemische en cytotoxiciteitsproblemen intrinsiek gerelateerd kunnen zijn aan de biofarmaceutische eigenschappen van de dihydrotriazinering zelf, werd vervolgens een 'scaffold hopping'-benadering onderzocht (figuur 10.1 B). De 2,4-diamino-1,3-diaza-farmacofoor, cruciaal voor DHFR-remming, werd geconserveerd in alle nieuwe analogen, bij voorkeur als onderdeel van een aromatisch systeem omdat deze een betere doorlaatbaarheid kan hebben, vergeleken met niet-aromatische dihydrotriazinen. In totaal werden 21 structureel diverse pyrimidine- en triazinederivaten gesynthetiseerd en geëvalueerd met variaties in 1) het linker-gedeelte en 2) het aryl-substitutiepatroon. Helaas bleken alle verbindingen die werden bereid door de scaffold-hopping-benadering volledig inactief te zijn in enzymatische en *whole-cell*-assays, wat het bijzondere belang lijkt te onderstrepen van de onverzadigde 1,6-dihydro-1,3,5-triazine- 2,4-diamine kern voor krachtige MtbDHFR remming. Verscheidene structureel gerelateerde diaminotriazines met een lage micromolaire *whole-cell*-activiteit tegen Mtb H37Rv werden onlangs gerapporteerd door Tawari et al. Deze resultaten zouden een interessant startpunt kunnen vormen voor verder onderzoek naar MtbDHFR-remmers met een aromatische heterocyclische kern.

10.3 Hydantoins as DprE1 inhibitors: Identification and SAR exploration

De initiële hydantoïne-hit 4.1 vertoonde een krachtige DprE1-remming en bezat een veelbelovend hitprofiel, zonder detecteerbare cytotoxiciteit in de HepG2-assay. Bovendien bleken deze eigenschappen gekoppeld aan een aanvaardbare oplosbaarheid en lipofiliciteit (Figuur 10.2). Er werd besloten om deze verbinding als basis te nemen voor een reeks nieuwe analogen. Volgende projectdoelstellingen werden gedefinieerd:

- Bereiding van nieuwe, hydantoïne-afgeleide DprE1 remmers met verhoogde potentie in enzymatische en *whole-cell* assays én met een uitgebalanceerd fysicochemisch profiel.
- Verwijdering of vervanging van onwenselijke functionele groepen en structuurelementen.
- Bekomen van *in vivo proof-of-concept* voor deze serie remmers.

Om deze objectieven te bereiken, werd het *hit-to-lead* optimalisatieproces onderverdeeld in twee cycli.

10.3.1 Eerste cyclus van hit-to-lead optimalisatie

In de eerste cyclus werd gefocust op twee potentieel compromitterende structuurelementen van de initiële hit **4.1** (het acetofenon fragment en de carbonitrile groep). Daarnaast werd een bredere screening van de chemische ruimte rond deze hit uitgevoerd om primaire SAR-data te bekomen. Meerbepaald werden modificaties uitgevoerd ter hoogte van de linker, werd de zijketen gevarieerd en

werd ring A gemodificeerd. In totaal werden 100 verbindingen met deze modificaties gesynthetiseerd onder OpenMedChem, waarvan ongeveer 30 moleculen beschreven werden in deze thesis. Figuur **10.2** vat de in deze cyclus bekomen SAR-conclusies, samen.
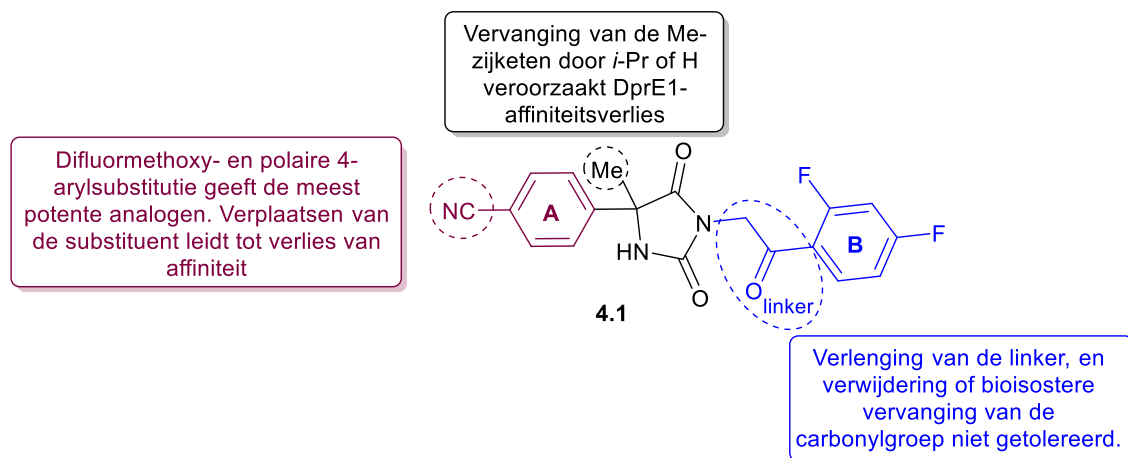
Figuur 10.2 Eerste cyclus H2L optimalisatie: SAR conclusies.

De initiële bezorgdheid over metabole instabiliteit (gerelateerd aan de aanwezigheid van de acetofenon groep), bleek op het eerste gezicht niet gegrond na microsomale stabiliteitsstudies. Aangezien alle geëvalueerde linkermodificaties resulteerden in een complete verlies van activiteit, werd de originele keton-bevattende linker behouden in alle bijkomende analogen met ring A of B modificaties. Ook de vervanging van de methyl-zijketen door een isopropylgroep of een waterstofatoom resulteerde in DprE1-affiniteitsverlies. In de reeks van A-ring gevarieerde verbindingen, werden een aantal vertegenwoordigers geïdentificeerd met verbeterde fenotypische en target-gebaseerde potentie. Over het algemeen bleek de introductie van polaire, hydrofiele substituenten in plaats van de carbonitril groep, de beste resultaten in de target-gebaseerde en de fenotypische assays te geven. Een sulfonamide (4-NHSO$_2$Me) substituent bleek een drievoudige verhoging van de activiteit te geven in de cellulaire evaluatie vergeleken met hit **4.1**. Verbinding **5.71** bleek de beste DprE1-remmer te zijn (pIC$_{50}$=7.4), maar slechts matige cellulaire potentie te hebben (MIC$_{90}$= 10 μM). (Figuur **10.3**) Verbindingen **4.1**, **5.50** en **5.71** werden gekozen als startpunt voor de tweede cyclus *Hit-to-Lead* optimalisatie.
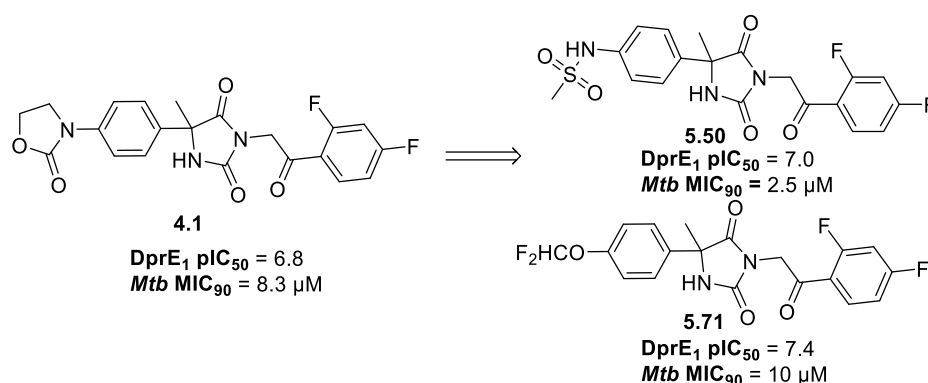
Figuur 10.3 Actieve stoffen die werden geselecteerd voor de tweede cyclus H2L optimalisatie.

_____

10.3.2 Tweede cyclus van hit-to-lead optimalisatie.

Ongeveer 75 analogen van **5.50** (4-NHSO$_2$Me, 'sulfonamide'), werden gesynthetiseerd en geëvalueerd tijdens de tweede cyclus van. De meest veelbelovende vertegenwoordigers worden voorgesteld in **Figuur 9.4**.
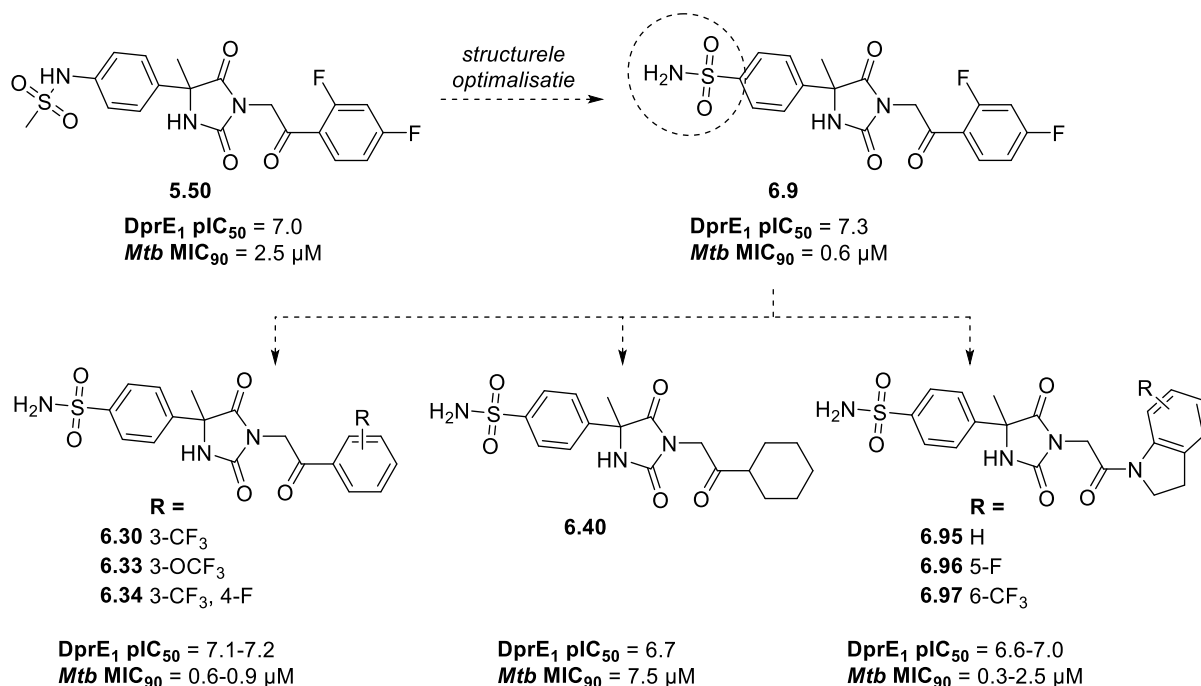
Figuur 9.4 Tweede cyclus H2L optimalisatie: geselecteerde voorbeelden.

Eerst werden modificaties van de sulfonamidegroep bestudeerd. De meest actieve vertegenwoordiger bleek het 'retro-sulfonamide' **6.9** (4-SO$_2$NH$_2$) te zijn. Deze molecule combineerde zeer uitgesproken affiniteit voor DprE1 (pIC$_{50}$=7.3) met sub-micromolaire cellulaire activiteit (MIC$_{90}$=0.6 µM). Daarom werd **6.9** gekozen als nieuwe referentie en de 4-SO$_2$NH$_2$ substituent in de A-ring werd geconserveerd gedurende de daaropvolgende SAR-exploratie van de B-ring en de linker.

Bij de verbindingen met een anders gesubstitueerde B-ring, waren de 3-gesubstitueerde analogen (**6.30**/3-CF$_3$, **6.33**/3-OCF$_3$ en **6.34**/3-CF$_3$, 4-F) het meest krachtig. Alle andere substituties die werden geëxploreerd, leidden tot een daling van de score in de enzymatische en fenotypische assays. Invoeren van een verzadigde cyclohexylring als B-ring in **6.40**, leidde tot een beperkte verbetering in potentie, vergeleken met het overeenkomstige fenyl-gesubstitueerde product **6.14**. Een aantal gesubstitueerde benzoxazoles, amides en arylsulfones erden geïntroduceerd in de plaats van het acetofenon fragment in **6.9**, wat analogen opleverde die partieel activiteit in de enzymatische en cellulaire assays behielden. In tegenstelling tot de eerdere resultaten, bleek de ketogroep in deze subreeks dus niet essentieel te zijn om activiteit te zien. Helaas bleken een paar gedecoreerde benzoxazoles ook cytotoxisch te zijn in de HepG$_2$ assay (IC$_{50}$< 100 µM). Verschillende indoline-bevattende structuren (**6.95-6.97**) bleken een zeer veelbelovende cellulaire activiteit te combineren met een eerder matige potentie in de enzymatische test. Verdere optimalisatie van deze reeks, gericht op verdere verhoging van de target-affiniteit, kan nochtans een veelbelovende strategie zijn voor de toekomstige, verdere explorering van deze reeks.

_____

10.3.3 Verdere biologisch onderzoek op de hydantoïne reeks.

Verschillende krachtige hydantoïne analogen werden geselecteerd voor een uitgebreide biologische profilering.

Overexpressie van DprE1 in Mycobacterium tuberculosis bleek voor resistentie te zorgen: de MIC-waarde bleek met een factor 5 te verhogen, vergeleken met de wild-type stam. Deze resultaten waren indicatief voor het feit dat DprE1 inderdaad het (belangrijkste) biologisch doelwit van deze moleculen is. Daarnaast werden de inhibitiekinetiek van **4.1** onderzocht op DprE1 en werd aangetoond dat de hydantoïnes geen covalente remmers zijn van het enzym. MIC-bepalingen voor 3 verbindingen uit de reeks tegen een panel van medisch relevante stammen gram positieve en gram negatieve bacterieën, toonden geen betekenisvolle remming van de groei. Deze resultaten wijzen op een selectieve activiteit tegen mycobacterieën, en meer bepaald tegen *M. tuberculosis*. Er bleek geen intrinsieke cytotoxiciteit (HepG$_2$) geassocieerd te zijn met de hydantoïne familie. Hoewel hERG inhibitie initieel gedetecteerd werd voor sommige analogen, kon aangetoond worden dat dit geen inherent probleem van de serie is: uiteindelijk bleken de meest actieve analogen geen inhibitie te geven van dit eiwit. Alle geëvalueerde verbindingen bezaten bevredigende metabole stabiliteit in de *in vitro* intrinsieke clearance test in muis en humane microsomen.

Verschillende vertegenwoordigers van de hydantoïne reeks hadden een krachtige activiteit in een intracellulair model van *M. tuberculosis* infectie van humane macrofagen. Niettemin werd ook gezien dat de intracellulaire activiteit verschilde van verbinding tot verbinding en niet altijd gecorreleerd was met de MIC$_{90}$ onder standaard omstandigheden.

Hydantoïne **6.9** toonde statistisch significante efficaciteit in een acuut muismodel van intratracheale infectie, waarmee *in vivo* proof-of-concept werd geleverd voor de reeks.

10.3.4 Hydantoins als DprE1 inhibitors: samenvatting en perspectieven

Er werd een uitgebreide SAR karakterisering uitgevoerd voor hydantoïne-afgeleide DprE1 remmers. Dit resulteerde in een aantal zeer actieve DprE1 remmers (pIC$_{50}$ = 7.0-7.3) met sub-micromolaire cellulaire activiteit, een gebalanceerd fysicochemisch profiel en geen cytotoxiciteit in de HepG2 assay.

Hoewel dit profiel zeer veelbelovend is, lijkt een verdere optimalisatie van zowel de cellulaire activiteit als de target-affiniteit wenselijk voor de reeks om verdere ontwikkeling tot antimycobacterieel geneesmiddel toe te laten. Verschillende strategieën kunnen hiervoor gebruikt worden, waaronder een verdere verfijning van de SAR, ondersteund door computationele studies voor rationele optimalisatie van het design van deze moleculen.

_____

Acknowledgments

_____

References

(1)   Hershkovitz, I.; Donoghue, H. D.; Minnikin, D. E.; Besra, G. S.; Lee, O. Y.-C.; Gernaey, A. M.; Galili, E.; Eshed, V.; Greenblatt, C. L.; Lemma, E.; Bar-Gal, G. K.; Spigelman, M. Detection and Molecular Characterization of 9000-Year-Old Mycobacterium Tuberculosis from a Neolithic Settlement in the Eastern Mediterranean. *PLoS One* **2008**, *3* (10), 6.

(2)   *Tuberculosis*; Madkour, M. M., Ed.; Springer Berlin Heidelberg: Berlin, Heidelberg, 2004. https://doi.org/10.1007/978-3-642-18937-1.

(3)   Murray, J. F. A Century of Tuberculosis. *Am. J. Respir. Crit. Care Med.* **2004**, *169* (11), 1181–1186. https://doi.org/10.1164/rccm.200402-140oe.

(4)   Wallstedt, H.; Maeurer, M. The History of Tuberculosis Management in Sweden. *Int. J. Infect. Dis.* **2015**, *32*, 179–182. https://doi.org/10.1016/j.ijid.2015.01.018.

(5)   Barberis, I.; Bragazzi, N. L.; Galluzzo, L.; Martini, M. The History of Tuberculosis: From the First Historical Records to the Isolation of Koch's Bacillus. *J. Prev. Med. Hyg.* **2017**, *58* (1), E9–E12. https://doi.org/10.15167/2421-4248/jpmh2017.58.1.728.

(6)   World Health Organization. *Global Tuberculosis Report 2018*, 20th ed.; 2018.

(7)   Maher, D.; Raviglione, M. Global Epidemiology of Tuberculosis. *Clin. Chest Med.* **2005**, *26* (2), 167–182. https://doi.org/10.1016/j.ccm.2005.02.009.

(8)   World Health Organization. *Global Tuberculosis Report 2019*; 2019.

(9)   World Health Organization (WHO). Target Regimen Profiles for TB Treatment. *Geneva Contract No. WHO/HTM/TB/2016.16* **2016**.

(10)   Tuberculosis surveillance and monitoring in Europe 2020 –2018 data https://www.ecdc.europa.eu/en/publications-data/tuberculosis-surveillance-and-monitoring-europe-2020-2018-data#:~:text=Epidemiology and treatment outcome,population in the EU%2FEEA (accessed Jul 5, 2021).

(11)   Tuberculosis - For a Healthy Belgium https://www.healthybelgium.be/en/health-status/communicable-diseases/tuberculosis (accessed Jul 5, 2021).

(12)   Gillespie, S. H. Evolution of Drug Resistance in Mycobacterium Tuberculosis: Clinical and Molecular Perspective. *Antimicrob. Agents Chemother.* **2002**, *46* (2), 267–274. https://doi.org/10.1128/AAC.46.2.267-274.2002.

(13)   Akbar Velayati, A.; Farnia, P.; Reza Masjedi, M. The Totally Drug Resistant Tuberculosis (TDR-TB). *Int. J. Clin. Exp. Med.* **2013**, *6* (4), 307–309.

(14)   Udwadia, Z. F.; Amale, R. A.; Ajbani, K. K.; Rodrigues, C. Totally Drug-Resistant Tuberculosis in India. *Clin. Infect. Dis.* **2012**, *54* (4), 579–581. https://doi.org/10.1093/cid/cir889.

(15)   World Health Organisation. End TB Strategy. *World Heal. Origanisation* **2013**, *53* (9), 1689–1699. https://doi.org/10.1017/CBO9781107415324.004.

(16)   Schlegel, H. G.; Zaborosch, C. *General Microbiology*; Cambridge University Press, 1993.

(17)   Brosch, R.; Gordon, S. V.; Marmiesse, M.; Brodin, P.; Buchrieser, C.; Eiglmeier, K.; Garnier, T.; Gutierrez, C.; Hewinson, G.; Kremer, K.; Parsons, L. M.; Pym, A. S.; Samper, S.; Van Soolingen, D.; Cole, S. T. A New Evolutionary Scenario for the Mycobacterium Tuberculosis Complex. *Proc. Natl. Acad. Sci. U. S. A.* **2002**, *99* (6), 3684–3689. https://doi.org/10.1073/pnas.052548299.

(18)   Pai, M.; Behr, M. A.; Dowdy, D.; Dheda, K.; Divangahi, M.; Boehme, C. C.; Ginsberg, A.; Swaminathan, S.; Spigelman, M.; Getahun, H.; Menzies, D.; Raviglione, M. Tuberculosis. *Nat.*

_____

Rev. Dis. Prim. **2016**, *2* (1), 16076. https://doi.org/10.1038/nrdp.2016.76.

(19) Pieters, J. Mycobacterium Tuberculosis and the Macrophage: Maintaining a Balance. *Cell Host and Microbe*. Cell Press June 2008, pp 399–407. https://doi.org/10.1016/j.chom.2008.05.006.

(20) Birkeland, H. C. G.; Stenmark, H. Protein Targeting to Endosomes and Phagosomes via FYVE and PX Domains. *Current Topics in Microbiology and Immunology*. Springer, Berlin, Heidelberg 2003, pp 89–115. https://doi.org/10.1007/978-3-642-18805-3_4.

(21) Marakalala, M. J.; Raju, R. M.; Sharma, K.; Zhang, Y. J.; Eugenin, E. A.; Prideaux, B.; Daudelin, I. B.; Chen, P.-Y.; Booty, M. G.; Kim, J. H.; Eum, S. Y.; Via, L. E.; Behar, S. M.; Barry, C. E.; Mann, M.; Dartois, V.; Rubin, E. J. Inflammatory Signaling in Human Tuberculosis Granulomas Is Spatially Organized. *Nat. Med.* **2016**, *22* (5), 531–538. https://doi.org/10.1038/nm.4073.

(22) Grosset, J. Mycobacterium Tuberculosis in the Extracellular Compartment: An Underestimated Adversary. *Antimicrob. Agents Chemother.* **2003**, *47* (3), 833–836. https://doi.org/10.1128/AAC.47.3.833-836.2003.

(23) Yang, D.; Kong, Y. The Bacterial and Host Factors Associated with Extrapulmonary Dissemination of Mycobacterium Tuberculosis. *Front. Biol. (Beijing).* **2015**, *10* (3), 252–261. https://doi.org/10.1007/s11515-015-1358-y.

(24) Johansen, M. D.; Herrmann, J. L.; Kremer, L. Non-Tuberculous Mycobacteria and the Rise of Mycobacterium Abscessus. *Nat. Rev. Microbiol.* **2020**. https://doi.org/10.1038/s41579-020-0331-1.

(25) Falkinham, J. O. Environmental Sources of Nontuberculous Mycobacteria. *Clin. Chest Med.* **2015**, *36* (1), 35–41. https://doi.org/10.1016/j.ccm.2014.10.003.

(26) Falkinham, J. O. Nontuberculous Mycobacteria from Household Plumbing of Patients with Nontuberculous Mycobacteria Disease. *Emerg. Infect. Dis.* **2011**, *17* (3), 419–424. https://doi.org/10.3201/eid1703.101510.

(27) Prevots, D. R.; Marras, T. K. Epidemiology of Human Pulmonary Infection with Nontuberculous Mycobacteria a Review. *Clin. Chest Med.* **2015**, *36* (1), 13–34. https://doi.org/10.1016/j.ccm.2014.10.002.

(28) Ringshausen, F. C.; Wagner, D.; de Roux, A.; Diel, R.; Hohmann, D.; Hickstein, L.; Welte, T.; Rademacher, J. Prevalence of Nontuberculous Mycobacterial Pulmonary Disease, Germany, 2009-2014. *Emerg. Infect. Dis.* **2016**, *22* (6), 1102–1105. https://doi.org/10.3201/eid2206.151642.

(29) Namkoong, H.; Kurashima, A.; Morimoto, K.; Hoshino, Y.; Hasegawa, N.; Ato, M.; Mitarai, S. Epidemiology of Pulmonary Nontuberculous Mycobacterial Disease, Japan. *Emerging Infectious Diseases*. Centers for Disease Control and Prevention (CDC) June 2016, pp 1116–1117. https://doi.org/10.3201/eid2206.151086.

(30) Adjemian, J.; Olivier, K. N.; Seitz, A. E.; Holland, S. M.; Prevots, D. R. Prevalence of Nontuberculous Mycobacterial Lung Disease in U.S. Medicare Beneficiaries. *Am. J. Respir. Crit. Care Med.* **2012**, *185* (8), 881–886. https://doi.org/10.1164/rccm.201111-2016OC.

(31) Swenson, C.; Zerbe, C. S.; Fennelly, K. Host Variability in NTM Disease: Implications for Research Needs. *Front. Microbiol.* **2018**, *9* (December). https://doi.org/10.3389/fmicb.2018.02901.

(32) Bryant, J. M.; Grogono, D. M.; Rodriguez-Rincon, D.; Everall, I.; Brown, K. P.; Moreno, P.; Verma, D.; Hill, E.; Drijkoningen, J.; Gilligan, P.; Esther, C. R.; Noone, P. G.; Giddings, O.; Bell, S. C.; Thomson, R.; Wainwright, C. E.; Coulter, C.; Pandey, S.; Wood, M. E.; Stockwell, R. E.; Ramsay, K. A.; Sherrard, L. J.; Kidd, T. J.; Jabbour, N.; Johnson, G. R.; Knibbs, L. D.; Morawska, L.; Sly, P. D.; Jones, A.; Bilton, D.; Laurenson, I.; Ruddy, M.; Bourke, S.; Bowler, I. C. J. W.; Chapman, S. J.;

Clayton, A.; Cullen, M.; Dempsey, O.; Denton, M.; Desai, M.; Drew, R. J.; Edenborough, F.; Evans, J.; Folb, J.; Daniels, T.; Humphrey, H.; Isalska, B.; Jensen-Fangel, S.; Jönsson, B.; Jones, A. M.; Katzenstein, T. L.; Lillebaek, T.; MacGregor, G.; Mayell, S.; Millar, M.; Modha, D.; Nash, E. F.; O'Brien, C.; O'Brien, D.; Ohri, C.; Pao, C. S.; Peckham, D.; Perrin, F.; Perry, A.; Pressler, T.; Prtak, L.; Qvist, T.; Robb, A.; Rodgers, H.; Schaffer, K.; Shafi, N.; van Ingen, J.; Walshaw, M.; Watson, D.; West, N.; Whitehouse, J.; Haworth, C. S.; Harris, S. R.; Ordway, D.; Parkhill, J.; Floto, R. A. Emergence and Spread of a Human-Transmissible Multidrug-Resistant Nontuberculous Mycobacterium. *Science (80-.).* **2016**, *354* (6313), 751–757. https://doi.org/10.1126/science.aaf8156.

(33)   Wu, M. L.; Aziz, D. B.; Dartois, V.; Dick, T. NTM Drug Discovery: Status, Gaps and the Way Forward. *Drug Discov. Today* **2018**, *23* (8), 1502–1519. https://doi.org/10.1016/j.drudis.2018.04.001.

(34)   Vacchelli, E.; Galluzzi, L.; Eggermont, A.; Fridman, W. H.; Galon, J.; Sautès-Fridman, C.; Tartour, E.; Zitvogel, L.; Kroemer, G. Trial Watch: FDA-Approved Toll-like Receptor Agonists for Cancer Therapy. *Oncoimmunology* **2012**, *1* (6), 894–907. https://doi.org/10.4161/onci.20931.

(35)   Luca, S.; Mihaescu, T. History of BCG Vaccine. *Maedica (Buchar).* **2013**, *8* (1), 53–58.

(36)   Andersen, P.; Doherty, T. M. The Success and Failure of BCG — Implications for a Novel Tuberculosis Vaccine. *Nat. Rev. Microbiol.* **2005**, *3* (8), 656–662. https://doi.org/10.1038/nrmicro1211.

(37)   Abubakar, I.; Pimpin, L.; Ariti, C.; Beynon, R.; Mangtani, P.; Sterne, J.; Fine, P.; Smith, P.; Lipman, M.; Elliman, D.; Watson, J.; Drumright, L.; Whiting, P.; Vynnycky, E. Systematic Review and Meta-Analysis of the Current Evidence on the Duration of Protection by Bacillus Calmette-Guérin Vaccination against Tuberculosis. *Health Technol. Assess. (Rockv).* **2013**, *17* (37), 1–4. https://doi.org/10.3310/hta17370.

(38)   Nguipdop-Djomo, P.; Heldal, E.; Rodrigues, L. C.; Abubakar, I.; Mangtani, P. Duration of BCG Protection against Tuberculosis and Change in Effectiveness with Time since Vaccination in Norway: A Retrospective Population-Based Cohort Study. *Lancet Infect. Dis.* **2016**, *16* (2), 219–226. https://doi.org/10.1016/S1473-3099(15)00400-4.

(39)   Zodpey, S. P.; Shrikhande, S. N. The Geographic Location (Latitude) of Studies Evaluating Protective Effect of BCG Vaccine and It's Efficacy/Effectiveness against Tuberculosis. *Indian J. Public Health* **2007**, *51* (4), 205–210.

(40)   Brandt, L.; Cunha, J. F.; Olsen, A. W.; Chilima, B.; Hirsch, P.; Appelberg, R.; Andersen, P. Failure of the Mycobacterium Bovis BCG Vaccine: Some Species of Environmental Mycobacteria Block Multiplication of BCG and Induction of Protective Immunity to Tuberculosis. *Infect. Immun.* **2002**, *70* (2), 672–678. https://doi.org/10.1128/IAI.70.2.672-678.2002.

(41)   Ritz, N.; Hanekom, W. A.; Robins-Browne, R.; Britton, W. J.; Curtis, N. Influence of BCG Vaccine Strain on the Immune Response and Protection against Tuberculosis. *FEMS Microbiology Reviews*. August 2008, pp 821–841. https://doi.org/10.1111/j.1574-6976.2008.00118.x.

(42)   Trunz, B. B.; Fine, P.; Dye, C. Effect of BCG Vaccination on Childhood Tuberculous Meningitis and Miliary Tuberculosis Worldwide: A Meta-Analysis and Assessment of Cost-Effectiveness. *Lancet* **2006**, *367* (9517), 1173–1180. https://doi.org/10.1016/S0140-6736(06)68507-3.

(43)   World Health Organization. Revised BCG Vaccination Guidelines for Children with HIV Infection. *Wkly. Epidemiol. Rec.* **2007**, *82* (21), 193–196.

(44)   Martin, C.; Aguilo, N.; Marinova, D.; Gonzalo-Asensio, J. Update on TB Vaccine Pipeline. *Appl. Sci.* **2020**, *10* (7), 2632. https://doi.org/10.3390/app10072632.

(45)   Parida, S. K.; Kaufmann, S. H. E. The Quest for Biomarkers in Tuberculosis. *Drug Discov. Today*

2010, *15* (3–4), 148–157. https://doi.org/10.1016/j.drudis.2009.10.005.

(46) Bucsan, A. N.; Mehra, S.; Khader, S. A.; Kaushal, D. The Current State of Animal Models and Genomic Approaches towards Identifying and Validating Molecular Determinants of Mycobacterium Tuberculosis Infection and Tuberculosis Disease. *Pathog. Dis.* **2019**, *77* (4), 1–17. https://doi.org/10.1093/femspd/ftz037.

(47) Scriba, T. J.; Tameris, M.; Mansoor, N.; Smit, E.; van der Merwe, L.; Isaacs, F.; Keyser, A.; Moyo, S.; Brittain, N.; Lawrie, A.; Gelderbloem, S.; Veldsman, A.; Hatherill, M.; Hawkridge, A.; Hill, A. V. S.; Hussey, G. D.; Mahomed, H.; McShane, H.; Hanekom, W. A. Modified Vaccinia Ankara-Expressing Ag85A, a Novel Tuberculosis Vaccine, Is Safe in Adolescents and Children, and Induces Polyfunctional CD4+ T Cells. *Eur. J. Immunol.* **2011**, *41* (5), 1501–1501. https://doi.org/10.1002/eji.201190030.

(48) Tameris, M. D.; Hatherill, M.; Landry, B. S.; Scriba, T. J.; Snowden, M. A.; Lockhart, S.; Shea, J. E.; McClain, J. B.; Hussey, G. D.; Hanekom, W. A.; Mahomed, H.; McShane, H. Safety and Efficacy of MVA85A, a New Tuberculosis Vaccine, in Infants Previously Vaccinated with BCG: A Randomised, Placebo-Controlled Phase 2b Trial. *Lancet* **2013**, *381* (9871), 1021–1028. https://doi.org/10.1016/S0140-6736(13)60177-4.

(49) Van Der Meeren, O.; Hatherill, M.; Nduba, V.; Wilkinson, R. J.; Muyoyeta, M.; Van Brakel, E.; Ayles, H. M.; Henostroza, G.; Thienemann, F.; Scriba, T. J.; Diacon, A.; Blatner, G. L.; Demoitie, M. A.; Tameris, M.; Malahleha, M.; Innes, J. C.; Hellstrom, E.; Martinson, N.; Singh, T.; Akite, E. J.; Khatoon Azam, A.; Bollaerts, A.; Ginsberg, A. M.; Evans, T. G.; Gillard, P.; Tait, D. R. Phase 2b Controlled Trial of M72/AS01E Vaccine to Prevent Tuberculosis. *N. Engl. J. Med.* **2018**, *379* (17), 1621–1634. https://doi.org/10.1056/NEJMoa1803484.

(50) The Bill & Melinda Gates Medical Research Institute obtains license for continued development of M72/AS01E tuberculosis vaccine candidate from GSK - Bill & Melinda Gates Foundation.

(51) World Health Organization (WHO). *Operational Handbook on Tuberculosis*; 2020.

(52) Hinshaw, C.; Feldman, W. H.; Pfuetze, K. H. Treatment of Tuberculosis with Streptomycin: A Summary of Observations on One Hundred Cases. *J. Am. Med. Assoc.* **1946**, *132* (13), 778–782. https://doi.org/10.1001/jama.1946.02870480024007.

(53) Treatment of Pulmonary Tuberculosis with Streptomycin and Para-Aminosalicylic Acid; a Medical Research Council Investigation. *Br. Med. J.* **1950**, *2* (4688), 1073–1085.

(54) Daniel, T. M. Rifampin — A Major New Chemotherapeutic Agent for the Treatment of Tuberculosis. *N. Engl. J. Med.* **1969**, *280* (11), 615–616. https://doi.org/10.1056/NEJM196903132801112.

(55) Vall-Spinosa, A.; Lester, W.; Moulding, T.; Davidson, P. T.; McClatchy, J. K. Rifampin in the Treatment of Drug-Resistant Mycobacterium Tuberculosis Infections. *N. Engl. J. Med.* **1970**, *283* (12), 616–621. https://doi.org/10.1056/NEJM197009172831202.

(56) Keshavjee, S.; Farmer, P. E. Tuberculosis, Drug Resistance, and the History of Modern Medicine. *N. Engl. J. Med.* **2012**, *367* (10), 931–936. https://doi.org/10.1056/NEJMra1205429.

(57) Chakraborty, S.; Rhee, K. Y. Tuberculosis Drug Development: History and Evolution of the Mechanism-Based Paradigm. *Cold Spring Harb. Perspect. Med.* **2015**, *5* (8), 1–11. https://doi.org/10.1101/cshperspect.a021147.

(58) Zumla, A.; Nahid, P.; Cole, S. T. Advances in the Development of New Tuberculosis Drugs and Treatment Regimens. *Nat. Rev. Drug Discov.* **2013**, *12* (5), 388–404. https://doi.org/10.1038/nrd4001.

(59) Fox, W.; Ellard, G. A.; Mitchison, D. A. Studies on the Treatment of Tuberculosis Undertaken by

the British Medical Research Council Tuberculosis Units, 1946-1986, with Relevant Subsequent Publications. *International Journal of Tuberculosis and Lung Disease*. October 1999.

(60)   Ma, Z.; Lienhardt, C.; McIlleron, H.; Nunn, A. J.; Wang, X. Global Tuberculosis Drug Development Pipeline: The Need and the Reality. *Lancet* **2010**, *375* (9731), 2100–2109. https://doi.org/10.1016/S0140-6736(10)60359-9.

(61)   Bahuguna, A.; Rawat, D. S. An Overview of New Antitubercular Drugs, Drug Candidates, and Their Targets. *Med. Res. Rev.* **2020**, *40* (1), 263–292. https://doi.org/10.1002/med.21602.

(62)   Zha, B. S.; Nahid, P. Treatment of Drug-Susceptible Tuberculosis. *Clin. Chest Med.* **2019**, *40* (4), 763–774. https://doi.org/10.1016/j.ccm.2019.07.006.

(63)   Mitchison, D.; Davies, G. The Chemotherapy of Tuberculosis: Past, Present and Future. *Int. J. Tuberc. Lung Dis.* **2012**, *16* (6), 724–732. https://doi.org/10.5588/ijtld.12.0083.

(64)   *Guidelines for Treatment of Drug-Susceptible Tuberculosis and Patient Care.*, 2017 updat.; Geneva: World Health Organization, 2017.

(65)   Diacon, A. H.; Donald, P. R. The Early Bactericidal Activity of Antituberculosis Drugs. *Expert Rev. Anti. Infect. Ther.* **2014**, *12* (2), 223–237. https://doi.org/10.1586/14787210.2014.870884.

(66)   Connolly, L. E.; Edelstein, P. H.; Ramakrishnan, L. Why Is Long-Term Therapy Required to Cure Tuberculosis? *PLoS Medicine*. March 2007, pp 435–442. https://doi.org/10.1371/journal.pmed.0040120.

(67)   Nath, H.; Ryoo, S. First– and Second–Line Drugs and Drug Resistance. In *Tuberculosis - Current Issues in Diagnosis and Management*; InTech, 2013. https://doi.org/10.5772/54960.

(68)   Koul, A.; Arnoult, E.; Lounis, N.; Guillemont, J.; Andries, K. The Challenge of New Drug Discovery for Tuberculosis. *Nature* **2011**, *469* (7331), 483–490. https://doi.org/10.1038/nature09657.

(69)   Sotgiu, G.; Tiberi, S.; D'Ambrosio, L.; Centis, R.; Alffenaar, J. W.; Caminero, J. A.; Abdo Arbex, M.; Alarcon Guizado, V.; Aleksa, A.; Dore, S.; Gaga, M.; Gualano, G.; Kunst, H.; Payen, M.-C.; Roby Arias, A. J.; Skrahina, A.; Solovic, I.; Sulis, G.; Tadolini, M.; Zumla, A.; Migliori, G. B. Faster for Less: The New "Shorter" Regimen for Multidrug-Resistant Tuberculosis. *Eur. Respir. J.* **2016**, *48* (5), 1503–1507. https://doi.org/10.1183/13993003.01249-2016.

(70)   McIlleron, H.; Meintjes, G.; Burman, W. J.; Maartens, G. Complications of Antiretroviral Therapy in Patients with Tuberculosis: Drug Interactions, Toxicity, and Immune Reconstitution Inflammatory Syndrome. *J. Infect. Dis.* **2007**, *196* (s1), S63–S75. https://doi.org/10.1086/518655.

(71)   Bernstein, J.; Lott, W. A.; Steinberg, B. A.; Yale, H. L. Chemotherapy of Experimental Tuberculosis. V. Isonicotinic Acid Hydrazide (Nydrazid) and Related Compounds. *Am. Rev. Tuberc.* **1952**, *65* (4), 357–364. https://doi.org/10.1164/art.1952.65.4.357.

(72)   Isoniazid. *Tuberculosis* **2008**, *88* (2), 112–116. https://doi.org/10.1016/S1472-9792(08)70011-8.

(73)   Banerjee, A.; Dubnau, E.; Quemard, A.; Balasubramanian, V.; Um, K. S.; Wilson, T.; Collins, D.; De Lisle, G.; Jacobs, W. R. InhA, a Gene Encoding a Target for Isoniazid and Ethionamide in Mycobacterium Tuberculosis. *Science (80-.).* **1994**, *263* (5144), 227–230. https://doi.org/10.1126/science.8284673.

(74)   Timmins, G. S.; Deretic, V. Mechanisms of Action of Isoniazid. *Molecular Microbiology*. December 2006, pp 1220–1227. https://doi.org/10.1111/j.1365-2958.2006.05467.x.

(75)   Unissa, A. N.; Subbian, S.; Hanna, L. E.; Selvakumar, N. Overview on Mechanisms of Isoniazid Action and Resistance in Mycobacterium Tuberculosis. *Infect. Genet. Evol.* **2016**, *45*, 474–492.

https://doi.org/10.1016/j.meegid.2016.09.004.

(76) Sensi, P.; Margalith, P.; Timbal, M. T. Rifomycin, a New Antibiotic; Preliminary Report. *Farmaco. Sci.* **1959**, *14* (2), 146–147.

(77) Wehrli, W.; Knusel, F.; Schmid, K.; Staehelin, M. Interaction of Rifamycin with Bacterial RNA Polymerase. *Proc. Natl. Acad. Sci.* **1968**, *61* (2), 667–673. https://doi.org/10.1073/pnas.61.2.667.

(78) Wehrli, W. Rifampin: Mechanisms of Action and Resistance. *Rev. Infect. Dis.* **1983**, *5*, S407–S411. https://doi.org/10.1093/clinids/5.Supplement_3.S407.

(79) Ramaswamy, S.; Musser, J. M. Molecular Genetic Basis of Antimicrobial Agent Resistance in Mycobacterium Tuberculosis: 1998 Update. *Tuber. Lung Dis.* **1998**, *79* (1), 3–29. https://doi.org/10.1054/tuld.1998.0002.

(80) Rifampin. *Tuberculosis* **2008**, *88* (2), 151–154. https://doi.org/10.1016/S1472-9792(08)70024-6.

(81) de Steenwinkel, J. E. M.; de Knegt, G. J.; ten Kate, M. T.; van Belkum, A.; Verbrugh, H. A.; Kremer, K.; van Soolingen, D.; Bakker-Woudenberg, I. A. J. M. Time-Kill Kinetics of Anti-Tuberculosis Drugs, and Emergence of Resistance, in Relation to Metabolic Activity of Mycobacterium Tuberculosis. *J. Antimicrob. Chemother.* **2010**, *65* (12), 2582–2589. https://doi.org/10.1093/jac/dkq374.

(82) Rosenthal, I. M.; Zhang, M.; Williams, K. N.; Peloquin, C. A.; Tyagi, S.; Vernon, A. A.; Bishai, W. R.; Chaisson, R. E.; Grosset, J. H.; Nuermberger, E. L. Daily Dosing of Rifapentine Cures Tuberculosis in Three Months or Less in the Murine Model. *PLoS Med.* **2007**, *4* (12), 1931–1939. https://doi.org/10.1371/journal.pmed.0040344.

(83) Semvua, H. H.; Kibiki, G. S.; Kisanga, E. R.; Boeree, M. J.; Burger, D. M.; Aarnoutse, R. Pharmacological Interactions Between Rifampicin and Antiretroviral Drugs. *Ther. Drug Monit.* **2015**, *37* (1), 22–32. https://doi.org/10.1097/FTD.0000000000000108.

(84) Mitchison, D. A. The Action of Antituberculosis Drugs in Short-Course Chemotherapy. *Tubercle* **1985**, *66* (3), 219–225. https://doi.org/10.1016/0041-3879(85)90040-6.

(85) Falzon, D.; Schünemann, H. J.; Harausz, E.; González-Angulo, L.; Lienhardt, C.; Jaramillo, E.; Weyer, K. World Health Organization Treatment Guidelines for Drug-Resistant Tuberculosis, 2016 Update. *Eur. Respir. J.* **2017**, *49* (3), 1602308. https://doi.org/10.1183/13993003.02308-2016.

(86) Nuermberger, E.; Tyagi, S.; Tasneen, R.; Williams, K. N.; Almeida, D.; Rosenthal, I.; Grosset, J. H. Powerful Bactericidal and Sterilizing Activity of a Regimen Containing PA-824, Moxifloxacin, and Pyrazinamide in a Murine Model of Tuberculosis. *Antimicrob. Agents Chemother.* **2008**, *52* (4), 1522–1524. https://doi.org/10.1128/AAC.00074-08.

(87) Veziris, N.; Ibrahim, M.; Lounis, N.; Chauffour, A.; Truffot-Pernot, C.; Andries, K.; Jarlier, V. A Once-Weekly R207910-Containing Regimen Exceeds Activity of the Standard Daily Regimen in Murine Tuberculosis. *Am. J. Respir. Crit. Care Med.* **2009**, *179* (1), 75–79. https://doi.org/10.1164/rccm.200711-1736OC.

(88) Konno, K.; Feldmann, F. M.; McDermott, W. Pyrazinamide Susceptibility and Amidase Activity of Tubercle Bacilli. *Am. Rev. Respir. Dis.* **1967**, *95* (3), 461–469. https://doi.org/10.1164/arrd.1967.95.3.461.

(89) Zhang, Y.; Mitchison, D. The Curious Characteristics of Pyrazinamide: A Review. *International Journal of Tuberculosis and Lung Disease*. January 1, 2003, pp 6–21.

(90) Zhang, Y. Mode of Action of Pyrazinamide: Disruption of Mycobacterium Tuberculosis

Membrane Transport and Energetics by Pyrazinoic Acid. *J. Antimicrob. Chemother.* **2003**, *52* (5), 790–795. https://doi.org/10.1093/jac/dkg446.

(91)   Zhang, Y.; Shi, W.; Zhang, W.; Mitchison, D. Mechanisms of Pyrazinamide Action and Resistance. *Microbiol. Spectr.* **2014**, *2* (4), 1. https://doi.org/10.1128/microbiolspec.mgm2-0023-2013.

(92)   Hu, Y.; Coates, A. R.; Mitchison, D. A. Sterilising Action of Pyrazinamide in Models of Dormant and Rifampicin-Tolerant Mycobacterium Tuberculosis. *Int. J. Tuberc. Lung Dis.* **2006**, *10* (3), 317–322.

(93)   Ethambutol. *Tuberculosis* **2008**, *88* (2), 102–105. https://doi.org/10.1016/S1472-9792(08)70008-8.

(94)   Takayama, K.; Kilburn, J. O. Inhibition of Synthesis of Arabinogalactan by Ethambutol in Mycobacterium Smegmatis. *Antimicrob. Agents Chemother.* **1989**, *33* (9), 1493–1499. https://doi.org/10.1128/AAC.33.9.1493.

(95)   Wolucka, B. A.; McNeil, M. R.; De Hoffmann, E.; Chojnacki, T.; Brennan, P. J. Recognition of the Lipid Intermediate for Arabinogalactan/Arabinomannan Biosynthesis and Its Relation to the Mode of Action of Ethambutol on Mycobacteria. *J. Biol. Chem.* **1994**, *269* (37), 23328–23335.

(96)   Zhang, Y.; Yew, W.-W. Mechanisms of Drug Resistance in Mycobacterium Tuberculosis: Update 2015. *Int. J. Tuberc. Lung Dis.* **2015**, *19* (11), 1276–1289. https://doi.org/10.5588/ijtld.15.0389.

(97)   *WHO Consolidated Guidelines on Drug-Resistant Tuberculosis Treatment.*; Geneva: World Health Organization, 2019.

(98)   Sharma, S. K.; Dheda, K. What Is New in the WHO Consolidated Guidelines on Drug-Resistant Tuberculosis Treatment? *Indian Journal of Medical Research*. Wolters Kluwer Medknow Publications March 1, 2019, pp 309–312. https://doi.org/10.4103/ijmr.IJMR_579_19.

(99)   Sotgiu, G.; Tiberi, S.; Centis, R.; D'Ambrosio, L.; Fuentes, Z.; Zumla, A.; Migliori, G. B. Applicability of the Shorter 'Bangladesh Regimen' in High Multidrug-Resistant Tuberculosis Settings. *Int. J. Infect. Dis.* **2017**, *56*, 190–193. https://doi.org/10.1016/j.ijid.2016.10.021.

(100) Keam, S. J. Pretomanid: First Approval. *Drugs* **2019**, *79* (16), 1797–1803. https://doi.org/10.1007/s40265-019-01207-9.

(101) Conradie, F.; Diacon, A. H.; Ngubane, N.; Howell, P.; Everitt, D.; Crook, A. M.; Mendel, C. M.; Egizi, E.; Moreira, J.; Timm, J.; McHugh, T. D.; Wills, G. H.; Bateson, A.; Hunt, R.; Van Niekerk, C.; Li, M.; Olugbosi, M.; Spigelman, M. Treatment of Highly Drug-Resistant Pulmonary Tuberculosis. *N. Engl. J. Med.* **2020**, *382* (10), 893–902. https://doi.org/10.1056/nejmoa1901814.

(102) *WHO Consolidated Guidelines on Tuberculosis. Module 4: Treatment - Drug-Resistant Tuberculosis Treatment*; Geneva: World Health Organization, 2020.

(103) Lewis, R. J.; Mohr, J. F. Dysglycaemias and Fluoroquinolones. *Drug Saf.* **2008**, *31* (4), 283–292. https://doi.org/10.2165/00002018-200831040-00002.

(104) Spies, F. S.; Almeida da Silva, P. E.; Ribeiro, M. O.; Rossetti, M. L.; Zaha, A. Identification of Mutations Related to Streptomycin Resistance in Clinical Isolates of Mycobacterium Tuberculosis and Possible Involvement of Efflux Mechanism. *Antimicrob. Agents Chemother.* **2008**, *52* (8), 2947–2949. https://doi.org/10.1128/AAC.01570-07.

(105) Tiberi, S.; Scardigli, A.; Centis, R.; D'Ambrosio, L.; Muñoz-Torrico, M.; Salazar-Lezama, M. Á.; Spanevello, A.; Visca, D.; Zumla, A.; Migliori, G. B.; Caminero Luna, J. A. Classifying New Anti-Tuberculosis Drugs: Rationale and Future Perspectives. *Int. J. Infect. Dis.* **2017**, *56*, 181–184. https://doi.org/10.1016/j.ijid.2016.10.026.

(106) Ginsburg, A. S.; Grosset, J. H.; Bishai, W. R. Fluoroquinolones, Tuberculosis, and Resistance.

Lancet Infect. Dis. **2003**, *3* (7), 432–442. https://doi.org/10.1016/S1473-3099(03)00671-6.

(107) Moxifloxacin. *Tuberculosis* **2008**, *88* (2), 127–131. https://doi.org/10.1016/S1472-9792(08)70016-7.

(108) Levofloxacin. *Tuberculosis* **2008**, *88* (2), 119–121. https://doi.org/10.1016/S1472-9792(08)70013-1.

(109) Field, S. K. Bedaquiline for the Treatment of Multidrug-Resistant Tuberculosis: Great Promise or Disappointment? *Ther. Adv. Chronic Dis.* **2015**, *6* (4), 170–184. https://doi.org/10.1177/2040622315582325.

(110) Avorn, J. Approval of a Tuberculosis Drug Based on a Paradoxical Surrogate Measure. *JAMA* **2013**, *309* (13), 1349. https://doi.org/10.1001/jama.2013.623.

(111) Diacon, A. H.; Pym, A.; Grobusch, M.; Patientia, R.; Rustomjee, R.; Page-Shipp, L.; Pistorius, C.; Krause, R.; Bogoshi, M.; Churchyard, G.; Venter, A.; Allen, J.; Palomino, J. C.; De Marez, T.; van Heeswijk, R. P. G.; Lounis, N.; Meyvisch, P.; Verbeeck, J.; Parys, W.; de Beule, K.; Andries, K.; Neeley, D. F. M. The Diarylquinoline TMC207 for Multidrug-Resistant Tuberculosis. *N. Engl. J. Med.* **2009**, *360* (23), 2397–2405. https://doi.org/10.1056/NEJMoa0808427.

(112) Andries, K.; Verhasselt, P.; Guillemont, J.; Göhlmann, H. W. H.; Neefs, J.-M.; Winkler, H.; Van Gestel, J.; Timmerman, P.; Zhu, M.; Lee, E.; Williams, P.; de Chaffoy, D.; Huitric, E.; Hoffner, S.; Cambau, E.; Truffot-Pernot, C.; Lounis, N.; Jarlier, V. A Diarylquinoline Drug Active on the ATP Synthase of Mycobacterium Tuberculosis. *Science (80-.).* **2005**, *307* (5707), 223–227. https://doi.org/10.1126/science.1106753.

(113) Haagsma, A. C.; Podasca, I.; Koul, A.; Andries, K.; Guillemont, J.; Lill, H.; Bald, D. Probing the Interaction of the Diarylquinoline TMC207 with Its Target Mycobacterial ATP Synthase. *PLoS One* **2011**, *6* (8), e23575. https://doi.org/10.1371/journal.pone.0023575.

(114) Haagsma, A. C.; Abdillahi-Ibrahim, R.; Wagner, M. J.; Krab, K.; Vergauwen, K.; Guillemont, J.; Andries, K.; Lill, H.; Koul, A.; Bald, D. Selectivity of TMC207 towards Mycobacterial ATP Synthase Compared with That towards the Eukaryotic Homologue. *Antimicrob. Agents Chemother.* **2009**, *53* (3), 1290–1292. https://doi.org/10.1128/AAC.01393-08.

(115) Esposito, S.; Bianchini, S.; Blasi, F. Bedaquiline and Delamanid in Tuberculosis. *Expert Opin. Pharmacother.* **2015**, *16* (15), 2319–2330. https://doi.org/10.1517/14656566.2015.1080240.

(116) Shinabarger, D. Mechanism of Action of the Oxazolidinone Antibacterial Agents. *Expert Opin. Investig. Drugs* **1999**, *8* (8), 1195–1202. https://doi.org/10.1517/13543784.8.8.1195.

(117) Leach, K. L.; Brickner, S. J.; Noe, M. C.; Miller, P. F. Linezolid, the First Oxazolidinone Antibacterial Agent. *Ann. N. Y. Acad. Sci.* **2011**, *1222* (1), 49–54. https://doi.org/10.1111/j.1749-6632.2011.05962.x.

(118) Bressler, A. M.; Zimmer, S. M.; Gilmore, J. L.; Somani, J. Peripheral Neuropathy Associated with Prolonged Use of Linezolid. *Lancet Infectious Diseases*. Elsevier August 1, 2004, pp 528–531. https://doi.org/10.1016/S1473-3099(04)01109-0.

(119) Rucker, J. C.; Hamilton, S. R.; Bardenstein, D.; Isada, C. M.; Lee, M. S. Linezolid-Associated Toxic Optic Neuropathy. *Neurology* **2006**, *66* (4), 595–598. https://doi.org/10.1212/01.wnl.0000201313.24970.b8.

(120) Jadhavar, P.; Vaja, M.; Dhameliya, T.; Chakraborti, A. Oxazolidinones as Anti-Tubercular Agents: Discovery, Development and Future Perspectives. *Curr. Med. Chem.* **2015**, *22* (38), 4379–4397. https://doi.org/10.2174/0929867323666151106125759.

(121) Cholo, M. C.; Steel, H. C.; Fourie, P. B.; Germishuizen, W. A.; Anderson, R. Clofazimine: Current Status and Future Prospects. *J. Antimicrob. Chemother.* **2012**, *67* (2), 290–298.

_____

https://doi.org/10.1093/jac/dkr444.

(122) Clofazimine. *Tuberculosis*. Churchill Livingstone March 1, 2008, pp 96–99. https://doi.org/10.1016/S1472-9792(08)70006-4.

(123) Lechartier, B.; Cole, S. T. Mode of Action of Clofazimine and Combination Therapy with Benzothiazinones against Mycobacterium Tuberculosis. *Antimicrob. Agents Chemother.* **2015**, *59* (8), 4457–4463. https://doi.org/10.1128/AAC.00395-15.

(124) Shi, W.; Zhang, S.; Feng, J.; Cui, P.; Zhang, W.; Zhang, Y. Clofazimine Targets Essential Nucleoid Associated Protein, Mycobacterial Integration Host Factor (MIHF), in Mycobacterium Tuberculosis. *bioRxiv* **2017**, 192161. https://doi.org/10.1101/192161.

(125) Ren, Y. R.; Pan, F.; Parvez, S.; Fleig, A.; Chong, C. R.; Xu, J.; Dang, Y.; Zhang, J.; Jiang, H.; Penner, R.; Liu, J. O. Clofazimine Inhibits Human Kv1.3 Potassium Channel by Perturbing Calcium Oscillation in T Lymphocytes. *PLoS One* **2008**, *3* (12), e4009. https://doi.org/10.1371/journal.pone.0004009.

(126) Wallis, R. S. Cardiac Safety of Extensively Drug-Resistant Tuberculosis Regimens Including Bedaquiline, Delamanid and Clofazimine. *Eur. Respir. J.* **2016**, *48* (5), 1526–1527. https://doi.org/10.1183/13993003.01207-2016.

(127) Cycloserine. *Tuberculosis* **2008**, *88* (2), 100–101. https://doi.org/10.1016/S1472-9792(08)70007-6.

(128) Caminero, J. A.; Sotgiu, G.; Zumla, A.; Migliori, G. B. Best Drug Treatment for Multidrug-Resistant and Extensively Drug-Resistant Tuberculosis. *Lancet Infect. Dis.* **2010**, *10* (9), 621–629. https://doi.org/10.1016/S1473-3099(10)70139-0.

(129) Hwang, T. J.; Wares, D. F.; Jafarov, A.; Jakubowiak, W.; Nunn, P.; Keshavjee, S. Safety of Cycloserine and Terizidone for the Treatment of Drug-Resistant Tuberculosis: A Meta-Analysis [Review Article]. *Int. J. Tuberc. Lung Dis.* **2013**, *17* (10), 1257–1266. https://doi.org/10.5588/ijtld.12.0863.

(130) Gurumurthy, M.; Mukherjee, T.; Dowd, C. S.; Singh, R.; Niyomrattanakit, P.; Tay, J. A.; Nayyar, A.; Lee, Y. S.; Cherian, J.; Boshoff, H. I.; Dick, T.; Barry, C. E.; Manjunatha, U. H. Substrate Specificity of the Deazaflavin-Dependent Nitroreductase from Mycobacterium Tuberculosis Responsible for the Bioreductive Activation of Bicyclic Nitroimidazoles. *FEBS J.* **2012**, *279* (1), 113–125. https://doi.org/10.1111/j.1742-4658.2011.08404.x.

(131) Matsumoto, M.; Hashizume, H.; Tomishige, T.; Kawasaki, M.; Tsubouchi, H.; Sasaki, H.; Shimokawa, Y.; Komatsu, M. OPC-67683, a Nitro-Dihydro-Imidazooxazole Derivative with Promising Action against Tuberculosis In Vitro and In Mice. *PLoS Med.* **2006**, *3* (11), e466. https://doi.org/10.1371/journal.pmed.0030466.

(132) Ryan, N. J.; Lo, J. H. Delamanid: First Global Approval. *Drugs* **2014**, *74* (9), 1041–1045. https://doi.org/10.1007/s40265-014-0241-5.

(133) Gupta, R.; Geiter, L. J.; Hafkin, J.; Wells, C. D. Delamanid and QT Prolongation in the Treatment of Multidrug-Resistant Tuberculosis. *Int. J. Tuberc. Lung Dis.* **2015**, *19* (10), 1261–1262. https://doi.org/10.5588/ijtld.15.0541.

(134) Singh, R.; Manjunatha, U.; Boshoff, H. I. M.; Ha, Y. H.; Niyomrattanakit, P.; Ledwidge, R.; Dowd, C. S.; Lee, I. Y.; Kim, P.; Zhang, L.; Kang, S.; Keller, T. H.; Jiricek, J.; Barry, C. E. PA-824 Kills Nonreplicating Mycobacterium Tuberculosis by Intracellular NO Release. *Science (80-.).* **2008**, *322* (5906), 1392–1395. https://doi.org/10.1126/science.1164571.

(135) Manjunatha, U.; Boshoff, H. I. M.; Barry, C. E. The Mechanism of Action of PA-824. *Commun. Integr. Biol.* **2009**, *2* (3), 215–218. https://doi.org/10.4161/cib.2.3.7926.

(136) Kesado, T.; Hashizume, T.; Asahi, Y. Antibacterial Activities of a New Stabilized Thienamycin, N-Formimidoyl Thienamycin, in Comparison with Other Antibiotics. *Antimicrob. Agents Chemother.* **1980**, *17* (6), 912–917. https://doi.org/10.1128/AAC.17.6.912.

(137) Edwards, J. R. Meropenem: A Microbiological Overview. *J. Antimicrob. Chemother.* **1995**, *36* (suppl A), 1–17. https://doi.org/10.1093/jac/36.suppl_A.1.

(138) Sotgiu, G.; D'Ambrosio, L.; Centis, R.; Tiberi, S.; Esposito, S.; Dore, S.; Spanevello, A.; Migliori, G. Carbapenems to Treat Multidrug and Extensively Drug-Resistant Tuberculosis: A Systematic Review. *Int. J. Mol. Sci.* **2016**, *17* (3), 373. https://doi.org/10.3390/ijms17030373.

(139) Hugonnet, J.-E.; Blanchard, J. S. Irreversible Inhibition of the Mycobacterium Tuberculosis β-Lactamase by Clavulanate †. *Biochemistry* **2007**, *46* (43), 11998–12004. https://doi.org/10.1021/bi701506h.

(140) Hugonnet, J. E.; Tremblay, L. W.; Boshoff, H. I.; Barry, C. E.; Blanchard, J. S. Meropenem-Clavulanate Is Effective against Extensively Drug-Resistant Mycobacterium Tuberculosis. *Science (80-.).* **2009**, *323* (5918), 1215–1218. https://doi.org/10.1126/science.1167498.

(141) Cordillot, M.; Dubée, V.; Triboulet, S.; Dubost, L.; Marie, A.; Hugonnet, J.-E.; Arthur, M.; Mainardi, J.-L. In Vitro Cross-Linking of Mycobacterium Tuberculosis Peptidoglycan by l,d-Transpeptidases and Inactivation of These Enzymes by Carbapenems. *Antimicrob. Agents Chemother.* **2013**, *57* (12), 5940–5945. https://doi.org/10.1128/AAC.01663-13.

(142) Scholar, E. Carbapenems. In *xPharm: The Comprehensive Pharmacology Reference*; Elsevier, 2007; pp 1–3. https://doi.org/10.1016/B978-008055232-3.62935-6.

(143) Streptomycin. *Tuberculosis* **2008**, *88* (2), 162–163. https://doi.org/10.1016/S1472-9792(08)70027-1.

(144) Amikacin. *Tuberculosis* **2008**, *88* (2), 87–88. https://doi.org/10.1016/S1472-9792(08)70003-9.

(145) De Jager, R.; Van Altena, R. Hearing Loss and Nephrotoxicity in Long-Term Aminoglycoside Treatment in Patients with Tuberculosis. *Int. J. Tuberc. Lung Dis.* **2002**, *6* (7), 622–627.

(146) Wang, F.; Langley, R.; Gulten, G.; Dover, L. G.; Besra, G. S.; Jacobs, W. R.; Sacchettini, J. C. Mechanism of Thioamide Drug Action against Tuberculosis and Leprosy. *J. Exp. Med.* **2007**, *204* (1), 73–78. https://doi.org/10.1084/jem.20062100.

(147) Ethionamide. *Tuberculosis*. Churchill Livingstone March 1, 2008, pp 106–108. https://doi.org/10.1016/S1472-9792(08)70009-X.

(148) Prothionamide. *Tuberculosis*. Churchill Livingstone March 1, 2008, pp 139–140. https://doi.org/10.1016/S1472-9792(08)70020-9.

(149) Para-Aminosalicylic Acid. *Tuberculosis* **2008**, *88* (2), 137–138. https://doi.org/10.1016/S1472-9792(08)70019-2.

(150) Lehmann, J. PARA-AMINOSALICYLIC ACID IN THE TREATMENT OF TUBERCULOSIS. *Lancet* **1946**, *247* (6384), 15–16. https://doi.org/10.1016/S0140-6736(46)91185-3.

(151) Zheng, J.; Rubin, E. J.; Bifani, P.; Mathys, V.; Lim, V.; Au, M.; Jang, J.; Nam, J.; Dick, T.; Walker, J. R.; Pethe, K.; Camacho, L. R. Para-Aminosalicylic Acid Is a Prodrug Targeting Dihydrofolate Reductase in Mycobacterium Tuberculosis. *J. Biol. Chem.* **2013**, *288* (32), 23447–23456. https://doi.org/10.1074/jbc.M113.475798.

(152) McKenna, L. Pipeline Report 2019. **2019**.

(153) Stop TB Partnership. WGND Global TB Drug Pipeline https://www.newtbdrugs.org/pipeline/clinical (accessed May 21, 2020).

(154) New Study 31/A5349 on the treatment of drug-susceptible TB

_____

https://www.who.int/news/item/22-10-2020-new-study-31-a5349-on-the-treatment-of-drug-susceptible-tb (accessed Jan 13, 2021).

(155) Fätkenheuer, G.; Taelman, H.; Lepage, P.; Schwenk, A.; Wenzel, R. The Return of Tuberculosis. *Diagn. Microbiol. Infect. Dis.* **1999**, *34* (2), 139–146. https://doi.org/10.1016/S0732-8893(99)00006-1.

(156) Mfinanga, S. G.; Kirenga, B. J.; Chanda, D. M.; Mutayoba, B.; Mthiyane, T.; Yimer, G.; Ezechi, O.; Connolly, C.; Kapotwe, V.; Muwonge, C.; Massaga, J.; Sinkala, E.; Kohi, W.; Lyantumba, L.; Nyakoojo, G.; Luwaga, H.; Doulla, B.; Mzyece, J.; Kapata, N.; Vahedi, M.; Mwaba, P.; Egwaga, S.; Adatu, F.; Pym, A.; Joloba, M.; Rustomjee, R.; Zumla, A.; Onyebujoh, P. Early versus Delayed Initiation of Highly Active Antiretroviral Therapy for HIV-Positive Adults with Newly Diagnosed Pulmonary Tuberculosis (TB-HAART): A Prospective, International, Randomised, Placebo-Controlled Trial. *Lancet Infect. Dis.* **2014**, *14* (7), 563–571. https://doi.org/10.1016/S1473-3099(14)70733-9.

(157) Fitzgerald, D. W.; Desvarieux, M.; Severe, P.; Joseph, P.; Johnson, W. D.; Pape, J. W. Effect of Post-Treatment Isoniazid on Prevention of Recurrent Tuberculosis in HIV-1-Infected Individuals: A Randomised Trial. *Lancet* **2000**, *356* (9240), 1470–1474. https://doi.org/10.1016/S0140-6736(00)02870-1.

(158) Ahmad Khan, F.; Minion, J.; Al-Motairi, A.; Benedetti, A.; Harries, A. D.; Menzies, D. An Updated Systematic Review and Meta-Analysis on the Treatment of Active Tuberculosis in Patients With HIV Infection. *Clin. Infect. Dis.* **2012**, *55* (8), 1154–1163. https://doi.org/10.1093/cid/cis630.

(159) Havlir, D. V.; Kendall, M. A.; Ive, P.; Kumwenda, J.; Swindells, S.; Qasba, S. S.; Luetkemeyer, A. F.; Hogg, E.; Rooney, J. F.; Wu, X.; Hosseinipour, M. C.; Lalloo, U.; Veloso, V. G.; Some, F. F.; Kumarasamy, N.; Padayatchi, N.; Santos, B. R.; Reid, S.; Hakim, J.; Mohapi, L.; Mugyenyi, P.; Sanchez, J.; Lama, J. R.; Pape, J. W.; Sanchez, A.; Asmelash, A.; Moko, E.; Sawe, F.; Andersen, J.; Sanne, I. Timing of Antiretroviral Therapy for HIV-1 Infection and Tuberculosis. *N. Engl. J. Med.* **2011**, *365* (16), 1482–1491. https://doi.org/10.1056/NEJMoa1013607.

(160) Amogne, W.; Aderaye, G.; Habtewold, A.; Yimer, G.; Makonnen, E.; Worku, A.; Sonnerborg, A.; Aklillu, E.; Lindquist, L. Efficacy and Safety of Antiretroviral Therapy Initiated One Week after Tuberculosis Therapy in Patients with CD4 Counts < 200 Cells/ML: TB-HAART Study, a Randomized Clinical Trial. *PLoS One* **2015**, *10* (5), e0122587. https://doi.org/10.1371/journal.pone.0122587.

(161) Abdool Karim, S. S.; Naidoo, K.; Grobler, A.; Padayatchi, N.; Baxter, C.; Gray, A.; Gengiah, T.; Nair, G.; Bamber, S.; Singh, A.; Khan, M.; Pienaar, J.; El-Sadr, W.; Friedland, G.; Abdool Karim, Q. Timing of Initiation of Antiretroviral Drugs during Tuberculosis Therapy. *N. Engl. J. Med.* **2010**, *362* (8), 697–706. https://doi.org/10.1056/NEJMoa0905848.

(162) Critchley, J. A.; Young, F.; Orton, L.; Garner, P. Corticosteroids for Prevention of Mortality in People with Tuberculosis: A Systematic Review and Meta-Analysis. *Lancet Infect. Dis.* **2013**, *13* (3), 223–237. https://doi.org/10.1016/S1473-3099(12)70321-3.

(163) *Latent Tuberculosis Infection: Updated and Consolidated Guidelines for Programmatic Management.*; Geneva: World Health Organization, 2018.

(164) Houben, R. M. G. J.; Dodd, P. J. The Global Burden of Latent Tuberculosis Infection: A Re-Estimation Using Mathematical Modelling. *PLOS Med.* **2016**, *13* (10), e1002152. https://doi.org/10.1371/journal.pmed.1002152.

(165) Huaman, M. A.; Sterling, T. R. Treatment of Latent Tuberculosis Infection—An Update. *Clin. Chest Med.* **2019**, *40* (4), 839–848. https://doi.org/10.1016/j.ccm.2019.07.008.

(166) Getahun, H.; Matteelli, A.; Chaisson, R. E.; Raviglione, M. Latent Mycobacterium Tuberculosis

_____

Infection. *N. Engl. J. Med.* **2015**, *372* (22), 2127–2135. https://doi.org/10.1056/NEJMra1405427.

(167) Hirsch-Moverman, Y.; Daftary, A.; Franks, J.; Colson, P. W. Adherence to Treatment for Latent Tuberculosis Infection: Systematic Review of Studies in the US and Canada. *International Journal of Tuberculosis and Lung Disease*. November 2008, pp 1235–1254.

(168) Fox, G. J.; Dobler, C. C.; Marais, B. J.; Denholm, J. T. Preventive Therapy for Latent Tuberculosis Infection—the Promise and the Challenges. *International Journal of Infectious Diseases*. Elsevier B.V. March 1, 2017, pp 68–76. https://doi.org/10.1016/j.ijid.2016.11.006.

(169) Balcells, M. E.; Thomas, S. L.; Godfrey-Faussett, P.; Grant, A. D. Isoniazid Preventive Therapy and Risk for Resistant Tuberculosis. *Emerg. Infect. Dis.* **2006**, *12* (5), 744–751. https://doi.org/10.3201/eid1205.050681.

(170) Den Boon, S.; Matteelli, A.; Getahun, H. Rifampicin Resistance after Treatment for Latent Tuberculous Infection: A Systematic Review and Meta-Analysis. *International Journal of Tuberculosis and Lung Disease*. International Union against Tubercul. and Lung Dis. August 1, 2016, pp 1065–1071. https://doi.org/10.5588/ijtld.15.0908.

(171) Ballell, L.; Bates, R. H.; Young, R. J.; Alvarez-Gomez, D.; Alvarez-Ruiz, E.; Barroso, V.; Blanco, D.; Crespo, B.; Escribano, J.; González, R.; Lozano, S.; Huss, S.; Santos-Villarejo, A.; Martín-Plaza, J. J.; Mendoza, A.; Rebollo-Lopez, M. J.; Remuiñan-Blanco, M.; Lavandera, J. L.; Pérez-Herran, E.; Gamo-Benito, F. J.; García-Bustos, J. F.; Barros, D.; Castro, J. P.; Cammack, N. Fueling Open-Source Drug Discovery: 177 Small-Molecule Leads against Tuberculosis. *ChemMedChem* **2013**, *8* (2), 313–321. https://doi.org/10.1002/cmdc.201200428.

(172) Garnier, T.; Eiglmeier, K.; Camus, J.-C.; Medina, N.; Mansoor, H.; Pryor, M.; Duthoy, S.; Grondin, S.; Lacroix, C.; Monsempe, C.; Simon, S.; Harris, B.; Atkin, R.; Doggett, J.; Mayes, R.; Keating, L.; Wheeler, P. R.; Parkhill, J.; Barrell, B. G.; Cole, S. T.; Gordon, S. V; Hewinson, R. G. The Complete Genome Sequence of Mycobacterium Bovis. *Proc. Natl. Acad. Sci. U. S. A.* **2003**, *100* (13), 7877–7882. https://doi.org/10.1073/pnas.1130426100.

(173) Stanley, S. a; Grant, S. S.; Kawate, T.; Iwase, N.; Shimizu, M.; Wivagg, C.; Silvis, M.; Kazyanskaya, E.; Aquadro, J.; Golas, A.; Fitzgerald, M.; Dai, H.; Zhang, L.; Hung, D. T. Identification of Novel Inhibitors of M. Tuberculosis Growth Using Whole Cell Based High-Throughput Screening. *ACS Chem. Biol.* **2012**, *7* (8), 1377–1384. https://doi.org/10.1021/cb300151m.

(174) Lipinski, C. A.; Lombardo, F.; Dominy, B. W.; Feeney, P. J. Experimental and Computational Approaches to Estimate Solubility and Permeability in Drug Discovery and Development Settings. *Adv. Drug Deliv. Rev.* **2001**, *46* (1–3), 3–26.

(175) Chemical Computing Group ULC. MOE: Molecular Operating Environment https://www.chemcomp.com/MOE-Molecular_Operating_Environment.htm.

(176) Malarone-GSK Product https://gskpro.com/content/dam/global/hcpportal/en_US/Prescribing_Information/Malarone/pdf/MALARONE.PDF (accessed Apr 21, 2021).

(177) Kumar, A.; Guardia, A.; Colmenarejo, G.; Pérez, E.; Gonzalez, R. R.; Torres, P.; Calvo, D.; Gómez, R. M.; Ortega, F.; Jiménez, E.; Gabarro, R. C.; Rullás, J.; Ballell, L.; Sherman, D. R. A Focused Screen Identifies Antifolates with Activity on Mycobacterium Tuberculosis. *ACS Infect. Dis.* **2016**, *1* (12), 604–614. https://doi.org/10.1021/acsinfecdis.5b00063.

(178) Yuthavong, Y.; Tarnchompoo, B.; Vilaivan, T.; Chitnumsub, P.; Kamchonwongpaisan, S.; Charman, S. a; McLennan, D. N.; White, K. L.; Vivas, L.; Bongard, E.; Thongphanchang, C.; Taweechai, S.; Vanichtanankul, J.; Rattanajak, R.; Arwon, U.; Fantauzzi, P.; Yuvaniyama, J.; Charman, W. N.; Matthews, D. Malarial Dihydrofolate Reductase as a Paradigm for Drug

Development against a Resistance-Compromised Target. *Proc. Natl. Acad. Sci. U. S. A.* **2012**, *109* (42), 16823–16828. https://doi.org/10.1073/pnas.1204556109.

(179) Hughes, W. T.; Jacobus, D. P.; Canfield, C.; Killmar, J. Anti-Pneumocystis Carinii Activity of PS-15, a New Biguanide Folate Antagonist. *Antimicrob. Agents Chemother.* **1993**, *37* (7), 1417–1419.

(180) Rao, A.; Tapale, S. A Study on Dihydrofolate Reductase and Its Inhibitors: A Review. *Int. J. Pharm. Sci. Res.* **2013**, *4* (7), 2535–2547. https://doi.org/10.13040/IJPSR.0975-8232.4(7).2535-47.

(181) Sader, H. S.; Fritsche, T. R.; Jones, R. N. Potency and Bactericidal Activity of Iclaprim against Recent Clinical Gram-Positive Isolates. *Antimicrob. Agents Chemother.* **2009**, *53* (5), 2171–2175. https://doi.org/10.1128/AAC.00129-09.

(182) Debnath, A. K. Pharmacophore Mapping of a Series of 2,4-Diamino-5-Deazapteridine Inhibitors of Mycobacterium Avium Complex Dihydrofolate Reductase. *J. Med. Chem.* **2002**, *45* (1), 41–53. https://doi.org/10.1021/jm010360c.

(183) Shah, L. M.; Stefano, M. S. D. E. Enhanced in Vitro Activity of WR99210 in Combination with Dapsone against Mycobacterium Avium Complex . Enhanced In Vitro Activity of WR99210 in Combination with Dapsone against Mycobacterium Avium Complex. **1996**, *40* (11), 2644–2646.

(184) Meyer, S. C.; Majumder, S. K.; Cynamon, M. H. In Vitro Activities of PS-15, a New Dihydrofolate Reductase Inhibitor, and Its Cyclic Metabolite against Mycobacterium Avium Complex. *Antimicrob. Agents Chemother.* **1995**, *39* (8), 1862–1863.

(185) Blakley, R. L. Eukaryotic Dihydrofolate Reductase. *Adv. Enzymol. Relat. Areas Mol. Biol.* **1995**, *70*, 23–102.

(186) Jensen, D. E.; Black, A. R.; Swick, A. G.; Azizkhan, J. C. Distinct Roles for Sp1 and E2F Sites in the Growth/Cell Cycle Regulation of the DHFR Promoter. *J. Cell. Biochem.* **1997**, *67* (1), 24–31. https://doi.org/10.1002/(SICI)1097-4644(19971001)67:1<24::AID-JCB3>3.0.CO;2-Y.

(187) Kompis, I. M.; Islam, K.; Then, R. L. DNA and RNA Synthesis: Antifolates. *Chem. Rev.* **2005**, *105* (2), 593–620. https://doi.org/10.1021/cr0301144.

(188) Hansch, C.; Hathaway, B. A.; Zong-ru, g.; Selassie, D.; Dietrich, S. W.; Blaney, J. M.; Langridge, R.; Vz, K. W.; Kaufmang, B. T. No Title. **1984**, 129–143.

(189) Fleming, G. F.; Schilsky, R. L. Antifolates: The next Generation. *Semin. Oncol.* **1992**, *19* (6), 707–719. https://doi.org/10.5555/uri:pii:0093775492900394.

(190) Morales, C.; García, M. J.; Ribas, M.; Miró, R.; Muñoz, M.; Caldas, C.; Peinado, M. A. Dihydrofolate Reductase Amplification and Sensitization to Methotrexate of Methotrexate-Resistant Colon Cancer Cells. *Mol. Cancer Ther.* **2009**, *8* (2), 424–432. https://doi.org/10.1158/1535-7163.MCT-08-0759.

(191) Schweitzer, B. I.; Dicker, A. P.; Bertino, J. R. Dihydrofolate Reductase as a Therapeutic Target. *FASEB J.* **1990**, *4* (8), 2441–2452.

(192) Genestier, L.; Paillot, R.; Fournel, S.; Ferraro, C.; Miossec, P.; Revillard, J. P. Immunosuppressive Properties of Methotrexate: Apoptosis and Clonal Deletion of Activated Peripheral T Cells. *J. Clin. Invest.* **1998**, *102* (2), 322–328. https://doi.org/10.1172/JCI2676.

(193) M Cutolo, A Sulli, C Pizzorni, B. S. Anti-Inflammatory Mechanisms of Methotrexate in Rheumatoid Arthritis. *Ann. Rheum. Dis.* **2001**, *60* (8), 729–735. https://doi.org/10.1136/ard.60.8.729.

(194) Roth, B.; Rauckman, B. S.; Ferone, R.; Baccanari, D. P.; Champness, J. N.; Hyde, R. M. 2,4-Diamino-5-Benzylpyrimidines as Antibacterial Agents. 7. Analysis of the Effect of 3,5-Dialkyl

Substituent Size and Shape on Binding to Four Different Dihydrofolate Reductase Enzymes. *J. Med. Chem.* **1987**, *30* (2), 348–356. https://doi.org/10.1021/jm00385a017.

(195) Plowe, C. V.; Kublin, J. G.; Dzinjalamala, F. K.; Kamwendo, D. S.; Mukadam, R. A. G.; Chimpeni, P.; Molyneux, M. E.; Taylor, T. E. Sustained Clinical Efficacy of Sulfadoxine-Pyrimethamine for Uncomplicated Falciparum Malaria in Malawi after 10 Years as First Line Treatment: Five Year Prospective Study. *Br. Med. J.* **2004**, *328* (7439), 545–548. https://doi.org/10.1136/bmj.37977.653750.ee.

(196) Watkins, W. M.; Mberu, E. K.; Winstanley, P. A.; Plowe, C. V. The Efficacy of Antifolate Antimalarial Combinations in Africa: A Predictive Model Based on Pharmacodynamic and Pharmacokinetic Analyses. *Parasitology Today*. Elsevier Ltd December 1, 1997, pp 459–464. https://doi.org/10.1016/s0169-4758(97)01124-1.

(197) Zuccotto, F.; Martin, a C.; Laskowski, R. a; Thornton, J. M.; Gilbert, I. H. Dihydrofolate Reductase: A Potential Drug Target in Trypanosomes and Leishmania. *J. Comput. Aided. Mol. Des.* **1998**, *12* (3), 241–257.

(198) Raimondi, M.; Randazzo, O.; La Franca, M.; Barone, G.; Vignoni, E.; Rossi, D.; Collina, S. DHFR Inhibitors: Reading the Past for Discovering Novel Anticancer Agents. *Molecules* **2019**, *24* (6), 1140. https://doi.org/10.3390/molecules24061140.

(199) Sharma, M.; Chauhan, P. M. Dihydrofolate Reductase as a Therapeutic Target for Infectious Diseases: Opportunities and Challenges. *Future Med. Chem.* **2012**, *4* (10), 1335–1365. https://doi.org/10.4155/fmc.12.68.

(200) Kumar, A.; Zhang, M.; Zhu, L.; Liao, R. P.; Mutai, C.; Hafsat, S.; Sherman, D. R.; Wang, M.-W. High-Throughput Screening and Sensitized Bacteria Identify an M. Tuberculosis Dihydrofolate Reductase Inhibitor with Whole Cell Activity. *PLoS One* **2012**, *7* (6), e39961. https://doi.org/10.1371/journal.pone.0039961.

(201) Nixon, M. R.; Saionz, K. W.; Koo, M. S.; Szymonifka, M. J.; Jung, H.; Roberts, J. P.; Nandakumar, M.; Kumar, A.; Liao, R.; Rustad, T.; Sacchettini, J. C.; Rhee, K. Y.; Freundlich, J. S.; Sherman, D. R. Folate Pathway Disruption Leads to Critical Disruption of Methionine Derivatives in Mycobacterium Tuberculosis. *Chem. Biol.* **2014**, *21* (7), 819–830. https://doi.org/10.1016/j.chembiol.2014.04.009.

(202) Canfield, C. J.; Milhous, W. K.; Ager, A. L.; Rossan, R. N.; Sweeney, T. R.; Lewis, N. J.; Jacobus, D. P. PS-15: A Potent, Orally Active Antimalarial from a New Class of Folic Acid Antagonists. *Am. J. Trop. Med. Hyg.* **1993**, *49* (1), 121–126.

(203) Jensen, N. P.; Ager, a L.; Bliss, R. a; Canfield, C. J.; Kotecka, B. M.; Rieckmann, K. H.; Terpinski, J.; Jacobus, D. P. Phenoxypropoxybiguanides, Prodrugs of DHFR-Inhibiting Diaminotriazine Antimalarials. *J. Med. Chem.* **2001**, *44* (23), 3925–3931.

(204) White, E. L.; Ross, L. J.; Cunningham, A.; Escuyer, V. Cloning, Expression, and Characterization of Mycobacterium Tuberculosis Dihydrofolate Reductase. *FEMS Microbiol. Lett.* **2004**, *232* (1), 101–105. https://doi.org/10.1016/S0378-1097(04)00038-2.

(205) Li, R.; Sirawaraporn, R.; Chitnumsub, P.; Sirawaraporn, W.; Wooden, J.; Athappilly, F.; Turley, S.; Hol, W. G. Three-Dimensional Structure of M. Tuberculosis Dihydrofolate Reductase Reveals Opportunities for the Design of Novel Tuberculosis Drugs. *J. Mol. Biol.* **2000**, *295* (2), 307–323. https://doi.org/10.1006/jmbi.1999.3328.

(206) Gerum, A. B.; Ulmer, J. E.; Jacobus, D. P.; Jensen, N. P.; Sherman, D. R.; Sibley, C. H. Novel Saccharomyces Cerevisiae Screen Identifies WR99210 Analogues That Inhibit Mycobacterium Tuberculosis Dihydrofolate Reductase. *Antimicrob. Agents Chemother.* **2002**, *46* (11), 3362–3369. https://doi.org/10.1128/AAC.46.11.3362-3369.2002.

References

_____

(207) El-Hamamsy, M. H. R. I.; Smith, A. W.; Thompson, A. S.; Threadgill, M. D. Structure-Based Design, Synthesis and Preliminary Evaluation of Selective Inhibitors of Dihydrofolate Reductase from Mycobacterium Tuberculosis. *Bioorg. Med. Chem.* **2007**, *15* (13), 4552–4576. https://doi.org/10.1016/j.bmc.2007.04.011.

(208) Hong, W.; Wang, Y.; Chang, Z.; Yang, Y.; Pu, J.; Sun, T.; Kaur, S.; Sacchettini, J. C.; Jung, H.; Lin Wong, W.; Fah Yap, L.; Fong Ngeow, Y.; Paterson, I. C.; Wang, H. The Identification of Novel Mycobacterium Tuberculosis DHFR Inhibitors and the Investigation of Their Binding Preferences by Using Molecular Modelling. *Sci. Rep.* **2015**, *5* (July), 15328. https://doi.org/10.1038/srep15328.

(209) Kumar, A.; Guardia, A.; Colmenarejo, G.; Pérez, E.; Gonzalez, R. R.; Torres, P.; Calvo, D.; Gómez, R. M.; Ortega, F.; Jiménez, E.; Gabarro, R. C.; Rullás, J.; Ballell, L.; Sherman, D. R. A Focused Screen Identifies Antifolates with Activity on *Mycobacterium Tuberculosis*. *ACS Infect. Dis.* **2015**, acsinfecdis.5b00063. https://doi.org/10.1021/acsinfecdis.5b00063.

(210) Wang, N.; Ren, J. X.; Xie, Y. Identification of Novel DHFR Inhibitors for Treatment of Tuberculosis by Combining Virtual Screening with in Vitro Activity Assay. *J. Biomol. Struct. Dyn.* **2019**, *37* (4), 1054–1061. https://doi.org/10.1080/07391102.2018.1448721.

(211) Sittikornpaiboon, P.; Toochinda, P.; Lawtrakul, L. Structural and Dynamics Perspectives on the Binding of Substrate and Inhibitors in Mycobacterium Tuberculosis DHFR. *Sci. Pharm.* **2017**, *85* (3). https://doi.org/10.3390/scipharm85030031.

(212) Akhter, M. Identification of Novel Mycobacterium Tuberculosis Dihydrofolate Reductase Inhibitors through Rational Drug Design. *Int. J. Mycobacteriology* **2016**, *5*, S96. https://doi.org/10.1016/j.ijmyco.2016.09.026.

(213) Sharma, K.; Neshat, N.; Sharma, S.; Giri, N.; Srivastava, A.; Almalki, F.; Saifullah, K.; Alam, M. M.; Shaquiquzzaman, M.; Akhter, M. Identification of Novel Selective Mtb-DHFR Inhibitors as Antitubercular Agents through Structure-Based Computational Techniques. *Arch. Pharm. (Weinheim).* **2020**, *353* (2). https://doi.org/10.1002/ardp.201900287.

(214) Sharma, K.; Tanwar, O.; Deora, G. S.; Ali, S.; Alam, M. M.; Zaman, M. S.; Krishna, V. S.; Sriram, D.; Akhter, M. Expansion of a Novel Lead Targeting M. Tuberculosis DHFR as Antitubercular Agents. *Bioorganic Med. Chem.* **2019**, *27* (7), 1421–1429. https://doi.org/10.1016/j.bmc.2019.02.053.

(215) Ribeiro, J. A.; Hammer, A.; Libreros Zúñiga, G. A.; Chavez-Pacheco, S. M.; Tyrakis, P.; de Oliveira, G. S.; Kirkman, T.; Bakali, J. El; Rocco, S. A.; Sforça, M. L.; Parise-Filho, R.; Coyne, A.; Blundell, T.; Abell, C.; Bertacine Dias, M. V. Using a Fragment-Based Approach to Identify Novel Chemical Scaffolds Targeting the Dihydrofolate Reductase (DHFR) from Mycobacterium Tuberculosis. *bioRxiv* **2020**, 2020.03.30.016204. https://doi.org/10.1101/2020.03.30.016204.

(216) Ribeiro, J. A.; Hammer, A.; Libreros-Zúñiga, G. A.; Chavez-Pacheco, S. M.; Tyrakis, P.; De Oliveira, G. S.; Kirkman, T.; El Bakali, J.; Rocco, S. A.; Sforça, M. L.; Parise-Filho, R.; Coyne, A. G.; Blundell, T. L.; Abell, C.; Dias, M. V. B. Using a Fragment-Based Approach to Identify Alternative Chemical Scaffolds Targeting Dihydrofolate Reductase from Mycobacterium Tuberculosis. *ACS Infect. Dis.* **2020**, *6* (8), 2192–2201. https://doi.org/10.1021/acsinfecdis.0c00263.

(217) Mamalis, P. Di-Hydro Triazine Derivatives. *US Pat. 3,723,429* **1973**.

(218) Ma, X.; Woon, R. S.-P.; Ho, P. C.-L.; Chui, W.-K. Antiproliferative Activity against MCF-7 Breast Cancer Cells by Diamino-Triazaspirodiene Antifolates. *Chem. Biol. Drug Des.* **2009**, *74* (3), 322–326. https://doi.org/10.1111/j.1747-0285.2009.00860.x.

(219) Ma, X.; Tan, S.-T.; Khoo, C.-L.; Sim, H.-M.; Chan, L.-W.; Chui, W.-K. Synthesis and Antimicrobial Activity of N^1-Benzyl or N^1-Benzyloxy-1,6-Dihydro-1,3,5-Triazine-2,4-Diamines. *Bioorg. Med.*

Chem. Lett. **2011**, *21* (18), 5428–5431. https://doi.org/10.1016/j.bmcl.2011.06.125.

(220) Balabon, O. Master Thesis, Université Lille1, 2013.

(221) Bag, S.; Tawari, N. R.; Queener, S. F.; Degani, M. S. Synthesis and Biological Evaluation of Biguanide and Dihydrotriazine Derivatives as Potential Inhibitors of Dihydrofolate Reductase of Opportunistic Microorganisms. *J. Enzyme Inhib. Med. Chem.* **2010**, *25* (3), 331–339. https://doi.org/10.3109/14756360903179443.

(222) Kidwai, M.; Mothsra, P.; Mohan, R.; Biswas, S. 1-Aryl-4,6-Diamino-1,2-Dihydrotriazine as Antimalarial Agent: A New Synthetic Route. *Bioorg. Med. Chem. Lett.* **2005**, *15* (4), 915–917. https://doi.org/10.1016/j.bmcl.2004.12.049.

(223) Wang, W.; Sheng, C.; Che, X.; Ji, H.; Miao, Z.; Yao, J.; Zhang, W. N. Design, Synthesis, and Antifungal Activity of Novel Conformationally Restricted Triazole Derivatives. *Arch. Pharm. (Weinheim).* **2009**, *342* (12), 732–739. https://doi.org/10.1002/ardp.200900103.

(224) Che, X.; Sheng, C.; Wang, W.; Cao, Y.; Xu, Y.; Ji, H.; Dong, G.; Miao, Z.; Yao, J.; Zhang, W. New Azoles with Potent Antifungal Activity: Design, Synthesis and Molecular Docking. *Eur. J. Med. Chem.* **2009**, *44* (10), 4218–4226. https://doi.org/10.1016/j.ejmech.2009.05.018.

(225) Hurst, D. Application of the Elbs Persulfate Oxidation to the Preparation of 5-Hydroxypyrimidines. *Aust. J. Chem.* **1983**, *36* (6), 1285. https://doi.org/10.1071/CH9831285.

(226) Otzen, T.; Wempe, E. G.; Kunz, B.; Bartels, R.; Lehwark-Yvetot, G.; Hänsel, W.; Schaper, K.-J.; Seydel, J. K. Folate-Synthesizing Enzyme System as Target for Development of Inhibitors and Inhibitor Combinations against Candida Albicans-Synthesis and Biological Activity of New 2,4-Diaminopyrimidines and 4'-Substituted 4-Aminodiphenyl Sulfones. *J. Med. Chem.* **2004**, *47* (1), 240–253. https://doi.org/10.1021/jm030931w.

(227) Bag, S.; Tawari, N. R.; Degani, M. S.; Queener, S. F. Design, Synthesis, Biological Evaluation and Computational Investigation of Novel Inhibitors of Dihydrofolate Reductase of Opportunistic Pathogens. *Bioorg. Med. Chem.* **2010**, *18* (9), 3187–3197. https://doi.org/10.1016/j.bmc.2010.03.031.

(228) Hull, R. 399. Pyrimidines. Part I. The Synthesis of Some 5-Hydroxypyrimidines. *J. Chem. Soc.* **1956**, 2033. https://doi.org/10.1039/jr9560002033.

(229) Makarov, V.; Manina, G.; Mikusova, K.; Mollmann, U.; Ryabova, O.; Saint-Joanis, B.; Dhar, N.; Pasca, M. R.; Buroni, S.; Lucarelli, A. P.; Milano, A.; De Rossi, E.; Belanova, M.; Bobovska, A.; Dianiskova, P.; Kordulakova, J.; Sala, C.; Fullam, E.; Schneider, P.; McKinney, J. D.; Brodin, P.; Christophe, T.; Waddell, S.; Butcher, P.; Albrethsen, J.; Rosenkrands, I.; Brosch, R.; Nandi, V.; Bharath, S.; Gaonkar, S.; Shandil, R. K.; Balasubramanian, V.; Balganesh, T.; Tyagi, S.; Grosset, J.; Riccardi, G.; Cole, S. T. Benzothiazinones Kill Mycobacterium Tuberculosis by Blocking Arabinan Synthesis. *Science (80-.).* **2009**, *324* (5928), 801–804. https://doi.org/10.1126/science.1171583.

(230) Batt, S. M.; Jabeen, T.; Bhowruth, V.; Quill, L.; Lund, P. a.; Eggeling, L.; Alderwick, L. J.; Fütterer, K.; Besra, G. S.; Futterer, K.; Besra, G. S. Structural Basis of Inhibition of Mycobacterium Tuberculosis DprE1 by Benzothiazinone Inhibitors. *Proc. Natl. Acad. Sci.* **2012**, *109* (28), 11354–11359. https://doi.org/10.1073/pnas.1205735109.

(231) Trefzer, C.; Škovierová, H.; Buroni, S.; Bobovská, A.; Nenci, S.; Molteni, E.; Pojer, F.; Pasca, M. R.; Makarov, V.; Cole, S. T.; Riccardi, G.; Mikušová, K.; Johnsson, K. Benzothiazinones Are Suicide Inhibitors of Mycobacterial Decaprenylphosphoryl-β-d-Ribofuranose 2'-Oxidase DprE1. *J. Am. Chem. Soc.* **2012**, *134* (2), 912–915. https://doi.org/10.1021/ja211042r.

(232) Neres, J.; Pojer, F.; Molteni, E.; Chiarelli, L. R.; Dhar, N.; Boy-Röttger, S.; Buroni, S.; Fullam, E.; Degiacomi, G.; Lucarelli, A. P.; Read, R. J.; Zanoni, G.; Edmondson, D. E.; De Rossi, E.; Pasca, M.

R.; McKinney, J. D.; Dyson, P. J.; Riccardi, G.; Mattevi, A.; Cole, S. T.; Binda, C.; Boy-Rottger, S.; Buroni, S.; Fullam, E.; Degiacomi, G.; Lucarelli, A. P.; Read, R. J.; Zanoni, G.; Edmondson, D. E.; De Rossi, E.; Pasca, M. R.; McKinney, J. D.; Dyson, P. J.; Riccardi, G.; Mattevi, A.; Cole, S. T.; Binda, C.; Boy-Röttger, S.; Buroni, S.; Fullam, E.; Degiacomi, G.; Lucarelli, A. P.; Read, R. J.; Zanoni, G.; Edmondson, D. E.; De Rossi, E.; Pasca, M. R.; McKinney, J. D.; Dyson, P. J.; Riccardi, G.; Mattevi, A.; Cole, S. T.; Binda, C.; Boy-Rottger, S.; Buroni, S.; Fullam, E.; Degiacomi, G.; Lucarelli, A. P.; Read, R. J.; Zanoni, G.; Edmondson, D. E.; De Rossi, E.; Pasca, M. R.; McKinney, J. D.; Dyson, P. J.; Riccardi, G.; Mattevi, A.; Cole, S. T.; Binda, C. Structural Basis for Benzothiazinone-Mediated Killing of Mycobacterium Tuberculosis. *Sci. Transl. Med.* **2012**, *4* (150), 150ra121-150ra121. https://doi.org/10.1126/scitranslmed.3004395.

(233) Tiwari, R.; Moraski, G. C.; Krchňák, V.; Miller, P. A.; Colon-Martinez, M.; Herrero, E.; Oliver, A. G.; Miller, M. J. Thiolates Chemically Induce Redox Activation of BTZ043 and Related Potent Nitroaromatic Anti-Tuberculosis Agents. *J. Am. Chem. Soc.* **2013**, *135* (9), 3539–3549. https://doi.org/10.1021/ja311058q.

(234) Landge, S.; Mullick, A. B.; Nagalapur, K.; Neres, J.; Subbulakshmi, V.; Murugan, K.; Ghosh, A.; Sadler, C.; Fellows, M. D.; Humnabadkar, V.; Mahadevaswamy, J.; Vachaspati, P.; Sharma, S.; Kaur, P.; Mallya, M.; Rudrapatna, S.; Awasthy, D.; Sambandamurthy, V. K.; Pojer, F.; Cole, S. T.; Balganesh, T. S.; Ugarkar, B. G.; Balasubramanian, V.; Bandodkar, B. S.; Panda, M.; Ramachandran, V. Discovery of Benzothiazoles as Antimycobacterial Agents: Synthesis, Structure–Activity Relationships and Binding Studies with Mycobacterium Tuberculosis Decaprenylphosphoryl-β-d-Ribose 2'-Oxidase. *Bioorg. Med. Chem.* **2015**, *23* (24), 7694–7710. https://doi.org/10.1016/j.bmc.2015.11.017.

(235) Wang, F.; Sambandan, D.; Halder, R.; Wang, J.; Batt, S. M.; Weinrick, B.; Ahmad, I.; Yang, P.; Zhang, Y.; Kim, J.; Hassani, M.; Huszar, S.; Trefzer, C.; Ma, Z.; Kaneko, T.; Mdluli, K. E.; Franzblau, S.; Chatterjee, A. K.; Johnsson, K.; Johnson, K.; Mikusova, K.; Besra, G. S.; Fütterer, K.; Robbins, S. H.; Barnes, S. W.; Walker, J. R.; Jacobs, W. R.; Schultz, P. G. Identification of a Small Molecule with Activity against Drug-Resistant and Persistent Tuberculosis. *Proc. Natl. Acad. Sci. U. S. A.* **2013**, *110* (27), E2510-7. https://doi.org/10.1073/pnas.1309171110.

(236) Shirude, P. S.; Shandil, R.; Sadler, C.; Naik, M.; Hosagrahara, V.; Hameed, S.; Shinde, V.; Bathula, C.; Humnabadkar, V.; Kumar, N.; Reddy, J.; Panduga, V.; Sharma, S.; Ambady, A.; Hegde, N.; Whiteaker, J.; McLaughlin, R. E.; Gardner, H.; Madhavapeddi, P.; Ramachandran, V.; Kaur, P.; Narayan, A.; Guptha, S.; Awasthy, D.; Narayan, C.; Mahadevaswamy, J.; Vishwas, K.; Ahuja, V.; Srivastava, A.; Prabhakar, K.; Bharath, S.; Kale, R.; Ramaiah, M.; Choudhury, N. R.; Sambandamurthy, V. K.; Solapure, S.; Iyer, P. S.; Narayanan, S.; Chatterji, M. Azaindoles: Noncovalent DprE1 Inhibitors from Scaffold Morphing Efforts, Kill Mycobacterium Tuberculosis and Are Efficacious in Vivo. *J. Med. Chem.* **2013**, *56* (23), 9701–9708. https://doi.org/10.1021/jm401382v.

(237) Shirude, P. S.; Shandil, R. K.; Manjunatha, M. R.; Sadler, C.; Panda, M.; Panduga, V.; Reddy, J.; Saralaya, R.; Nanduri, R.; Ambady, A.; Ravishankar, S.; Sambandamurthy, V. K.; Humnabadkar, V.; Jena, L. K.; Suresh, R. S.; Srivastava, A.; Prabhakar, K. R.; Whiteaker, J.; McLaughlin, R. E.; Sharma, S.; Cooper, C. B.; Mdluli, K.; Butler, S.; Iyer, P. S.; Narayanan, S.; Chatterji, M. Lead Optimization of 1,4-Azaindoles as Antimycobacterial Agents. *J. Med. Chem.* **2014**, *57* (13), 5728–5737. https://doi.org/10.1021/jm500571f.

(238) Naik, M.; Humnabadkar, V.; Tantry, S. J.; Panda, M.; Narayan, A.; Guptha, S.; Panduga, V.; Manjrekar, P.; Jena, L. K.; Koushik, K.; Shanbhag, G.; Jatheendranath, S.; Manjunatha, M. R.; Gorai, G.; Bathula, C.; Rudrapatna, S.; Achar, V.; Sharma, S.; Ambady, A.; Hegde, N.; Mahadevaswamy, J.; Kaur, P.; Sambandamurthy, V. K.; Awasthy, D.; Narayan, C.; Ravishankar, S.; Madhavapeddi, P.; Reddy, J.; Prabhakar, K.; Saralaya, R.; Chatterji, M.; Whiteaker, J.; McLaughlin, B.; Chiarelli, L. R.; Riccardi, G.; Pasca, M. R.; Binda, C.; Neres, J.; Dhar, N.; Signorino-

Gelo, F.; McKinney, J. D.; Ramachandran, V.; Shandil, R.; Tommasi, R.; Iyer, P. S.; Narayanan, S.; Hosagrahara, V.; Kavanagh, S.; Dinesh, N.; Ghorpade, S. R. 4-Aminoquinolone Piperidine Amides: Noncovalent Inhibitors of DprE1 with Long Residence Time and Potent Antimycobacterial Activity. *J. Med. Chem.* **2014**, *57* (12), 5419–5434. https://doi.org/10.1021/jm5005978.

(239) Panda, M.; Ramachandran, S.; Ramachandran, V.; Shirude, P. S.; Humnabadkar, V.; Nagalapur, K.; Sharma, S.; Kaur, P.; Guptha, S.; Narayan, A.; Mahadevaswamy, J.; Ambady, A.; Hegde, N.; Rudrapatna, S. S.; Hosagrahara, V. P.; Sambandamurthy, V. K.; Raichurkar, A. Discovery of Pyrazolopyridones as a Novel Class of Noncovalent DprE1 Inhibitor with Potent Anti-Mycobacterial Activity. *J. Med. Chem.* **2014**, *57* (11), 4761–4771. https://doi.org/10.1021/jm5002937.

(240) Neres, J.; Hartkoorn, R. C.; Chiarelli, L. R.; Gadupudi, R.; Pasca, M. R.; Mori, G.; Venturelli, A.; Savina, S.; Makarov, V.; Kolly, G. S.; Molteni, E.; Binda, C.; Dhar, N.; Ferrari, S.; Brodin, P.; Delorme, V.; Landry, V.; de Jesus Lopes Ribeiro, A. L.; Farina, D.; Saxena, P.; Pojer, F.; Carta, A.; Luciani, R.; Porta, A.; Zanoni, G.; De Rossi, E.; Costi, M. P.; Riccardi, G.; Cole, S. T. 2-Carboxyquinoxalines Kill Mycobacterium Tuberculosis through Noncovalent Inhibition of DprE1. *ACS Chem. Biol.* **2015**, *10* (3), 705–714. https://doi.org/10.1021/cb5007163.

(241) Chikhale, R.; Menghani, S.; Babu, R.; Bansode, R.; Bhargavi, G.; Karodia, N.; Rajasekharan, M. V.; Paradkar, A.; Khedekar, P. Development of Selective DprE1 Inhibitors: Design, Synthesis, Crystal Structure and Antitubercular Activity of Benzothiazolylpyrimidine-5-Carboxamides. *Eur. J. Med. Chem.* **2015**, *96*, 30–46.

(242) Liu, R.; Lyu, X.; Batt, S. M.; Hsu, M.-H. H.; Harbut, M. B.; Vilchèze, C.; Cheng, B.; Ajayi, K.; Yang, B.; Yang, Y.; Guo, H.; Lin, C.; Gan, F.; Wang, C.; Franzblau, S. G.; Jacobs, W. R.; Besra, G. S.; Johnson, E. F.; Petrassi, M.; Chatterjee, A. K.; Fütterer, K.; Wang, F.; Wang, F. Determinants of the Inhibition of DprE1 and CYP2C9 by Antitubercular Thiophenes. **2017**, *56* (42), 13011–13015. https://doi.org/10.1002/anie.201707324.

(243) Oh, S.; Park, Y.; Engelhart, C. A.; Wallach, J. B.; Schnappinger, D.; Arora, K.; Manikkam, M.; Gac, B.; Wang, H.; Murgolo, N.; Olsen, D. B.; Goodwin, M.; Sutphin, M.; Weiner, D. M.; Via, L. E.; Boshoff, H. I. M.; Barry, C. E. Discovery and Structure–Activity-Relationship Study of N -Alkyl-5-Hydroxypyrimidinone Carboxamides as Novel Antitubercular Agents Targeting Decaprenylphosphoryl-β- d -Ribose 2'-Oxidase. *J. Med. Chem.* **2018**, *61* (22), 9952–9965. https://doi.org/10.1021/acs.jmedchem.8b00883.

(244) Chikhale, R. V.; Barmade, M. A.; Murumkar, P. R.; Yadav, M. R. Overview of the Development of DprE1 Inhibitors for Combating the Menace of Tuberculosis. *J. Med. Chem.* **2018**, *61* (19), 8563–8593. https://doi.org/10.1021/acs.jmedchem.8b00281.

(245) Vjecha, M. J.; Tiberi, S.; Zumla, A. Accelerating the Development of Therapeutic Strategies for Drug-Resistant Tuberculosis. *Nat. Rev. Drug Discov.* **2018**, *17* (9), 607–608. https://doi.org/10.1038/nrd.2018.28.

(246) Wolucka, B. A. Biosynthesis of D-Arabinose in Mycobacteria - A Novel Bacterial Pathway with Implications for Antimycobacterial Therapy. *FEBS J.* **2008**, *275* (11), 2691–2711. https://doi.org/10.1111/j.1742-4658.2008.06395.x.

(247) Brecik, M.; Centárová, I.; Mukherjee, R.; Kolly, G. S.; Huszár, S.; Bobovská, A.; Kilacsková, E.; Mokošová, V.; Svetlíková, Z.; Šarkan, M.; Neres, J.; Korduláková, J.; Cole, S. T.; Mikušová, K. DprE1 Is a Vulnerable Tuberculosis Drug Target Due to Its Cell Wall Localization. *ACS Chem. Biol.* **2015**, *10* (7), 1631–1636. https://doi.org/10.1021/acschembio.5b00237.

(248) Mikušová, K.; Huang, H.; Yagi, T.; Holsters, M.; Vereecke, D.; D'Haeze, W.; Scherman, M. S.; Brennan, P. J.; McNeil, M. R.; Crick, D. C. Decaprenylphosphoryl Arabinofuranose, the Donor of

the D-Arabinofuranosyl Residues of Mycobacterial Arabinan, Is Formed via a Two-Step Epimerization of Decaprenylphosphoryl Ribose. *J. Bacteriol.* **2005**, *187* (23), 8020–8025. https://doi.org/10.1128/JB.187.23.8020-8025.2005.

(249) Kolly, G. S.; Boldrin, F.; Sala, C.; Dhar, N.; Hartkoorn, R. C.; Ventura, M.; Serafini, A.; McKinney, J. D.; Manganelli, R.; Cole, S. T. Assessing the Essentiality of the Decaprenyl-Phospho-d-Arabinofuranose Pathway in Mycobacterium Tuberculosis Using Conditional Mutants. *Mol. Microbiol.* **2014**, *92* (1), 194–211. https://doi.org/10.1111/mmi.12546.

(250) Lu, H.; Kopcho, L.; Ghosh, K.; Witmer, M.; Parker, M.; Gupta, S.; Paul, M.; Krishnamurthy, P.; Laksmaiah, B.; Xie, D.; Tredup, J.; Zhang, L.; Abell, L. M. Development of a RapidFire Mass Spectrometry Assay and a Fluorescence Assay for the Discovery of Kynurenine Aminotransferase II Inhibitors to Treat Central Nervous System Disorders. *Anal. Biochem.* **2016**, *501*, 56–65. https://doi.org/10.1016/j.ab.2016.02.003.

(251) Leveridge, M.; Collier, L.; Edge, C.; Hardwicke, P.; Leavens, B.; Ratcliffe, S.; Rees, M.; Stasi, L. P.; Nadin, A.; Reith, A. D. A High-Throughput Screen to Identify LRRK2 Kinase Inhibitors for the Treatment of Parkinson's Disease Using RapidFire Mass Spectrometry. *J. Biomol. Screen.* **2016**, *21* (2), 145–155. https://doi.org/10.1177/1087057115606707.

(252) Rogacki, M. K.; Pitta, E.; Balabon, O.; Huss, S.; Lopez-Roman, E. M.; Argyrou, A.; Blanco-Ruano, D.; Cacho, M.; Vande Velde, C. M. L.; Augustyns, K.; Ballell, L.; Barros, D.; Bates, R. H.; Cunningham, F.; Van der Veken, P. Identification and Profiling of Hydantoins—A Novel Class of Potent Antimycobacterial DprE1 Inhibitors. *J. Med. Chem.* **2018**, *61* (24), 11221–11249. https://doi.org/10.1021/acs.jmedchem.8b01356.

(253) Balabon, O.; Pitta, E.; Rogacki, M. K.; Meiler, E.; Casanueva, R.; Guijarro, L.; Huss, S.; Lopez-Roman, E. M.; Santos-Villarejo, Á.; Augustyns, K.; Ballell, L.; Aguirre, D. B.; Bates, R. H.; Cunningham, F.; Cacho, M.; Van der Veken, P. Optimization of Hydantoins as Potent Antimycobacterial Decaprenylphosphoryl-β- <scp>d</Scp> -Ribose Oxidase (DprE1) Inhibitors. *J. Med. Chem.* **2020**, *63* (10), 5367–5386. https://doi.org/10.1021/acs.jmedchem.0c00107.

(254) Young, R. J.; Green, D. V. S. S.; Luscombe, C. N.; Hill, A. P. Getting Physical in Drug Discovery II: The Impact of Chromatographic Hydrophobicity Measurements and Aromaticity. *Drug Discov. Today* **2011**, *16* (17–18), 822–830. https://doi.org/10.1016/j.drudis.2011.06.001.

(255) Oballa, R. M.; Truchon, J. F.; Bayly, C. I.; Chauret, N.; Day, S.; Crane, S.; Berthelette, C. A Generally Applicable Method for Assessing the Electrophilicity and Reactivity of Diverse Nitrile-Containing Compounds. *Bioorganic Med. Chem. Lett.* **2007**, *17* (4), 998–1002. https://doi.org/10.1016/j.bmcl.2006.11.044.

(256) Potashman, M. H.; Duggan, M. E. Covalent Modifiers: An Orthogonal Approach to Drug Design. *J. Med. Chem.* **2009**, *52* (5), 1231–1246. https://doi.org/10.1021/jm8008597.

(257) Alanazi, A. M.; El-Azab, A. S.; Al-Swaidan, I. a.; Maarouf, A. R.; El-Bendary, E. R.; Abu El-Enin, M. a.; Abdel-Aziz, A. a.-M. Synthesis, Single-Crystal, in Vitro Antitumor Evaluation and Molecular Docking of 3-Substitued 5,5-Diphenylimidazolidine-2,4-Dione Derivatives. *Med. Chem. Res.* **2013**, *22* (12), 6129–6142. https://doi.org/10.1007/s00044-013-0597-1.

(258) Pitta, E. PhD Thesis, Universiteit Antwerpen, 2017.

(259) Balabon, O.; Rogacki, M. K.; Pitta, E. Unpublished Work.

(260) Peretto, I.; Forlani, R.; Fossati, C.; Giardina, G. a M.; Giardini, A.; Guala, M.; La Porta, E.; Petrillo, P.; Radaelli, S.; Radice, L.; Raveglia, L. F.; Santoro, E.; Scudellaro, R.; Scarpitta, F.; Bigogno, C.; Misiano, P.; Dondio, G. M.; Rizzi, A.; Armani, E.; Amari, G.; Civelli, M.; Villetti, G.; Patacchini, R.; Bergamaschi, M.; Delcanale, M.; Salcedo, C.; Fernández, A. G.; Imbimbo, B. P. Discovery of Diaryl Imidazolidin-2-One Derivatives, a Novel Class of Muscarinic M3 Selective Antagonists (Part 1).

J. Med. Chem. **2007**, *50* (7), 1571–1583. https://doi.org/10.1021/jm061159a.

(261) Safari, J.; Javadian, L. A One-Pot Synthesis of 5,5-Disubstituted Hydantoin Derivatives Using Magnetic Fe3O4 Nanoparticles as a Reusable Heterogeneous Catalyst. *Comptes Rendus Chim.* **2013**, *16* (12), 1165–1171. https://doi.org/10.1016/j.crci.2013.06.005.

(262) Safari, J.; Gandomi-Ravandi, S.; Javadian, L. Microwave-Promoted Facile and Rapid Synthesis Procedure for the Efficient Synthesis of 5,5-Disubstituted Hydantoins. *Synth. Commun.* **2013**, *43* (23), 3115–3120. https://doi.org/10.1080/00397911.2012.730647.

(263) Ooms, F.; Wouters, J.; Oscari, O.; Happaerts, T.; Bouchard, G.; Carrupt, P.-A.; Testa, B.; Lambert, D. M. Exploration of the Pharmacophore of 3-Alkyl-5-Arylimidazolidinediones as New CB(1) Cannabinoid Receptor Ligands and Potential Antagonists: Synthesis, Lipophilicity, Affinity, and Molecular Modeling. *J. Med. Chem.* **2002**, *45* (9), 1748–1756.

(264) Dumbris, S. M.; Díaz, D. J.; McElwee-White, L. Preparation of Hydantoins by Catalytic Oxidative Carbonylation of Alpha-Amino Amides. *J. Org. Chem.* **2009**, *74* (22), 8862–8865. https://doi.org/10.1021/jo9016138.

(265) Konnert, L.; Reneaud, B.; De Figueiredo, R. M.; Campagne, J. M.; Lamaty, F.; Martinez, J.; Colacino, E. Mechanochemical Preparation of Hydantoins from Amino Esters: Application to the Synthesis of the Antiepileptic Drug Phenytoin. *J. Org. Chem.* **2014**, *79* (21), 10132–10142. https://doi.org/10.1021/jo5017629.

(266) Colacino, E.; Lamaty, F.; Martinez, J.; Parrot, I. Microwave-Assisted Solid-Phase Synthesis of Hydantoin Derivatives. *Tetrahedron Lett.* **2007**, *48* (30), 5317–5320. https://doi.org/10.1016/j.tetlet.2007.05.084.

(267) Stilz, H. U.; Guba, W.; Jablonka, B.; Just, M.; Klingler, O.; König, W.; Wehner, V.; Zoller, G. Discovery of an Orally Active Non-Peptide Fibrinogen Receptor Antagonist Based on the Hydantoin Scaffold. *J. Med. Chem.* **2001**, *44* (8), 1158–1176. https://doi.org/10.1021/jm001068s.

(268) Olimpieri, F.; Bellucci, M. C.; Volonterio, A.; Zanda, M. A Mild, Efficient Approach for the Synthesis of 1,5-Disubstituted Hydantoins. *European J. Org. Chem.* **2009**, *2009* (35), 6179–6188. https://doi.org/10.1002/ejoc.200900868.

(269) Rosen, B. R.; Ruble, J. C.; Beauchamp, T. J.; Navarro, A. Mild Pd-Catalyzed N -Arylation of Methanesulfonamide and Related Nucleophiles: Avoiding Potentially Genotoxic Reagents and Byproducts. *Org. Lett.* **2011**, *13* (10), 2564–2567. https://doi.org/10.1021/ol200660s.

(270) Chemical Shift http://www.chem.wisc.edu/areas/reich/nmr/05-hmr-02-delta.htm (accessed Jul 25, 2017).

(271) Rogacki, M. K. PhD Thesis (Unpublished), Universiteit Antwerpen, 2017.

(272) Liao, W.; Hu, G.; Guo, Z.; Sun, D.; Zhang, L.; Bu, Y.; Li, Y.; Liu, Y.; Gong, P. Design and Biological Evaluation of Novel 4-(2-Fluorophenoxy)Quinoline Derivatives Bearing an Imidazolone Moiety as c-Met Kinase Inhibitors. *Bioorg. Med. Chem.* **2015**, *23* (15), 4410–4422. https://doi.org/10.1016/j.bmc.2015.06.026.

(273) Crozet, M. D.; Botta, C.; Gasquet, M.; Curti, C.; Rémusat, V.; Hutter, S.; Chapelle, O.; Azas, N.; De Méo, M.; Vanelle, P. Lowering of 5-Nitroimidazole's Mutagenicity: Towards Optimal Antiparasitic Pharmacophore. *Eur. J. Med. Chem.* **2009**, *44* (2), 653–659. https://doi.org/10.1016/j.ejmech.2008.05.015.

(274) Antane, S.; Bernotas, R.; Li, Y.; McDevitt, R.; Yan, Y. Chloromethyl Sulfones from Sulfonyl Chlorides via a One-Pot Procedure. *Synth. Commun.* **2004**, *34* (13), 2443–2449. https://doi.org/10.1081/SCC-120039498.

(275) Trefzer, C.; Rengifo-Gonzalez, M.; Hinner, M. J.; Schneider, P.; Makarov, V.; Cole, S. T.; Johnsson, K. Benzothiazinones: Prodrugs That Covalently Modify the Decaprenylphosphoryl-β-<scp>d</Scp> -Ribose 2'-Epimerase DprE1 of *Mycobacterium Tuberculosis*. *J. Am. Chem. Soc.* **2010**, *132* (39), 13663–13665. https://doi.org/10.1021/ja106357w.

(276) Danielsson, B. R.; Lansdell, K.; Patmore, L.; Tomson, T. Phenytoin and Phenobarbital Inhibit Human HERG Potassium Channels. *Epilepsy Res.* **2003**, *55* (1–2), 147–157. https://doi.org/10.1016/S0920-1211(03)00119-0.

(277) van der Stelt, M.; Cals, J.; Broeders-Josten, S.; Cottney, J.; van der Doelen, A. A.; Hermkens, M.; de Kimpe, V.; King, A.; Klomp, J.; Oosterom, J.; Pols-de Rooij, I.; de Roos, J.; van Tilborg, M.; Boyce, S.; Baker, J. Discovery and Optimization of 1-(4-(Pyridin-2-Yl)Benzyl)Imidazolidine-2,4-Dione Derivatives As a Novel Class of Selective Cannabinoid CB2 Receptor Agonists. *J. Med. Chem.* **2011**, *54* (20), 7350–7362. https://doi.org/10.1021/jm200916p.

(278) Easton, J. D. Potential Hazards of Hydantoin Use. *Ann. Intern. Med.* **1972**, *77* (6), 998. https://doi.org/10.7326/0003-4819-77-6-998.

(279) Nicolai, J.; Vles, J. S. H.; Aldenkamp, A. P. Neurodevelopmental Delay in Children Exposed to Antiepileptic Drugs in Utero: A Critical Review Directed at Structural Study-Bias. *J. Neurol. Sci.* **2008**, *271* (1–2), 1–14. https://doi.org/10.1016/j.jns.2008.03.004.

(280) Sanguinetti, M. C.; Tristani-Firouzi, M. HERG Potassium Channels and Cardiac Arrhythmia. *Nature* **2006**, *440* (7083), 463–469. https://doi.org/10.1038/nature04710.

(281) Thomas, D.; Karle, C.; Kiehn, J. The Cardiac HERG/IKr Potassium Channel as Pharmacological Target: Structure, Function, Regulation, and Clinical Applications. *Curr. Pharm. Des.* **2006**, *12* (18), 2271–2283. https://doi.org/10.2174/138161206777585102.

(282) Pitta, E.; Rogacki, M. K.; Balabon, O.; Huss, S.; Cunningham, F.; Lopez-Roman, E. M.; Joossens, J.; Augustyns, K.; Ballell, L.; Bates, R. H.; Van der Veken, P. Searching for New Leads for Tuberculosis: Design, Synthesis, and Biological Evaluation of Novel 2-Quinolin-4-Yloxyacetamides. *J. Med. Chem.* **2016**, *59* (14), 6709–6728. https://doi.org/10.1021/acs.jmedchem.6b00245.

(283) Kumar, A.; Zhang, M.; Zhu, L.; Liao, R. P.; Mutai, C.; Hafsat, S.; Sherman, D. R.; Wang, M.-W. High-Throughput Screening and Sensitized Bacteria Identify an M. Tuberculosis Dihydrofolate Reductase Inhibitor with Whole Cell Activity. *PLoS One* **2012**, *7* (6), e39961. https://doi.org/10.1371/journal.pone.0039961.

(284) Batt, S. M.; Cacho Izquierdo, M.; Castro Pichel, J.; Stubbs, C. J.; Vela-Glez Del Peral, L.; Pérez-Herrán, E.; Dhar, N.; Mouzon, B.; Rees, M.; Hutchinson, J. P.; Young, R. J.; McKinney, J. D.; Barros Aguirre, D.; Ballell, L.; Besra, G. S.; Argyrou, A. Whole Cell Target Engagement Identifies Novel Inhibitors of Mycobacterium Tuberculosis Decaprenylphosphoryl-β- d -Ribose Oxidase. *ACS Infect. Dis.* **2016**, *1* (12), 615–626. https://doi.org/10.1021/acsinfecdis.5b00065.

(285) Warrier, T.; Kapilashrami, K.; Argyrou, A.; Ioerger, T. R.; Little, D.; Murphy, K. C.; Nandakumar, M.; Park, S.; Gold, B.; Mi, J.; Zhang, T.; Meiler, E.; Rees, M.; Somersan-Karakaya, S.; Porras-De Francisco, E.; Martinez-Hoyos, M.; Burns-Huang, K.; Roberts, J.; Ling, Y.; Rhee, K. Y.; Mendoza-Losana, A.; Luo, M.; Nathan, C. F. N-Methylation of a Bactericidal Compound as a Resistance Mechanism in Mycobacterium Tuberculosis. *Proc. Natl. Acad. Sci. U. S. A.* **2016**, *113* (31), E4523-30. https://doi.org/10.1073/pnas.1606590113.

(286) Gillie, D. J.; Novick, S. J.; Donovan, B. T.; Payne, L. A.; Townsend, C. Development of a High-Throughput Electrophysiological Assay for the Human Ether-à-Go-Go Related Potassium Channel HERG. *J. Pharmacol. Toxicol. Methods* **2013**, *67* (1), 33–44. https://doi.org/10.1016/j.vascn.2012.10.002.

(287)   Remuiñán, M. J.; Pérez-Herrán, E.; Rullás, J.; Alemparte, C.; Martínez-Hoyos, M.; Dow, D. J.; Afari, J.; Mehta, N.; Esquivias, J.; Jiménez, E.; Ortega-Muro, F.; Fraile-Gabaldón, M. T.; Spivey, V. L.; Loman, N. J.; Pallen, M. J.; Constantinidou, C.; Minick, D. J.; Cacho, M.; Rebollo-López, M. J.; González, C.; Sousa, V.; Angulo-Barturen, I.; Mendoza-Losana, A.; Barros, D.; Besra, G. S.; Ballell, L.; Cammack, N. Tetrahydropyrazolo[1,5-a]Pyrimidine-3-Carboxamide and N-Benzyl-6',7'-Dihydrospiro[Piperidine-4,4'-Thieno[3,2-c]Pyran] Analogues with Bactericidal Efficacy against Mycobacterium Tuberculosis Targeting MmpL3. *PLoS One* **2013**, *8* (4), e60933. https://doi.org/10.1371/journal.pone.0060933.

(288)   Tawari, N. R.; Bag, S.; Raju, A.; Lele, A. C.; Bairwa, R.; Ray, M. K.; Rajan, M.; Nawale, L. U.; Sarkar, D.; Degani, M. S. Rational Drug Design, Synthesis and Biological Evaluation of Dihydrofolate Reductase Inhibitors as Antituberculosis Agents. *Future Med. Chem.* **2015**, *7* (8), 979–988. https://doi.org/10.4155/fmc.15.48.

Curriculum Vitae

Olga BALABON

Via Caselline, 317, 41058 Vignola (MO), Italy | balabonolga@gmail.com | +393755300592

Education

Ph.D. IN MEDICINAL CHEMISTRY

Universiteit Antwerpen (Belgium) | 2013 - 2017

- OpenMedChem project
- Funding: Marie Curie Actions (FP7-PEOPLE-2012-ITN)
- Thesis titile: "Profiling and structural investigation of dihydrotriazine-based DHFR inhibitors and hydantoin-derived DprE1 inhibitors in search of novel antimycobacterials"

M. Sc. MASTER ADVANCED SPECTROSCOPY IN CHEMISTRY (ASC)

Universität Leipzig (Germany) & Université Lille1 (France) | 2011 – 2013

- Funding: Erasmus Mundus
- Thesis title: "Novel dihydro-2,4-diamino-1,3,5-triazines as inhibitors of DHFR in Mycobacterium tuberculosis"

B.Sc. CHEMISTRY

Taras Shevchenko National University of Kyiv (Ukraine) | 2007 – 2011

- Specialization: organic chemistry

Professional Experience

HEAD OF CORPORATE MARKETING

Life Chemicals Inc. (Italy & Canada) | 2019 – present

- Define, coordinate & oversee implementation of the Marketing strategy
- Develop and maintain the corporate website and social media content
- Represent company at international conferences and specialized events

MANAGER, MARKETING & SALES

Life Chemicals Inc. (Italy & Canada) | 2018 – 2019

- Responsible for customer support in >10 European countries
- Identified and developped new business opportunities

RESEARCH SCIENTIST

Universiteit Antwerpen (Belgium) | 2013 – 2014, 2016 – 2017

GSK DDW (Spain) | 2014 – 2015

- Design, synthesis, purification and spectroscopical characterization of novel organic molecules
- Analysis and interpretation biological evaluation findings
- Scientific writing and literature review
- Decision making and planning for the research project

Skills & Competences

Language proficiency

- English, Italian, Spanish – fluent
- Russian, Ukrainian – native

IT skills

- Excellent knowledge of the MS Office Word-Excel-PowerPoint-Outlook, internet.
- Chemistry-orientated software proficiency: Experimental data and reference management: CambridgeSoft E-Notebook, Mendeley. Chemical drawing & NMR processing tools: ChemOffice (ChemDraw), ACDLabs, MestReNova

Non-technical competences

- Proactive, flexible and effective in acquiring new skills
- Capable of delivering successfully results, both independently and in team settings
- Strong skills in identifying issues, finding solutions and alternatives
- Reliable and accountable team-player

Publications

- Pazenok, S.; Lui, N.; Gerus, I.; **Balabon, O**. Novel Dioxolane And Dioxane Derivatives And A Process For Their Preparation, June 23, 2011. *(patent)*
- Vdovenko, S.; Gerus, I.; **Balabon, O**.; Kukhar, V. Distinctive Features of Push-Pull Enaminoketones. III: β-Dialkylaminovinyl Perfluoromethyl Ketones and β-Dialkylaminovinyl Trichloromethyl Ketones. *Trends Org. Chem.* 2013, *16*, 93–113.
- Pitta, E.; Rogacki, M. K.; **Balabon, O.** *et al.* Searching for New Leads for Tuberculosis: Design, Synthesis, and Biological Evaluation of Novel 2-Quinolin-4-Yloxyacetamides. *J. Med. Chem.* 2016, *59* (14), 6709–6728.
- Pitta, E.; **Balabon, O.**; Rogacki, M. K. *et al.* Differential Characterization Using Readily Accessible NMR Experiments of Novel N- and O-Alkylated Quinolin-4-Ol, 1,5-Naphthyridin-4-Ol and Quinazolin-4-Ol Derivatives with Antimycobacterial Activity. *Eur. J. Med. Chem.* 2017, *125*, 890–901.
- Rogacki, M. K.; Pitta, E.; **Balabon, O.**; *et al.* Identification and Profiling of Hydantoins—A Novel Class of Potent Antimycobacterial DprE1 Inhibitors. *J. Med. Chem.* 2018, *61* (24), 11221–11249.

- Gerus, I. I.; **Balabon, O. A.;** Pazenok, S. V.; *et al.* Synthesis and Properties of Polyfunctional Cyclic β-Alkoxy-α,β-Unsaturated Ketones Based on 4-Methylene-1,3-Dioxolanes. *European J. Org. Chem.* 2018, *2018* (27–28), 3853–3861.

- Pinchuk, V.; Bondar, G.; **Balabon, O.** Epigenetic and PPI Targeted Libraries from Life Chemicals. *Proceedings* **2019**, *22* (1), 96.

- Shaitanova, E. N.; Gerus, I. I.; **Balabon, O. A.;** *et al.* Synthesis of Fluorine-Containing 3-Aminocyclopent-2-enones via Intramolecular Cyclization. *European J. Org. Chem.* 2020, *2020* (46), 7156–7163.

- **Balabon, O.**; Pitta, E.; Rogacki, M. K. *et al.* Optimization of Hydantoins as Potent Antimycobacterial Decaprenylphosphoryl-β-d-Ribose Oxidase (DprE1) Inhibitors. *J. Med. Chem.* 2020, *63* (10), 5367–5386.